(NASA-CR-150313) FLAW GROWTH OF 7075, 7475, 7050 AND 7049 ALUMINUM ALLOY PLATE IN STRESS CORROSION ENVIRONMENTS Final Report (Kaiser Aluminum and Chemical Corp.) 214 p HC A10/MF A01 CSCL 11F G3/26

N77-26272

Unclas 38267

KAISER ALUMINUM & CHEMICAL CORPORATION

CENTER FOR TECHNOLOGY

NAS 8-30890

RESEARCH REPORT
CFT RR 76-32

October 15, 1976

FLAW GROWTH OF 7075, 7475, 7050 AND 7049 ALUMINUM ALLOY PLATE IN STRESS CORROSION ENVIRONMENTS: CONTRACT NAS8-30890

R. C. Dorward and K. R. Hasse

N77-26272

FLAW GROWTH OF 7075, 7475, 7050 AND 7049 ALUMINUM PLATE IN STRESS CORROSION ENVIRONMENTS

by

R. C. DORWARD and K. R. HASSE

KAISER ALUMINUM & CHEMICAL CORPORATION
CENTER FOR TECHNOLOGY
PLEASANTON, CALIFORNIA 94566

prepared for

GEORGE C. MARSHALL SPACE FLIGHT CENTER
NATIONAL AERONAUTICS & SPACE ADMINISTRATION
MARSHALL SPACE FLIGHT CENTER, ALABAMA

FINAL REPORT

CONTRACT NAS8 - 30890
(REQUEST NO. 8-1-4-50 - 42566 RDH)

October 15, 1976

Prepared by

R. C. Dorward

Approved by

T. J. Summerson

K. R. Hasse

ABSTRACT.

Marine atmosphere and laboratory stress corrosion tests on smooth and precracked specimens from 7075, 7475, 7050, and 7049 alloy plates (1.25 and 3.0-in. thick) show that for a given strength level, alloys 7050-T7X and 7049-T7X have superior short-transverse stress corrosion resistance (SCR) to 7X75-T7X. At typical strength levels above the minimum of 7075-T6, for example, SCR of these alloys is considerably better than that of 7075-T76, and approaches that of 7075-T73. Alloy 7475 maintains an advantage in the area of fracture toughness, however, because it can be thermally processed to give particularly "clean" microstructures.

According to tests in synthetic seawater and a marine atmosphere on bolt-loaded DCB specimens containing pop-in precracks, 7050-T7X and 7049-T7X have SL threshold stress intensities (K_{Iscc}) of about 24 MPa$\sqrt{m}$ (22 ksi$\sqrt{in.}$) at a yield strength of 450 MPa (65.3 ksi). The corresponding K_{Iscc} value for 7X75-T7X at this strength level is about 19 MPa$\sqrt{m}$. In these environments K_{Iscc} is independent of plate thickness, per se; absolute strength level appears to be the controlling factor, K_{Iscc} being inversely proportional to yield strength. In a salt-chromate solution, however, the thicker material appeared inherently more resistant than the thin plate.

Results from precracked specimens are in good qualitative agreement with those obtained from smooth specimens. Although both specimen types are capable of distinguishing between -T6, -T76 and -T73 tempers in relatively short time periods (<2 weeks), the precracked specimen provides more information about crack growth rates.

Examination of fracture surfaces and metallographic cross sections showed a considerable amount of crack blunting, crack jogging, crack branching, unfailed ligaments, and mechanical fracturing in the precracked specimens. Stress corrosion cracks generated from pop-in precracks show these features to a greater extent than specimens containing fatigue precracks. In view of these crack morphologies, it is apparent that measured stress intensities can be higher than effective values at the crack tip. Apparent (measured) stress intensities should therefore be considered as phenomenological parameters only, useful for comparing alloys and tempers under a particular set of experimental conditions. They are also useful from a practical point of view in estimating crack velocities that could be expected under known environmental conditions.

CONTENTS

CONTENTS (Contd)

CONTENTS (Contd)

FOREWORD

This report was prepared by Kaiser Aluminum & Chemical Corporation under Contract NAS8-30890 for the George C. Marshall Space Flight Center of the National Aeronautics and Space Administration. The work was performed in the period October 1, 1974 to September 30, 1976, and was administered under the technical direction of the Propulsion and Vehicle Engineering Laboratory, Materials Division of the George C. Marshall Space Flight Center, with T. S. Humphries serving as Contracting Officer's Representative.

All investigations on alloys 7075-T7351, 7475-T7351, and 7050-T73651 were sponsored by NASA; costs incurred for the concurrent evaluation of alloy 7049 and for the inclusion of 7075-T651 and 7075-T7651 control materials were supported by KACC.

The investigation conducted under this contract has been completed with the writing of this report. However, marine atmospheric exposure tests will be continued, the results to be reported on a biannual basis.

I. INTRODUCTION

The overaged alloy 7075-T73 was the first of the stress-corrosion resistant 7000-series aluminum alloys to be used in aerospace applications. Although this alloy offers excellent stress-corrosion resistance (SCR) in the short-transverse orientation, its use can result in weight penalties because of its lower strength compared to 7075-T6, 7178-T6, and 7079-T6. This situation has provided the impetus for the development of alloys designed to have good SCR in combination with high strength (Refs 1, 2). Fracture toughness has also become increasingly important in aerospace applications requiring high strength and stress-corrosion resistance. Commercially available alloys developed to satisfy these needs are 7050-T736X, 7475-T73X and 7049-T73X. Before these alloys are to be utilized to their full capability, however, it must be demonstrated that they have SCR comparable to the established alloy 7075-T73.

Measurements of stress-corrosion susceptibility have traditionally been given in terms of the time-to-failure of "smooth" specimens which have been loaded at various stresses and then exposed to an appropriate corrosive environment. In recent years, stress-corrosion tests utilizing precracked specimens have become popular because they provide a means of determining quantitative crack growth rate information. Such data are a valuable addition to smooth-specimen results in the same way that fatigue crack growth rate data are a valuable addition to the standard S-N fatigue curves for different alloys.

Actual stress-corrosion crack growth rate data are also useful for setting inspection intervals and for monitoring purposes in a variety of structures. Moreover, if a stress intensity actually does exist below which stress-corrosion cracks do not propagate (K_{Iscc}), this stress intensity value can be determined. (Appendix A describes stress intensity and its relevance to

stress corrosion). In addition, a precracked specimen has the particular advantage of representing a practical situation in which flaws are always present.

The objective of this evaluation was to compare the stress-corrosion crack growth behavior of the newer stress-corrosion resistant, high strength alloys (7475-T7351, 7050-T73561 and 7049-T7351) with that of the established alloy 7075-T7351. The crack growth tests were supplemented with conventional time-to-failure results for smooth tensile-type specimens.

II. GENERAL PLAN OF STUDY

The alloys under consideration were evaluated in plate of two thicknesses; stress-corrosion is known to be dependent on section thickness for reasons that are not completely resolved (metallurgical factors involved are grain structure, strength level, and quench rate). In addition, two aging conditions were included, one intended to produce a "typical" -T73X temper, and the other to give a "borderline" (high strength) -T73X temper. For control purposes, 7075-T651 and 7075-T7651 were also evaluated.

Stress-corrosion tests using smooth specimens were conducted in the short-transverse and long-transverse plate directions using round tensile-type samples subjected to alternate immersion in synthetic seawater and to a seacoast atmosphere (Daytona Beach, Florida). Times to failure were determined at a number of stress levels for each alloy, orientation (short- and long-transverse), and test environment.

Most of the crack growth evaluations were conducted on bolt-loaded double-cantilever beam (DCB) specimens. This type of specimen has a favorable history for characterizing crack growth of aluminum alloys in environments conducive to stress corrosion (Refs 6,7). Crack growth data can be determined as a function of stress intensity, K_I, on a single portable sample that can be machined to test the short-transverse direction of material of almost any thickness. The precracked specimens were tested in three environments by the constant deflection method: a seacoast atmosphere at Daytona Beach, Florida, synthetic seawater, and a salt-chromate solution. A few additional precracked DCB specimens were tested by the constant load technique in the laboratory environments.

In addition to the stress-corrosion tests, supplemental data on fracture toughness and other mechanical properties (tensile and yield strength, elongation), chemical compositions, and electrical conductivities were also determined.

III. MATERIAL FABRICATION

A. CASTING AND HOT ROLLING

One 907 kg (2000 lb), 30.5 cm (12 in.) thick ingot of each of the compositions given in Table I was cast in Kaiser's Center for Technology pilot plant. For comparative purposes, all the new alloys had the same purity level (0.06% Si, 0.10% Fe). The ingots were stress relieved at 316°C (600°F) for 12 hr, and then homogenized for 24 hr at 468°C (875°F). They were then scalped (10 mm per side) and end cropped in preparation for hot rolling. In sawing the heads and butts, cracks were found in the 7050 and 7049 ingots. Successive end slices were taken until no cracks were visually apparent, and as a precaution all the ingots were inspected ultrasonically. This examination showed all ingots to be sound.

The ingots were preheated to 400°C (750°F) and hot rolled to 150 mm (6 in.) slab in six passes of approximately equal drafts. Final slab temperatures were about 370°C (700°F), ranging from 363°C (685°F) for 7050 and 380°C (720°F) for 7075. Figure 1 shows a plot of cumulative horsepower-hour/ton values (measure of the specific energy or work required for deformation) against exit thickness for each pass reduction. It appears that of the four alloys, 7050 required the least deformation energy. 7049 and 7475 were about equal, and 7075 was the "hardest" to roll. We also note that the 7050 slab was the coldest, whereas 7075 was the hottest. Had these temperatures been the same, the curves for the two alloys would probably have been more divergent. Differences in the amount of magnesium in solution at the rolling temperature probably account for the varying deformation energies. 7050 had only about 2.1% Mg, compared to 2.5% for 7075 and 7049. Furthermore, the relatively high copper level in 7050 increases its solvus temperature so that less magnesium is in solution during rolling.

At the 15.2 cm slab stage, the 7050, 7475 and 7049 alloys were given an additional thermal treatment of 20 hr at 493°C (920°F). This type of practice is recognized to be beneficial in alloys that are intended to be used in applications requiring good fracture toughness. The slabs were then hot rolled further to final gage: 76 mm (3.0 in.) and 32 mm (1.25 in.).

B. HEAT TREATMENT

After hot rolling, 10-ft lengths of each plate were solution heat treated at 482°C (900°F) for 6 hr and quenched in cold water. They were then stretched 1.75%, held at ambient temperature for 2 (1.25-in. plates) or 4 (3.0-in. plate) days, and step-1 aged for 24 hr at 121°C (250°F), i.e., -T651 temper.

Ultrasonic inspection of the plates showed all the 3-in. thick materials to conform to Class A discontinuity limits (Ref 10). The 1.25-in. thick plates conformed to Class B limits. In any case, however, test samples were taken only from areas shown to be free of defects giving responses equal to, or greater than, that from a 3/64 in. flat-bottomed hole, i.e., exceeding Class A limits.

To establish the step-2 aging conditions necessary for the desired "minimum" and "typical" -T73 temper conditions, long-transverse tensile blanks from each of the eight plates were aged at 165°C (330°F) for times ranging from 6 to 36 hr. Aging treatments were then selected primarily on the basis of target tensile properties. The desired yield strength for "typical" 7075 and 7475 was 34.5 MPa (5 ksi) above the minimum specified strength level for the particular plate thickness. The corresponding difference for the borderline condition was 75.8 MPa (11 ksi); at the same time, a minimum electrical conductivity of 38% IACS

was chosen.* Similarly, for 7050 and 7049, the desired typical yield strength was 27.6 MPa (4 ksi) above the minimum value, and the strength for the borderline condition was set at 55.1 MPa (8 ksi) above the minimum. Again, the electrical conductivity had to be greater than 38% IACS. Table II gives the minimum yield strengths and the target values for all the materials.

C. AGING CURVES

Figure 2 shows the electrical conductivities as a function of aging time at 165°C (330°F) for each plate thickness. 7075 had the lowest conductivity for a given aging practice, whereas 7475 gave the highest values. This is probably related to higher purity and a slightly lower magnesium content in 7475. Although alloys 7050 and 7049 had the lowest conductivities in the -T6 temper, they had intermediate levels when step-2 aged.

Long-transverse yield strengths (1/2t position for the 1.25-in. plates and 1/4t position for the 3.0-in. plates) as a function of aging time are shown in Figures 3 and 4. For the 1.25-in. thickness, 7050 and 7049 had the same as-overaged strength levels for a given aging time. 7050 revealed its characteristic pronounced peak in strength at short overaging times (Ref 12). 7075 and 7475 also had similar aging curves. For the 3.0-in. thickness, 7050 had higher strength levels for a given overaging time than any of the other alloys. This is probably related to its relatively low quench sensitivity (Ref 13), which would be revealed to a

*Lot acceptance criteria for 7075-T73 are (Ref 11):

Elec. Conductivity	Tensile Properties	Status
>40.0	Above min.	Acceptable
<38.0, ≤39.9	<11.9 ksi above min.	Acceptable
>38.0 ≤39.9	>12.0 ksi above min.	Suspect
≤38.0	Any level	Unacceptable

greater extent in the thicker gage. 7049 and 7075 had similar strengths after about 20 hours of overaging, but 7475 strength levels were considerably lower for all aging times. This could be related to the lower magnesium content in 7475 (2.2% vs. 2.5% in 7075).

Correlation plots of electrical conductivity with yield strength for all the alloys are given in Figure 5. For a given conductivity level, 7075 was the weakest, and 7050 was the strongest. The difference between the curves for 7075 and 7475 is noteworthy, considering their similar compositions.

Based on the overaging curves in Figures 3 and 4, aging times were chosen to just given the desired strength levels for the "typical" and "minimum" -T73X51 temper conditions. These times, together with the resultant yield strengths are given in Table III. Strength levels were generally within 14 MPa (2 ksi) of the target value (average deviation of 9 MPa), thereby allowing an evaluation of the alloys at comparable strength levels and over a fairly wide strength range. The typical and minimum temper conditions will be denoted by the designations -T73X51(T) and -T73X51(M), respectively.

IV. MATERIAL CHARACTERIZATION

In addition to evaluating the plates for stress-corrosion resistance, supplemental data were obtained on microstructures, chemical compositions, tensile properties and fracture toughness. The results of these evaluations follow.

A. METALLOGRAPHIC EVALUATION

The grain structures of the eight plates (mid-plane location) are shown in Figures 6 and 7. Grain size and shape were quite comparable between alloys for each thickness. There were some minor differences in extent of recrystallization, however (see also Figure 8). Both 7475 plates were essentially unrecrystallized, whereas the 7050 materials were about 20% recrystallized. The thinner 7075 plate was also about 20% recrystallized, but only a trace was evident in the 3-in. thick material. Both 7049 plates were slightly recrystallized (≃5%).

All the plates had a discernible sub-grain structure (Fig. 9), but it was most evident in alloys 7049 and 7050. Subgrains in the 3.0-in. thick 7050 plate were particularly well developed.

Figures 10 and 11 show the "insoluble" constituent dispersions in each of the plates. As would be expected on the basis of differences in composition (higher Fe and Si in 7075) and fabrication processes (more thorough homogenization for 7475, 7050 and 7049), there were more, and larger, constituents in the 7075 plates. These phases were Al_2CuMg, Al_7Cu_2Fe, and Mg_2Si in all materials (see Figure 12).

B. CHEMICAL COMPOSITIONS

Table IV shows the compositions of each plate. Zinc, magnesium, and copper contents were determined by "wet" chemical analysis on each plate (both plates of each alloy were rolled from the same ingot). Agreement between the two samples was generally within experimental error. Other elements (Si, Fe, Cr, Ti, Zr, etc.) were analyzed spectrographically; determinations on melt buttons and on plate samples gave the same results.

C. TENSILE PROPERTIES

All the plates were tested for ultimate tensile strength, 0.2% offset yield strength, and elongation. We used 0.505-in. rounds for the long-transverse and longitudinal directions, and miniature specimens for the short-transverse direction (0.125-in. diam for 1.25-in. plate, 0.250. diam for 3-in. plate). All tests were conducted in triplicate using an Instron model TTD testing machine. The test location was the midpoint of each 1.25-in. plate and at quarter thickness for the 3.0-in. plate (except for short-transverse direction).

The tensile data are listed in Table V, and the short and long transverse yield strength levels for all the materials are compared in Figure 13. The "typical" strengths for alloys 7050 and 7049 were 34-48 MPa (5-7 ksi) higher than those of 7075 and 7475. Minimum-aged 7049 and 7050 were stronger than the corresponding 7075-T7651 plates. We also note that the typically aged 7050 and 7049 materials had yield strengths equal to, or greater than, the minimum values for 7075-T651 (420 and 462 MPa for 3.0 and 1.25-in. thick plate, respectively).

D. FRACTURE TOUGHNESS

K_{Ic} data were determined using compact tension specimens according to ASTM E 399-72. Fatigue precracks were introduced with a 6-kip MTS axial-stress fatigue machine. Fracture toughness measurements were made in three directions (SL, TL, LT) using triplicate specimens. The test location was the midplane for the 1.25-in. plates; SL measurements in the 3.0-in. plates were also made at midplane, but LT and TL values were determined at quarter thickness.

In addition to the K_{Ic} values obtained as described above, approximate fracture toughness values were generated by mechanical precracking of the DCB specimens used in the stress-corrosion evaluation. This value is known as K_{Ia}, the stress intensity at which mechanical crack arrest occurs.

The results are given in Table I, and K_{Ic} values are correlated with yield strength in Figures 14 to 16. The usual inverse relationship was obtained, each 35 MPa increase in strength generally giving about 2 MPa$\sqrt{m}$ decrease in K_{Ic}. The TL values, however, appeared somewhat less dependent on strength than those in the LT and SL orientations.

LT and TL K_{Ic} values for the 3-in. thick plates were about 3 MPa$\sqrt{m}$ lower than those of the 1.25-in. materials. In the SL orientation, the same relationship was observed for the 7075 plates. With the exception of the 3.0-in. 7049 plates, K_{Ic} values for the other materials seemed to be independent of both plate thickness and alloy. The 3.0-in. thick 7049 plate had a lower K_{Ic} value than the other high-purity materials; it also had lower fracture toughness in the LT and TL orientations. K_{Ic} values for the 1.25-in. thick 7049 plate, however, were in good agreement with the 7475 and 7050 materials.

Need correspondence | ksi√in. for consistency

The fracture toughness levels of the 7475 plates were somewhat lower than the tentative minimums published for the alloy (Ref 14): LT-42 MPa$\sqrt{m}$ (38 ksi$\sqrt{in.}$) and TL-36 MPa$\sqrt{m}$ (33 ksi$\sqrt{in.}$) in thicknesses ranging from 0.75 to 1.5 in. Values obtained for 1.25-in. thick plate in this study were 38.5-42 MPa$\sqrt{m}$ (LT) and 32 MPa$\sqrt{m}$ (TL). The reason for this difference undoubtedly lies in the fabrication practice. We used the same practice for alloys 7475, 7050 and 7049. Achieving optimum fracture toughness in alloy 7475 requires high-temperature thermal treatments that are not possible with the other alloys because their liquidus temperatures are too low. To demonstrate the effect of high fracture toughness (and correspondingly high K_{Ia}, the initial stress intensity in a bolt-loaded DCB specimen) on crack growth behavior, a few stress-corrosion tests will also be run on a 3.5-in. thick plate having an SL K_Q level of 48 MPa$\sqrt{m}$ (43.4 ksi$\sqrt{in.}$).*

In addition to fracture toughness tests, fatigue crack growth rate curves were determined for the 1.25-in. plates ("typical" -T73 temper only) in the TL orientation. These tests were conducted on 1-in. wide compact specimens using a stress ratio of 0.1 and a cyclic frequency of 60 Hz. The relative humidity of the laboratory air was 20-25%. Logarithmic plots of da/dN versus ΔK are given in Figure 17. Although the high-purity materials had higher fracture toughness than the 7075 plates, fatigue crack growth rates for all the alloys were about equal over the ΔK range evaluated. This finding agrees with the work of Van Orden and Pettit (Ref 15) in which they concluded that high fracture toughness does not necessarily improve resistance to fatigue crack growth.

*Results will be given with first biannual report on long-term marine atmosphere performance of stress corrosion specimens exposed at Daytona Beach.

V. STRESS CORROSION TEST PROCEDURES

A. SMOOTH SPECIMENS

Tensile-round stress-corrosion specimens from the short- and long-transverse directions of each plate were tested by alternate immersion in the laboratory for 6 months (details are given in Appendix B) and in the coastal marine atmosphere at Daytona Beach, Florida, for an indefinite time period. A 3.6% synthetic sea salt (ASTM D1141, without heavy metal salts) was used rather than NaCl for the laboratory test in order to inhibit the amount of general corrosion (Refs 16 and 17), and thus reduce the frequency of tensile overload failures common to the conventional 3-1/2% NaCl test. The specimens used were 3.175 mm (0.125-in.) diameter tensile rounds, which were stressed in window frame jigs (Fig. 18).

In the laboratory test, the minimum and typical -T73 temper materials were exposed at four stress levels between 172 and 379 MPa (25, 35, 45 and 55 ksi). The 7075-T651 and 7075-T7651 materials were stressed at 34 to 172 MPa (5, 15 and 25 ksi) and 172 to 310 MPa (25, 35 and 45 ksi), respectively. Only the typical -T73 temper conditions were evaluated in the marine atmosphere; stress levels were the same as those used in the laboratory tests. The specimens were examined for failures on a daily basis in the laboratory, and weekly in the marine atmosphere.

B. PRECRACKED SPECIMENS

The crack-line loaded double cantilever beam (DCB) specimen was used for these tests. The details of this specimen are given in Appendix C together with relationships for the stress intensity factor as a function of loading and specimen geometry.

Two methods of loading were used in this study. Most of the specimens were bolt-loaded (decreasing stress intensity), but a few were tested under constant load conditions (increasing stress intensity). Details of each type of test follow.

1. CONSTANT DEFLECTION (DECREASING K) TESTS

Bolt loaded SL and TL specimens machined from the midplane of the plates were exposed to three environments:

1. Marine atmosphere (Daytona Beach)--typical -T73 temper only.
2. Synthetic seawater, alternate immersion--typical -T73 temper only.
3. Salt-chromate solution (0.6M NaCl + 0.02M $Na_2Cr_2O_7$ + 0.07M $NaC_2H_3O_2$ + $HC_2H_3O_2$ to pH4), constant immersion--minimum and typical -T73 tempers.

Specimens from the 7075-T651 and 7075-T7651 control materials were also tested in each environment. The salt-chromate environment was included because it inhibits general corrosion and provides faster crack growth than standard salt solutions (Ref 7). Synthetic seawater was again chosen because it promotes less general corrosion than NaCl; we have also encountered considerable difficulty in measuring crack lengths during alternate immersion in NaCl solutions.

Most of the DCB specimens were 25 mm (1-in.) wide by 25 mm (1-in.) high by 125 mm (5-in.) long, and were precracked by mechanical pop-in. In addition a few 75-mm (3.0-in.) high SL specimens were tested in each environment, and a number of fatigue-precracked SL specimens were also included. All the specimens had chevron notches, and were sidegrooved to help provide a straight crack front, suppress formation of shear lips, and keep

the crack growing in the proper plane (Refs 18 & 20). Drawings of the specimens used are given in Figures 19 and 20. Tables VII and VIII show a schedule of all the bolt-loaded specimens that were tested.

Prior to precracking and testing, the specimens were etch-cleaned in 5% NaOH solution at 180°C, desmutted in cold 50% HNO_3, and rinsed in hot deionized water. The specimens were precracked by turning a pair of stainless steel bolts into the machined slot at the end of the specimen. The cracks were propagated about 2-3 mm (0.1-in.) beyond the end of the chevron; total crack lengths were about 28 mm (1.1-in.) as measured from the load point. Deflections were measured with a clip-in strain gage at the integral knife edges, and crack lengths were measured optically at the specimen edges with the help of a binocular microscope.

Stress intensities for crack arrest (K_{Ia}) were then calculated from the relation given by Mostovoy et al. (Ref 18):

$$K = \frac{\delta E h^{3/2} \phi \left[3(a + .6h)^2 + h^2\right]^{1/2}}{4\left[(a + .6h)^3 + h^2 a\right]} \qquad (1)$$

where a is the crack length; h is the specimen beam height; δ is the deflection at the load point (determined by applying an empirical correction factor to the end measurements); E is the modulus of elasticity; and ϕ, a correction factor for side grooves, was assumed to be equal to $(b/b_n)^{0.5}$, where b and b_n are the full and reduced sections, respectively. The K_{Ia} values for the materials are given in Appendix D.

Specimens that were fatigue precracked were bolt loaded to two stress intensities, one to about 90% of K_{Ia}, and the other to 75% of K_{Ia}. All the specimens that were precracked by pop-in were tested at an initial stress intensity of K_{Ia}. Fatigue

precracks have some possible advantages since the zone of plastic deformation at the crack front is smaller than that of a mechanical pop-in crack. However, the latter type of crack, being much less time-consuming to produce is considerably more economical.

For the laboratory tests, the bolts were coated in paraffin wax, and the specimens were placed bolt-end up in the solutions. Specimens exposed at Daytona Beach were suspended from racks with the bold end down (Fig. 21). Measurements of crack length were made optically, with the help of a binocular microscope, on a logarithmic time basis of approximately 1 day, 2 days, 4 days, 1 week, 2 weeks, 1 month, 2 months, etc. The average of the crack lengths measured at each edge was then used in the calculation of stress intensity (using Eq. 1) and crack growth rate.

We recognize that crack front locations estimated from edge measurements are likely to be short due to crack-front bowing of both the precrack (see Appendix D, Figure D2) and the subsequent stress corrosion crack (side grooves minimize this problem, however). Since crack-front bowing causes an underestimation of crack length, stress intensity is overestimated (cf. Eq. 1). To circumvent this problem, other methods of crack length measurement have been proposed, such as ultrasonic techniques (Ref 24). However, the ultrasonic method is apparently accurate to only about ±1.5 mm (±0.06 in.), so although it may be quite adequate for alloys that undergo fast crack growth (e.g., 7075-T6) it is not sufficiently accurate for resistant materials that may grow a crack less than 1.5 mm (0.06 in.) long in one month of testing i.e., a crack velocity of 6×10^{-9} m/sec ($\approx 10^{-4}$ in./hr).

Total exposure periods for the laboratory tests were 6 months. The specimens were then broken open for visual and metallographic examination. At the end of 6 months, one specimen was also removed from the marine atmosphere for detailed examination. The

other specimens will be left at the test site for prolonged exposure (results will be reported biannually).

2. CONSTANT LOAD (INCREASING K) TESTS

As a check on the constant deflection method of loading, a number of DCB specimens from the 3.0 in. plates were also subjected to constant load tests in both laboratory environments (synthetic seawater and salt-chromate solution). The specimens were loaded as shown in Figure 22 after fatigue precracking. Specimen deflection was monitored with a linear voltage differential transducer (LVDT); these readings were then converted to crack length - stress intensity data. The test solutions were automatically metered to the crack--previously used methods of manually introducing solution at certain intervals (Ref 6) gave erratic results due to excessive drying overnight and on weekends.

VI. RESULTS AND DISCUSSION

A. SMOOTH SPECIMEN TESTS

1. LABORATORY ENVIRONMENT

The results for the 6-month exposure of tensile-type short-transverse specimens to alternate immersion in synthetic seawater are summarized in Tables IX and X for the 1.25-in. and the 3.0-in. plates, respectively. As expected, early failures occurred in all the susceptible control materials. 7075-T651 plates of both thicknesses failed in short times at 103 MPa (15 ksi) and 172 MPa (25 ksi) stress levels. Specimens stressed at 34 MPa (5 ksi) did not fail in the 6-month exposure period. The 1.25-in. 7075-T7651 plate failed at stresses as low as 172 MPa (25 ksi)--over 100 days; the corresponding 3.0-in. material survived at 172 MPa (25 ksi), but failed at 241 MPa (35 ksi). It is noteworthy that tests at stress levels of 172 and 310 MPa (25 and 45 ksi) clearly distinguished the three 7075 tempers within 2 weeks of exposure time.

All the -T73 temper plates survived 30 days at stress levels of 310 MPa (45 ksi) and below. The only materials failing in less than 30 days at 379 MPa (55 ksi) were 1.25-in. 7075 and 3.0-in. 7049 in the minimum-aged condition.

Among the minimum-aged 1.25-in. thick -T73 temper materials, only 7049 survived the total 6-month exposure at 310 and 379 MPa (45 and 55 ksi) stress levels. Of the typical -T73 temper plates, only 7050 did not survive the total exposure at these stress levels (it was the strongest material, however).

Metallographic examination of the specimens showed little general pitting corrosion, and only a few secondary intergranular stress corrosion cracks. Cases where intergranular attack was noted are indicated in the summary tables.

The stress-corrosion results for the 1.25-in. thick plates are represented graphically in Figure 23 on the basis of a pass/fail (100 days at 310 MPa) criterion.* At approximately equal strength levels, both 7050-T7365l and 7049-T7351 appear to have somewhat better stress corrosion resistance (SCR) than the 7X75-T7351 materials. We also note that these alloys had yield strengths above the minimum value for 7075-T651 (426 MPa).

In the 3.0-in. thickness, minimum-aged 7475 and 7049 did not survive the 6-month exposure (Table X). However, at equal strength levels both 7050-T7365l and 7049-T7351 again appear superior to 7075. The minimum-aged materials, for example, were stronger than 7075-T7651, yet had better SCR. These plates also had higher yield strengths in the typical condition than the 420 MPa minimum for 7075-T651.

These points are emphasized further in the survival rate (100 days at 310 MPa) curves shown in Figure 24. Data for the 7075 and 7475 plates fit the same pattern, showing well-defined "critical" yield strength levels at which SCR dropped sharply: about 480 and 450 MPa (70 and 65 ksi) for the 1.25 and 3.0-in. thick materials, respectively. For these particular test conditions, critical strengths for the corresponding 7050 and 7049 plates were obviously higher than these values, but the data were insufficient to estimate absolute levels.

There were no long-transverse failures in any of the -T73 temper materials at 310 and 379 MPa (45 and 55 ksi) stress levels (Table XI). The only failures in this orientation occurred in the 3.0-in. thick 7075-T651 plate stressed to 379 MPa (75% of the LT yield strength).

*Graphical representation is for the particular arbitrary test conditions indicated; different criteria could give different rankings.

2. MARINE ATMOSPHERE

As Tables XII and XIII show, short transverse failures in specimens exposed at Daytona Beach, Florida occurred in the relatively susceptible 7075-T651 and 7075-T7651 control materials and in the highly stressed (310-379 MPa) 1.25-in. 7050-T7365l and 7049-T7351 plates. At stress levels of 172 MPa (25 ksi) and higher, failure times for the control materials were <2.3 months and <6.9 months for the 1.25-in. and 3.0-in. plates, respectively. The 7049 and 7050 specimens failed in 8.9 months at 310 MPa (45 ksi). For 7050 these results confirm the long-term laboratory failures (>125 days) for the same material; there were no laboratory failures in the 7049 plate in 180 days of testing.

The results to date are not in agreement with a previous comparison of web-flange-type die forgings in which the calculated critical strength of 7049 was reported by Staley to be about 40 MPa (6 ksi) lower than that of 7050 (Refs 13 and 25). Although it is possible that marine and industrial atmospheres could give different rankings, misleading conclusions can be drawn if such comparisons are not made at the same time and at equal strength levels.*

As in the laboratory tests, failures in the long-transverse direction occurred only in the 3.0-in. 7075-T651 plate stressed at 379 MPa (55 ksi).

All the marine atmosphere tests will continue for an indefinite time period, and results will be reported on a biannual basis.

*The same program showed that in the 30-day alternate immersion test (3-1/2% NaCl) 7049 equaled or exceeded the performance of similar 7050 forgings.

B. PRECRACKED SPECIMEN TESTS: CONSTANT DEFLECTION SPECIMENS

1. CRACK LENGTH MEASUREMENTS

Crack extensions as determined on bolt-loaded specimens for the total test period in each environment (marine atmosphere, synthetic seawater, salt-chromate solution) are listed in Tables XV (SL orientation) and XVI (TL orientation).* Estimates based on edge measurements and lengths measured at the 1/4w location on the fracture surface are given. The fracture surface lengths were related back to the original (precracked) edge measurements for specimens tested at Daytona Beach and in synthetic seawater, because general corrosion occurring over the 6-month exposure period made it impossible in most cases to tell where the precrack ended and stress corrosion began. Since the cracks were bowed (see Section VI.B.4), the lengths based on these fracture surface measurements tend to overestimate actual crack extension. Nevertheless, agreement between the two measurements was quite good.

In a few instances, the actual presence of stress corrosion cracking was questionable according to visual examination of the surface morphology (see Appendix E for fracture surface examination and metallographic cross sections). Specimens from the 3.0-in. 7075 and 7475-T7351 plates tested at Daytona Beach and in synthetic seawater, for example, did not appear to have any significant stress corrosion crack growth (edge measurements indicated only 0.5 to 1 mm of crack extension--probably due to pitting attack).

*Crack extensions by themselves are representative only for the particular specimen used. They are also dependent on the initial stress intensity. A more rigorous assessment of crack growth behavior is given in a subsequent section on crack velocity - stress intensity relationships.

A feature of interest in the TL-oriented specimens was the presence of numerous small cracks in the short-transverse plane (normal to the precrack surface) on all specimens from the 1.25-in. plates and on specimens from the 3.0-in. 7050 and 7049 plates. These cracks extended 0.5-1.0 mm beyond the measured crack tip, and were slightly longer in 7075-T651 than in the -T73 temper materials. If they are in fact stress-corrosion cracks (and their intergranular nature suggests that they are), the usefulness of crack growth measurements and subsequent stress intensity values for the TL specimens is questionable.

The crack length measurements reveal a number of qualitative factors:

1. the typical -T73 temper materials were much more resistant than the 7075-T651 and 7075-T7651 control materials;
2. the 3.0-in. thick plates were more resistant than the corresponding 1.25-in. materials;
3. the "typical" -T73 temper condition was considerably more resistant than the minimum-aged condition;
4. at comparable yield strengths of 475 to 500 MPa, all 1.25-in. thick plates underwent about the same amount of crack extension;
5. crack extensions (SL orientation) in the 1.25-in. plates were considerably greater for the salt-chromate exposure than for the atmospheric and synthetic seawater environments;
6. crack extensions in the 3.0-in. materials were about the same in all three environments; and
7. as expected, the TL orientation was much more resistant than the SL orientation.

The foregoing results are for specimens containing mechanical pop-in precracks; SL specimens from the 1.25-in. plates (typical -T73 temper only) were also tested after fatigue precracking. A comparison of edge and fracture surface measurements for these specimens is shown in Table XVII. In cases where little crack growth was observed, as in the synthetic seawater environment, negative values are reported. This is because the fatigue precracks lead at the specimen edges (probably due to a notch effect at the side grooves). Consequently, the crack front in the center of the specimen has to "catch-up" to the initial reference location at the specimen edge. Once this occurs, the stress corrosion crack then usually assumes a bowed shape, leading in the center.

Crack extensions in the fatigue precracked specimens were generally somewhat less than those observed in the specimens having pop-in precracks. This is not unexpected, however, because the initial stress intensities were lower in the former specimens, i.e., 80-90% of K_{Ia}. As with the pop-in precrack, crack growth in these 1.25-in. thick plates was much more extensive in the salt-chromate solution than in synthetic seawater or at Daytona Beach.

Crack lengths for the total exposure time can alternatively be expressed in terms of a change in stress intensity (difference between initial and residual values) or an average crack velocity. These values are listed in Tables XVII to XX for the three environments. Combining these values (crack velocity over a certain stress intensity range) allows a more realistic comparison of stress corrosion resistance than crack length alone. These relationships will be discussed further in a subsequent section.

We nevertheless made an effort to compare the alloys on a stress intensity change basis by dividing ΔK by K_{Ia}. This was an attempt at normalization to allow for the dependence of ΔK on K_{Ia}.

(Since crack velocity is normally a function of stress intensity, ΔK increases with increasing K_{Ia}, all other factors being equal.) Figures 25 to 27 show $\Delta K/K_{Ia}$ vs. yield strength plots for each of the environments. For the Daytona Beach and synthetic seawater exposures, all the data fell on one general curve, with no obvious indication of an alloy or plate thickness effect, i.e., the factor $\Delta K/K_{Ia}$ seems to be dependent only on yield strength level. Data for the salt-chromate test fell on two curves, one for each plate thickness, the thinner material appearing much more susceptible for a given strength level. Again, no significant alloy effect was evident.

2. CRACK LENGTH VS. TIME

Crack lengths were measured at the edges of the bolt-loaded specimen on an approximate logarithmic basis of 1 day, 2 days, 4 days, 1 week, etc. Representative data for each environment are expressed as the form of length vs. exposure time plots. However, as mentioned previously, crack lengths for a given exposure time are dependent on specimen geometry and K_{Ia} levels. A more rigorous treatment of the time dependency of crack length is given in Section VI.B.3.

a. Marine Atmosphere

Figure 28 shows crack length vs time curves (SL orientation) for the 1.25 and 3.0-in. 7075 plates. The 1.25-in. -T651 material, in particular, shows the characteristic rapid crack growth at early exposure times (high stress intensity) followed by decreasing crack growth rate (decreasing stress intensity). There was an indication of abnormally fast crack growth in both -T6 plates over the last examination period. This could be due to the beginning of exfoliation and/or corrosion product wedging, common effects found in DCB specimens from alloys such as 7075-T6. It

could also reflect seasonal changes in temperature and humidity--longer exposure times are necessary to determine if "breakaway" is occurring.

Crack length-time curves for the -T73 temper materials (Fig. 29) showed a considerable amount of scatter between the triplicate specimens, especially for early exposure times. Agreement for the 6.5-month examination period, however, was fairly good. It is apparent that 7050 was influenced by an incubation factor. Crack growth for the first month was very slow, but from then on it seemed to accelerate.

b. Synthetic Seawater

Crack growth curves for the 7075 materials (Fig. 30) were similar to those obtained at Daytona Beach, except crack extension appeared to be more rapid in the early stages of exposure. As in the Daytona Beach exposure, crack growth was more extensive in the thinner plates. Crack growth in the -T73 temper was very slow; no crack growth occurred in the 3.0-in. material over the 6-month exposure period (in excellent agreement with the Daytona Beach results).

Figure 31 shows crack length vs. time curves for all the 1.25-in. thick typical -T73 temper materials. There appeared to be less scatter between replicate samples than at Daytona Beach (cf. Fig. 29). There again was evidence of an incubation period, especially notable for 7475, after which the crack growth rate increased with time, and then finally began to level off.

Reasons for an incubation period in the resistant materials are not obvious. It could be due to the zone of plastic deformation ahead of the crack tip, or it may be related to a slow transition process by which the stress corrosion crack develops from

the mechanical precrack. The latter type of crack is at least partly transgranular, whereas the former is intergranular. For a stress corrosion crack to initiate, therefore, it first must "find" an intergranular crack plane. This requires either transgranular stress corrosion (an extremely slow process) or a mixed mode of intergranular stress corrosion and mechanical rupturing of remaining ligaments (see Appendices E and F). Either mechanism would account for abnormally slow crack growth in the initial stages of testing.

c. Salt-Chromate Solution

Figure 32 shows crack extension curves for the 7075 plates tested in the salt-chromate solution (continuous immersion). Curves for the -T6 and -T76 tempers were similar to those obtained in the other environments. Also, as in the Daytona Beach and synthetic seawater tests, there was no crack growth in the 3.0-in. thick typical -T73 temper plate. Crack growth in the 1.25-in. thick -T73 temper materials, however, was much more extensive than in the other environments, approaching that obtained in 7075-T7651.

Six replicate specimens were tested for the 1.25-in. thick typical 7075-T7351 temper plate. As Figure 33 shows, agreement between the replicates was quite good. These curves also show an incubation effect; crack growth was very slow during the first 2 weeks of testing, and then it increased. Crack growth curves for the other alloys were similar to those of 7075 (Fig. 34).

Figure 35 shows crack growth curves for fatigue-precracked specimens tested in salt-chromate solution. Incubation times were even more evident for these specimens than those with pop-in precracks. It is unlikely therefore that incubation effects are related to the zone of plastic deformation ahead of the crack tip. The concept of a transition barrier for the propagation of a stress corrosion crack from a mechanical crack is more probable. Since

fatigue precracks are predominantly transgranular (more so than a pop-in precrack), stress corrosion is initially retarded until an intergranular path is established. The lower initial stress intensity could also affect the incubation time of a fatigue precrack compared to a pop-in precrack, i.e., a lower driving force for overcoming the transition barrier.

3. CRACK VELOCITY - STRESS INTENSITY RELATIONSHIPS

The data presented in the previous sections are not generalized--crack length vs. time relations are dependent on the geometry of the specimen, particularly the beam height. The length of the precrack and the magnitude of K_{Ia} also have an effect. A more rigorous evaluation involves analyzing the crack-front velocity in terms of the stress intensity at the crack tip. Appendix A gives a general description of crack velocity vs. stress intensity (V-K) plots.

Curve fitting methods have been proposed for determining crack velocities (derivative of crack length vs time plots), but this procedure does not work well for materials that are resistant to stress corrosion. Reference to Figures 28 and 29, for example, shows that curve fitting would be relatively straightforward for 7075-T651, but rather difficult for the -T73 temper materials. Although some of the crack length-time data (Figs. 29, 31 and 34) could perhaps be construed as having linear relationships (velocity independent of stress intensity), we have plotted crack growth rates as obtained from crack length changes over definite time increments versus the average calculated stress intensity for that time period.

a. Marine Atmosphere

V-K plots for the 1.25-in. thick 7075 plates shown in Figure 36 reveal the expected behavior: much higher crack growth rates at a given stress intensity for the -T6 material than for the -T73 temper, with the -T76 temper having an intermediate velocity. The V-K relationships for all four 1.25-in. -T73 temper alloys are compared in Figure 37 (data are based on three specimens per alloy). Alloys 7075, 7475, and 7049 show similar behavior; a good data fit for these alloys is also evident. The 7050 data were more scattered, and exhibited a somewhat higher average velocity for a given stress intensity (7050 was also stronger than the other materials, however--477 MPa yield strength vs 462 MPa for 7049 and 420-430 MPa for 7075 and 7475). The reason for scattered behavior in the 7050 plot is evident in the crack length vs. time curve for the alloy (Fig. 29). There appears to be an incubation time involved for appreciable crack growth; this leads to an inverse type of V-K relationship.

The V-K data for the 3.0-in. 7075 materials are shown in Figure 38. Crack growth rates were slower than in the corresponding 1.25-in. plates. In fact, 3.0-in. 7075-T7351 did not appear to undergo any stress corrosion (nor did 7475-T7351). Figure 39 gives V-K information for the 3.0-in 7050-T73651 and 7049-T7351 materials. Data for 7049 are limited, but the two alloys seem to be quite comparable. The larger specimen size (75 mm high vs 25 mm) appeared to give a lower velocity for a given stress intensity, but this was probably due to a slightly lower apparent initial K_{Ia} in the 75 mm specimens (see Table D2 in Appendix D).

Crack growth in specimens having fatigue precracks seemed to be occurring at lower stress intensities than in those with pop-in precracks. This may be related to the greater amount of plastic deformation associated with a pop-in crack. Pop-in cracks are

also more ragged, leading to stress corrosion cracks that are not well confined to a single short-transverse plane (see Appendixes E and F); this leads to an effective stress intensity, lower than the apparent (measured) value. This finding is in direct contrast to that of Sprowls et al. (Ref 7) in which pop-in precracks showed more crack extension. The DCB specimens used in that study were not side grooved, however; consequently, stress intensities were considerably greater in the samples containing pop-in precracks.

V-K data for the TL orientation are given in Figures 40 and 41. Although these data are limited due to the lack of extensive crack growth, it is apparent that the -T6 temper is less resistant than the -T73 temper. In fact, the resistance of the -T6 temper in the TL orientation is approximately the same as that of the -T73 temper in the SL orientation. For the 1.25-in. thickness, the 7050 plate seemed somewhat more susceptible than the 7475 and 7049 alloys. As mentioned previously, the significance of V-K data for the TL orientation is uncertain in view of the secondary (and leading) SL cracking in these specimens.

b. Synthetic Seawater

V-K plots (SL orientation) for the 1.25-in. 7075 plates (Fig. 42) show the same general behavior as noted in the atmospheric tests. As the alloy comparison in Figure 43 shows, all four 1.25-in. -T73 temper plate materials had fairly similar V-K behavior. However, in view of their higher strength levels, 7050 and 7049 may have an advantage over the 7X75 materials. Is is again apparent that the fatigue precracked specimens undergo crack extension at somewhat lower apparent stress intensities than those with pop-in precracks.

V-K plots for the 3.0-in. thick plates are shown in Figure 44. For 7075, all the 3.0-in. plates had greater resistance to crack

propagation than the corresponding 1.25-in. thick plates. Of the 3.0-in. thick -T73 materials, only 7050 and 7049 showed crack growth in the SL orientation. There did not appear to be any significant difference between the two alloys.

V-K data for the TL orientation* are given in Figure 45. The data for the -T6 and -T76 tempers seem to fall within a general band lying between the SL curves for 7075-T7651 and 7075-T7351. The 3.0-in. thick -T6 material appeared to be somewhat more susceptible than the others, however. All the 1.25-in. -T73 materials showed some crack growth in the TL orientation, but were more resistant than in the SL orientation. It is interesting that the 7075-T7351 plate appears to have a similar crack growth rate to 7475-T7351, but at a much lower stress intensity. As in the SL orientation, 7050 and 7049 were the only 3.0-in. thick materials showing significant crack growth.

c. Salt-Chromate Solution

V-K plots for the 1.25-in. thick -T6, -T76 and -T73 7075 plates are shown in Figure 46. The curves for the -T6 and -T76 materials are similar to those tested at Daytona Beach and in synthetic seawater, but the -T73 temper had faster crack growth rates at much lower stress intensities than in the other two environments. There was also an inverse relationship evident at high stress intensities (initial stages of test) which is probably an incubation effect. As Figure 47 shows, the other 1.25-in. materials also had relatively fast crack growth rates over a fairly wide stress intensity range. The minimum-aged materials naturally had faster crack growth rates than the typical -T73 temper conditions, their curves approaching that of 7075-T76 in most cases. It is also noteworthy that tendencies toward plateau velocities

*Results refer to in-plane crack growth only, not the perpendicular SL oriented cracking.

were more evident in the salt-chromate solution that in the other environments.

V-K curves for the fatigue-precracked specimens (Fig. 48) show definite inverse relationships due to the marked incubation times for these specimens. Different curves were also obtained from one specimen to another, depending on the initial stress intensity. In specimens loaded to about 90% of K_{Ic}, crack growth was intially slower for a given stress intensity than for those containing a pop-in precrack (due to stronger incubation effect). At longer exposure times crack growth rates appeared to reach a maximum at velocities above those obtained with pop-in precracks. It appears, therefore, that initial crack growth rates in specimens containing fatigue precrack are relatively slow (difficult transition from transgranular crack to intergranular stress corrosion crack), but once the incubation period is over, crack growth rates are faster than in specimens containing pop-in precracks. As postulated previously, this latter phenomenon could be related to the morphology of the stress corrosion cracks. Since fatigue precracks are smoother and more planar than pop-in precracks, this surface characteristic can be extended to the propagating stress corrosion crack as well--at least during the initial few millimeters of crack extension (see Appendix F). This would allow stress corrosion to proceed at a lower apparent stress intensity. Another possible factor is the extent of microbranching, which is expected to be less for lower initial stress intensities (Ref 26). This would result in crack growth at lower apparent stress intensities for fatigue-precracked specimens (Ref 27).

Contrary to the results for the 1.25-in. plates, crack growth rates for the 3.0-in. thick plates in the salt-chromate solution were comparable to those obtained in the other environments (Figs. 49 and 50). Crack growth rates in the minimum-aged alloys

were considerably faster than in the typical -T73 temper condition. We note, however, that the crack velocities in minimum-aged 7050 and 7049 were lower than those in 7075-T7651--and at higher strength levels (yield strengths of 475 and 481 MPa, respectively, vs. 460 MPa).

d. Comparison of Environments

A comparison of V-K plots for the 1.25-in. 7075 plates in the three environments is shown in Figure 51. For the -T6 temper, crack growth at Daytona Beach was considerably slower than in the laboratory tests; however, the relative difference for the -T76 temper appears dependent on the stress intensity. At low K levels, for example, the salt-chromate solution seems to give relatively high crack velocities, but at high stress intensities artificial seawater appears more aggressive.

For the -T73 temper, synthetic seawater and the marine atmosphere gave similar results, but crack growth in the salt-chromate solution was much more rapid than in the other environments. This difference was not nearly as great in the 3.0-in. materials, however.

4. K_{Iscc} ESTIMATES

The stress intensity at which crack velocities decrease to 1×10^{-5} in./hr (7×10^{-11} m/sec) or less is often taken to be the "threshold" stress intensity value (K_{Iscc}). Depending on the patience of the investigator, it becomes difficult to demonstrate that a crack is moving at velocities much less than this rate. Table XXI gives estimated values of K_{Iscc} for all the alloys in each of the environments as determined with specimens having pop-in precracks. In many cases we were able to establish only a minimum or maximum value, and in some instances bracket K_{Iscc} between two values.

The data are presented in graphical form as K_{Iscc} vs. yield strength plots in Figures 52 to 56. There appeared to be an inverse linear relationship between yield strength and K_{Iscc} as established in all environments (analogous to K_{Ic} - strength relations). In general, the SL data points for 7075 and 7475 tended to fall on the same trend line. K_{Iscc} values for 7050 and 7049, however, were about 3.5-6 MPa$\sqrt{m}$ (3-5.5 ksi$\sqrt{in.}$) higher than those for 7X75 at a given yield strength. There did not appear to be any significant difference between 7050 and 7049 at equal strength levels. In the TL orientation, there were no apparent alloy effects on K_{Iscc}. All materials fell into the same general data band.

Although it has been stated that general relationships between yield strength and K_{Iscc} do not exist for aluminum alloys (Ref 9), such relationships do apparently exist for the family of alloys evaluated in this study. Such a relationship is to be expected for 7075-type alloys in which overaging leads to a strength decrease in combination with an improvement in SCR. However, for alloys such as 2024, in which normal aging increases both strength and SCR, K_{Iscc} would be expected to increase with yield strength (as in aging from the -T3 to the -T8 temper).

For the Daytona Beach and synthetic seawater test, K_{Iscc} appeared to be independent of plate thickness (except as thickness affects strength). The 3.0-in. thick plates, however, had much higher K_{Iscc} values than the thinner plates according to the salt-chromate test. A "threshold" stress intensity was never attained for most of the 1.25-in. materials in the 6-month exposure period in this environment. With the exception of the 1.25-in. materials tested in salt-chromate solution, agreement between K_{Iscc} values as determined in each of the environments was quite good.

K_{Iscc} values estimated from fatigue-precracked specimen data were generally somewhat lower than those determined from specimens having pop-in precracks (see Table XXII). As discussed previously, the type of stress corrosion crack generated from a fatigue precrack seems to grow at lower stress intensities, at least during the first few millimeters of crack extension.

C. PRECRACKED SPECIMEN TESTS: CONSTANT LOAD SPECIMENS

Fatigue-precracked DCB specimens from the 3.0-in. plates of each alloy (typical -T73 temper only) were exposed under constant load conditions at stress intensities near K_{Ia} to both artificial seawater and salt-chromate environments for 60 to 90 days.

In the first series of tests, the samples were initially loaded to about 95% of K_{Ic} (the 7075 specimen tested with synthetic seawater corrodent was accidentally "popped" during loading--consequently the stress corrosion crack grew from a mechanical precrack, not a fatigue precrack). Crack growth rates as monitored with the linear voltage differential transducer (LVDT) system were so slow ($<10^{-10}$ m/sec) that the loads were increased until measurable crack extensions were obtained. Generation of meaningful V-K information was extremely difficult in these materials, however, because K_{Iscc} is so close to K_{Ic} (according to constant-deflection tests on pop-in precracks, K_{Iscc} in some cases is greater than K_{Ic}). A second set of specimens was then loaded to slightly lower stress intensities for 70 to 90 days. The specimens were broken open at test completion to confirm that little crack growth had taken place, thereby allowing an estimate of K_{Iscc} to be made.

Results of these tests are given in Table XXIII. One of the most noteworthy results was the occurrence of stable crack growth at apparent stress intensities above K_{Ic}--in one case 3 MPa$\sqrt{\text{in.}}$.

higher.* In view of the crack blunting and branching effects discussed earlier, this is not really unexpected.

Crack growth rates determined from crack opening displacement changes varied somewhat but did not appear to increase with increasing stress intensity over the ranges covered. Crack extension and stress intensity ranges calculated from crack measurements on the fracture surfaces compared reasonably well with those estimated from the LVDT measurements.

Crack velocities in the salt-chromate environment were about twice those in synthetic seawater for a given stress intensity. Unlike the synthetic seawater tests, all crack extension obtained in the salt-chromate environment was easily identified as stress corrosion by examination of the fracture surfaces.

The V-K data generated from this loading method are compared in Figures 57 and 58 to that obtained from the bolt-loaded (constant deflection) specimens containing pop-in precracks. In most cases the agreement was good. The 7075 and 7475 plates, however, appeared somewhat more susceptible in the constant load test.

K_{Iscc} estimates from the constant-load tests are given in Table XXV and compared to the values estimated from the constant-deflection (pop-in precrack) tests. As would be expected from the similarity between the V-K data for the two test methods, K_{Iscc} levels were quite comparable. There was a trend to lower values for the fatigue precracks as there was in the bolt-loaded, fatigue-precracked specimens from the 1.25-in. plates (cf. Table XXII).

Another feature of these results is the apparent advantage of 7475 over 7075 (K_{Iscc} difference of about 4 MPa$\sqrt{m}$). This

*In breaking these specimens open, apparent stress intensities up to 6 MPa$\sqrt{m}$ higher than true K_{Ic} were observed (see Table XXIV).

effect was not evident in specimens from the 1.25-in. plates when tested under constant deflection conditions with both fatigue and pop-in precracks. Both 3.0-in. thick materials also appeared similar in the constant-deflection, salt-chromate test (no crack growth was observed in either alloy when tested in synthetic seawater or at Daytona Beach).

D. COMPARISON WITH PREVIOUS WORK

V-K plots from previous investigations and summary reports are given in Appendix A. As noted, comparisons are difficult, especially for -T73 type temper materials due to the lack of data. There is also the problem of SCR dependency on product form, strength level, and test conditions. Moreover, in some cases data are "averaged" and exact thermal treatment conditions and strength levels are not known.

Nevertheless, the previous investigations indicate that K_{Iscc} values for 7075-T651 range from 3 to 7 MPa$\sqrt{m}$ in 3-1/2% NaCl, 6.5 MPa$\sqrt{m}$ in salt-chromate solution, and 5.5 MPa$\sqrt{m}$ in an industrial atmosphere. On bolt-loaded specimens containing pop-in precracks, we obtained values of 4 to 9 MPa$\sqrt{m}$ for 1.25-in. plate (522 MPa yield strength) and 8 to 12.5 MPa$\sqrt{m}$ for 3.0-in. plate (500 MPa yield strength). In similar environments, K_{Iscc} values of 20.5 to 28 MPa$\sqrt{m}$ are indicated for 7075-T7351, compared to our values of 22.5 MPa$\sqrt{m}$ for 1.25-in. thick plate (429 MPa yield strength) tested in synthetic seawater and at Daytona Beach.* For 3.0-in. plate we obtained minimum values of 25 MPa$\sqrt{m}$ for 7075-T7351 and 29.5 MPa$\sqrt{m}$ for 7475-T7351 (382 and 384 MPa yield strengths, respectively).

*For the 3.0-in. thick plates our tests in salt-chromate solution gave comparable K_{Iscc} values to those established in synthetic seawater and at Daytona Beach. Salt-chromate gave much lower values for the 1.25-in. materials, however.

For 7050-T73651, a K_{Iscc} value of 25.5 MPa$\sqrt{m}$ has been reported for an industrial atmosphere (Ref 9). This compares favorably with values of 19.5 to 27 MPa$\sqrt{m}$ as determined in synthetic seawater and at Daytona Beach. Another report (Ref 28) showed a 4.0-in. thick 7050-T73651 plate (≃440 MPa yield strength) to have a K_{Iscc} of about 22 MPa$\sqrt{m}$ as determined on ring-loaded fatigue-precracked specimens in a NaCl environment. We obtained a value of 26.5 MPa$\sqrt{m}$ on 3.0-in. thick plate (430 MPa yield strength); the corresponding value for a fatigue precrack would probably be slightly lower.

K_{Iscc} values below 11 MPa$\sqrt{m}$ have been reported (Ref 9) for 7049-T73 die forgings tested in NaCl solution and an industrial atmosphere. It is unlikely that this particular sample was properly aged to the -T73 temper, however, because K_{Iscc} values in the present evaluation were about 24 MPa m for both synthetic seawater and marine atmosphere environments.

In no cases were plateau velocities observed as idealized in Appendix A, Figure A1, or as reported previously (Fig. A3). Trends towards stress intensity independent velocities were evident, however, in the more susceptible materials, especially when tested in the salt-chromate solution. The salt-chromate environment also produced relatively flat V-K curves for the 1.25-in. thick -T73 temper materials. The reason for the presence or absence of ideal Region II behavior (velocity independent of stress intensity) may be in the method of data analysis. Most previous methods of generating V-K plots have been based on curve fitting crack length-time data; a straight line drawn through the initial points naturally gives an ideal plateau velocity. We determined crack velocities for each time interval between measurements of crack length, and assigned to that velocity the average stress intensity over the time interval.

The fact that plateau velocities were not observed in the -T73 temper materials is not really surprising. As pointed out by Brown (Ref 29), alloys of relatively high resistance experience crack growth only at stress intensity levels near K_{Ic}, and do not demonstrate a clearly defined plateau value.

A particular area of interest from a mechanistic viewpoint is the functional dependence of crack growth rate on stress intensity. A number of stress corrosion theories, for example, predict a K^2 relationship; such a dependence has also been observed experimentally (Ref 30). Plots of ln V vs. ln K for the 1.25-in. thick 7075-T651 plate, however, reveal exponents of 4 to 16 (Fig. 59). A K^2 relationship was observed only in the transition between Regions I and II for the salt-chromate test. The exponent also varied from one material to another for a given test environment. As Figure 60 shows, the crack velocity of the 3.0-in. thick 7075-T651 plate was proportional to K^{6-7} in synthetic seawater and the salt-chromate solution. The exponent for the 1.25-in. thick 7075-T7651 material varied from 5 in the salt-chromate environment to 7 in synthetic seawater. It is apparent that a theory involving a unique functional dependence of crack velocity on apparent stress intensity does not exist for all thicknesses, thermal treatments and test conditions, even for the same alloy.

The previously established exponent of 2 (Ref 30) was determined by loading fatigue-precracked specimens to a series of incremental stress intensities and measuring the crack extension over a certain time period. Any incubation effects could therefore have influenced the results, especially since the incubation time is probably inversely dependent on the initial stress intensity.

Speidel (Ref 31) suggests that V-K results can best be represented by an equation of the form

$$V = A \exp(BK),$$

but as the semilogarithmic plots for 7075-T651 in Figures 42 and 46 indicate, this formalism may not be correct either. Figures 59 and 60 suggest that an equation of the form

$$V = CK^n$$

may be more appropriate (but where n is not restricted to the value 2).

In any case, theoretical arguments based on measured stress intensities are tenuous at best, because crack branching and blunting can lead to apparent stress intensities that are higher than the effective values (Ref 27). It is also possible that the extent of crack branching and blunting depends on the type of test, i.e., decreasing or increasing K. Another complicating factor is the possibility of corrosion product wedging (probably minimal in chromate-containing environments), the effects of which are impossible to assess quantitatively. Stress intensities measured in a stress corrosion test should therefore be considered as phenomenological parameters only, useful for comparing alloys and tempers under a particular set of experimental conditions.

VII. SUMMARY AND CONCLUSIONS

From this evaluation of plate products in the thickness range 1.25 to 3.0-in. we conclude that:

1. For a given strength level, alloys 7050 and 7049 have short-transverse stress corrosion resistance (SCR) superior to that of 7075 and 7475. 7050-T73651 and 7049-T7351, with typical strength levels above 7075-T7651 minimum, have significantly better SCR than 7075-T7651 although they are not in the "virtually immune" category of 7075-T7351.

2. At equal strength levels, there are no significant differences in short-transverse SCR between 7050 and 7049. At a long-transverse yield strength of 450 MPa (65.3 ksi), for example, both 7050 and 7049 have K_{Iscc} (SL orientation) values of about 24 MPa$\sqrt{m}$ (22 ksi$\sqrt{in.}$) as determined in synthetic seawater and in a marine atmosphere (vs. 18-19.5 MPa$\sqrt{m}$ for 7X75 at this strength level).*

3. Results from precracked specimen tests are in good qualitative agreement with those from smooth specimens. In addition to providing useful information about crack growth rates, however, precracked specimen tests have the additional advantage of giving a rapid assessment of a material's relative susceptibility. In test times as short as 1 to 2 days, for example, susceptibility associated with the -T6 temper can be easily identified; potential also exists for clear separation of -T76 and -T73 tempers in short test times (a week or less).

*As determined on bolt-loaded specimens containing pop-in precracks.

4. For synthetic seawater and marine atmosphere tests, K_{Iscc} values are a unique function of strength level (inverse relationship) and are not significantly affected by plate thickness, per se. Thickness effects are obvious in the salt-chromate solution, however. When tested in this media, the thicker plate showed similar behavior to that obtained in the other environments, but the thinner material underwent quite rapid crack growth, never approaching a "threshold" value over the 6-month test period.

5. Stable crack growth in stress corrosion environments is possible at apparent stress intensity levels well above K_{Ic}. Fatigue precracked specimens exposed to synthetic seawater and salt-chromate solutions, for example, were mechanically "popped" at stress intensities up to 6 $MPa\sqrt{m}$ above K_{Ic}.

6. Precracked specimens from fairly resistant materials reveal incubation periods during which initial crack growth is very slow. It is postulated that the incubation period is related to a transition barrier in which an intergranular stress corrosion crack develops from a predominantly transgranular mechanical precrack. The more susceptible the material, the faster this process is; and, in -T6 temper material incubation effects are not observable.

7. Incubation periods are more obvious in specimens containing fatigue precracks than in those having pop-in precracks. Two reasons for this behavior are: (1) initial stress intensities (driving force for crack extension) in the former are lower, and (2) transition barrier for a fatigue precrack involves the initiation

of an intergranular stress corrosion crack from a transgranular crack, whereas a pop-in crack is at least partially intergranular.

8. Once incubation periods are over, stress-corrosion cracks grow at lower apparent (measured) stress intensities in specimens containing fatigue precracks than in those with pop-in precracks. This effect is related to the difference in morphology of the stress corrosion crack generated in each case. Fatigue precracks generate relatively planar stress corrosion cracks, whereas those grown from pop-in precracks are non-planar, containing jogs and unfailed ligaments. The latter probably requires a higher stress intensity for crack propagation. Moreover, the average stress intensity acting at the crack tip is probably closer to the apparent (measured) value for the fatigue-precracked specimen; the ragged nature of the stress-corrosion crack generated by the pop-in precrack causes the actual stress intensity to be overestimated.

9. In view of the crack morphologies noted above, apparent (measured) stress intensities are likely to be higher than the average values acting at the corroding crack tip. Comparisons of theoretical crack velocity - stress intensity behavior to measured relationships may therefore be somewhat tenuous, but this does not detract from the usefulness of such information from a practical viewpoint.

10. In the TL orientation, all alloys have approximately equal K_{Iscc} values for a given strength level. However, stress corrosion crack growth in TL oriented DCB specimens proceeds primarily in a plane normal to the precrack.

Numerous SL-oriented cracks lead the TL stress corrosion crack (if any) by about 1 mm (for a 6-month exposure). These secondary cracks could be generated by a combination of residual stress and a transverse tensile stress ahead of the crack tip. The length of these cracks appears to be limited to the approximate size of the plastic zone. Cracks in the -T6 temper material, for example, are not much longer than those in the resistant -T73 temper.

11. A simple bolt-loaded DCB specimen has promise as a practical alternative to those now used for routine fracture toughness testing of high-strength aluminum alloys. Although machining costs may be no less, the specimens do not have to be fatigue precracked--nor is a tensile machine needed. All that is required is a clip-in extensometer with electronic display and a visual measurement of crack length.

VIII. RECOMMENDATIONS FOR FURTHER WORK

1. All specimens presently on exposure at the Daytona Beach atmosphere site will remain in test for at least 6 years. At the same time, however, additional samples of the newer 7000 series alloys should be put on exposure as material (plate and extrusions) of various section sizes becomes available from routine production. Samples from the 2000 alloy series, such as 2124 and 2048, should also be included.

2. Tests using bolt-loaded DCB specimens have potential for rapid screening and quality control checks of stress corrosion resistance. A simple crack length measurement after 2 days of exposure is capable of clearly separating the susceptible -T6 temper from the resistant -T73 temper. Further work is required, however, to optimize the test conditions (solution chemistry, temperature, specimen geometry) in order to discriminate between materials having intermediate to good SCR in both the 2000 and 7000 alloy series. The results of a study to develop a rapid test for smooth specimens (Ref 33) indicate that elevated temperature salt-chromate solutions hold promise.

REFERENCES

1. J. V. Luhan and T. J. Summerson, "Development of 7049-T73 High-Strength, Stress-Corrosion Resistant Aluminum Alloy Forgings," Metals Engineering Quarterly, 10, No. 4, p. 35 (1970).

2. J. T. Staley and H. Y. Hunsicker, "Exploratory Development of High-Strength, Stress-Corrosion Resistant Aluminum Alloy for Use in Thick Section Applications," Technical Report, AFML-TR-70-256, November 1970.

3. P. C. Paris and G. C. Sih, "Stress Analysis of Cracks," Fracture Toughness Testing and Its Application, ASTM STP 381, p. 30 (1965).

4. W. F. Brown and J. E. Srawley, "Plain Strain Crack Toughness Testing of High-Strength Metallic Materials," ASTM STP 410, (1966).

5. B. F. Brown and C. D. Beachem, "A Study of the Stress Factor in Corrosion Cracking by Use of the Precracked Cantilever Beam Specimen," Corrosion Science, 5, p. 745 (1965).

6. M. V. Hyatt, "Use of Precracked Specimens in Stress-Corrosion Testing of High-Strength Aluminum Alloys," Corrosion, 26, p. 487 (1972).

7. D. O. Sprowls, M. B. Shumaker, and J. D. Walsh, "Evaluation of Stress-Corrosion Cracking Susceptibility Using Fracture Mechanics Techniques," Contract No. NAS8-21487, Final Report - Part I, May 31, 1971.

8. M. V. Hyatt and M. O. Speidel, "Stress-Corrosion Cracking of High Strength Aluminum Alloys," Boeing Report D6-24840, June 1970.

9. M. O. Speidel, "Stress Corrosion Cracking of Aluminum Alloys," Metallurgical Transactions, 6A, p. 631 (1975).

10. Aluminum Standards and Data, The Aluminum Association, p. 62-64, 1974-75.

11. Ibid., p. 65.

12. J. T. Staley, H. Y. Hunsicker, and R. Schmidt, "New Aluminum Alloy X7050," ASM Metal Congress and AIME Fall Meeting, Detroit, Oct. 18-21, 1971.

13. J. T. Staley, "Comparison of Aluminum Alloy 7050, 7049, MA52 and 7175-T736 Die Forgings," Technical Report AMFL-TR-73-34, May, 1973.

14. P. L. Mehr, "Alcoa 7475 Sheet and Plate," Alcoa Green Letter, October, 1973.

15. J. M. Van Orden and D. E. Pettit, "Corrosion Fatigue Crack Growth in 7050-T7651 Aluminum Alloy Extrusions," 16th Structures, Structural Dynamics, and Materials Conference, Denver, May 1975.

16. T. S. Humphries and E. E. Nelson, "Synthetic Seawater--an Improved Stress Corrosion Test Medium for Aluminum Alloys," NASA Technical Memorandum NASA TM X-64733, March 21, 1973.

17. Round Robin Tests of 7075-T6, -T7X and -T73, Aluminum Association-ASTM Committee G.01.06.91.

18. S. Mostovoy, P. B. Crosley, and E. J. Ripling, "Use of Crack-Line-Loaded Specimens for Measuring Plane Strain Fracture Toughness," J. Materials, 2, p. 661 (1967).

19. C. N. Freed and J. M. Krafft, "Effect of Side Grooving on Measurements of Plane Strain Fracture Toughness," J. Materials, 1, p. 770 (1966).

20. B. F. Brown, "The Application of Fracture Mechanics to Stress-Corrosion Cracking," Metallurgical Reviews, 13, p. 171 (1968).

21. D. O. Sprowls, J. D. Welsh, and J. W. Coursen, "Evaluating Stress Corrosion Crack Propagation Rates in High Strength Aluminum Alloys with Bolt-loaded Precracked DCB Specimens," Tri-Service Conference on Corrosion of Military Equipment, Dayton, Ohio, October, 1974.

22. R. G. Hoagland, "On the Use of the DCB Specimen for Determining the Plane Strain Fracture Toughness of Metals," J. Basic Engineering (ASME), 89, p. 525 (1967).

23. R. C. Dorward and K. R. Hasse, "Estimating K_{Ic} of High-Strength Aluminum Alloys from Crack Arrest (K_{Ia}) Toughness," J. Testing and Evaluation, to be published.

24. P. J. Blau and W. M. Griffith, "Measurement of Stress-Corrosion Cracks in Aluminum Alloy DCB Specimens Using an Ultrasonic Pulse-Echo Technique," Technical Report AMFL-TR-75-200, January, 1976. (See also Met. Trans., 7A, p. 463, 1976).

25. J. T. Staley, "Stress Corrosion Cracking in Aluminum Alloys," Metals Engineering Quarterly, 13, No. 4, p. 52 (1973).

26. M. O. Speidel, "Branching of Stress Corrosion Cracks in Aluminum Alloys," in The Theory of Stress Corrosion Cracking in Alloys, J. C. Scully, Editor, p. 345, NATO, Brussels, 1971.

27. I. M. Austen, R. Brook, and J. M. West, "Effective Stress Intensities in Stress Corrosion Cracking," International Journal of Fracture, 12, p. 253 (1976).

28. R. E. Davies, G. E. Nordmark, and J. D. Walsh, "Design Mechanical Properties, Fracture Toughness, Fatigue Properties, Exfoliation and Stress-Corrosion Resistance of 7050 Sheet, Plate, Hand Forgings, Die Forgings and Extrusions," Report N00019-72-C-0512 (Naval Air Systems Command), July, 1975.

29. B. F. Brown, "Stress Corrosion Cracking in High-Strength Steels and in Titanium and Aluminum Alloys," Naval Research Laboratory Report, ARPA Order No. 878, 1972.

30. W. E. Wood and W. W. Gerberich, "The Mechanical Nature of Stress Corrosion Cracking in Al-Zn-Mg Alloys, Parts I & II," Metallurgical Trans., 5, p. 1285 and 1295 (1974).

31. M. O. Speidel, "Current Understanding of Stress Corrosion Crack Growth in Aluminum Alloys," in The Theory of Stress-Corrosion Cracking in Alloys, J. C. Scully, Editor, p. 289, NATO, Brussels, 1971.

32. N. Levy, P. V. Marcal, W. J. Ostergren and J. R. Rice, "Small Scale Yielding Near a Crack in Plane Strain: A Finite Element Analysis," Intern. J. Fracture Mechanics, 7, p. 143 (1971).

33. W. J. Helfrich, "Development of a Rapid Stress-Corrosion Test for Aluminum Alloys," Contract No. NAS8-20105, Final Report, May 15, 1968.

Table I. Chemical Composition of Melts,* % by Wt.

Alloy	Si	Fe	Cu	Mg	Cr	Zn	Ti	Zr
7075	0.14	0.16	1.40	2.40	0.20	5.7	0.03	0.00
(AA Limits)	0.40	0.50	1.2-2.0	2.1-2.9	0.18-0.35	5.0-6.1	0.25	Ti + Zr
7475	0.06	0.10	1.45	2.15	0.20	6.0	0.02	0.00
(AA Limits)	0.10	0.12	1.2-1.9	1.9-2.6	0.18-0.25	5.2-6.2	0.06	0.05
7050	0.06	0.11	2.15	2.15	0.00	6.2	0.02	0.12
(AA Limits)	0.12	0.15	2.0-2.6	1.9-2.6	0.04	5.7-6.7	0.06	0.08-0.15
7049	0.06	0.10	1.55	2.50	0.14	7.7	0.02	0.00
(AA Limits)**	0.15	0.20	1.2-1.9	2.0-2.9	0.10-0.22	7.2-8.2	0.10	0.05

All other elements <0.005% each; <0.05% total

*Spectrographic analysis of melt buttons.

**Limits given are for 7149 (higher purity version of 7049).

Table II. Desired Yield Strengths and Electrical Conductivities for Minimum and Typical -T73X51 Temper Conditions

Alloy	Plate Thickness, in.	-T73X51 Temper	Elec. Condy, % IACS	Min. Yield Strength, ksi	Desired Yield Strength, ksi (MPa)
7075	1.25	Minimum	>38	57.0	67-69 (468)
7075	1.25	Typical	>40		61-63 (427)
7075	3.0	Minimum	>38	49.0	59-61 (413)
7075	3.0	Typical	>40		53-55 (372)
7475	1.25	Minimum	>38	57.0	67-69 (468)
7475	1.25	Typical	>40		61-63 (427)
7475	3.0	Minimum	>38	52.0	62-64 (434)
7475	3.0	Typical	>40		56-58 (393)
7050	1.25	Minimum	>38	63.0	70-72 (489)
7050	1.25	Typical	>40		66-68 (462)
7050	3.0	Minimum	>38	60.0	67-69 (469)
7050	3.0	Typical	>40		63-65 (441)
7049	1.25	Minimum	>38	63.0	70-72 (489)
7049	1.25	Typical	>40		66-68 (462)
7049	3.0	Minimum	>38	60.0	67-69 (469)
7049	3.0	Typical	>40		63-65 (441)

Table III. Long Transverse Yield Strengths[a] and Electrical Conductivities of the Plate Materials

Material[b]	Plate Thickness, in.	Aging Time, hr at 330°F	Electrical Conductivity,[c] % IACS	Actual Yield Strength, Mpa (ksi)	Desired Yield Strength, ksi
7075-T651	1.25	0	33.2	522(75.7)	--
7075-T7651		9	38.4	489(71.0)	70
7075-T7351(M)		13	39.6	480(69.6)	68
7075-T7351(T)		27	41.6	429(62.2)	63
7075-T651	3.0	0	34.0	500(72.6)	--
7075-T7651		15	39.5	460(66.7)	68
7075-T7351(M)		32	41.6	405(58.8)	60
7075-T7351(T)		48	42.1	382(55.4)	55
7475-T7351(M)	1.25	14	41.2	482(70.0)	68
7475-T7351(T)		26	43.4	420(61.0)	63
7475-T7351(M)	3.0	15	42.3	444(64.4)	63
7475-T73651(T)		32	44.8	385(55.8)	58
7050-T73651(M)	1.25	15.5	41.3	500(72.5)	71
7059-T73651(T)		23	41.9	477(69.2)	67
7050-T73651(M)	3.0	20	41.7	475(69.0)	68
7050-T73651(T)		30	43.2	429(62.2)	64
7049-T7351(M)	1.25	15.5	40.8	493(71.5)	71
7049-T7351(T)		23	42.5	461(67.0)	67
7049-T7351(M)	3.0	13.5	40.1	481(69.8)	68
7049-T7351(T)		21	41.7	450(65.3)	64

[a]Average of three measurements: midplane for 1.25-in. plate, 1/4t for 3.0-in. plate.

[b](M) indicates minimum-aged condition (high tensile properties); (T) indicates typical condition.

[c]Measured on plate surface with Magnaflux eddy current tester.

Table IV. Chemical Compositions of the Plate Materials[a]

Alloy	Plate[b] Thickness, in.	% by Weight[c]							
		Si	Fe	Cu	Mg	Cr	Zn	Ti	Zr
7075	1.25	0.14	0.16	1.45	2.49	0.20	5.78	0.03	0.00
7075	3.0	0.14	0.16	1.46	2.50	0.20	5.91	0.03	0.00
7475	1.25	0.06	0.10	1.57	2.23	0.20	5.96	0.02	0.00
7475	3.0	0.06	0.10	1.55	2.20	0.20	5.97	0.02	0.00
7050	1.25	0.06	0.10	2.10	2.08	0.00	6.00	0.02	0.12
7050	3.0	0.06	0.10	2.09	2.07	0.00	6.10	0.02	0.12
7049	1.25	0.06	0.10	1.53	2.48	0.14	7.60	0.02	0.00
7049	3.0	0.06	0.10	1.55	2.54	0.14	7.54	0.02	0.00

[a]Cu, Mg and Zn based on atomic absorption analysis of the plates; Si, Fe, Cr, Ti, and Zr based on Quantometer analysis of the melts and plates.

[b]Both plates of each alloy were rolled from the same ingot.

[c]All other elements <0.005% each; <0.05% total.

Table V. Tensile Properties[a] of the Plate Materials

Material[b]		Tensile Strength, MPa(ksi)			Yield Strength[c], MPa(ksi)			Elongation[d], %		
		L	LT	ST	L	LT	ST	L	LT	ST
1.25"	7075-T651	594(86.2)	584(84.8)	541(78.5)	548(79.6)	522(75.7)	480(69.6)	10.5	10.7	4.0
3"	7075-T651	557(80.8)	559(81.1)	525(76.2)	520(75.4)	500(72.6)	455(66.1)	10.5	7.7	4.0
1.25"	7075-T7651	553(80.3)	544(79.0)	491(71.3)	503(73.0)	489(73.0)	456(66.2)	10.5	10.2	3.3
3"	7075-T7651	526(76.3)	521(75.6)	486(70.5)	474(68.8)	460(66.7)	428(62.1)	10.5	7.7	3.0
1.25"	7075-T7351(M)	542(78.6)	536(77.8)	494(71.7)	487(70.7)	480(69.6)	446(64.8)	11.0	9.8	4.0
1.25"	7075-T7351(T)	502(72.8)	498(72.3)	456(66.2)	432(62.7)	429(62.2)	406(58.9)	11.3	10.5	4.0
3"	7075-T7351(M)	482(69.9)	481(69.8)	440(63.8)	413(59.9)	405(58.8)	380(55.1)	10.5	9.0	4.0
3"	7075-T7351(T)	469(68.1)	464(67.4)	446(64.7)	392(56.9)	382(55.4)	361(52.4)	11.7	9.0	6.3
1.25"	7475-T7351(M)	583(80.2)	540(78.4)	502(72.8)	499(72.4)	482(70.0)	456(66.2)	11.0	11.2	4.0
1.25"	7475-T7351(T)	502(72.9)	495(71.9)	453(65.7)	429(62.3)	420(61.0)	400(58.1)	13.0	11.7	4.0
3"	7475-T7351(M)	513(74.5)	514(74.6)	484(70.3)	455(66.0)	444(64.4)	415(60.2)	11.3	9.5	4.0
3"	7475-T7351(T)	467(68.0)	470(68.2)	449(65.2)	391(56.8)	385(55.8)	364(52.9)	13.0	10.0	4.7
1.25"	7050-T73651(M)	562(81.6)	533(80.2)	517(75.0)	509(73.9)	500(72.5)	466(67.7)	12.2	11.2	4.0
1.25"	7050-T73651(T)	537(78.0)	537(77.9)	500(72.5)	480(69.7)	477(69.2)	440(63.9)	12.7	11.8	4.0
3"	7050-T73651(M)	526(76.3)	536(77.8)	493(71.5)	481(69.8)	475(69.0)	440(63.9)	11.3	8.5	5.0
3"	7050-T73651(T)	503(73.0)	502(72.9)	477(69.3)	438(63.6)	429(62.2)	408(59.2)	12.7	8.8	5.0
1.25"	7049-T73651(M)	559(81.1)	553(80.3)	514(74.6)	500(72.6)	493(71.5)	463(67.2)	11.7	10.7	4.0
1.25"	7049-T73651(T)	534(77.5)	520(75.5)	495(71.9)	466(67.6)	461(67.0)	436(63.3)	12.3	11.0	4.0
3"	7049-T73651(M)	541(78.5)	548(79.6)	515(74.8)	488(70.8)	481(69.8)	446(64.7)	11.2	9.0	4.0
3"	7049-T73651(T)	517(75.1)	525(76.2)	500(72.5)	452(65.5)	450(65.3)	416(60.4)	12.0	9.8	5.0

[a] Average of triplicate specimens

[b] M indicates minimum-aged condition; T indicates typical condition.

[c] 0.2% offset

[d] % in 2-in. for L and LT directions; % in 1-in. and 0.5-in. for ST direction in 3-in. and 1.25-in. respectively.

Table VI. Fracture Toughness of the Plate Materials[a]

Material[b]	Plate Thickness, in.	LT Yield Strength, MPa	Fracture Toughness[c], K_{Ic} or K_Q, MPa$\sqrt{m}$ (ksi$\sqrt{in.}$)		
			LT	TL	SL
7075-T651	1.25	522	30.6(27.8)	25.1(22.8)	24.2(22.0)
7075-T7651	1.25	489	31.5(28.6)	25.2(22.9)	23.1(21.0)
7075-T7351(M)	1.25	480	31.8(28.9)	- -	23.4(21.3)
7075-T7351(T)	1.25	429	33.3(30.3)	26.7(24.3)	24.3(22.1)
7075-T651	3.0	500	27.1(24.6)	22.4(20.4)	19.6(17.8)
7075-T7651	3.0	460	28.4(25.8)	22.0(20.0)	21.3(19.4)
7075-T7351(M)	3.0	405	31.9(29.0)	- -	23.2(21.1)
7075-T7351(T)	3.0	382	32.0(29.1)	24.8(22.5)	23.5(21.4)
7475-T7351(M)	1.25	482	38.2(34.7)	- -	25.7(23.4)
7475-T7351(T)	1.25	420	41.8(38.0)	31.7(28.8)	26.7(24.3)
7475-T7351(M)	3.0	444	35.0(31.8)	- -	26.7(24.3)
7475-T7351(T)	3.0	384	40.4(36.7)	30.5(27.7)	29.7(27.0)
7050-T73651(M)	1.25	500	37.0(33.6)	31.2(28.4)	25.7(23.4)
7050-T73651(T)	1.25	477	39.9(36.3)	- -	27.3(24.8)
7050-T73651(M)	3.0	475	34.6(31.5)	- -	26.8(24.4)
7050-T73651(T)	3.0	429	38.3(34.8)	29.2(26.5)	27.9(25.4)
7049-T7351(M)	1.25	493	35.5(32.3)	- -	25.9(23.5)
7049-T7351(T)	1.25	462	39.4(35.8)	31.2(28.4)	27.8(25.3)
7049-T7351(M)	3.0	481	28.4(25.8)	- -	23.8(21.6)
7049-T7351(T)	3.0	449	33.1(30.1)	27.2(24.7)	27.6(25.1)

[a]Average of triplicate compact tension specimens (best estimate of standard deviation: 0.8 MPa$\sqrt{m}$). Specimen thicknesses are given below

Plate Thickness (in.)	Specimen Thickness, B(in.)		
	LT	TL	SL
1.25	1.0	1.0	0.5
3.0	1.25	1.25	1.0

(LT values for minimum aged condition are from duplicate specimens.)

[b]M indicates minimum-aged condition; T indicates typical condition.

[c]2.5 $(K_Q/\sigma_{YS})^2$ thickness criterion was satisfied for all measurements.

State which values qualify as K_{Ic} & which K_Q according to ASTM E399

Table VII. Schedule of Bolt-Loaded DCB Tests: SL Orientation

Material	Thickness, in.	Number of Specimens[a] Daytona Beach	Synthetic Seawater	Salt Chromate
7075-T651	1.25	1	1	1
7075-T7651	1.25	1	1	1
7075-T7351(M)	1.25	-/3[b]	-/6[b]	1/6[b]
7075-T7351(T)	1.25			
7075-T651	3.0	1	1	1
7075-T7651	3.0	1	1	1
7075-T7351(M)	3.0	-/3[c]	-/2[c]	2/2[c]
7075-T7351(T)	3.0			
7475-T7351(M)	1.25	-/3[b]	-/2[b]	2/2[b]
7475-T7351(T)	1.25			
7475-T7351(M)	3.0	-/3[c]	-/2[c]	2/2[c]
7475-T7351(T)	3.0			
7050-T73651(M)	1.25	-/3[b]	-/2[b]	2/2[b]
7050-T73651(T)	1.25			
7050-T73651(M)	3.0	-/3[c]	-/2[c]	2/2[c]
7050-T73651(T)	3.0			
7049-T7351(M)	1.25	-/3[b]	-/2[b]	2/2[b]
7049-T7351(T)	1.25			
7049-T7351(M)	3.0	-/3[c]	-/2[c]	2/2[c]
7049-T7351(T)	3.0			

[a] All specimens 25-mm (1.0-in.) high with pop-in precracks;

[b] Indicates four 25-mm (1.0-in.) high fatigue-precracked specimens also tested (2 initial stress intensities);

[c] Indicates that two 75-mm (3.0-in.) high specimens also tested (pop-in precrack).

Table VIII. Schedule of Bolt-Loaded DCB Tests: TL Orientation

Material	Thickness, in.	Number of Specimens[a] Daytona Beach	Synthetic Seawater	Salt-Chromate
7075-T651	1.25	1	1	1
7075-T7651		1	1	1
7075-T7351(T)		3	2	2
7075-T651	3.0	1	1	1
7075-T7651		1	1	1
7075-T7351(T)		3	2	2
7475-T7351(T)	1.25	3	2	2
7475-T7351(T)	3.0	3	2	2
7050-T73651(T)	1.25	3	2	2
7050-T73651(T)	3.0	3	2	2
7049-T7351(T)	1.25	3	2	2
7049-T7351(T)	3.0	3	2	2

[a]All specimens 25 mm (1.0-inch) high with pop-in precracks.

Table IX. Summary of Laboratory Short-Transverse SCR Results[a] for 1.25-in. Plates--Smooth Specimens

Applied Stress MPa(ksi)	Alloy/Temper									
	7075				7475		7050		7049	
	-T651	-T7651	M[b]	T[b]	M	T	M	T	M	T
	[522][c]	[489]	[480]	[429]	[482]	[420]	[500]	[477]	[493]	[462]
34 (5)	OK	-	-	-	-	-	-	-	-	-
103(15)	2/3* (2,12 d)	-	-	-	-	-	-	-	-	-
172(25)	3/3 (1,2,2 d)	1/3* (103 d)	OK	OK	OK	OK	OK	OK	OK	OK
241(35)	-	1/3 (3 d)	OK*	OK	OK	OK	1/3 (125 d)	OK	OK	OK
310(45)	-	3/3 (all 2 d)	2/3* (62,95 d)	OK	1/3 (60 d)	OK	1/3* (114 d)	1/3 (125 d)	OK*	OK
379(55)	-	-	3/3 (19,22,60 d)	OK	3/3 (47,53,53 d)	OK	2/3 (92,152 d)	2/3 (125,133 d)	OK	OK

need definition for

[a]Number specimens failed/Number tested; OK indicates 3 specimens survived 6-month exposure
Test environment: Synthetic seawater, alternate immersion
Specimen: 3.175 mm diam. tensile type

[b]M indicates minimum-aged -T73 temper condition; T indicates typical -T73 temper.

[c]Numbers in brackets are LT yield strengths (MPa). Minimum yield strengths for 1.25-in. thick 7075-T651 and 7075-T7351 are 462 and 393 MPa, respectively.

*Secondary intergranular attack noted in metallographic exam.

Table X. Summary of Laboratory Short-Transverse SCR Results[a] for 3.0-in. Plates--Smooth Specimens

Applied Stress, MPa(ksi)	Alloy/Temper									
	7075				7475		7050		7049	
	-T651	-T7651	M[b]	T[b]	M	T	M	T	M	T
	[500][c]	[460]	[405]	[382]	[444]	[384]	[475]	[429]	[481]	[449]
34 (5)	OK	-	-	-	-	-	-	-	-	-
103(15)	3/3 (all 1 d)	-	-	-	-	-	-	-	-	-
172(25)	3/3 (all 1 d)	OK*	OK	OK	OK	OK	OK	OK	OK	OK
241(35)	-	3/3 (6,7,107 d)	OK	OK	OK	OK	OK	OK	OK*	OK
310(45)	-	3/3 (4,7,11 d)	OK	OK	2/3 (160,168 d)	OK	OK	OK	1/3 (39 d)	OK
379(55)	-	-	OK	OK	OK	OK	OK	OK	3/3 (13,106,152 d)	OK

[a] Number specimens failed/Number tested; OK indicates 3 specimens survived 6-months exposure.
Test environment: Synthetic seawater, alternate immersion.
Specimen: 3.175 mm diam. tensile type.

[b] M indicates minimum-aged -T73 temper condition; T indicates typical -T73 temper.

[c] Numbers in brackets are LT yield strengths (MPa). Minimum yield strengths for 2.5-3.0-in. 7075-T651 and 7075-T7351 are 420 and 338 MPa, respectively.

*Secondary intergranular attack noted in metallographic exam.

need definition of typ.

Table XI. Summary of Laboratory Long-Transverse SCR Results[a]--Smooth Specimens

Applied Stress, MPa(ksi)	Alloy/Temper					
	7075 -T651	7075 -T7651	7075 -T7351	7475-T7351	7050-T73651	7049-T7351
			1.25-in. Plate			
310(45)	-	OK	OK	OK	OK	OK
379(55)	OK	OK*	OK	OK	OK	OK
			3.0-in Plate			
310(45)	-		OK	OK	OK	OK
379(55)	2/3* (4,6 d)	OK*(50 ksi)	OK	OK	OK	OK

[a]Number specimens failed/number tested; OK indicates 3 specimens survived 6 months.
Test environment: synthetic seawater, alternate immersion
Specimen: 3.175 mm diam. tensile type.

*Secondary intergranular attack noted in metallographic exam.

Table XII. Summary of Marine Atmosphere Short-Transverse Results[a] for 1.25-in. Plates--Smooth Specimens

Applied Stress, MPa(ksi)	Alloy/Temper					
	7075					
	-T651	-T7651	-T7351(T)	7475-T7351(T)	7050-T73651(T)	7049-T7351(T)
	[522][b]	[489]	[429]	[420]	[477]	[462]
34 (5)	OK	-	-	-	-	-
103(15)	2/3 (.2,8.9 mo.)	-	-	-	-	-
172(25)	3/3 (.1-.2 mo.)	3/3 (.9-2.3 mo.)	OK	OK	OK	OK
241(35)	-	3/3 (.4-1.2 mo.)	OK	OK	OK	OK
310(45)	-	3/3 (.1-.4 mo.)	OK	OK	3/3 (8.9 mo.)	2/3 (8.9 mo.)
379(55)	-	-	OK	OK	2/3 (3.4,4.8 mo.)	2/3 (8.9 mo.)

[a]Number specimens failed/Number tested; OK indicates 3 specimens survived 9 months exposure. Specimen: 3.175 mm diam. tensile type.

[b]Numbers in brackets are LT yield strengths (MPa). Minimum yield strengths for 1.25-in. 7075-T651 and 7075-T7351 are 462 and 393 MPa, respectively.

Table XIII. Summary of Marine Atmosphere Short-Transverse SCR Results[a] for 3.0-in. Plates--Smooth Specimens

Applied Stress, ksi	Alloy/Temper					
	7075 -T651	7075 -T7651	7075 -T7351(T)	7475-T7351(T)	7050-T73651(T)	7049-T7351(T)
	[500][b]	[460]	[382]	[384]	[429]	[449]
34 (5)	OK	-	-	-	-	-
103(15)	3/3 (.1-.4 mo.)	-	-	-	-	-
172(25)	2/3 (.05 mo.)	OK	OK	OK	OK	OK
241(35)	-	1/3 (6.2 mo.)	OK	OK	OK	OK
310(45)	-	3/3 (.5-1.8 mo.)	OK	OK	OK	OK
379(55)	-	-	OK	OK	OK	OK

[a]Number specimens failed/Number tested; OK indicates 3 specimens survived 9-month exposure. Specimen: 3.175 mm diam. tensile type.

[b]Numbers in brackets are LT yield strengths (MPa). Minimum yield strengths for 2.5-3.0-in. 7075-T651 and 7075-T7351 are 420 and 338 MPa, respectively.

Table XIV. Summary of Marine Atmosphere Long-Transverse SCR Results[a]--Smooth Specimens

Applied Stress, MPa(ksi)	Alloy/Temper					
	7075					
	-T651	-T7651	-T7351(T)	7475-T7351(T)	7050-T73651(T)	7049-T7351(T)
			1.25-in. Plate			
310(45)	-	-	OK	OK	OK	OK
379(55)	OK	OK	OK	OK	OK	OK
			3.0-in. Plate			
310(45)	-		OK	OK	OK	OK
379(55)	2/3 (3.4-4.6 mo.)	OK(50 ksi)	OK	OK	OK	OK

[a]Number specimens failed/Number tested; OK indicates 3 specimens survived 9-month exposure.
Test environment: synthetic seawater, alternate immersion
Specimen: 3.175 mm diam. tensile type.

Table XV. Total Crack Growth Observed in DCB Specimens[a] with Pop-in Precracks: SL Orientation

Material	Plate Thickness, in.	LT Yield Strength, MPa	SL K_{Ia}, MPa$\sqrt{m}$	Average Crack Extension[b] (mm) Daytona Beach	Synthetic Seawater	Salt-Chromate Solution
7075-T651	1.25	522	21.3	20.8	30.5 (33.5)	22.4 (27.4)
7075-T7651	1.25	489	21.7	9.1	6.8 (6.1)	10.2 (13.0)
7075-T7351(M)	1.25	480	21.7	-	-	11.3 (12.6)
7075-T7351(T)	1.25	429	23.8	1.3 (2.0)	1.4 (1.1)	8.4 (8.5)
7075-T651	3.0	500	19.8	16.3	15.5 (16.0)	9.9 (11.7)
7075-T7651	3.0	460	21.2	1.8	3.8 (4.6)	2.8 (3.0)
7075-T7351(M)	3.0	405	24.2	-	-	0.6 (0.8)
7075-T7351(T)	3.0	382	24.8	0.5 (0.5)*	0.6 (0.5)*	0.0 (0.4)*
7075-T7351(T)	3.0	382	24.4	0.8 (0.8)*	1.3 (0.0)*	0.1 (0.3)
7475-T7351(M)	1.25	482	24.0	-	-	12.6 (13.0)
7475-T7351(T)	1.25	420	27.1	2.5 (2.8)	3.7 (3.7)	9.5 (10.2)
7475-T7351(M)	3.0	444	25.4	-	-	2.5 (3.3)
7475-T7351(T)	3.0	384	30.0	1.3 (1.0)*	1.1 (0.8)*	0.1 (1.0)
7475-T7351(T)	3.0	384	29.0	0.3 (0.3)*	1.1 (-0.3)*	0.3 (0.5)
7050-T73651(M)	1.25	500	24.2	-	-	9.8 (12.5)
7050-T73651(T)	1.25	477	25.2	5.3 (5.8)	2.8 (2.9)	8.3 (9.3)
7050-T73651(M)	3.0	475	24.7	-	-	2.2 (3.4)
7050-T73651(T)	3.0	429	28.3	2.0 (2.8)	1.8 (1.8)	1.3 (2.5)
7050-T73651(T)	3.0	429	27.8	2.8 (1.5)	3.4 (1.9)	1.5 (2.3)
7049-T7351(M)	1.25	493	23.0	-	-	12.4 (14.6)
7049-T7351(T)	1.25	462	27.5	3.3 (3.6)	2.8 (2.8)	9.5 (10.2)
7049-T7351(M)	3.0	481	24.2	-	-	3.4 (5.1)
7049-T7351(T)	3.0	449	26.3	2.5 (4.1)	1.9 (2.3)	2.8 (3.7)
7049-T7351(T)	3.0	449	25.9	3.3 (2.5)	4.3 (2.2)	1.5 (2.7)

[a]All specimens 25 mm (1 in.) high, except second set of data for 3-in. thick typical -T73 plates, which were 75 mm (3 in.) high.

[b]Estimate based on average of measurements at specimen edges at end of 6-month exposure period (numbers in parentheses based on fracture surface measurements).

*Presence of actual stress corrosion questionable according to visual examination of fracture surface.

Table XVI. Total Crack Growth Observed in DCB Specimen[a] with Pop-in Precracks: TL Orientation

Material	Plate Thickness, in.	LT Yield Strength, MPa	K_{Ia} MPa$\sqrt{m}$	Average Crack Extension[b], mm		
				Daytona Beach	Synthetic Seawater	Salt-Chromate Solution
7075-T651	1.25	522	23.6	2.0	1.8 (3.0)†	0.8 (1.8)†
7075-T7651	1.25	489	23.8	0.3	2.3 (1.0)†	0.5 (0.8)†
7075-T7351	1.25	429	26.1	0.5 (0.8)†	0.4 (0.9)†	0.0 (0.9)†
7075-T651	3.0	500	22.6	0.5	3.8 (2.3)†	0.0 (0.5)†
7075-T7651	3.0	460	23.8	0.0	0.8 (0.3)†	0.0 (0.0)*
7075-T7351	3.0	382	26.7	0.3 (0.8)*	0.3 (0.6)*	0.5 (0.0)*
7475-T7351	1.25	420	32.8	0.5 (1.3)†	0.3 (1.0)†	0.3 (0.4)
7475-T7351	3.0	384	33.9	0.0 (0.8)*	0.3 (0.3)*	0.0 (0.5)*
7050-T73651	1.25	477	28.3	1.5 (1.8)†	1.4 (0.9)†	0.1 (0.6)†
7050-T73651	3.0	429	30.5	0.8	1.8 (1.3)†	0.0 (0.1)†
7049-T7351	1.25	462	30.9	1.3 (0.8)†	1.7 (0.9)†	0.0 (1.3)†
7049-T7351	3.0	449	29.6	0.8 (-0.3)†	0.6 (0.8)†	0.0 (0.0)†

[a] All specimens 25 mm high.

[b] Estimate based on measurements at specimen edges at end of 6-month exposure period (numbers in parentheses based on fracture surface measurements).

*Presence of actual stress corrosion cracking is questionable according to visual examination.

†Fine cracks normal to, and leading crack tip were present.

Table XVII. Crack Growth in Fatigue-Precracked Specimens from 1.25-in. Plates: 6-Month Exposure

Material[a]	LT Yield Strength, MPa	K_{Ii},[b] MPa$\sqrt{m}$	K_{Ir},[c] MPa$\sqrt{m}$	Crack Extension, mm		Ave. Velocity,[d] m/sec x 10^{-10}
				Edge	Surface	
			Daytona Beach			
7075-T7351	429	21.8	20.3	0.5	1.3	0.76
7475-T7351	420	22.5	20.1	1.0	2.3	1.36
7050-T73651	477	22.0	16.8	3.0	5.1	3.01
7049-T7351	462	23.5	19.5	2.0	3.6	2.13
			Synthetic Seawater			
7075-T7351	429	20.0	20.1	0.8	-0.3*	0.00
7475-T7351	420	21.8	21.7	0.3	0.3	0.19
7050-T73651	477	21.5	19.5	2.0	2.0	1.24
7049-T7351	462	21.4	21.1	0.3	0.3	0.19
			Salt-Chromate Solution			
7075-T7351	429	19.7	14.2	5.8	6.6	4.20
7475-T7351	420	22.3	17.2	4.3	4.8	3.05
7050-T73651	477	21.8	14.2	7.4	8.6	5.47
7049-T7351	462	21.7	13.1	8.6	10.4	6.61

[a] All typical -T73 temper.

[b] Initial stress intensity based on edge measurement of precrack length.

[c] Residual stress intensity based on fracture surface measurement.

[d] Based on fracture surface crack length measurement (0.7×10^{-10} m/sec = 1×10^{-5} in./hr)

*Presence of stress-corrosion cracking questionable according to visual examination.

Table XVIII Residual Stress Intensity (K_{Ir}) and Average Crack Velocity for DCB Specimens[a] Exposed for 6.5 Months at Daytona Beach, Florida

Material	Plate Thickness, in.	Plate Strength, MPa	SL Orientation			TL Orientation		
			K_{Ia}, MPa$\sqrt{m}$	K_{Ir}, MPa$\sqrt{m}$	Ave. Velocity m/sec x 10^{-10}	K_{Ia}, MPa$\sqrt{m}$	K_{Ir}, Mpa$\sqrt{m}$	Ave. Velocity, m/sec x 10^{-10}
7075-T651	1.25	522	21.3	9.0	12	23.6	21.2	1.2
7075-T7651	1.25	489	21.7	16.2	5.4	23.8	23.5	0.18
7075-T7351(T)	1.25	429	23.8	22.3	0.77	26.1	25.5	0.30
7075-T651	3.0	500	19.8	9.6	9.6	22.6	22.0	0.30
7075-T7651	3.0	460	21.2	19.1	1.1	23.8	23.8	0
7075-T7351(T)	3.0	382	24.8	24.3	0.30*	26.7	26.5	0.18*
7075-T7351(T)	3.0	382	24.4	23.6	0.47*	-	-	-
7475-T7351(T)	1.25	420	27.1	23.7	1.5	32.8	31.6	0.30
7475-T7351(T)	3.0	384	30.0	27.8	0.77*	33.9	33.8	0*
7475-T7351(T)	3.0	384	29.0	28.9	0.18*	-	-	-
7050-T73651(T)	1.25	477	25.2	19.2	3.1	28.3	26.0	0.89
7050-T73651(T)	3.0	429	28.3	26.3	1.2	30.5	29.4	0.48
7050-T73651(T)	3.0	429	27.8	24.3	1.7	-	-	-
7049-T7351(T)	1.25	462	27.5	23.2	1.9	30.9	28.9	0.77
7049-T7351(T)	3.0	449	26.3	23.7	1.5	29.6	28.2	0.47
7049-T7351(T)	3.0	449	25.9	23.1	1.9	-	-	-

[a]All specimens 25 mm high, except second set of data for 3.0-in. thick -T73 temper plates, which were 75 mm high. Pop-in precracks.

*Presence of stress corrosion cracking questionable according to visual examination of fracture surfaces.

Table XIX. Residual Stress Intensity (K_{Ir}) and Average Crack Velocity for DCB Specimens[a] Exposed for 6 Months to Synthetic Seawater, Alternate Immersion

Material	Plate Thickness, in.	Plate Strength, MPa	SL Orientation			TL Orientation		
			K_{Ia}, MPa$\sqrt{m}$	K_{Ir}, MPa$\sqrt{m}$	Ave. Velocity, m/sec x 10^{-10}	K_{Ia}, MPa$\sqrt{m}$	K_{Ir}, MPa$\sqrt{m}$	Ave. Velocity m/sec x 10^{-10}
7075-T651	1.25	522	21.3	5.7	19	23.6	20.2	1.9
7075-T7651	1.25	489	21.7	15.7	3.9	23.8	22.6	0.64
7075-T7351(T)	1.25	429	23.8	22.5	0.70	26.1	25.0	0.57
7075-T651	3.0	500	19.8	9.6	10	22.6	20.1	1.5
7075-T7651	3.0	460	21.2	16.8	2.9	23.8	23.5	0.19
7075-T7351(T)	3.0	382	24.8	24.2	0.32*	26.7	26.0	0.38*
7075-T7351(T)	3.0	382	24.4	24.4	0*	-	-	-
7475-T7351(T)	1.25	420	27.1	22.5	2.4	32.8	31.5	0.64
7475-T7351(T)	3.0	384	30.0	28.8	0.51*	33.9	33.5	0.19*
7475-T7351(T)	3.0	384	29.0	29.3	0*	-	-	-
7050-T73651(T)	1.25	477	25.2	21.5	1.8	28.3	27.1	0.57
7050-T73651(T)	3.0	429	28.3	25.9	1.1	30.5	28.6	0.83
7050-T73651(T)	3.0	429	27.8	25.9	1.2	-	-	-
7049-T7351(T)	1.25	462	27.5	23.7	1.8	30.9	29.4	0.57
7049-T7351(T)	3.0	449	26.3	24.1	1.5	29.6	28.3	0.51
7049-T7351(T)	3.0	449	25.9	23.8	1.4	-	-	-

[a]All specimens 25 mm high, except second set of data for 3.0-in. thick -T73 temper plates, which were 75 mm high. Pop-in precracks.

*Presence of stress corrosion cracking questionable according to visual examinaton of fracture surfaces.

Table XX. Residual Stress Intensity (K_{Ir}) and Average Crack Velocity for DCB Specimens[a] Exposed for 6 Months to Salt-Chromate Solution

Material	Plate Thickness, in.	LT Yield Strength, MPa	SL Orientation			TL Orientation		
			K_{Ia}, MPa$\sqrt{m}$	K_{Ir}, MPa$\sqrt{m}$	Ave. Velocity, m/sec x 10^{-10}	K_{Ia}, MPa$\sqrt{m}$	K_{Ir}, MPa$\sqrt{m}$	Ave. Velocity m/sec x 10^{-10}
7075-T651	1.25	522	21.3	7.4	17.4	23.6	21.3	1.1
7075-T7651	1.25	489	21.7	11.9	8.3	23.8	22.6	0.51
7075-T7351(M)	1.25	480	21.7	12.1	8.0	-	-	-
7075-T7351(T)	1.25	429	23.8	15.7	5.4	26.1	24.9	0.57
7075-T651	3.0	500	19.8	11.4	7.4	22.6	22.3	0.32
7075-T7651	3.0	460	21.2	18.0	1.9	23.8	23:8	0*
7075-T7351(M)	3.0	405	24.2	23.2	0.51	-	-	-
7075-T7351(T)	3.0	382	24.8	24.3	0.25*	26.7	26.7	0*
7075-T7351(T)	3.0	382	24.4	24.2	0.19	-	-	-
7475-T7351(M)	1.25	482	24.0	13.1	8.3	-	-	-
7475-T7351(T)	1.25	420	27.1	16.6	6.5	32.8	32.3	0.25
7475-T7351(M)	3.0	444	25.4	21.3	2.1	-	-	-
7475-T7351(T)	3.0	384	30.0	28.6	0.64	33.9	33.9	0*
7475-T7351(T)	3.0	384	29.0	28.6	0.32	-	-	-
7050-T73651(M)	1.25	500	24.2	13.7	8.0	-	-	-
7050-T73651(T)	1.25	477	25.2	16.1	5.9	28.3	27.3	0.38
7050-T73651(M)	3.0	475	24.7	21.5	2.2	-	-	-
7050-T73651(T)	3.0	429	28.3	24.8	1.6	30.5	30.3	0.06
7050-T73651(T)	3.0	429	27.8	25.8	1.5	-	-	-
7049-T7351(M)	1.25	493	23.0	11.9	9.3	-	-	-
7049-T7351(T)	1.25	462	27.5	16.7	6.5	30.9	28.7	0.83
7049-T7351(M)	3.0	481	24.2	18.9	3.2	-	-	-
7049-T7351(T)	3.0	449	26.3	22.6	2.4	29.6	29.6	0#
7049-T7351(T)	3.0	449	25.9	23.7	1.7	-	-	-

[a]All specimens 25 mm high, except second set of data for 3.0-in. thick -T73 temper plates, which were 75 mm high. Pop-in precracks.

*Presence of actual stress corrosion cracking questionable according to visual examination of fracture surfaces.

#Slight stress corrosion noted.

Table XXI. K_{Iscc} Estimates for Bolt-Loaded DCB Specimens Having Pop-in Precracks: Constant Deflection Tests

Material	Plate Thickness, in.	LT Yield Strength, MPa	SL K_{Iscc}, MPa$\sqrt{m}$			TL K_{Iscc}[a], MPa$\sqrt{m}$		
			Daytona Beach	Synthetic Seawater	Salt-Chromate Solution	Daytona Beach	Synthetic Seawater	Salt-Chromate Solution
7075-T651	1.25	522	<9	4-6	9	22.5	21	22
7075-T7651	1.25	489	10.5-15.5	13.5-17	12	>22.5	21	23
7075-T7351(M)	1.25	480	-	-	<13.5	-	-	-
7075-T7351(T)	1.25	429	22.5	22.5	<15.5	>26.0	25.5	25.5
7075-T651	3.0	500	<10.5	8-10.5	12.5	>22	19	>22.5
7075-T7651	3.0	460	15.5-20	18	18	>23.5	23.5	>24
7075-T7351(M)	3.0	405	-	-	24	-	-	-
7075-T7351(T)	3.0	382	>25	>25	>25	>26.5	>26.5	>26.5
7475-T7351(M)	1.25	482	-	-	<13.5	-	-	-
7475-T7351(T)	1.25	420	25	20.5-23	<15.5	31.5	32	32.5
7475-T7351(M)	3.0	444	-	-	23	-	-	-
7475-T7351(T)	3.0	384	>30	30	29	>34	>34	>34
7050-T73651(M)	1.25	500	-	-	<15.5	-	-	-
7050-T73651(T)	1.25	477	18-21	22	<17.5	26.5	27	28.5
7050-T73651(M)	3.0	475	-	-	22.5	-	-	-
7050-T73651(T)	3.0	429	27	26	26	29	28.5	>30.5
7049-T7351(M)	1.25	493	-	-	<13.5	-	-	-
7049-T7351(T)	1.25	462	25	23.5	<17.5	29.5	29	29
7049-T7351(M)	3.0	481	-	-	20.5	-	-	-
7049-T7351(T)	3.0	449	25	25	24	29	28.5	>29.5

[a] K_{Iscc} values refer to in-plane crack growth only and do not reflect perpendicular SL cracking observed in TL specimens.

Table XXII. K_{Iscc}[a] Estimates for Fatigue Precracked Specimens from 1.25-in. Plates: Constant Deflection Tests

Material	LT Yield Strength, MPa	SL K_{Ic}, MPa$\sqrt{m}$	SL K_{Iscc}, MPa$\sqrt{m}$		
			Daytona Beach	Synthetic Seawater	Salt-Chromate Solution
7075-T7351(T)	429	24.3	21 (22.5)[b]	>20 (22.5)	<15 (<15.5)
7475-T7351(T)	420	26.7	22 (25)	22 (22)	<15.5 (<15.5)
7050-T73651(T)	477	27.3	19 (19.5)	20 (22)	<13.5 (<17.5)
7049-T7351(T)	462	27.8	21 (25)	22 (23.5)	<14.5 (<17.5)

[a] Stress intensity at which crack growth rate decreases to 0.7×10^{-10} m/sec (1×10^{-5} in./hr).

[b] Numbers in parentheses are K_{Iscc} estimates based on specimens containing pop-in precracks.

Table XXIII. Crack Growth in DCB Specimens from 3.0-in. Thick Plates: SL Orientation, Constant Load, Fatigue Precrack

Material	LT Yield Strength, MPa	SL K_{Ic}, MPa$\sqrt{m}$	Exposure Time, Days	Stress Intensity,[a] MPa$\sqrt{m}$	Crack Extension, mm	Ave. Crack Velocity, m/sec x 10^{-10}	Measured Crack Velocity,[b] m/sec x 10^{-10}	Cracks Visually Identified as SCC
				Synthetic Seawater (AI)				
7075-T7351(T)	382	23.5	61	24.9-25.3	0.5[c]	1.0	0.8-1.3	Yes
			90	23.9-24.1	0.5	0.6	-[e]	No
7474-T7351(T)	384	29.7	61	30.6-31.2	0.8	1.5	1.1-1.6	No
			90	28.5-28.9	0.5	0.6	-[e]	No
7050-T73651(T)	429	27.9	61	28.9-29.5	0.5	1.0	0.9-1.1	No
			90	27.9-28.5	0.8	1.0	0.5-1.6	Yes
7049-T7351(T)	449	27.6	61	27.1-27.6	0.8	1.5	1.3-1.4	Yes
			90	25.6-26.1	0.5	0.6	0.4-1.5	Yes
				Salt-Chromate Solution				
7075-T7351(T)	382	23.5	90	25.3-26.1	1.3	1.7	0.7-2.8	Yes
			67	23.1-23.4	0.3	0.5	-[e]	Yes
7475-T7351(T)	384	29.7	90	30.0-32.9	3.3	4.2	2.3-4.9	Yes
			67	28.3-29.2	1.0	1.7	0.8-2.7	Yes
7050-T73651(T)	429	27.9	90	27.6	0[d]	0	0	No[f]
			67	24.4-25.1	1.0	1.7	0.6-1.1	Yes
7049-T7351(T)	449	27.6	90	26.9-29.8	3.8	4.9	2.5-4.2	Yes
			67	24.6-26.6	2.5	4.3	1.7-4.6	Yes

[a] Stress intensity covered this range during the test period. The values were calculated from load and fracture surface crack length measurements.

[b] Range of crack growth rates determined over weekly intervals from deflection measurements and compliance relationship. There were no obvious trends toward increasing rates as stress intensity increased over the range indicated. (0.7 x 10^{-10} m/sec = 1 x 10^{-5} in./hr).

[c] Crack grew from pop-in precrack.

[d] Specimen was misoriented (TL orientation).

[e] Rates were too slow to measure with sufficient accuracy.

[f] SL cracks perpendicular to the precrack were present.

Table XXIV. Stress Intensities Required to Generate Unstable Crack Growth in DCB Specimens Containing Stress Corrosion Cracks

Material[a]	LT Yield Strength, MPa	SL K_{Ic}, MPa$\sqrt{m}$	K_{If}^{b}, MPa$\sqrt{m}$	
			Synthetic Seawater	Salt-Chromate Solution
7075-T7351(T)	382	23.5	27.4	27.2
7475-T7351(T)	384	29.7	32.1	35.5
7050-T73651(T)	429	27.9	30.8	30.0
7049-T7351(T)	449	27.6	30.9	31.1

[a]All 3.0-in. thick plate.

[b]Stress intensity required to initiate mechanical pop-in from stress corrosion crack.

Table XXV. K_{Iscc}[a] Estimates for Fatigue-Precracked Specimens from 3.0-in. Plates: Constant Load Tests

Material	LT Yield Strength, MPa	SL K_{Ic}, MPa$\sqrt{m}$	SL K_{Iscc}, MPa$\sqrt{m}$	
			Synthetic Seawater	Salt-Chromate Solution
7075-T7351(T)	382	23.5	24 (>25)[b]	23.5 (>25)
7475-T7351(T)	384	29.7	28.5 (>30)	<28.5 (29)
7050-T73651(T)	429	27.9	27.5 (26)	<24.5 (26)
7049-T7351(T)	449	27.6	25.5 (25)	<25.5 (24)

[a] Stress intensity at which crack growth rate decreases to 0.7 x 10^{-10} m/sec (1 x 10^{-5} in./hr).

[b] Numbers in parentheses are K_{Iscc} estimates based on specimens containing pop-in precracks and tested under constant deflection conditions.

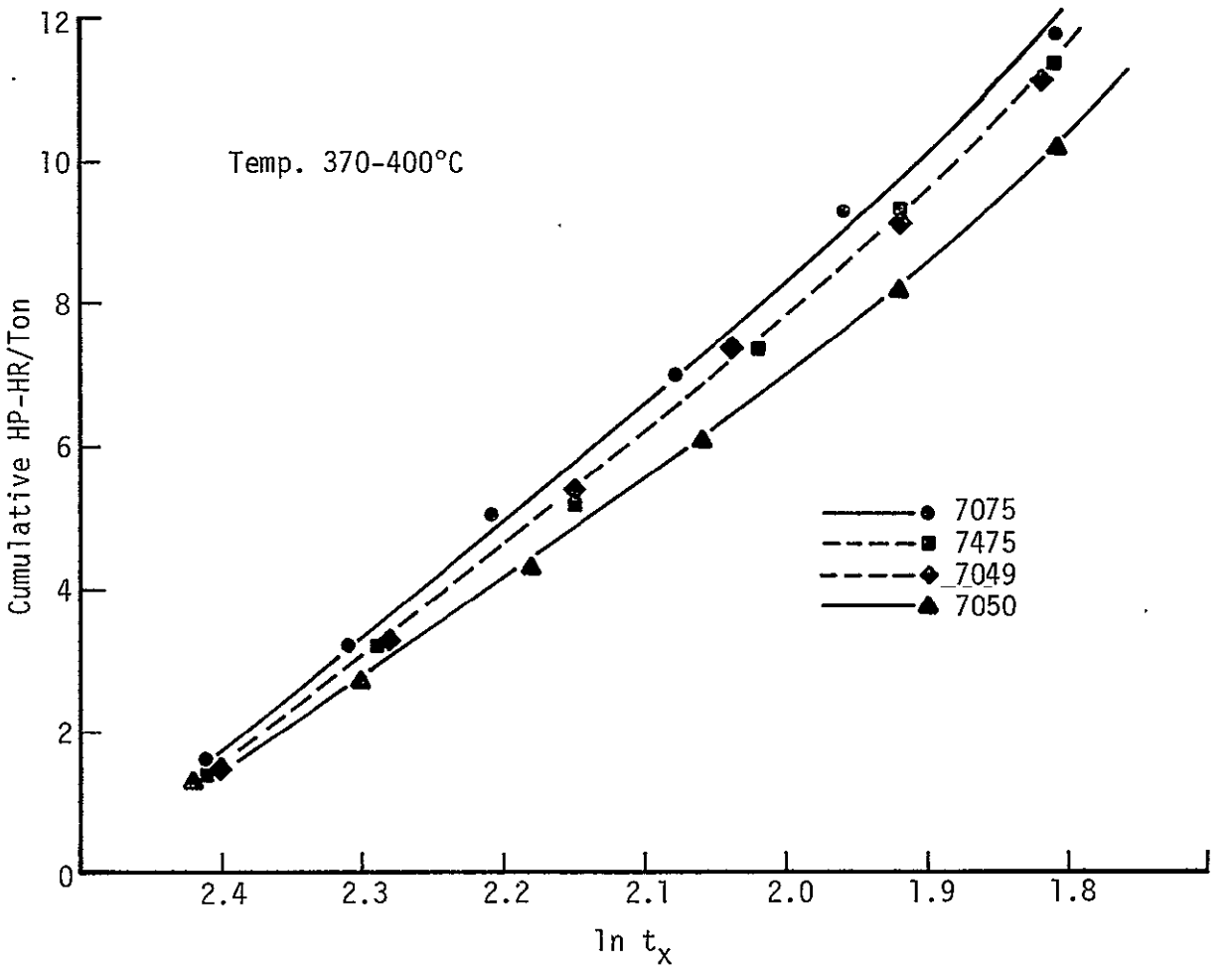

Figure 1. Cumulative deformation energy for hot rolling high-strength aluminum alloys from 12-in. ingot to 6-in. slab

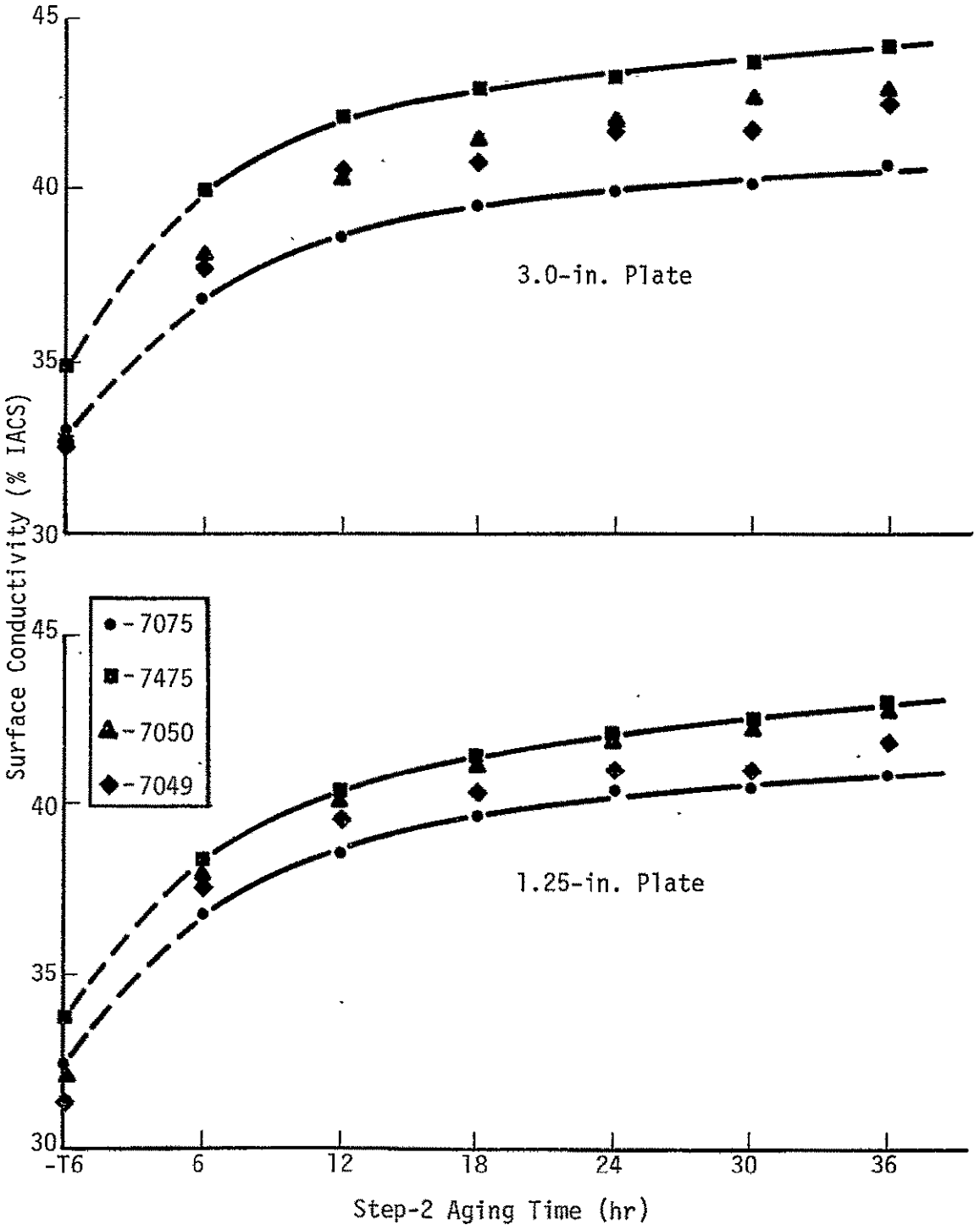

Figure 2. Plate electrical conductivity vs. step-2 aging time at 165°C (330°F)

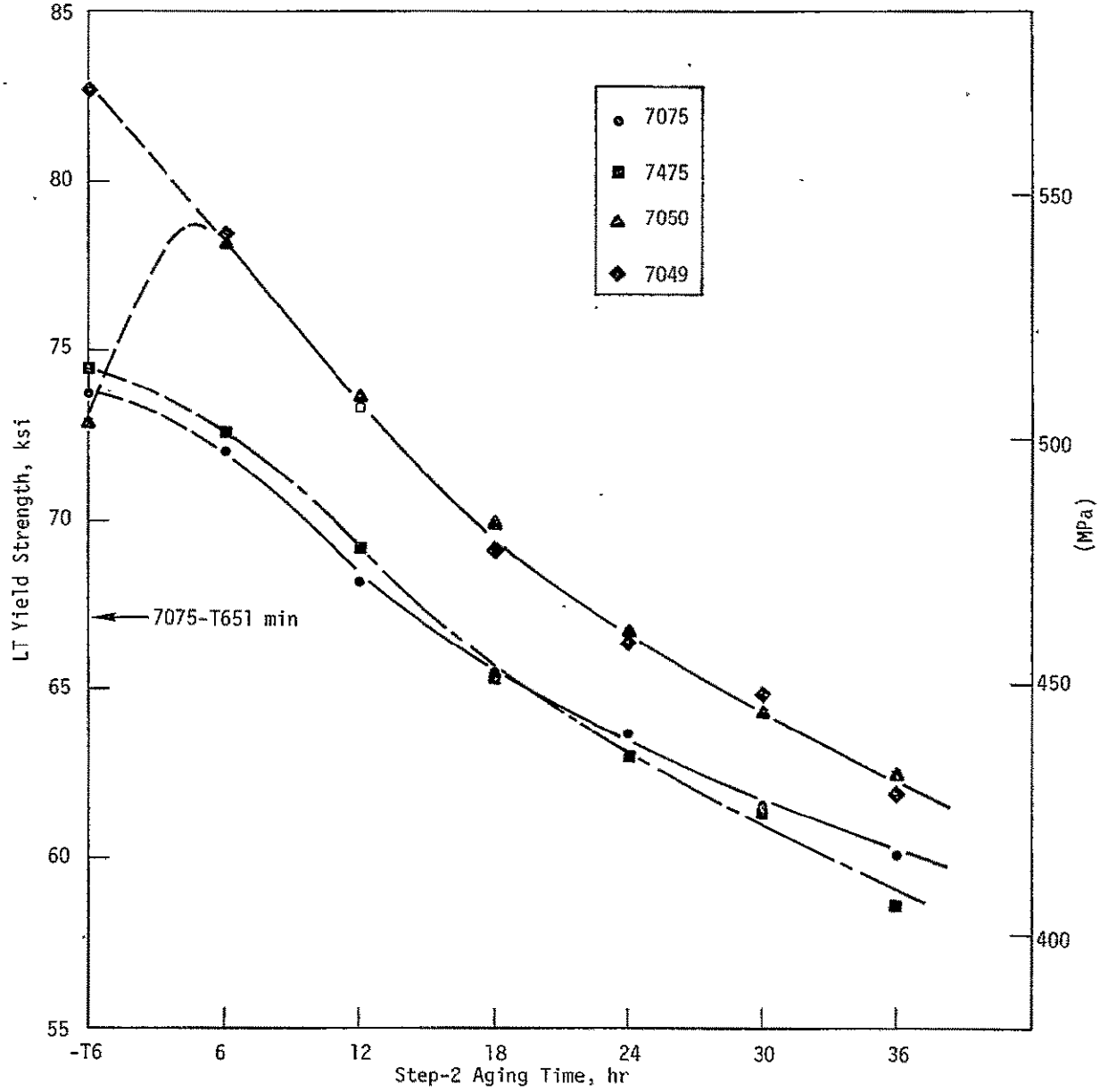

Figure 3. Overaging curves at 165°F 165°C (330°F) for 1.25-in. thick plates

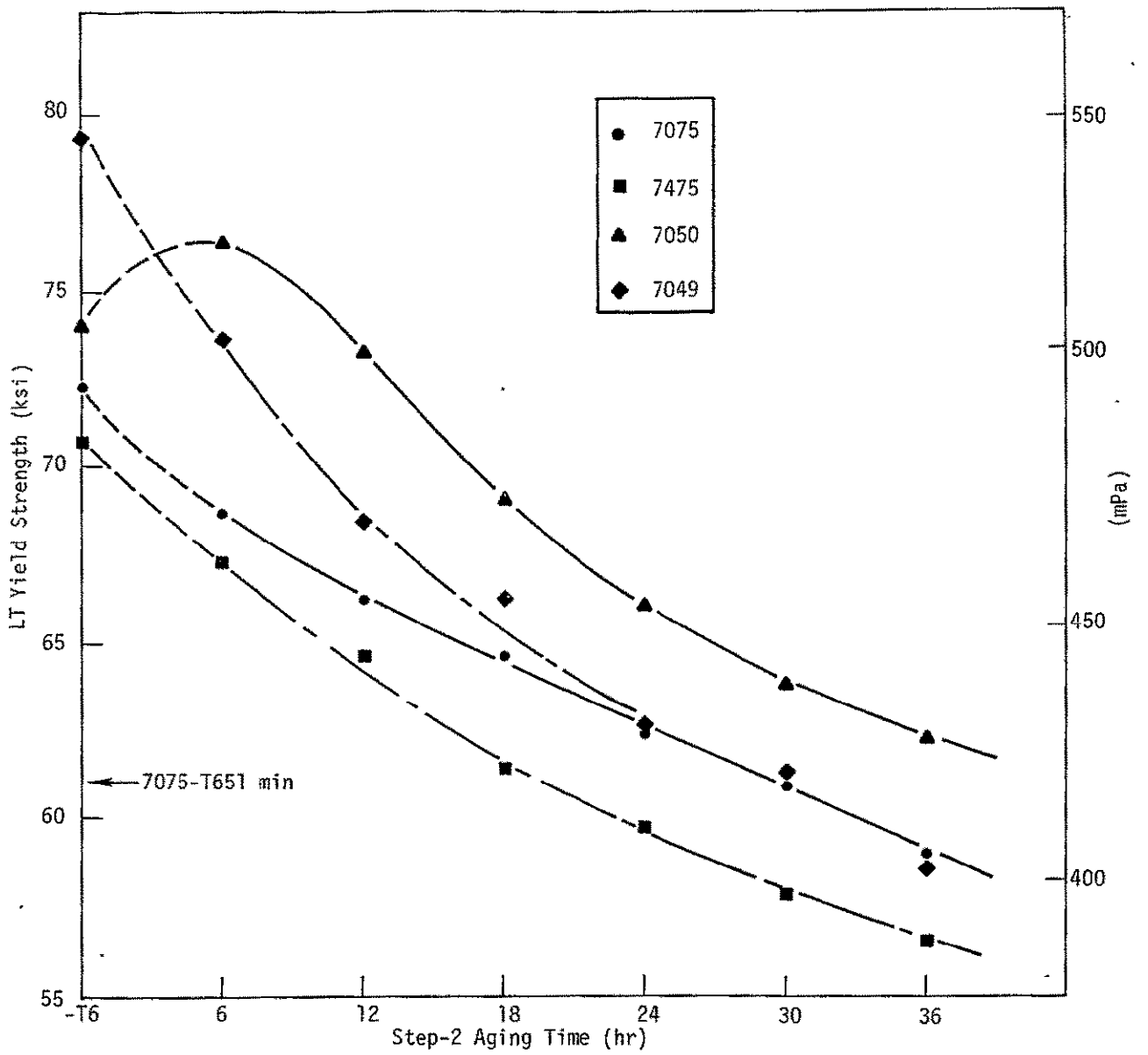

Figure 4. Overaging curves at 165°C (330°F) for 3.0-in. thick plates

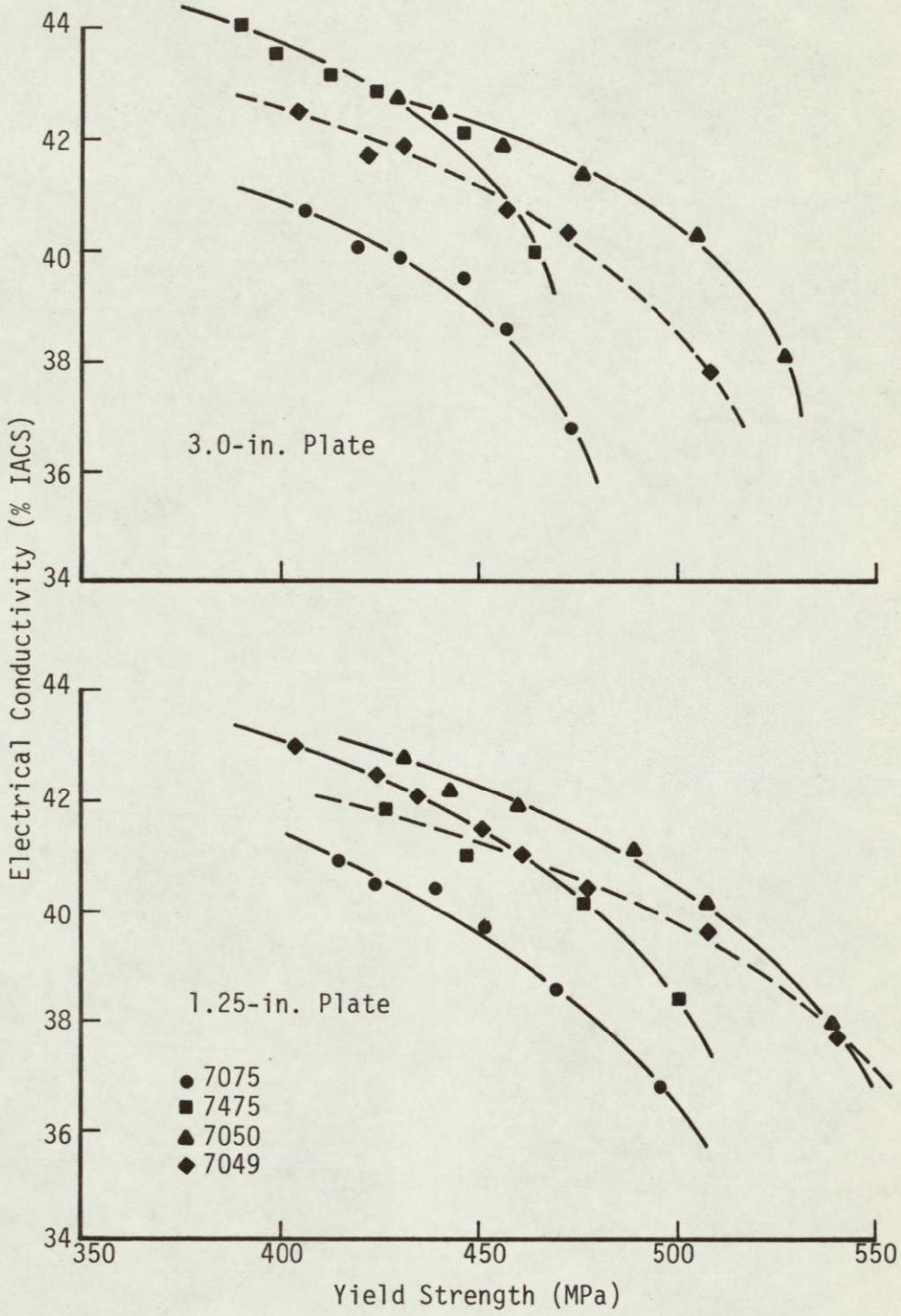

Figure 5. Correlation of yield strength and electrical conductivity for overaged alloys

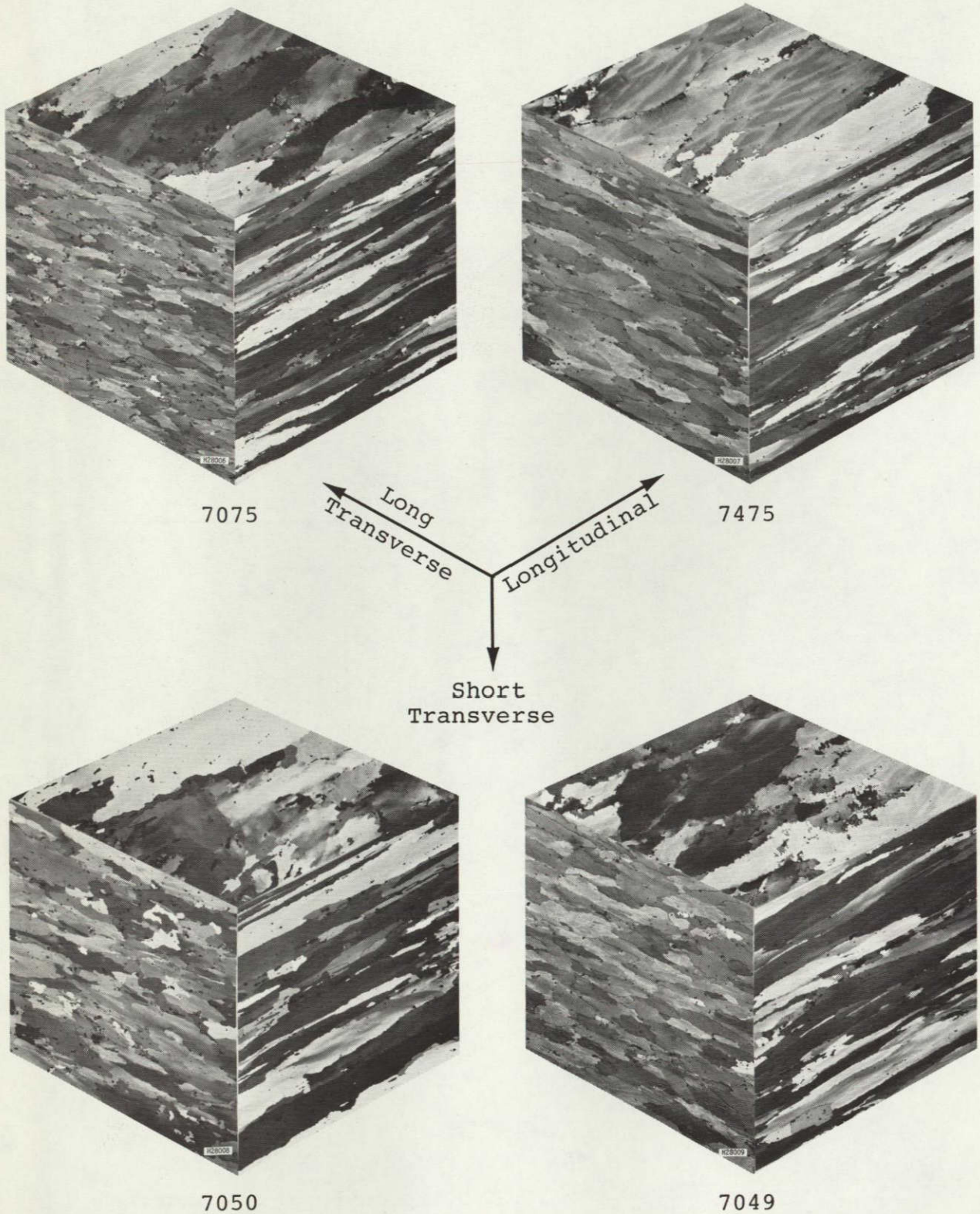

Figure 6. Grain structures of 3-in. thick plates (Barker's etch, polarized light, 25X)

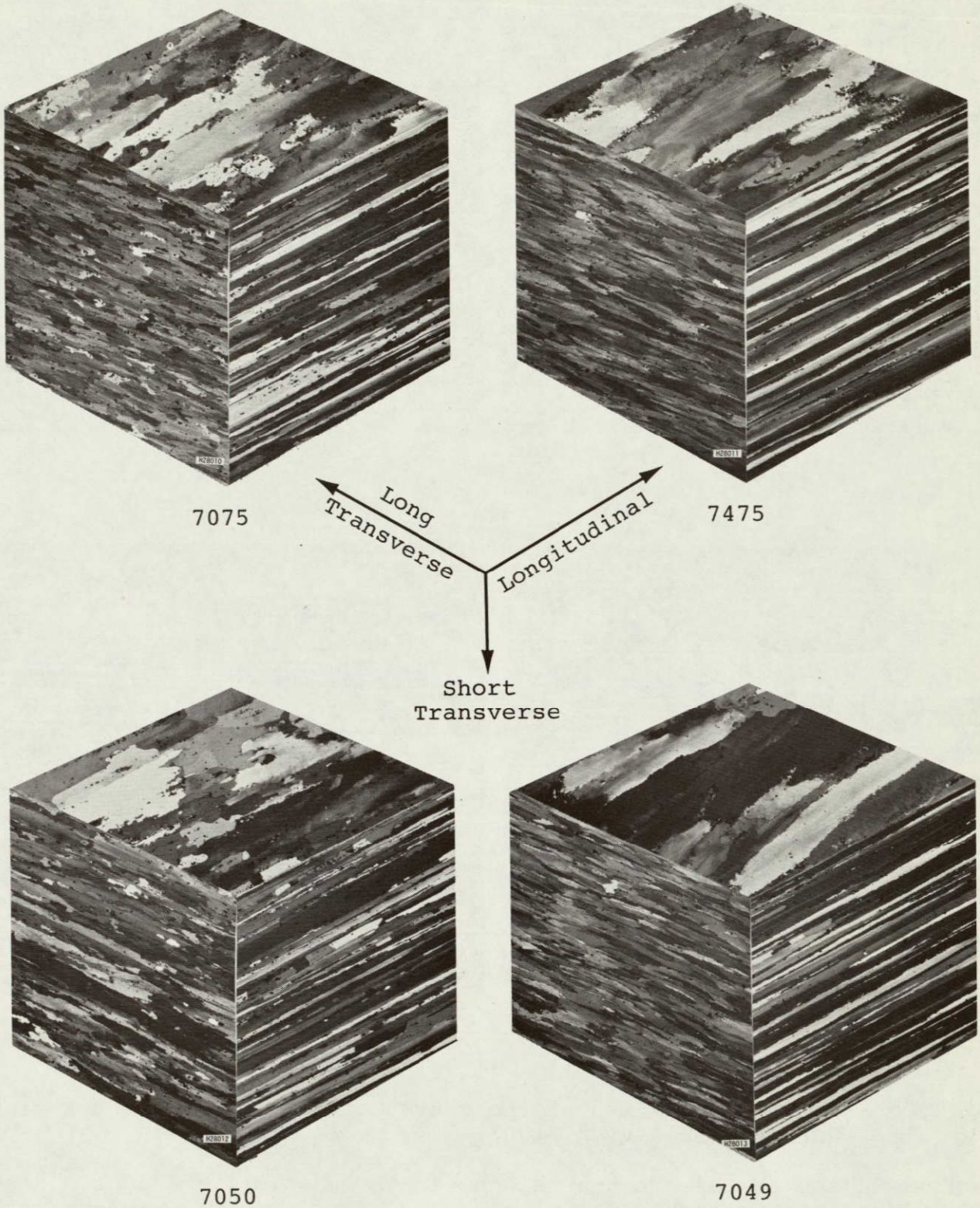

Figure 7. Grain structures of 1.25-in. thick plates (Barker's etch, polarized light, 25X)

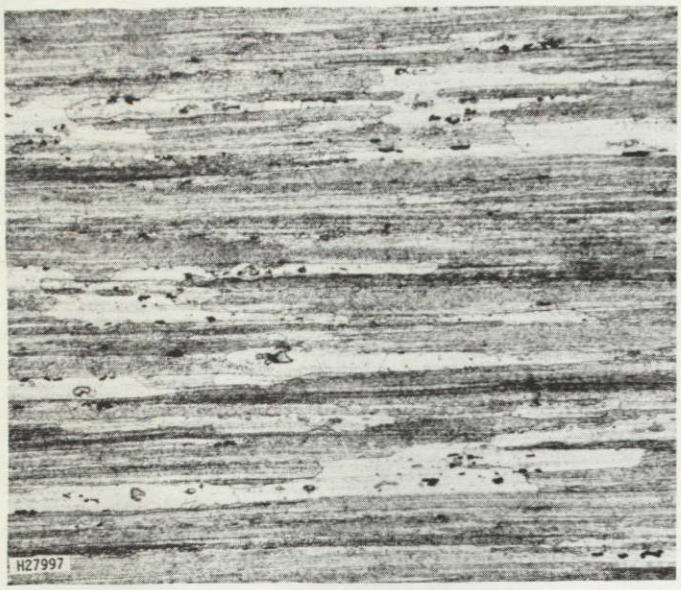

7075

7475

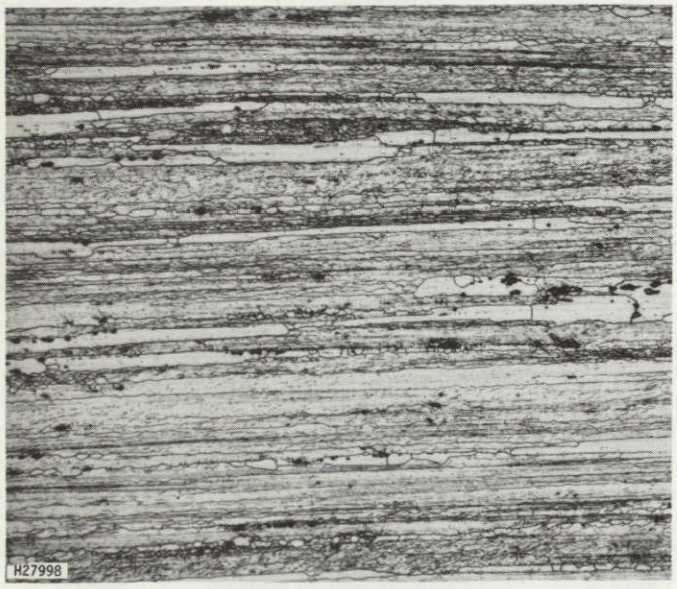

7050

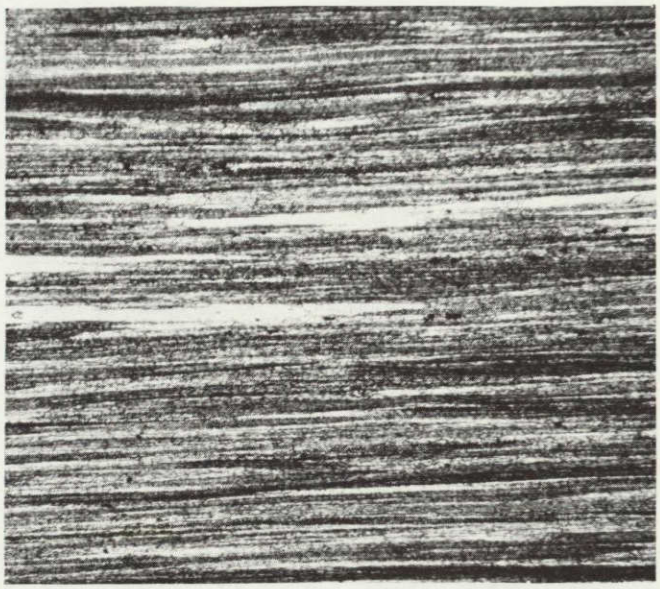

7049

Figure 8. Recrystallization at the center of the 1.25-in. thick plates (Chromic acid etch, 100X)

Recrystallized grains are unattacked (light in color). Amount of recrystallization in each material was:

Alloy	1.25-in.	3.0 in.
7075	20%	trace
7475	trace	trace
7050	20%	20%
7049	5%	5%

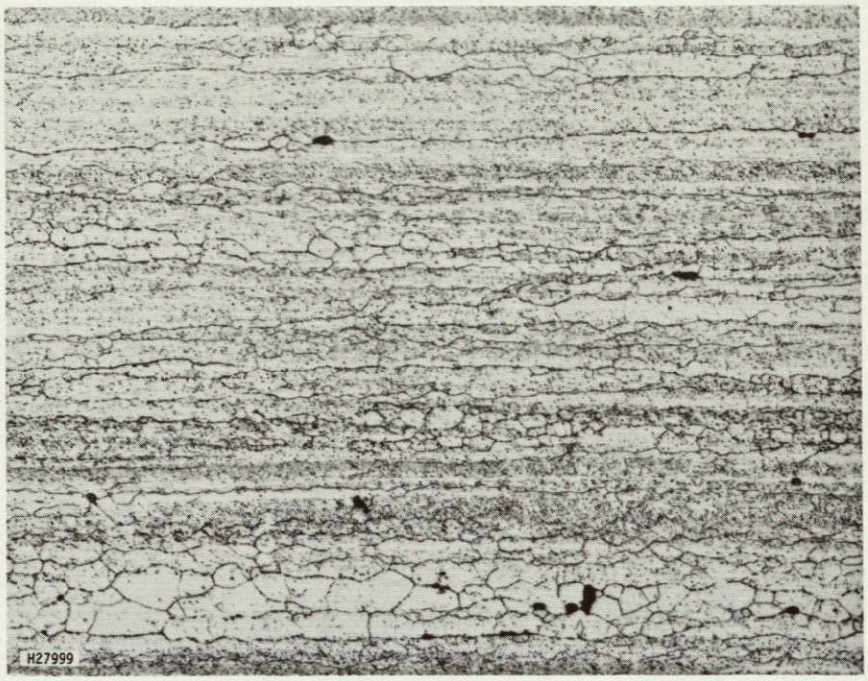

1.25-in. thick 7049

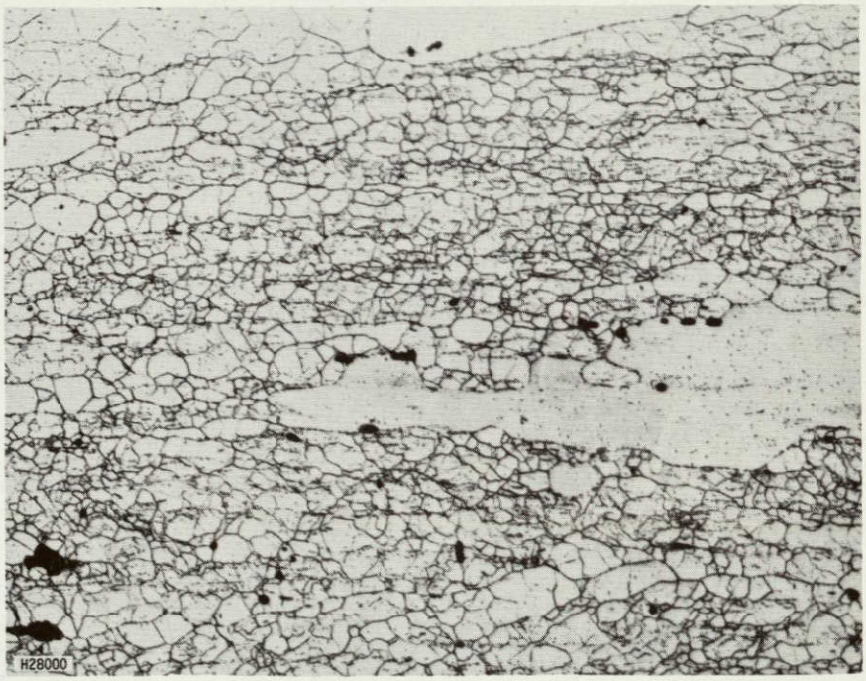

3.0-in. thick 7050

Figure 9. Subgrain structure in 7049 and 7050 plates (H_3PO_4 etch, 500X)

Subgrains were visible in all the plates, but were most evident in 7049 and 7050.

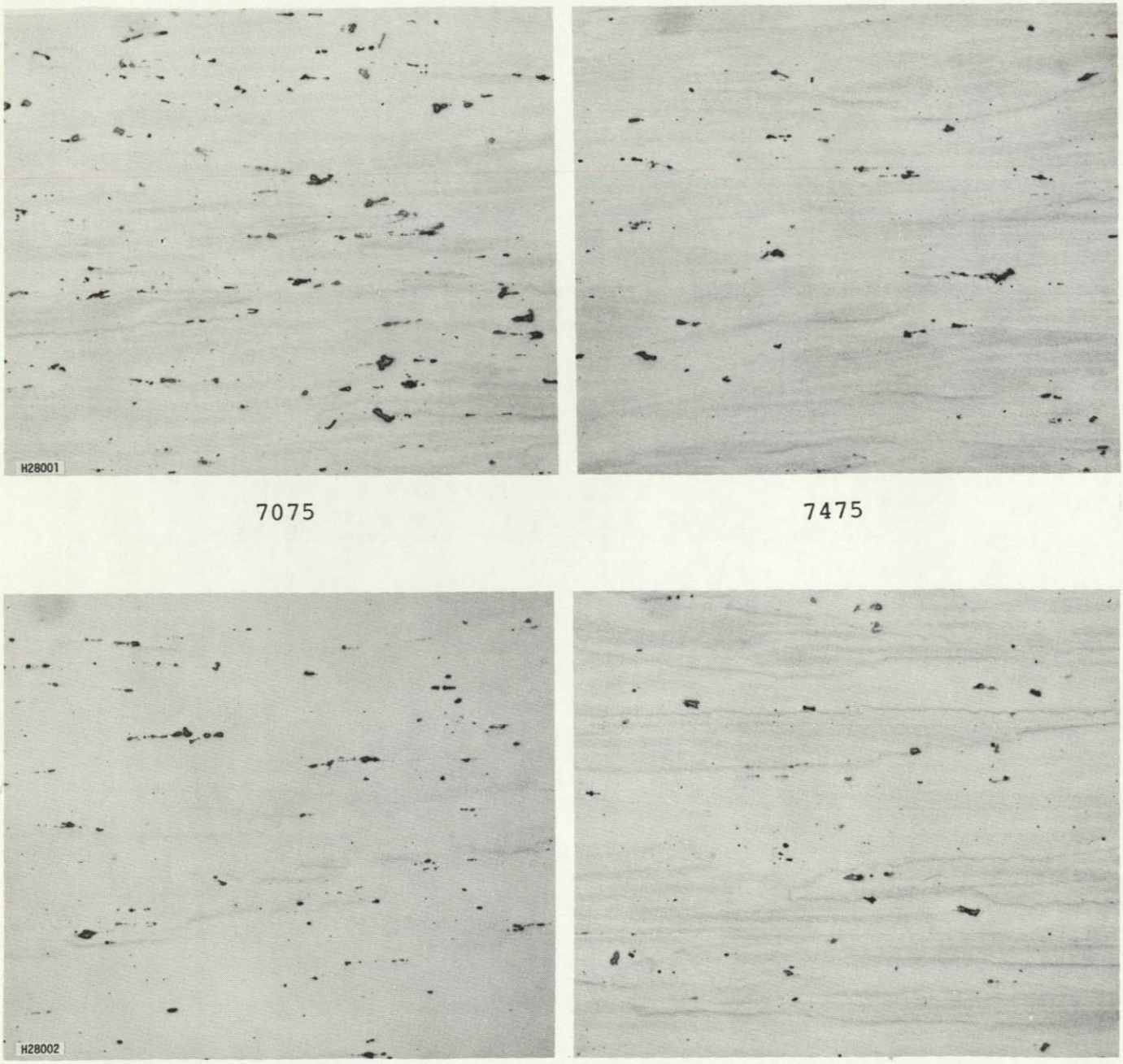

Figure 10. Coarse constituent dispersion in the center of the 3.0-in. thick plates (dilute Keller's etch, 100X)

Lower iron and silicon contents, and a more thorough homogenization treatment reduced the amount of "insoluble" phases in 7475, 7050 and 7049 compared to 7075.

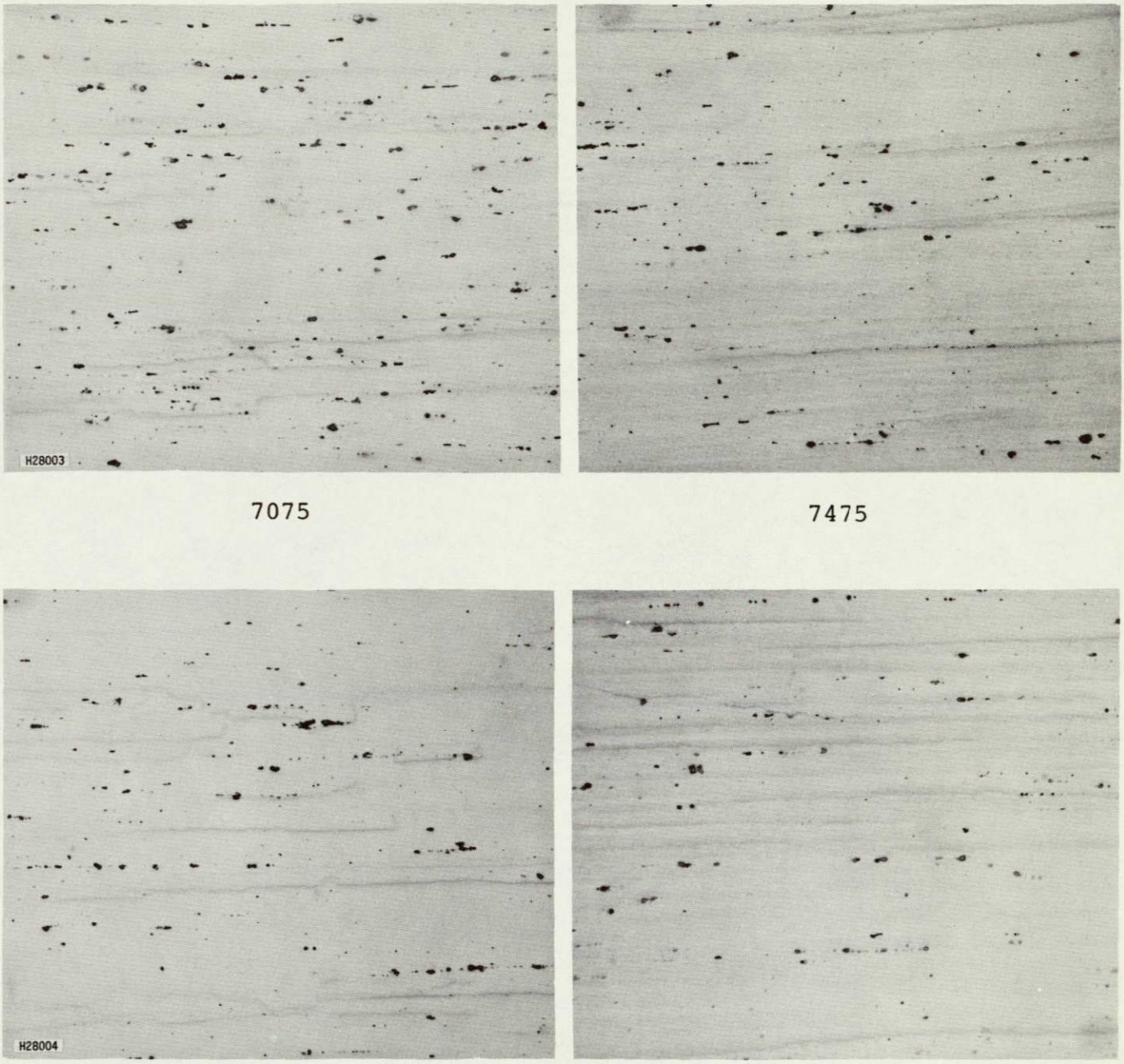

7075 7475

7050 7049

Figure 11. Coarse constituent dispersion in the center of the 1.25-in. thick plates (dilute Keller's etch, 100X)

As in the 3-in. thick material 7475, 7050 and 7049 contained fewer constituents than 7075. These phases were more strung-out in the thinner plates.

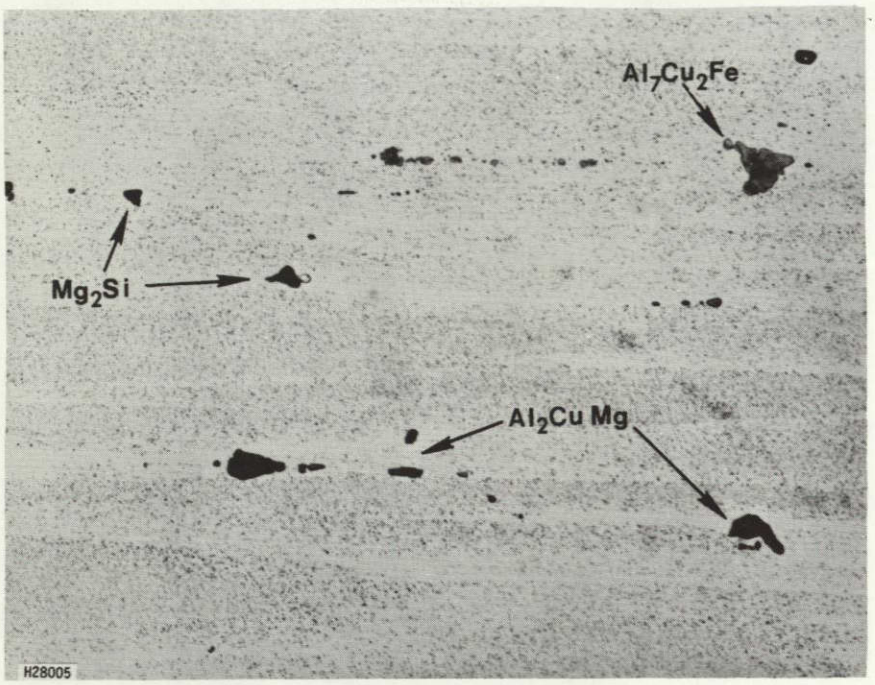

Figure 12. Constituents in 3-in. thick 7475 plate (dilute Keller's etch, 500X)

Most of the coarse "insoluble" phases in all four alloys were Al_7Cu_2Fe, Al_2CuMg and Mg_2Si.

Curves are meaningless

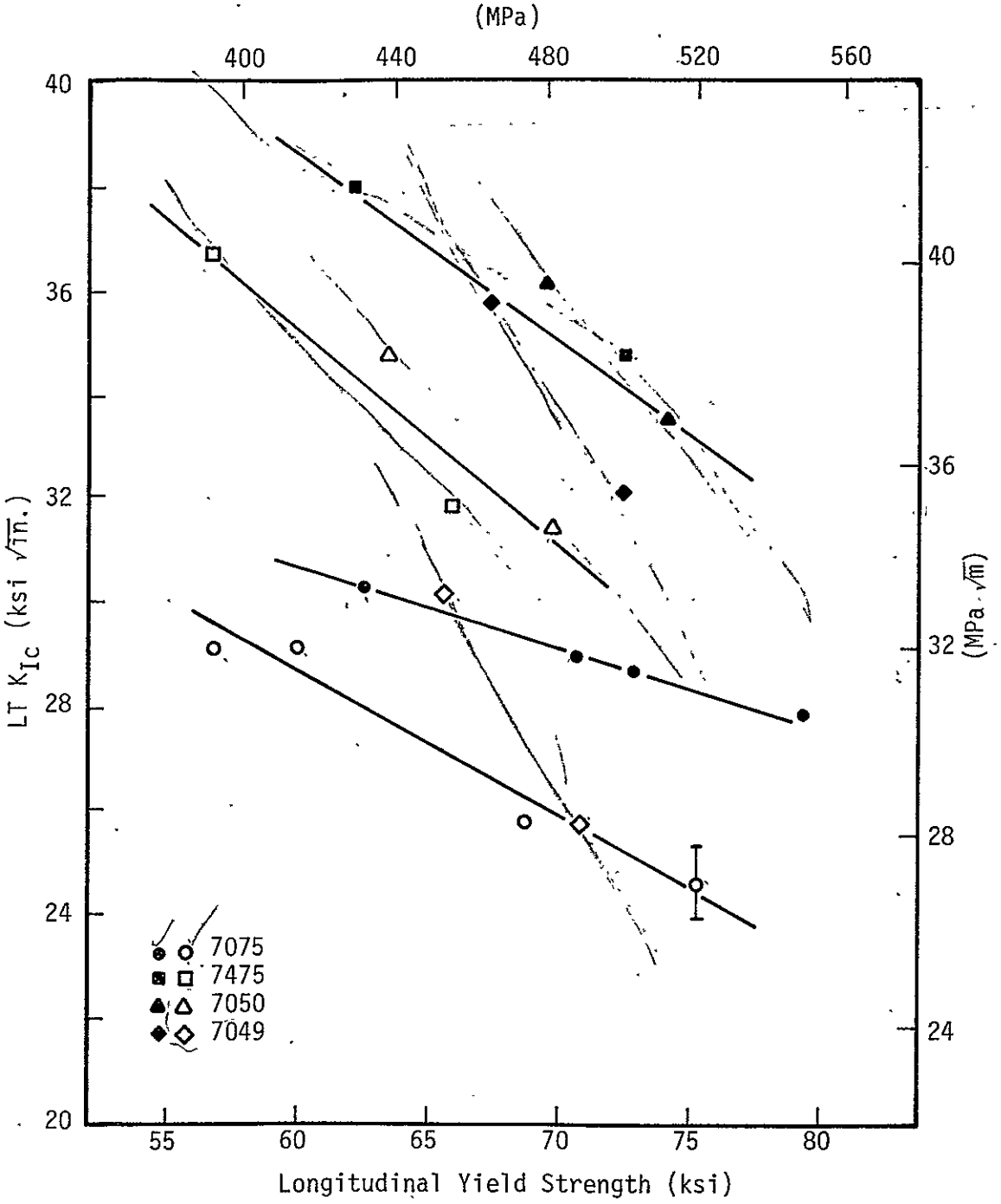

Figure 14. Relationship between longitudinal yield strength and LT fracture toughness

Solid symbols -- 1.25-in. plate
Open symbols -- 3.0-in. plate

Error bar shows best estimate of standard deviation.

Curves cannot be indicated as to direction in this graph for any other than 7075 alloy.

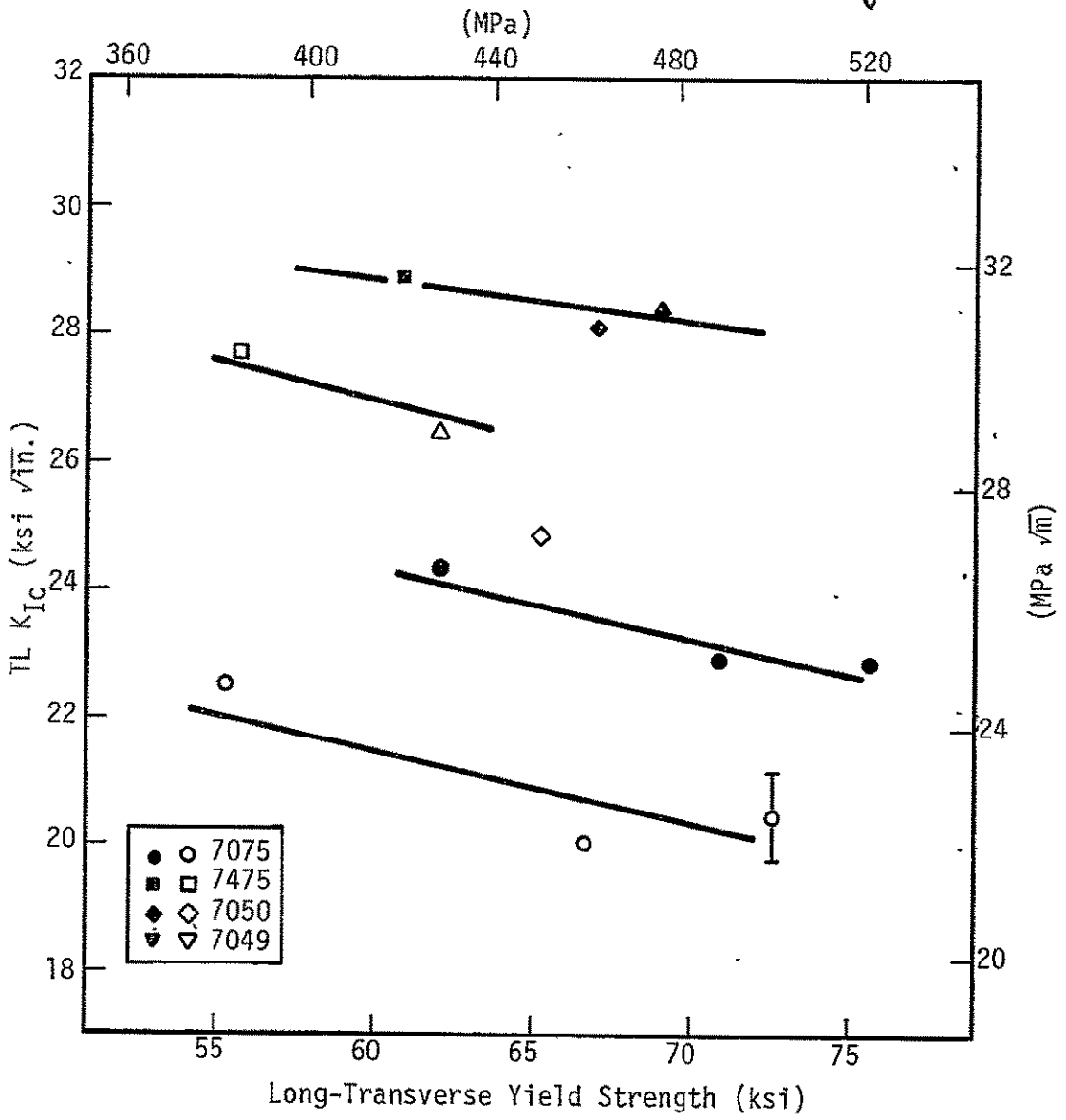

Figure 15. Relationship between long-transverse yield strength and TL fracture toughness

Solid symbols -- 1.25-in. plate
Open symbols -- 3.0-in. plate.

Error bar shows best estimate of standard deviation.

Curves are meaningless

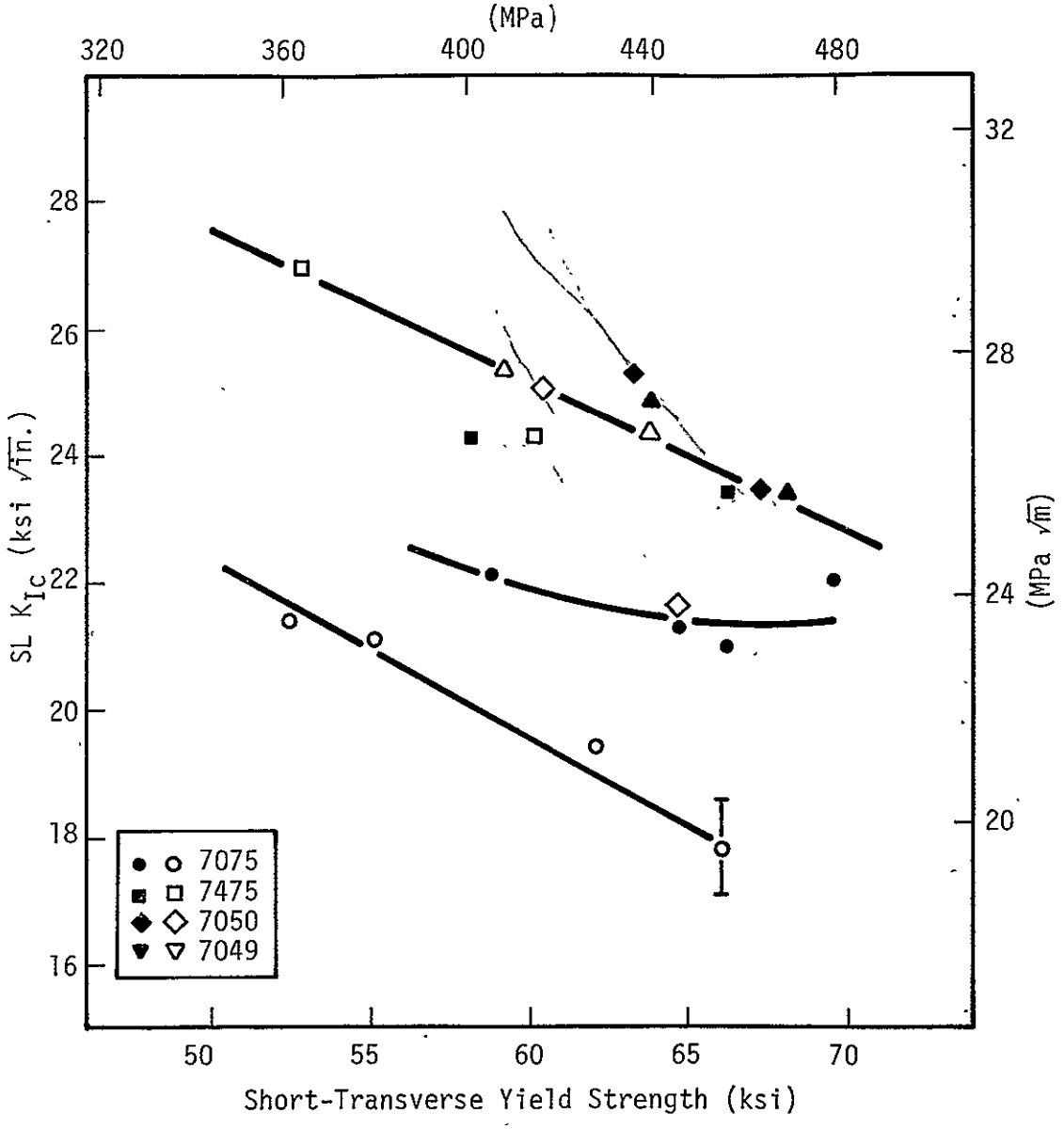

Figure 16. Relationship between short-transverse yield strength and SL fracture toughness.

Solid symbols -- 1.25-in. plate
Open symbols -- 3.0-in. plate

Error bar shows best estimate of standard deviation.

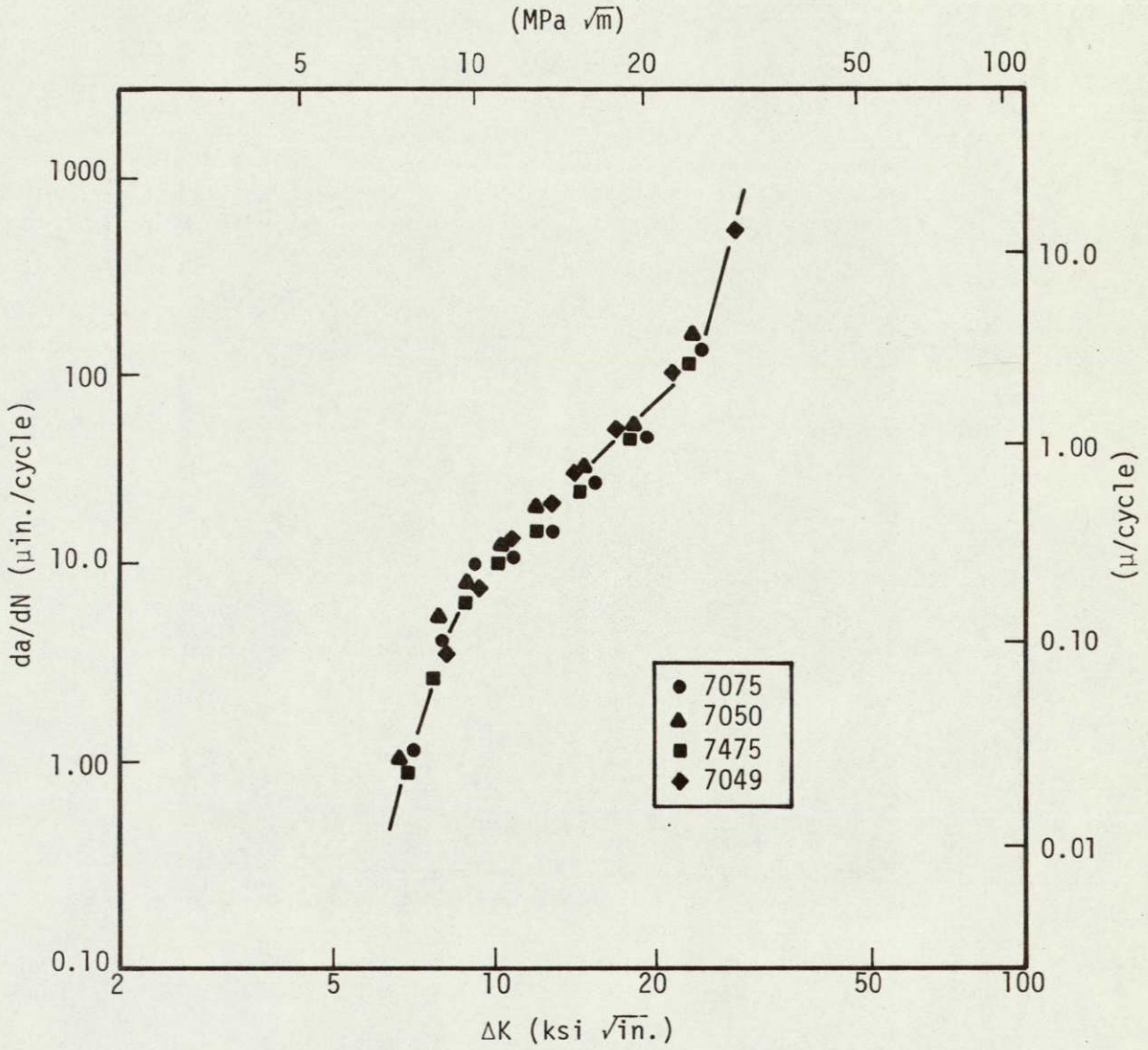

Figure 17. Fatigue crack growth rate curves for 1.25-in. thick plates, TL orientation. All plates in "typical" -T73 temper condition.

Test conditions: 0.1 load ratio, 63 cps frequency, laboratory air environment (20-25% relative humidity).

C-2

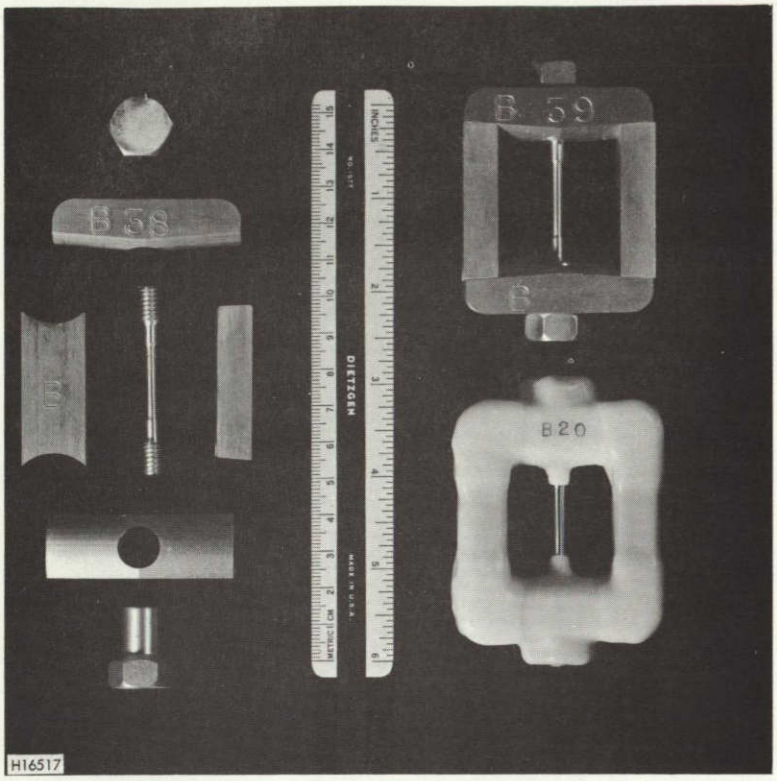

Figure 18. Tensile round stress-corrosion specimen and stressing frame

Left: 1/8-in. diameter tensile specimen and components of the stressing frame.

Upper Right: Assembled frame with specimen as it appears before stressing.

Lower Right: Stressed specimen and frame coated with 5% polyethylene-paraffin wax.

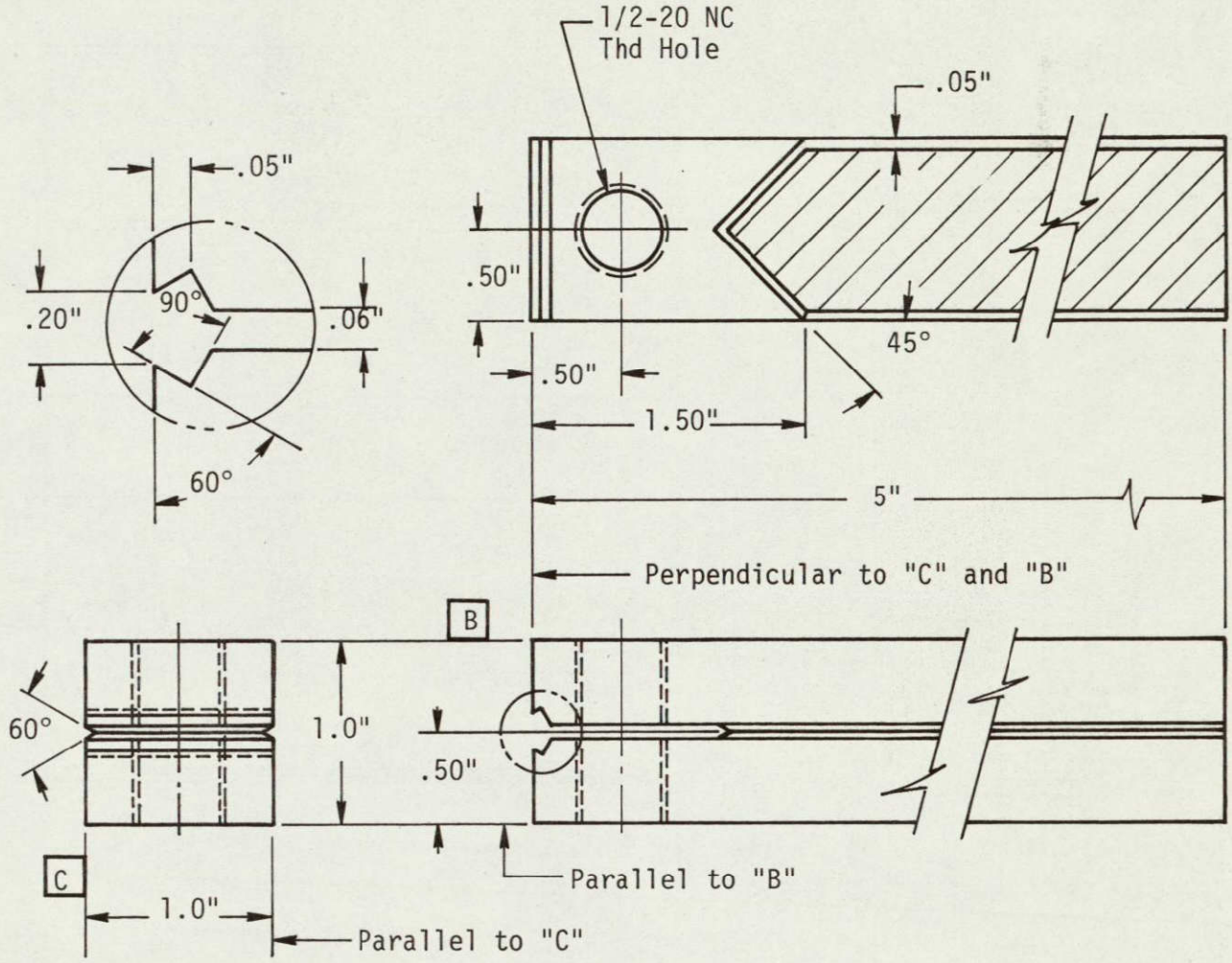

Figure 19. 25-mm constant deflection DCB specimen

The constant load specimens contained 0.25-in. diam. pin-loading holes rather than threaded bolt holes. Bolt-loaded fatigue-precracked specimens contained both bolt holes and pin-loading holes. (All dimensions in inches.)

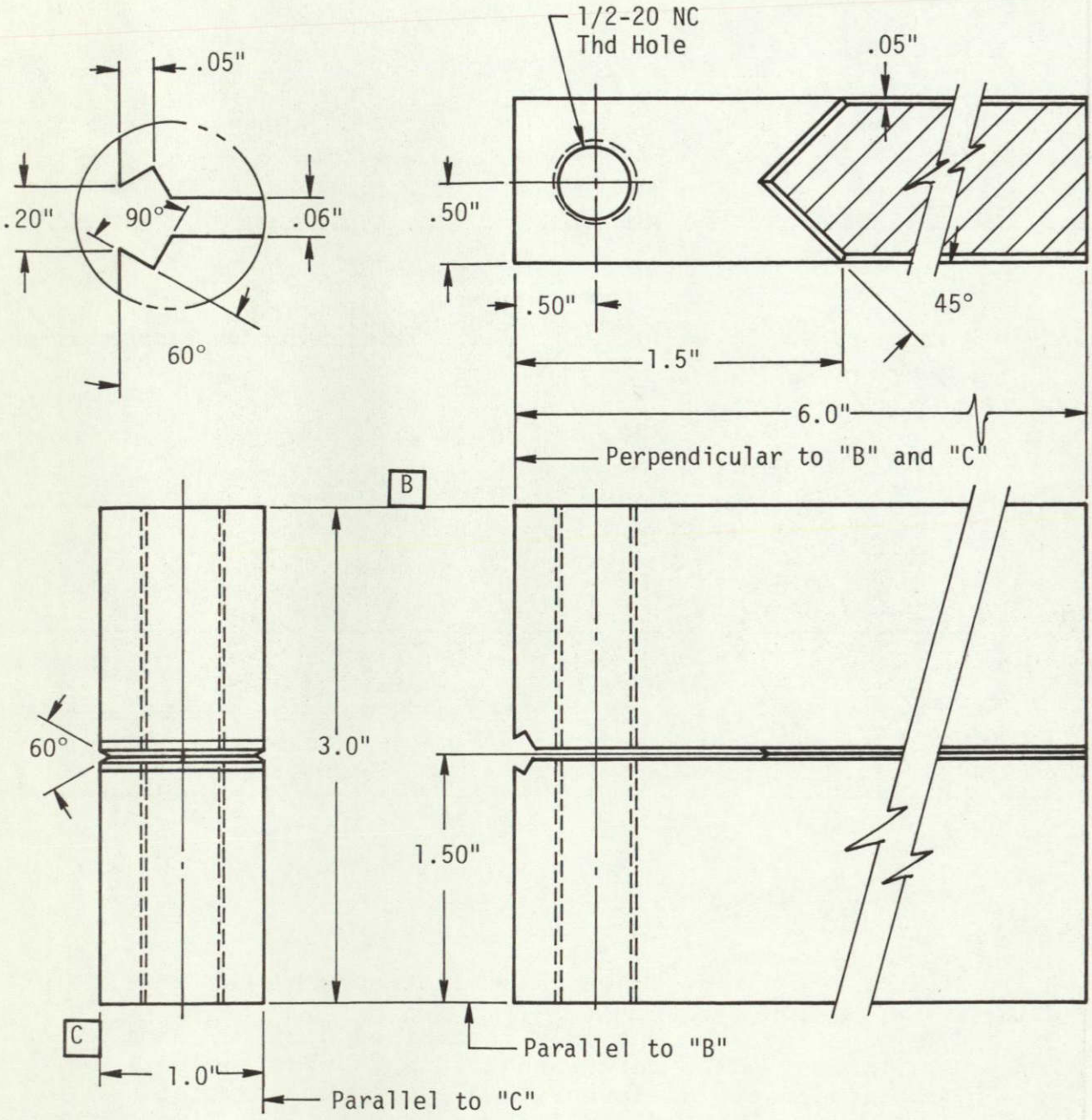

Figure 20. 75-mm constant deflection DCB specimen
(All dimensions in inches)

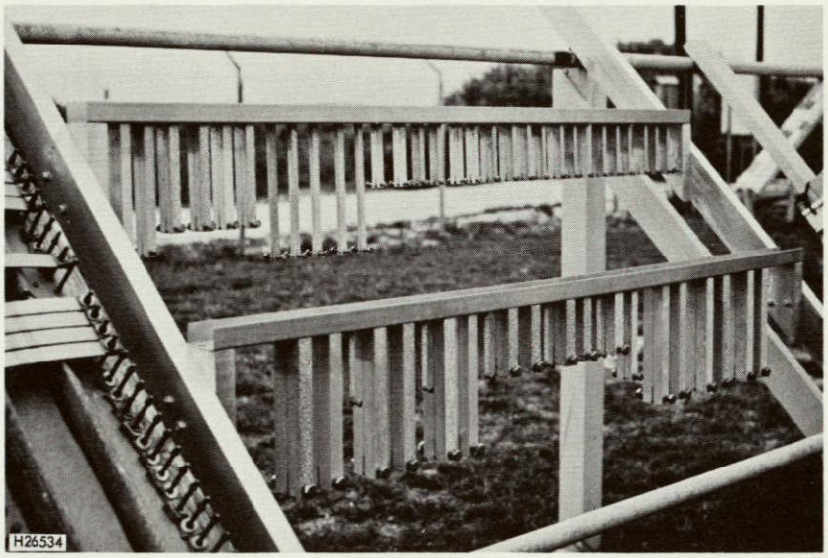

Figure 21. Bolt-loaded DCB specimens on exposure at the oceanfront site near Daytona Beach, Florida

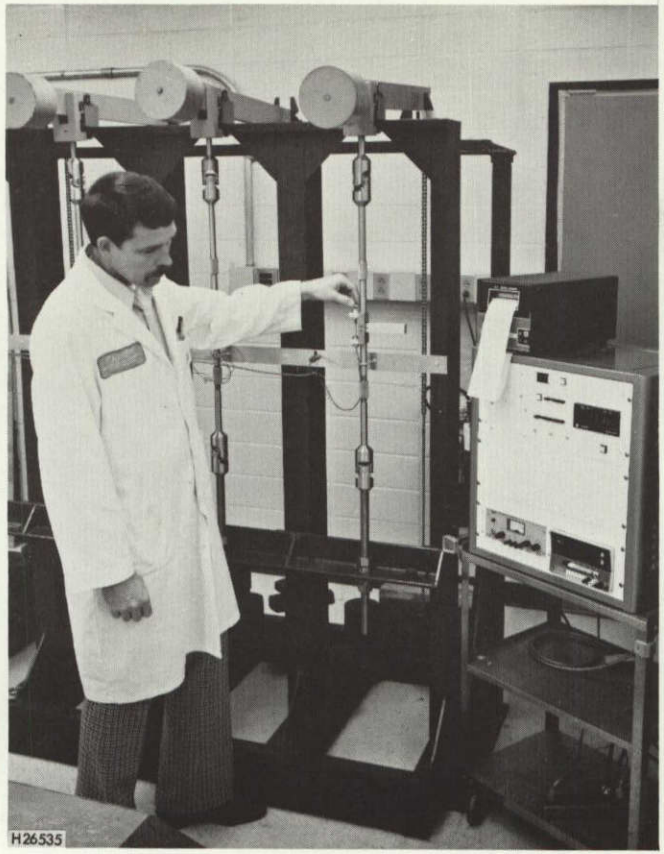

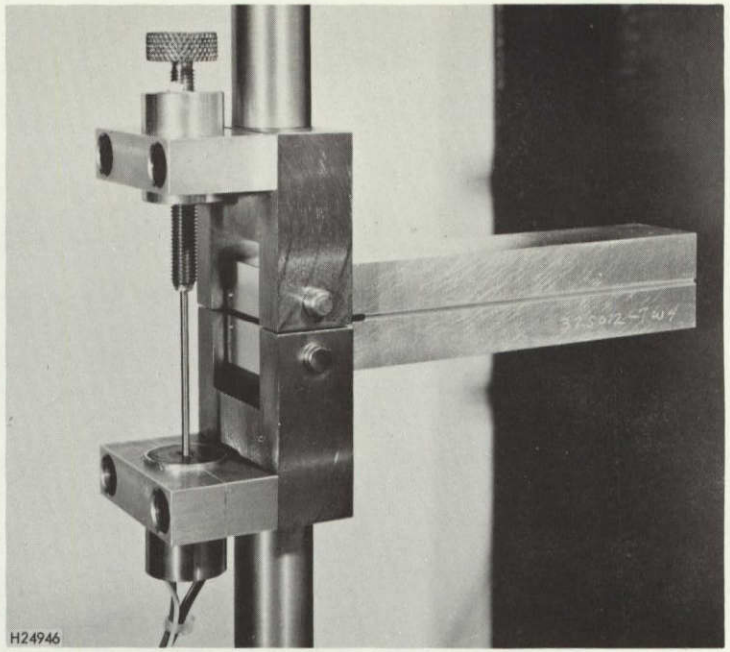

Figure 22. Direct load tests of DCB specimens

Left: Creep rupture stands used to apply a constant load to DCB specimens. Power supply and digital voltmeter for excitation and recording of output (respectively) from LVDT's.

Right: DCB specimen and the LVDT used to monitor deflection of the specimen are shown in greater detail.

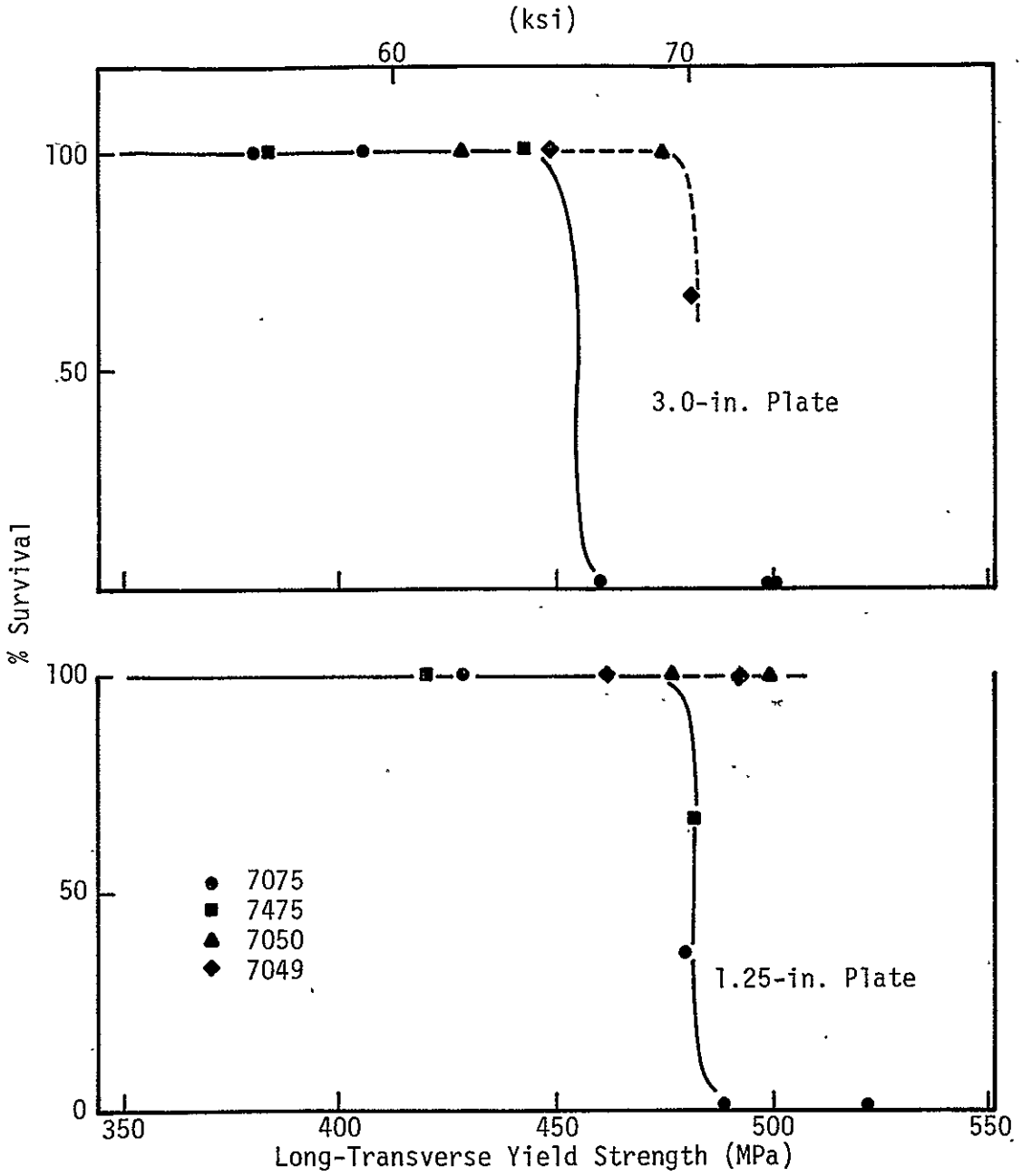

Figure 24. Effect of strength level on survival rate of smooth tensile specimens: synthetic seawater, alternate immersion, 45 ksi stress level, 100 days

Critical yield strength for 7075 was about 450 MPa (3.0-in. plate) and 480 MPa (1.25-in. plate).

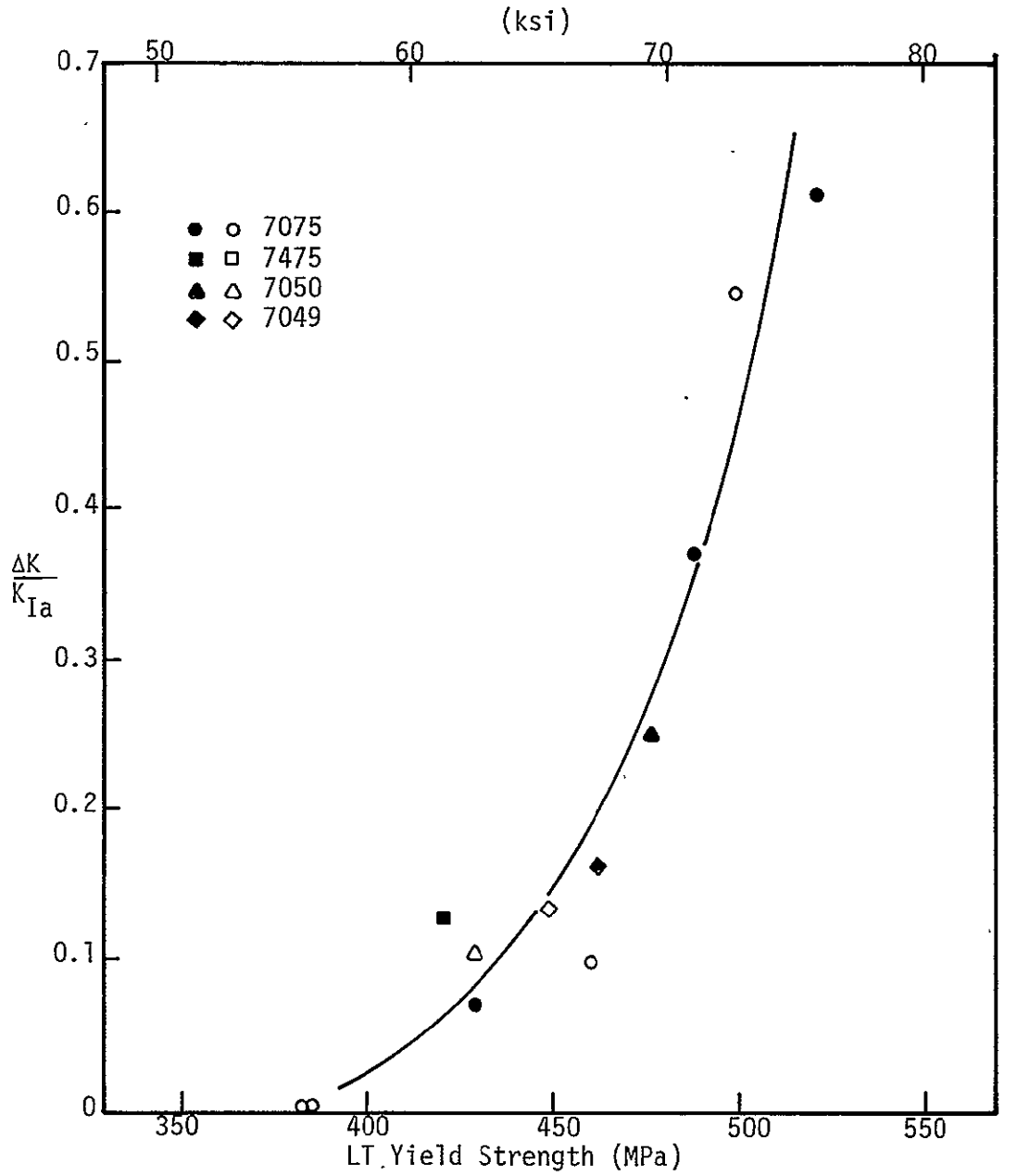

Figure 25. Dependence of $\Delta K/K_{Ia}$ on strength: 6.5-mo exposure at Daytona Beach

All materials fell on same general curve (solid symbols, 1.25-in. plate; open symbols, 3.0-in. plate).

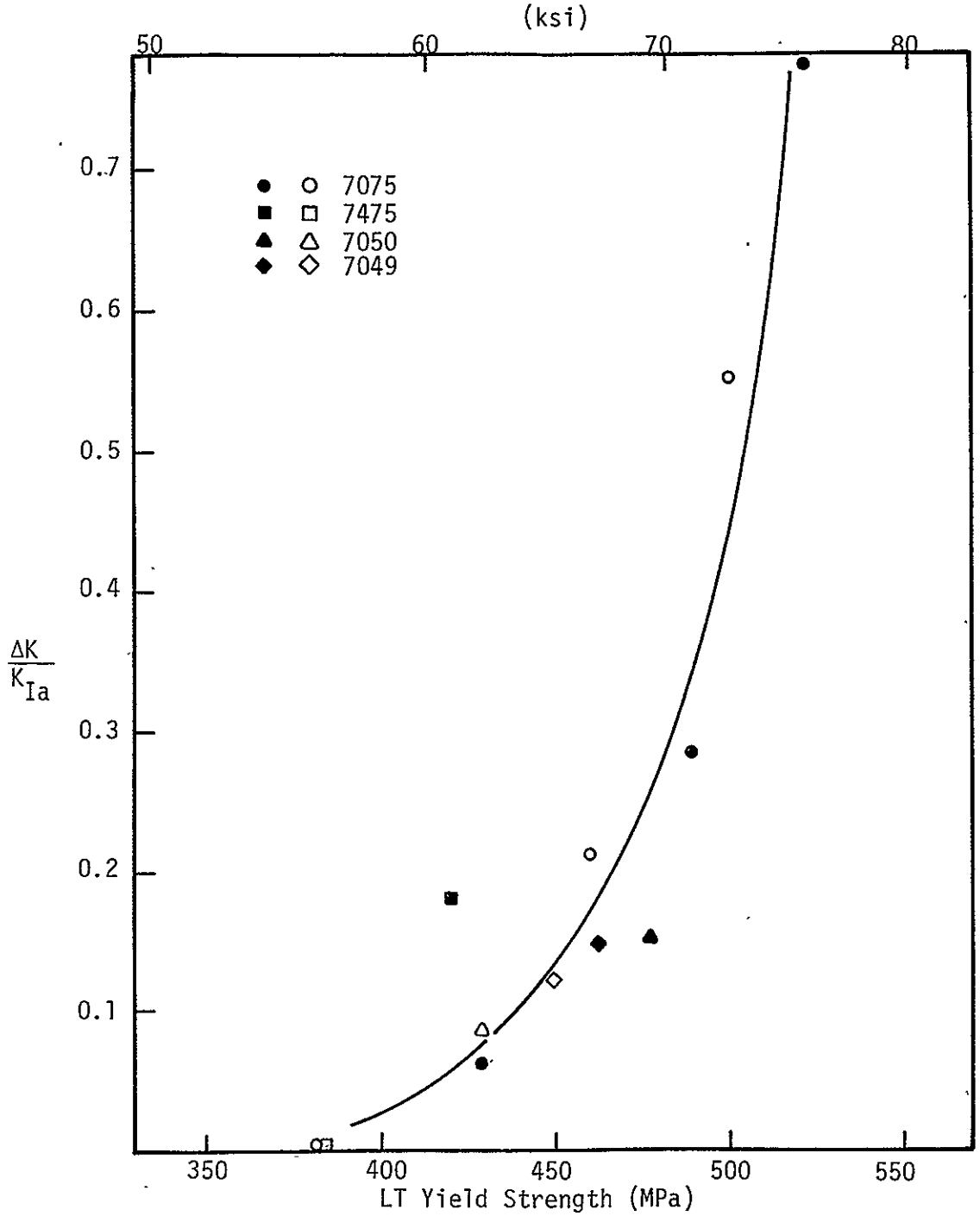

Figure 26. Dependence of $\Delta K/K_{Ia}$ on strength: 6-mo. synthetic seawater immersion (alternate immersion)

Relationship was quite similar to that for Daytona Beach exposure, with no alloy or thickness effects evident (solid symbols, 1.25-in. plate; open symbols, 3.0-in. plate).

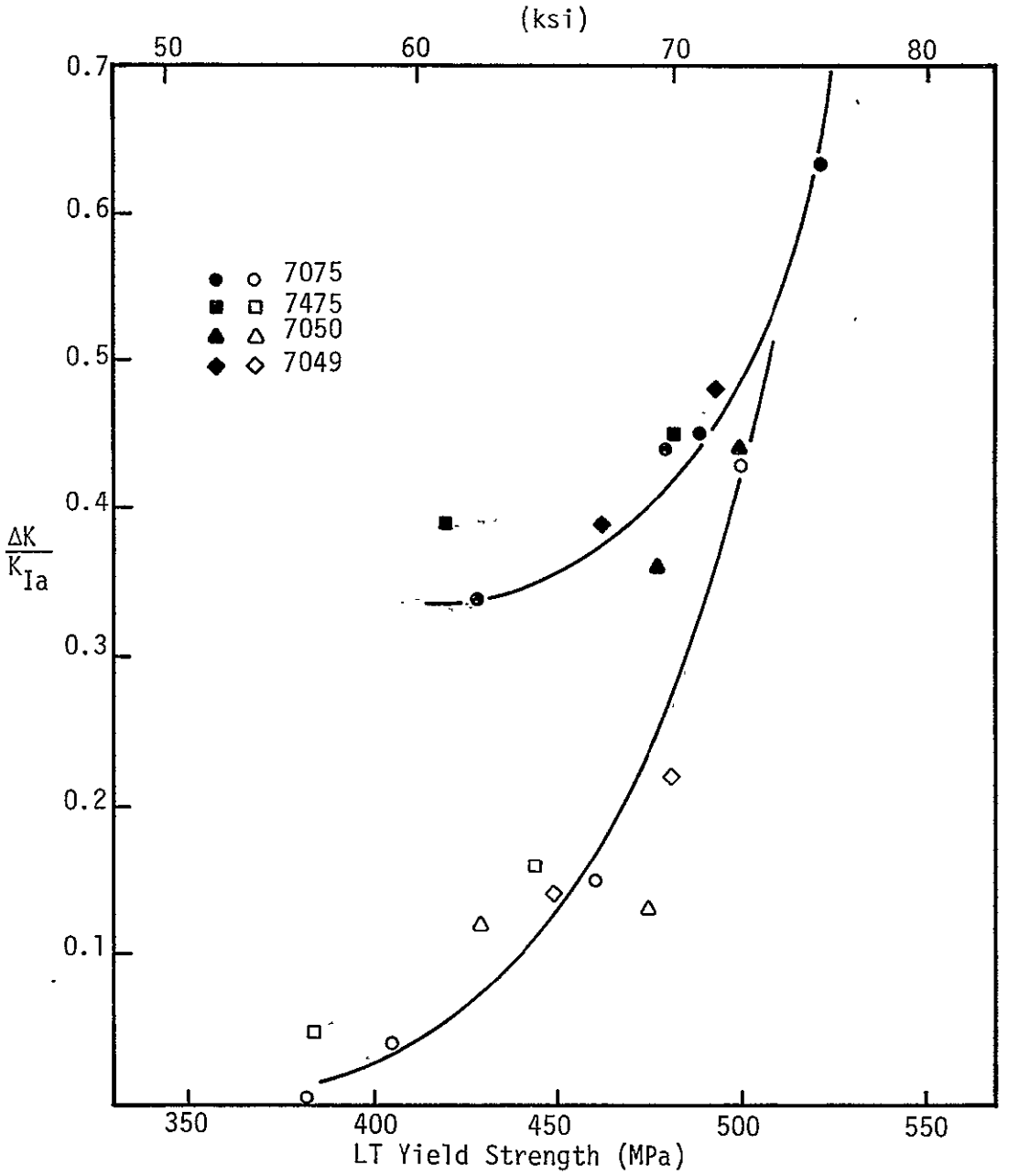

Figure 27. Dependence of $\Delta K/K_{Ia}$ on strength: 6-month exposure to salt-chromate solution

Unlike the other two environments, the two plate thicknesses fell on separate curves (solid symbols, 1.25-in. plate; open symbols, 3.0-in. plate).

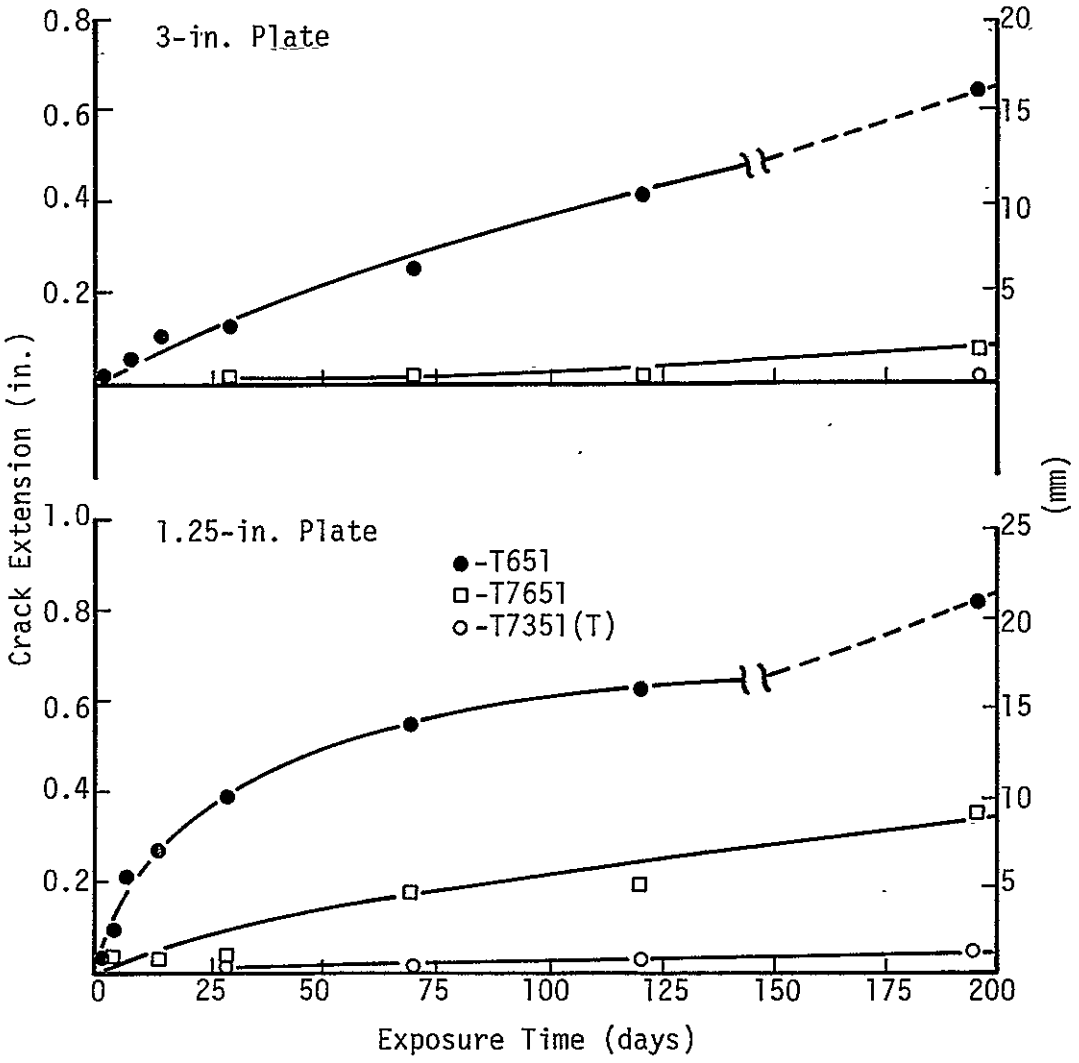

Figure 28. Crack growth in 7075 DCB specimens exposed to marine agmosphere (Daytona Beach): SL orientation, pop-in precrack

-T6 and -T76 tempers: single specimens
-T73 temper: average of 3 replicates

All data are for 1-in. high specimens. No crack growth occurred in the 3-in. thick -T7351 temper plate

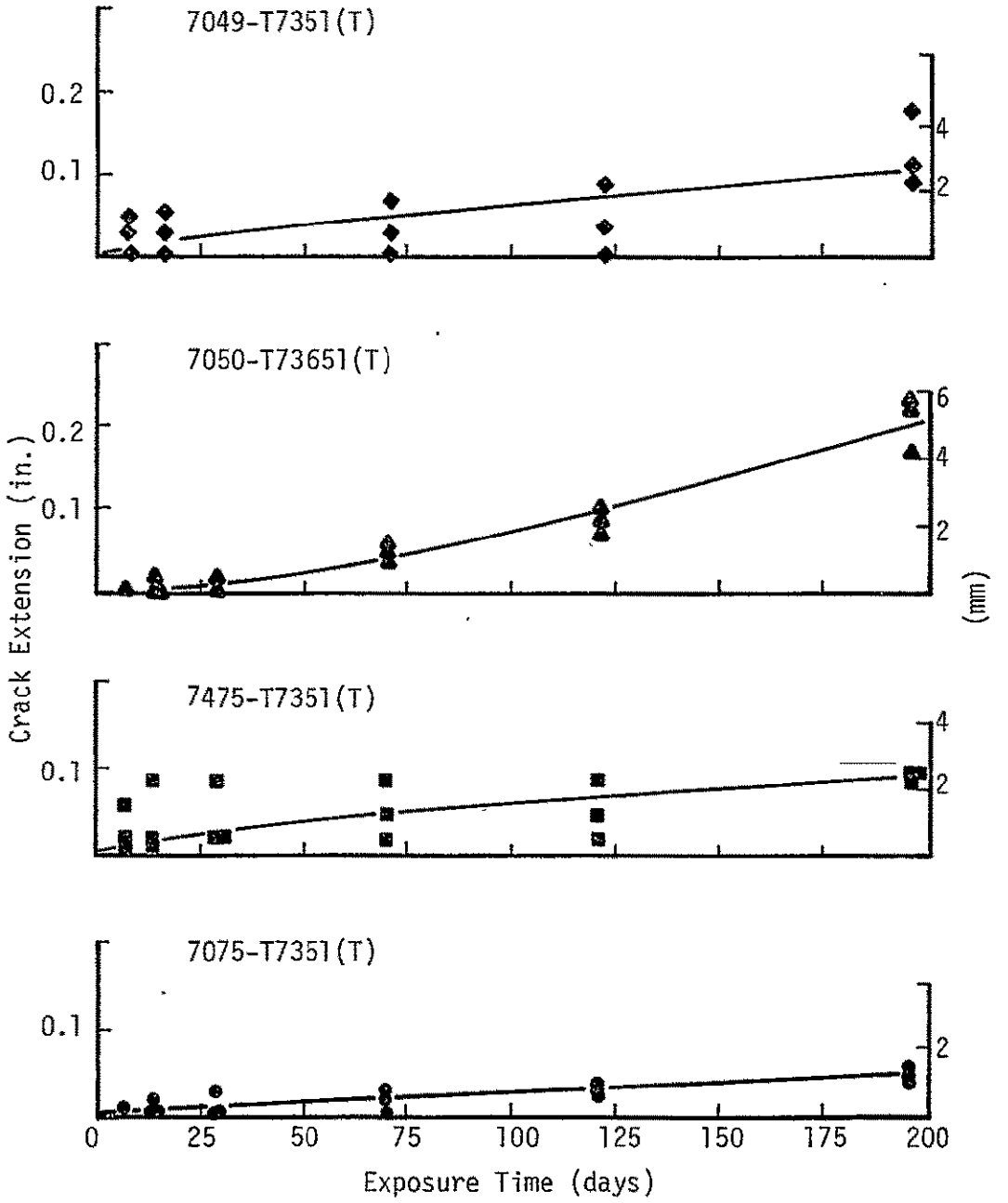

Figure 29. Crack growth in 1.25-in. -T73 temper plates at Daytona Beach: SL orientation, pop-in precrack

There was considerable scatter between replicate samples. Note also apparent incubation period for 7050.

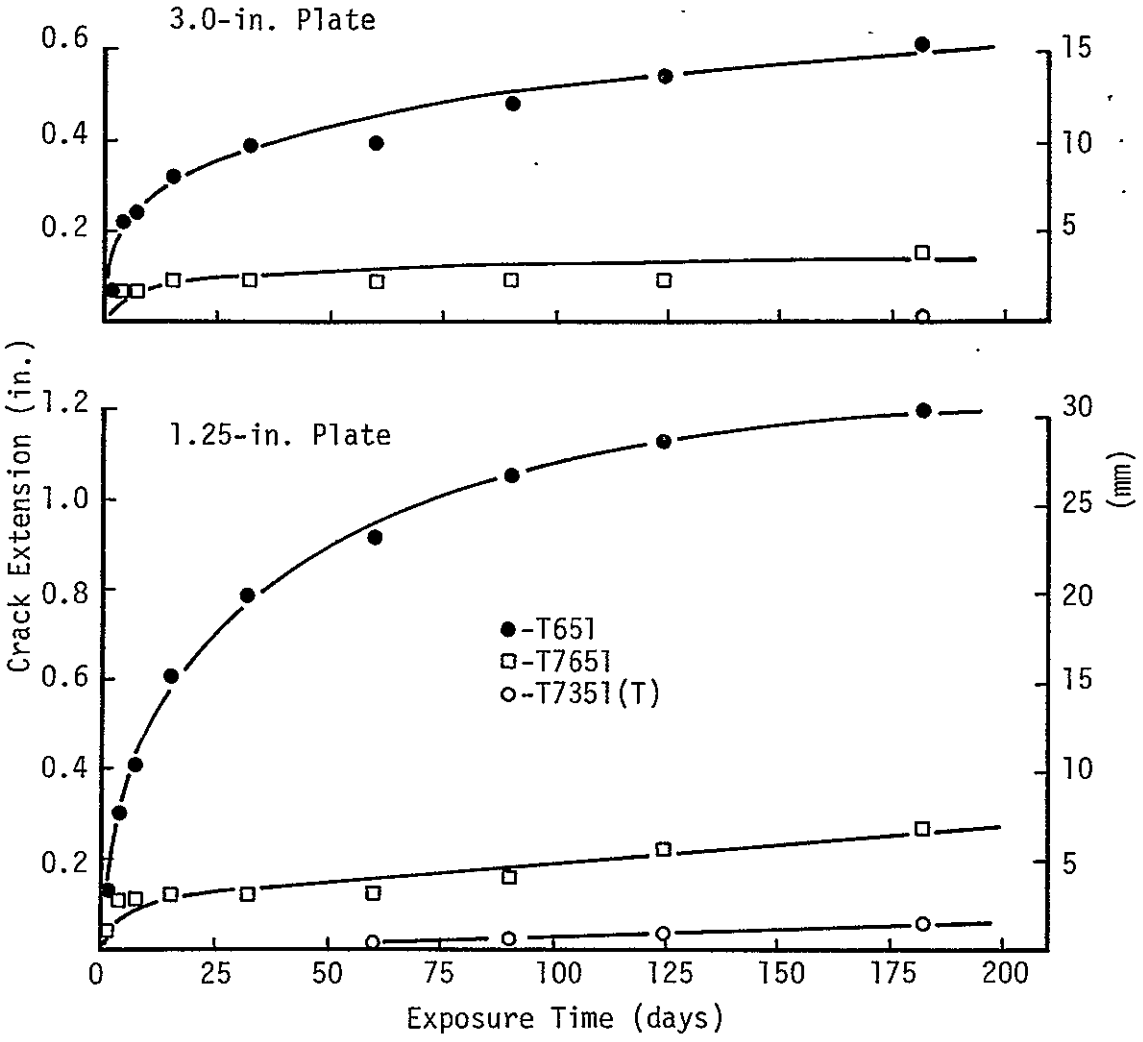

Figure 30. Crack growth in 7075 DCB specimens exposed to immersion in synthetic seawater: SL orientation, pop-in precrack

-T6 and -T76 temper: single specimens
-T73 temper: average of 2 replicates for 3.0-in. plate, 6 replicates for 1.25-in. plate

Crack growth was much more extensive in thinner plates (no crack extension was observed in 3.0-in. -T73 material).

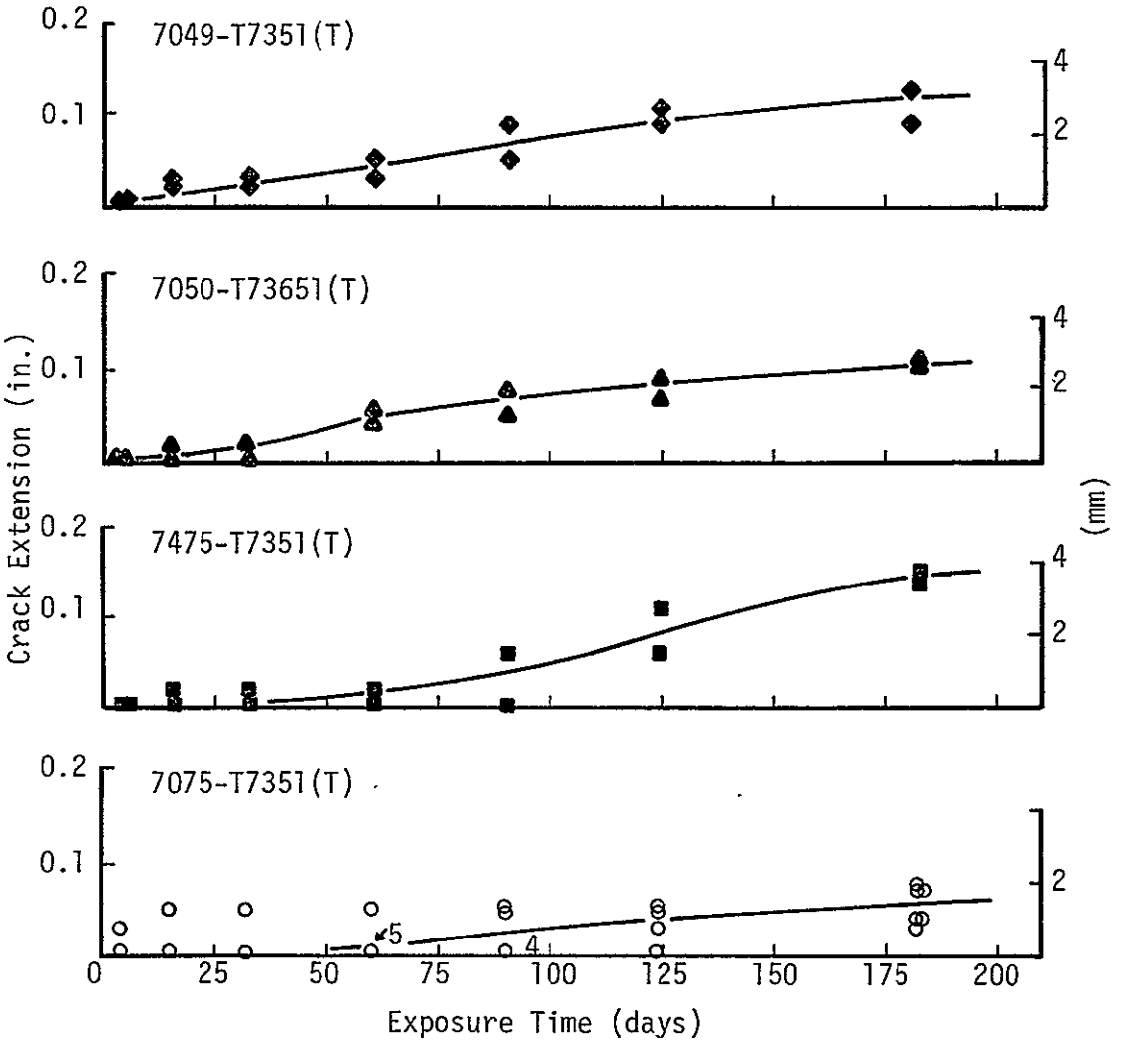

Figure 31. Crack growth in 1.25-in. -T73 temper plates for synthetic seawater exposure: SL orientation, pop-in precrack

An incubation period was evident for all materials.

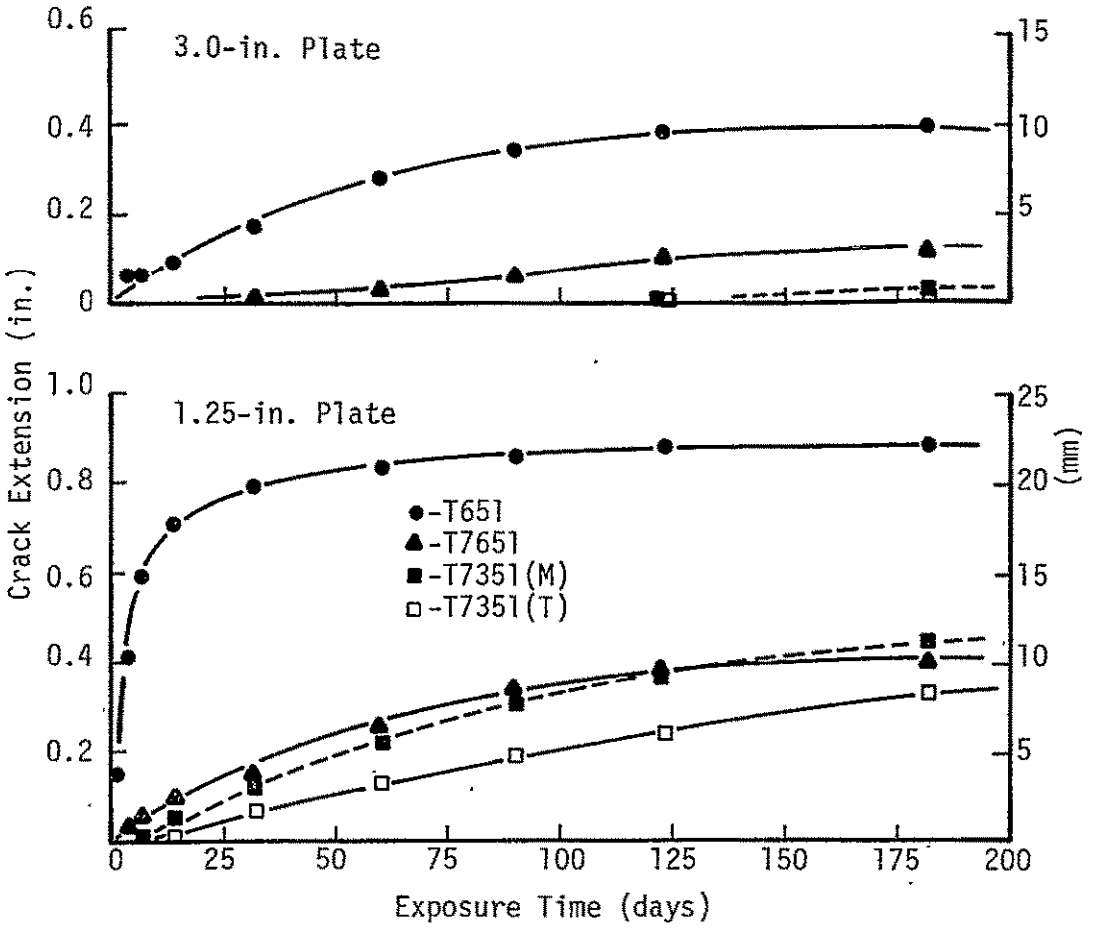

Figure 32. Crack growth in 7075 DCB specimens exposed to continuous immersion in salt-chromate solution: SL orientation, pop-in precrack

This environment produced a great deal of crack growth in the 1.25-in. -T73 materials.

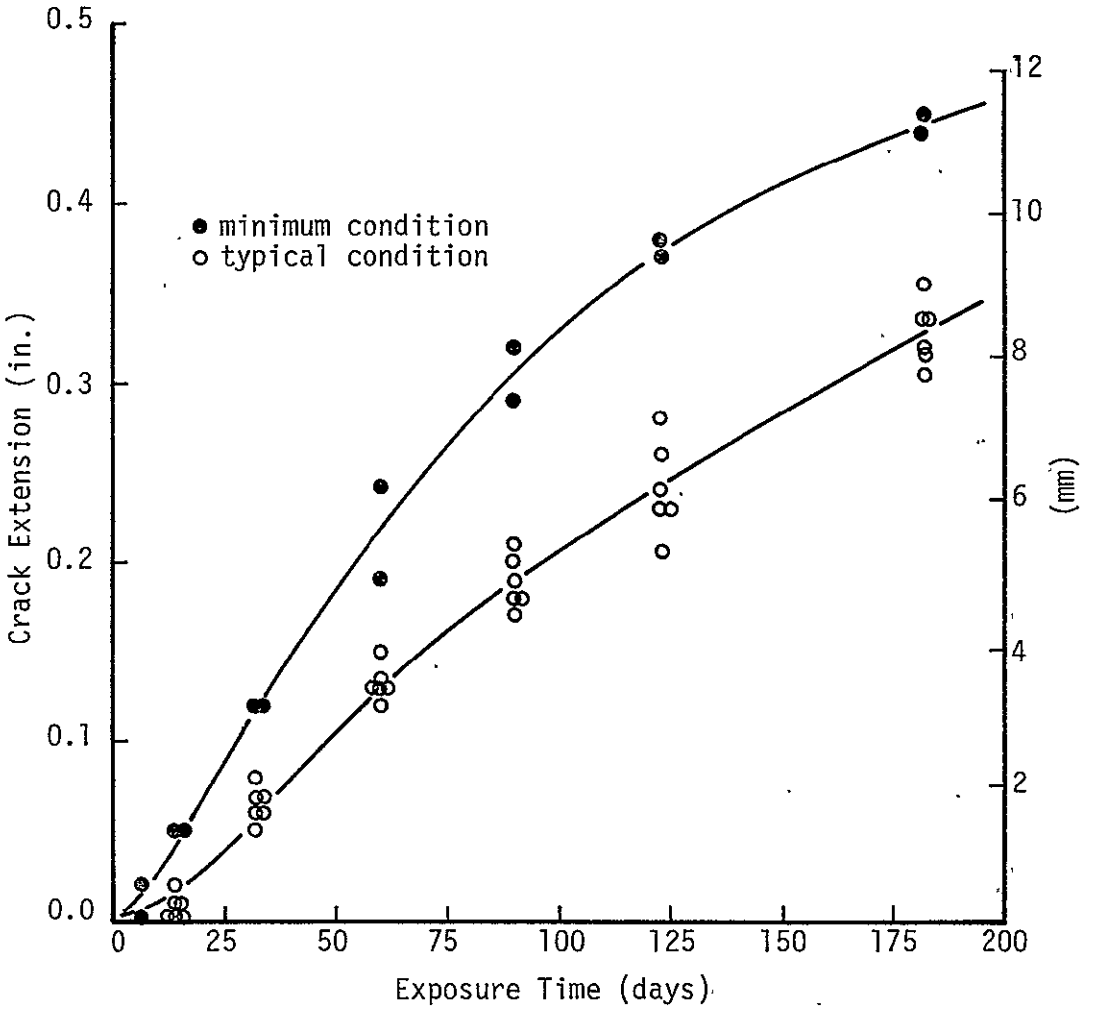

Figure 33. Crack growth in 7075-T7351 DCB specimens exposed to salt-chromate solution: SL orientation, pop-in precrack, 1.25-in. plate

Agreement between replicate specimens was quite good

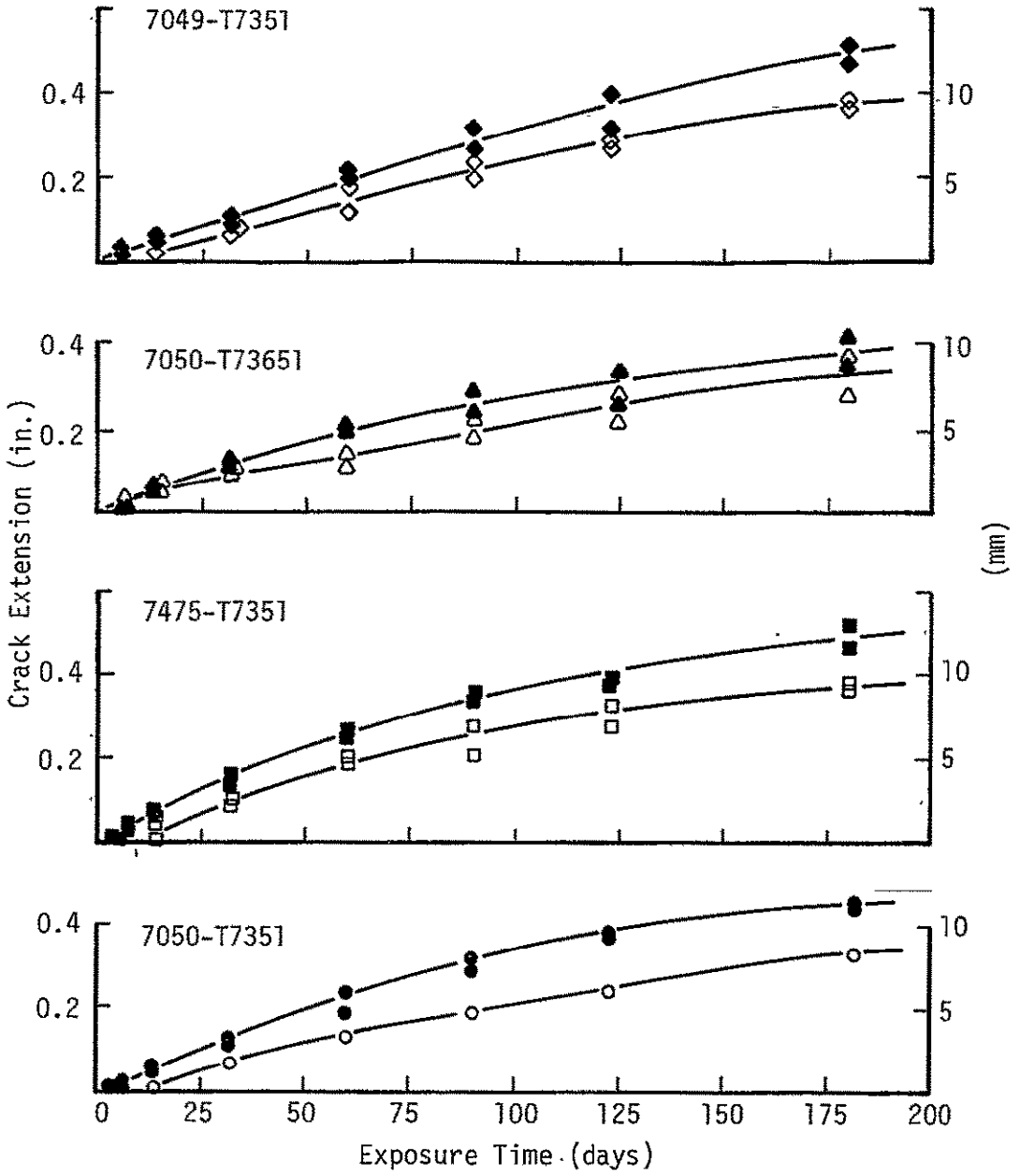

Figure 34. Crack growth in 1.25-in. -T73 temper plates exposed to salt-chromate solution: SL orientation, pop-in precrack

7075-T7351(T): Average of 6 replicates
Solid symbols--Minimum condition
Open symbols--typical condition

In spite of extensive crack growth in these materials, an incubation period was still evident.

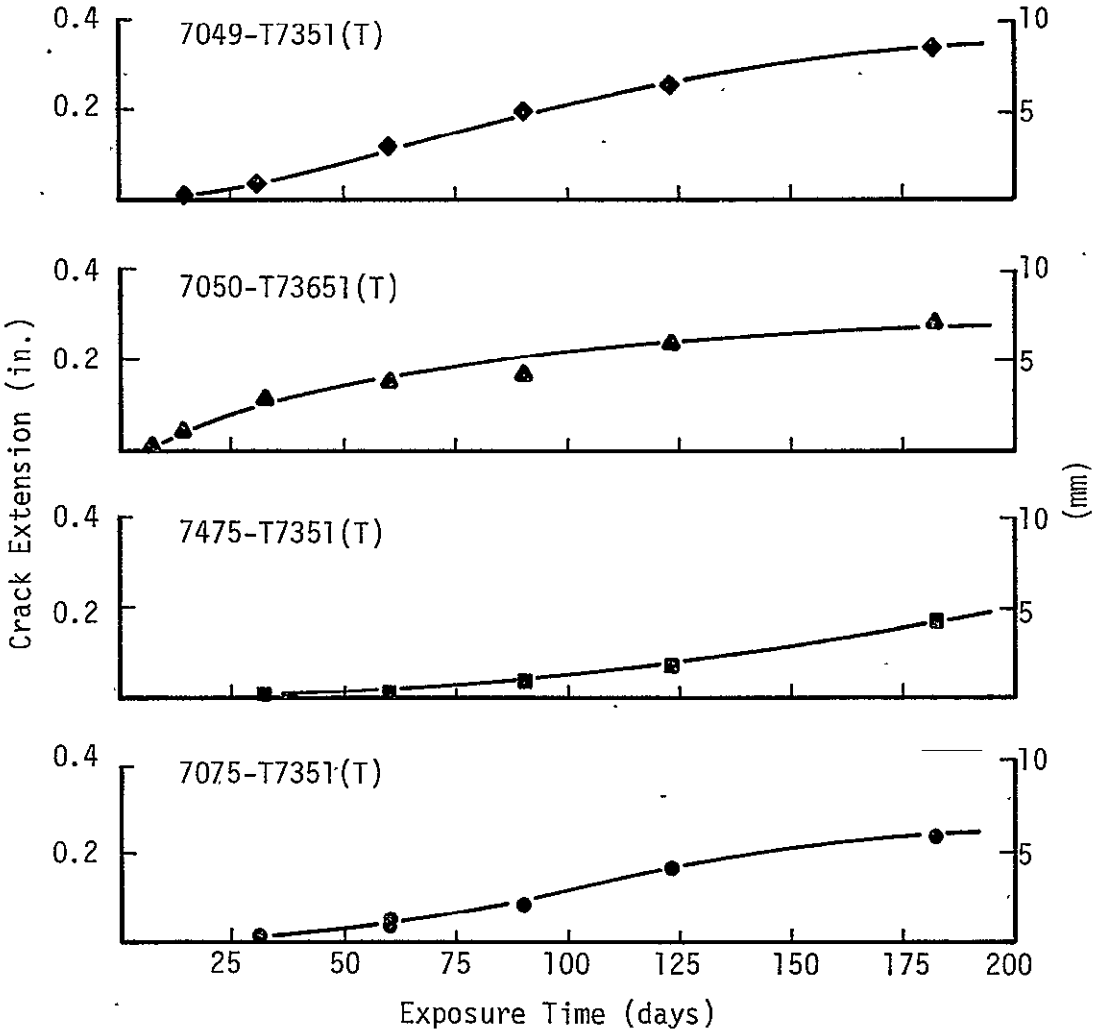

Figure 35. Crack growth in 1.25-in. -T73 temper plates exposed to salt-chromate solution: SL orientation, fatigue precrack

Incubation effects were more apparent in these specimens than in those containing pop-in precracks

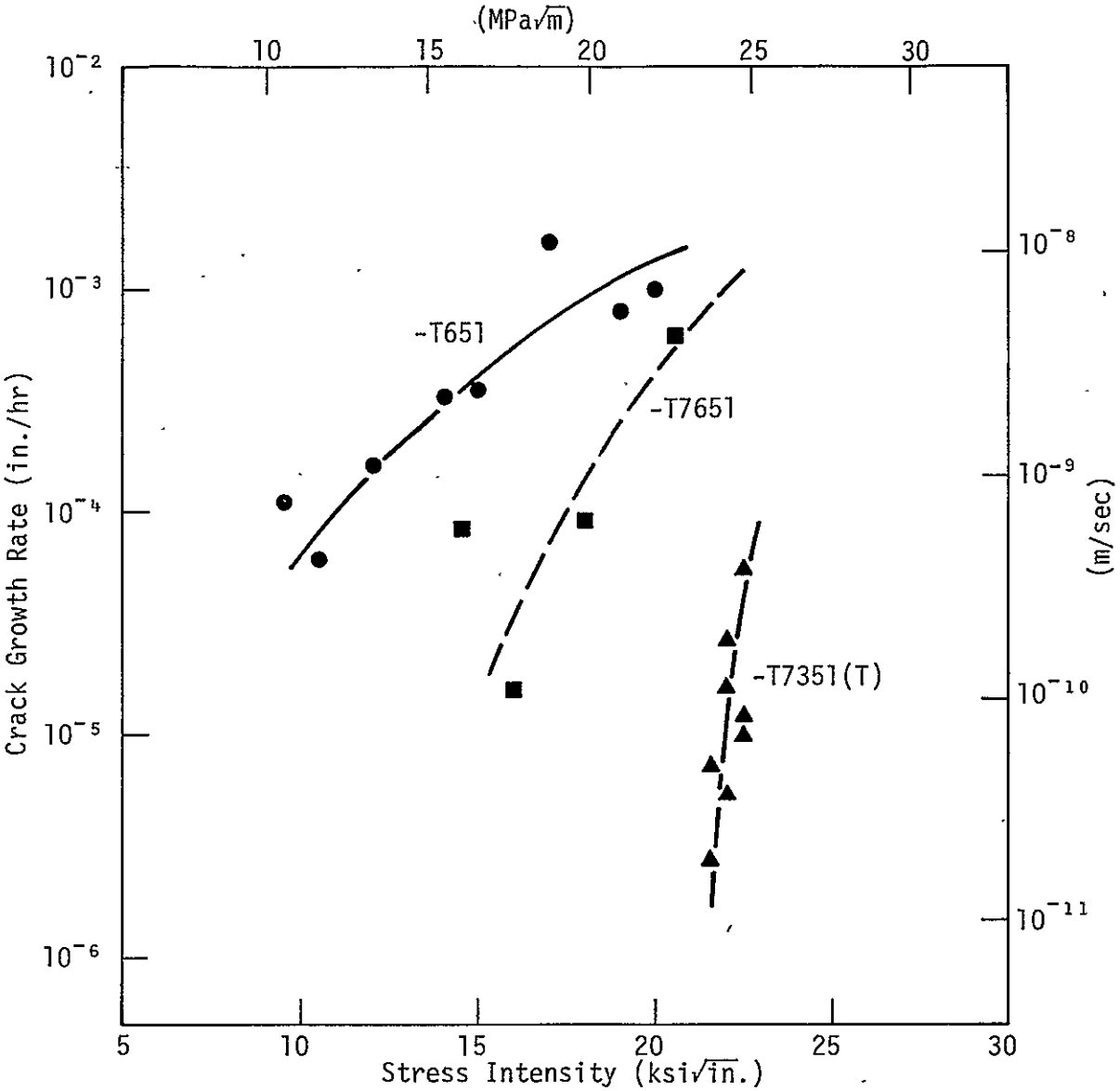

Figure 36. V-K plots for 1.25-in. thick 7075 plates at Daytona Beach: SL orientation, pop-in precracks

Crack velocity for a given stress intensity increased in the order -T7351, -T7651, -T651. Note trend towards a plateau region (V independent of K) for the -T651 temper.

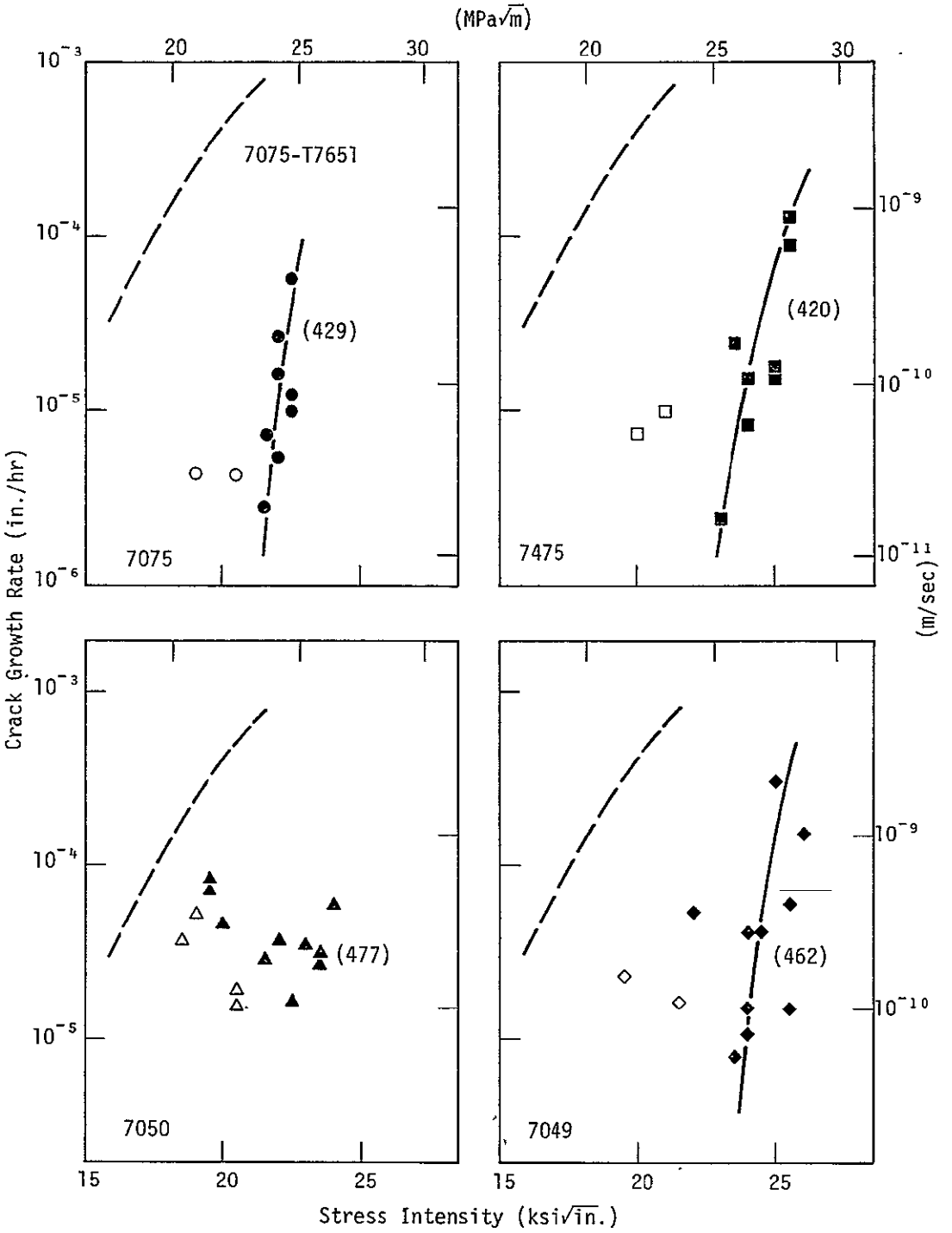

Figure 37. V-K plots for 1.25-in. thick -T73(T) temper plates at Daytona Beach: SL orientation

Solid symbols: pop-in precracks
Open symbols: fatigue precracks

Numbers in brackets are LT yield strengths (MPa). Dashed line represents 7075-T7651 in all cases (489 MPa yield strength). Specimens with fatigue precracks appeared more susceptible than those with pop-in precracks.

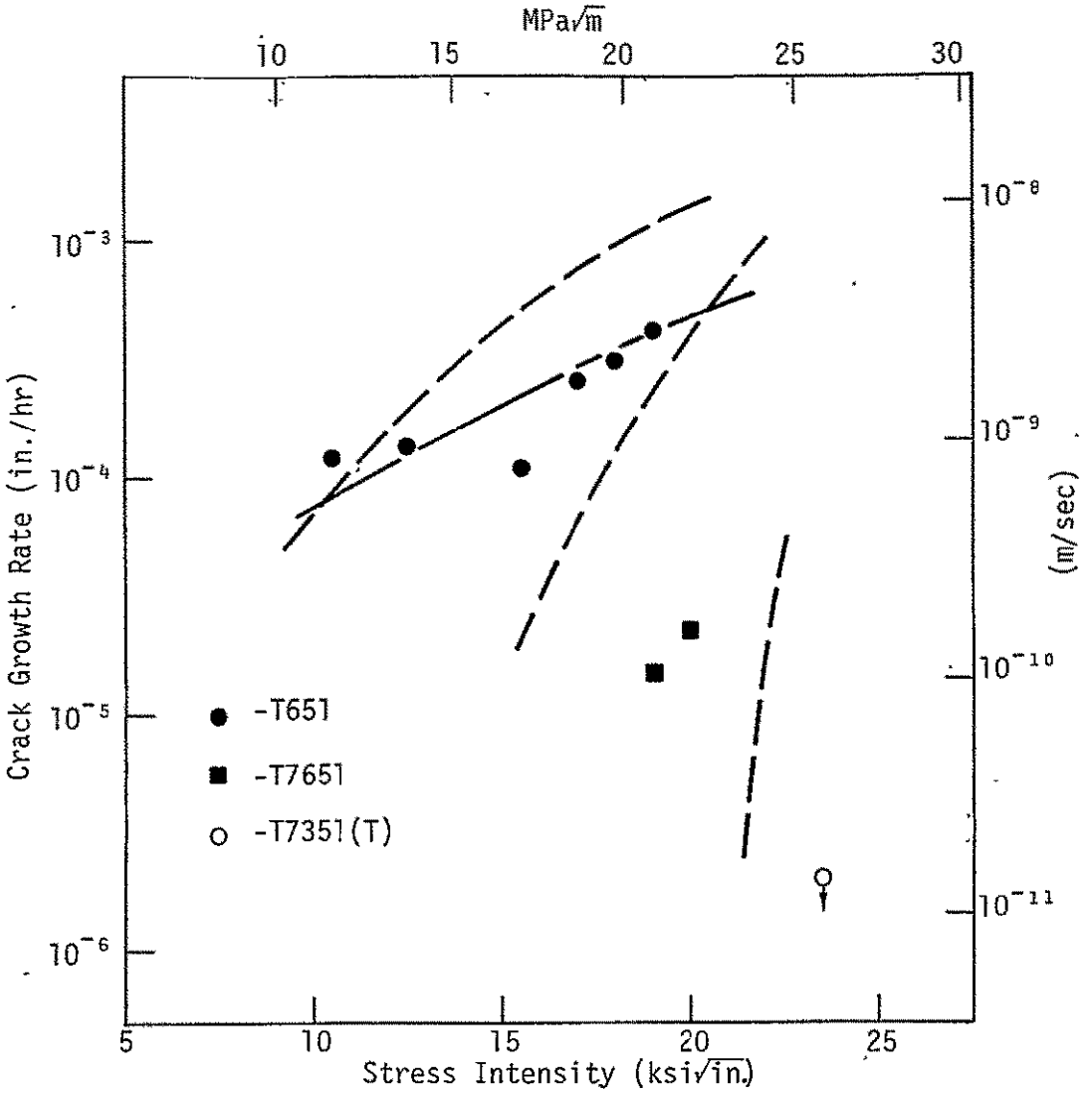

Figure 38. V-K data for 3.0-in. thick 7075 plates at Daytona Beach: SL orientation, pop-in precracks.

Dashed lines are corresponding plots for 1.25-in. plate. The 3.0-in. plates were more resistant than the thinner materials (no crack growth was evident in the 3.0-in. -T7351 temper plate).

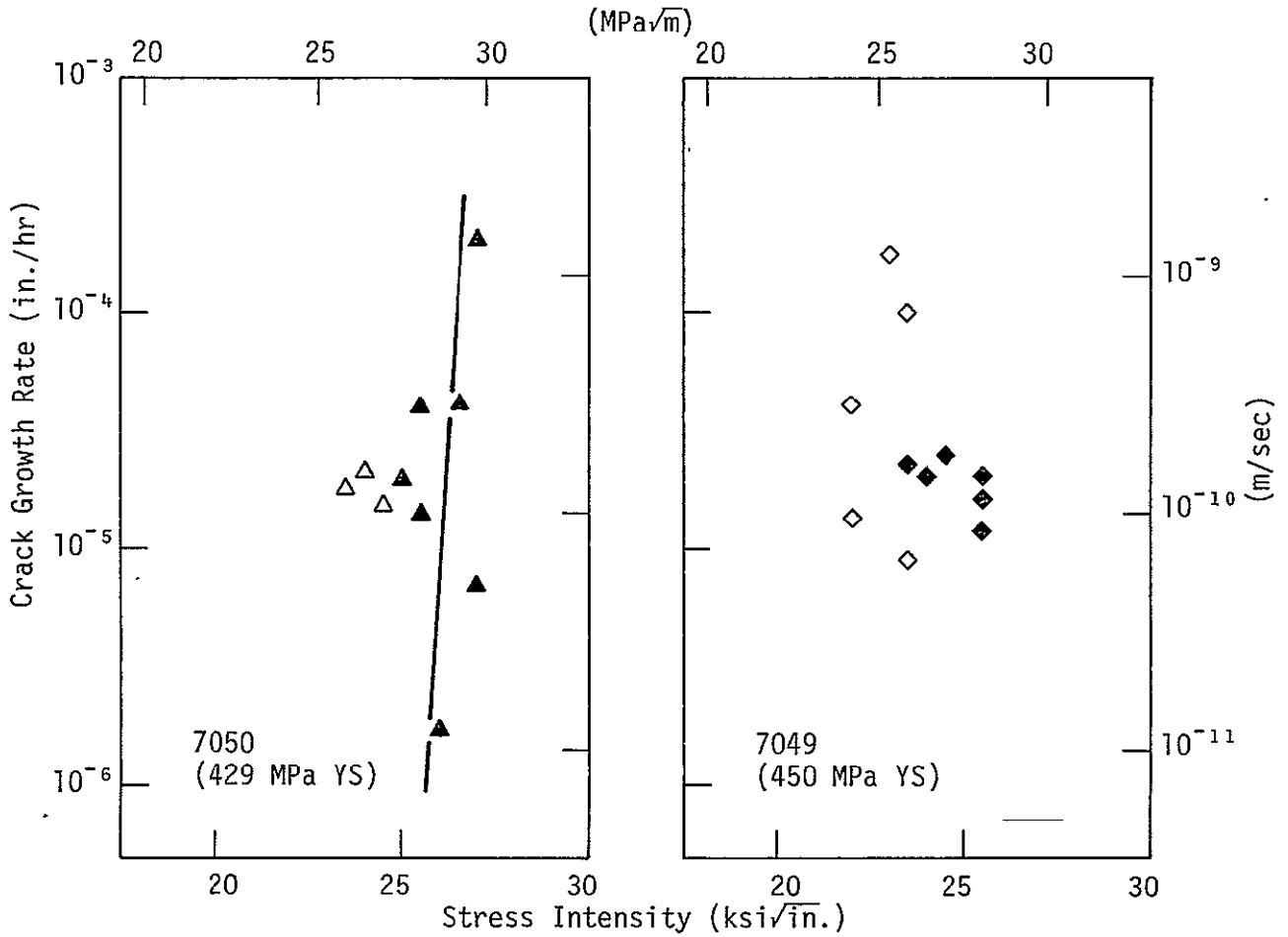

Figure 39. V-K plots for 3-in. thick 7050-T73651(T) and 7049-T7351(T) plates at Daytona Beach: SL orientation, pop-in precracks

Solid symbols: 25-mm high specimens
Open symbols: 75-mm high specimens

Larger specimens seem to give lower velocity for a given K; this may be due to slightly lower apparent initial stress intensity in the 75 mm specimens.

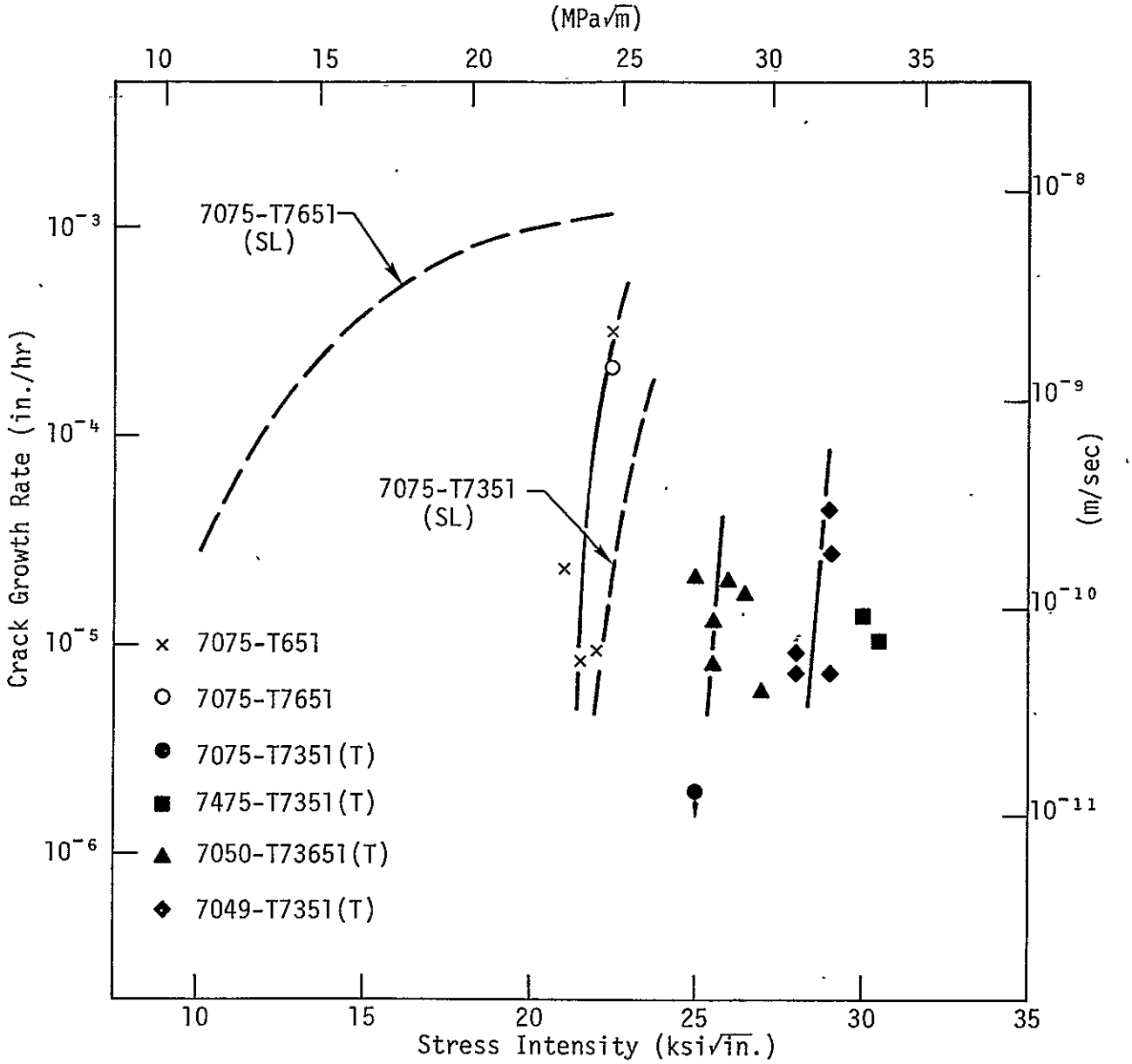

Figure 40. V-K data for 1.25-in. thick plates at Daytona Beach: TL orientation, pop-in precracks

Of the -T73 temper materials, only 7050 and 7049 showed significant crack growth, with 7050 somewhat more susceptible than 7049.

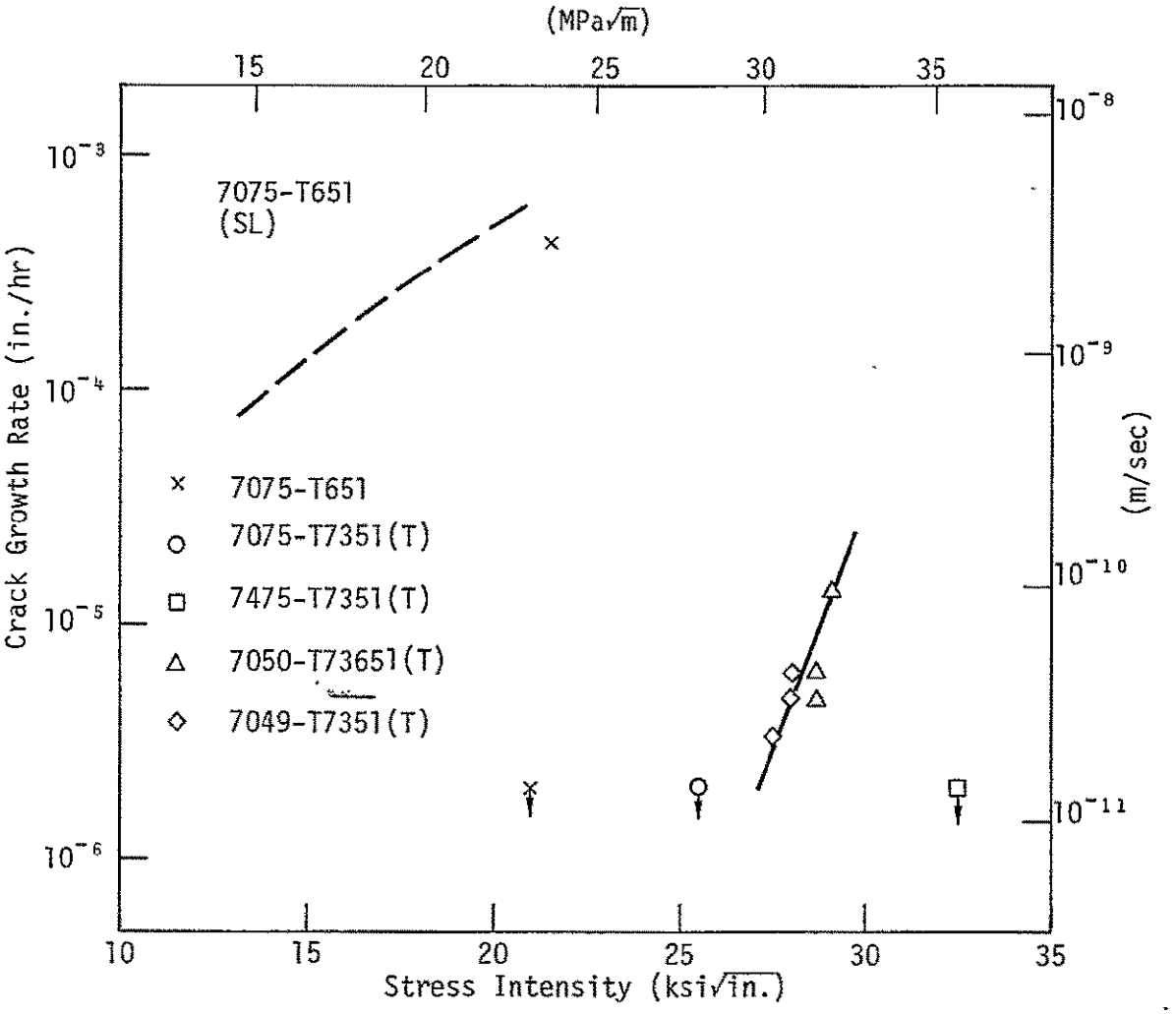

Figure 41. V-K data for 3.0-in. thick plates at Daytona Beach: pop-in precracks, TL orientation

As in the 1.25-in. plates, only 7050 and 7049 showed significant crack growth.

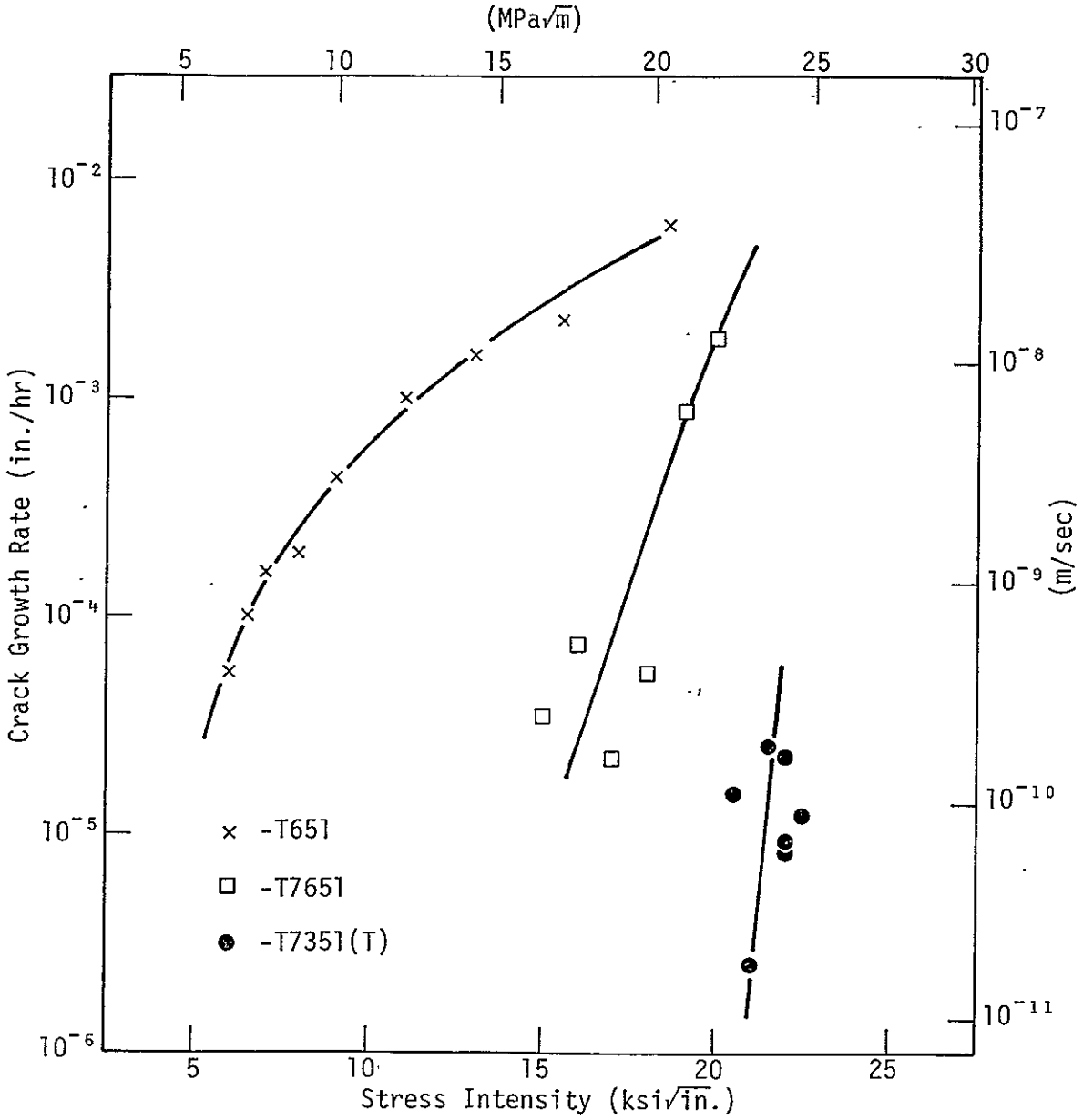

Figure 42. V-K plots for 1.25-in. thick 7075 plates in synthetic seawater (AI): SL orientation, pop-in precracks

Crack growth behavior was similar to that in the marine atmosphere (cf. Fig. 36).

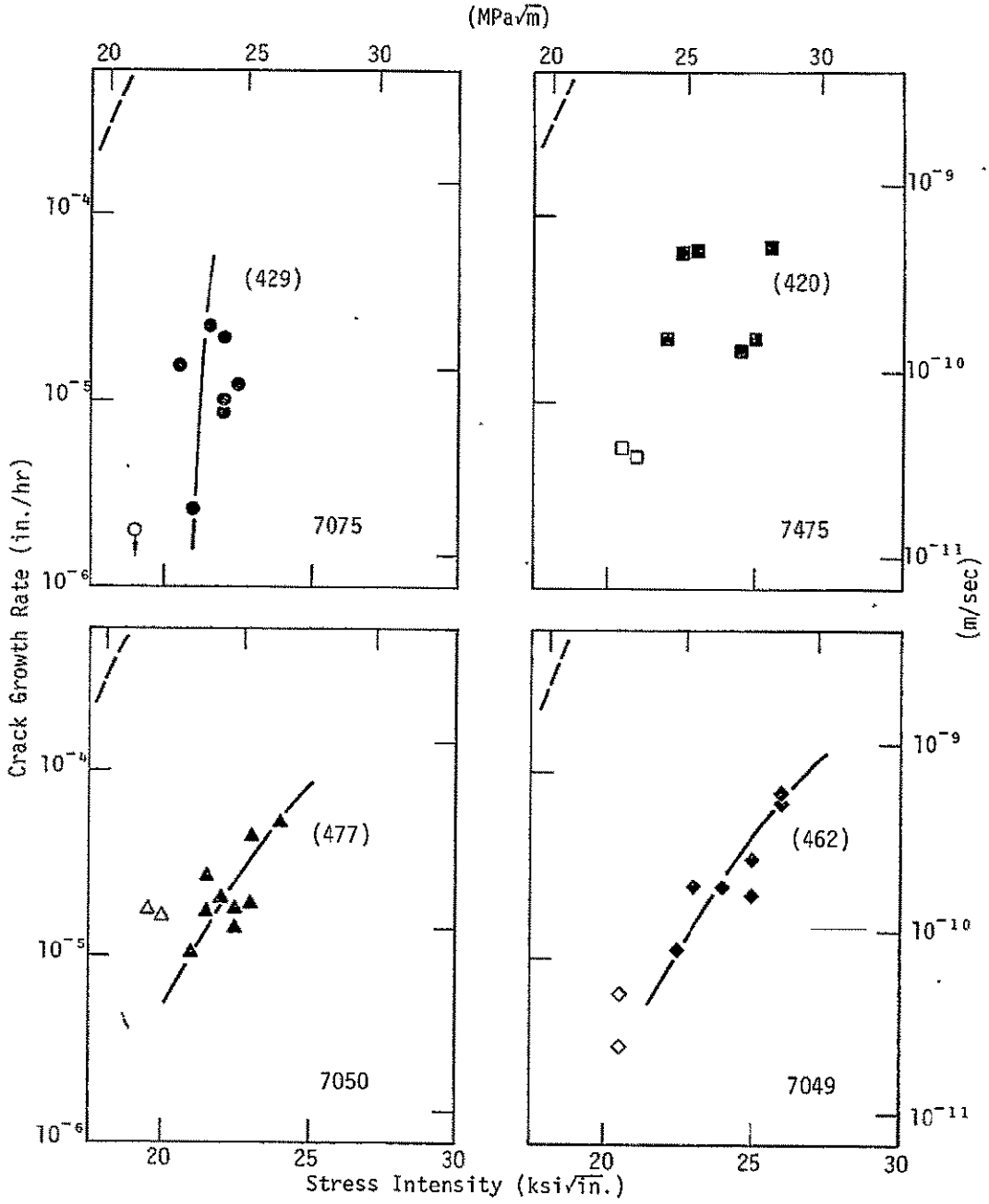

Figure 43. V-K plots for 1.25-in. thick -T73(T) temper plates in synthetic seawater (AI): SL orientation

Solid symbols: pop-in precracks
Open symbols: fatigue precracks

Numbers in brackets are LT yield strengths (MPa). Dashed line in upper l.h. corner represents 7075-T7651 in all cases (489 MPa yield strength).

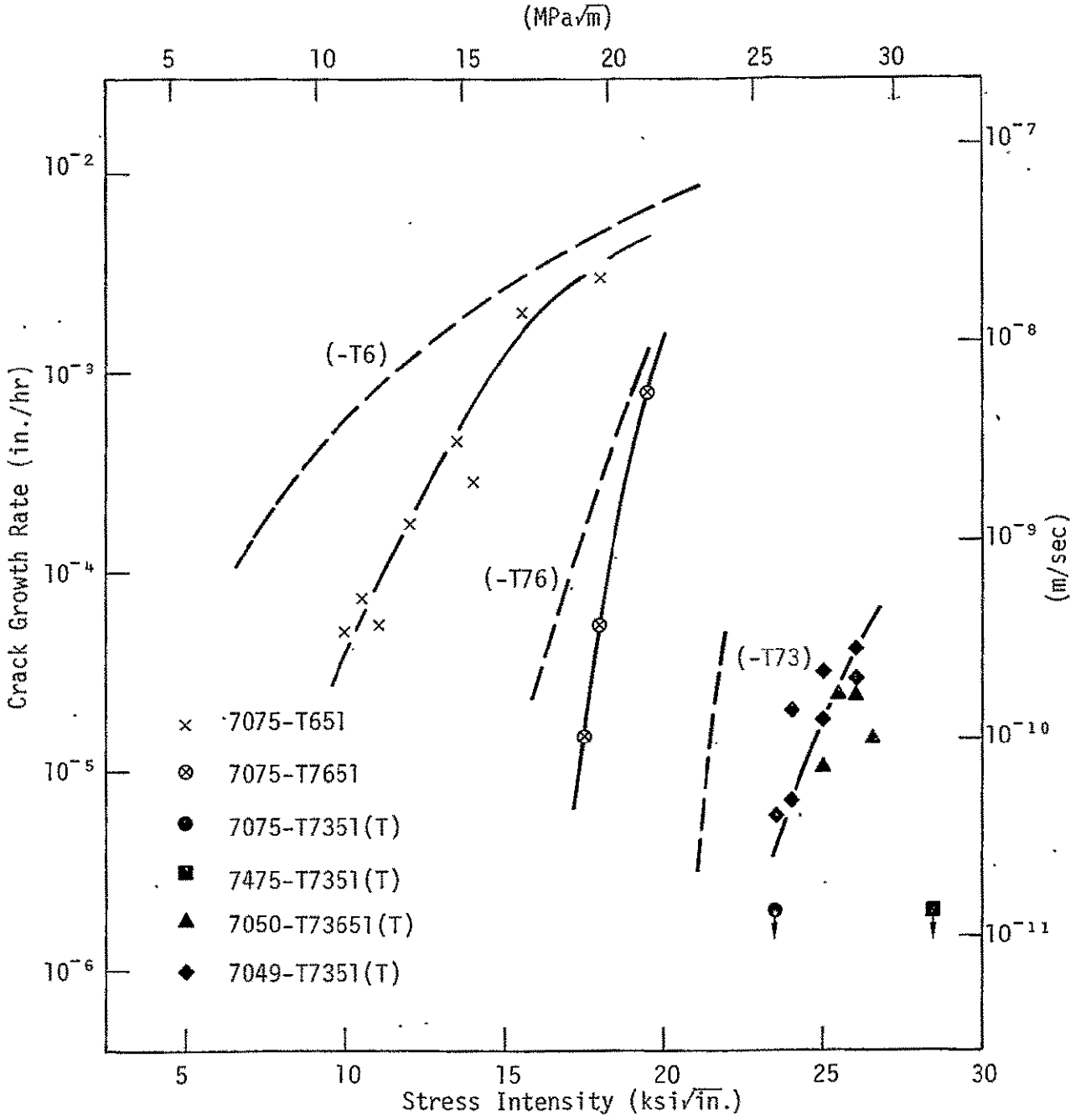

Figure 44. V-K plots for 3.0-in. thick plates in synthetic seawater (AI): S1 orientation, pop-in precracks

The dashed lines are for corresponding 1.25-in. 7075 plates. Of the -T73 temper materials, only 7050 and 7049 showed crack growth.

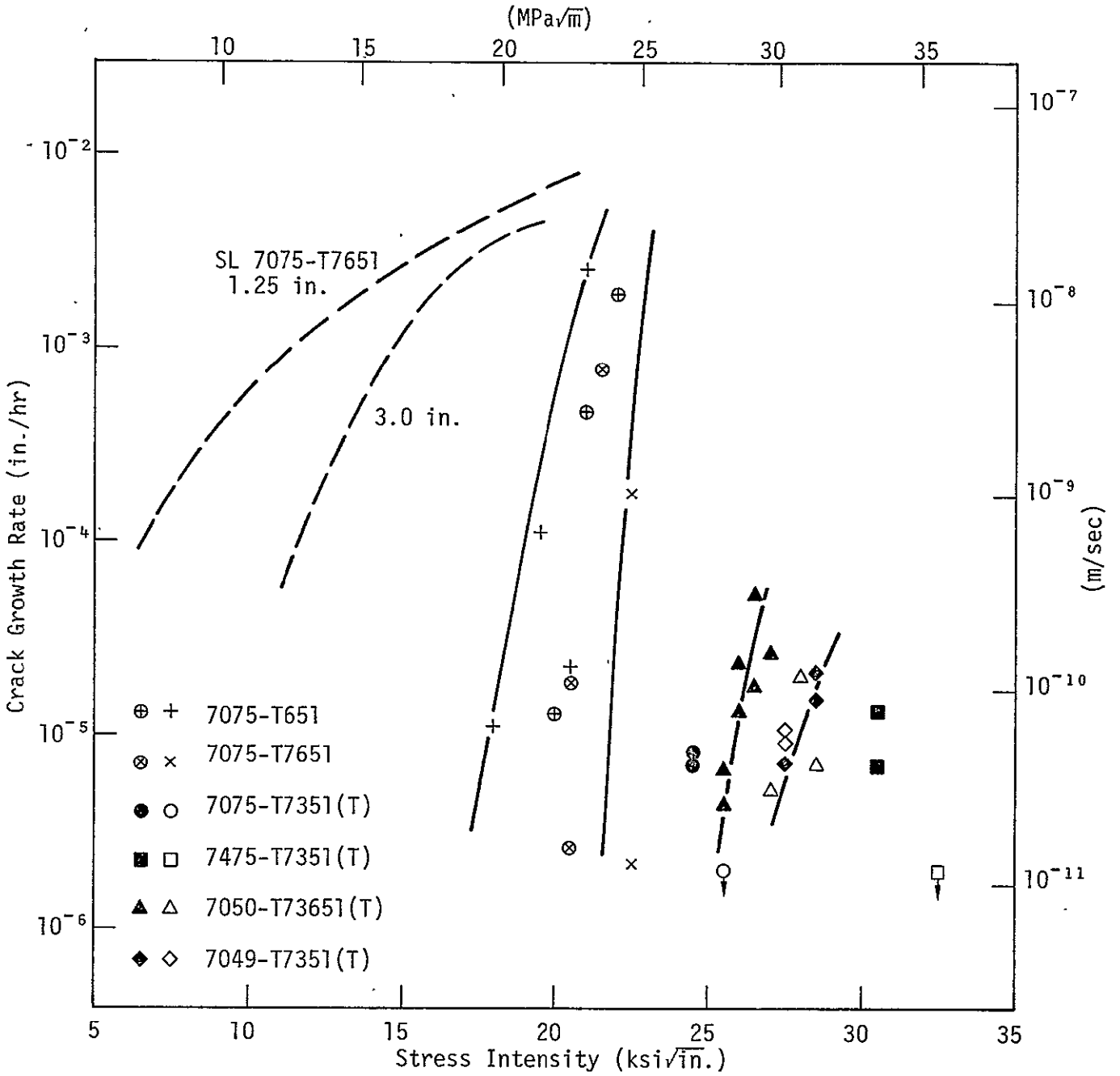

Figure 45. V-K data for TL orientation in synthetic seawater (AI): pop-in precrack.

Symbols in first column: 1.25-in. plate; second column: 3.0-in. plate.

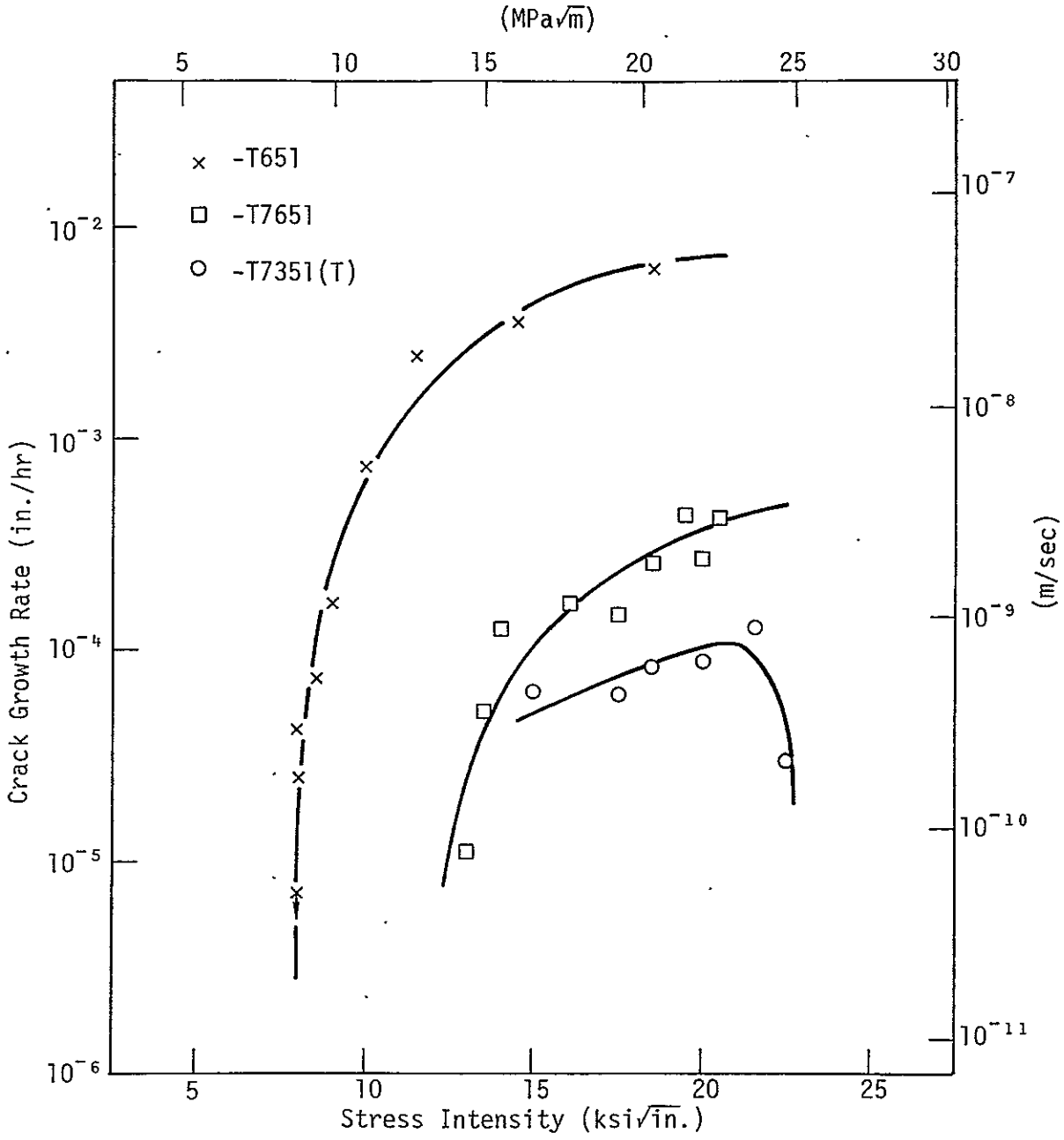

Figure 46. V-K plots for 1.25-in. thick 7075 plates in salt chromate solution: SL orientation, pop-in precracks.

Data for -T7351 temper is based on average crack growth rates for 6 replicates. Initial inverse V-K relationship may be due to incubation factor.

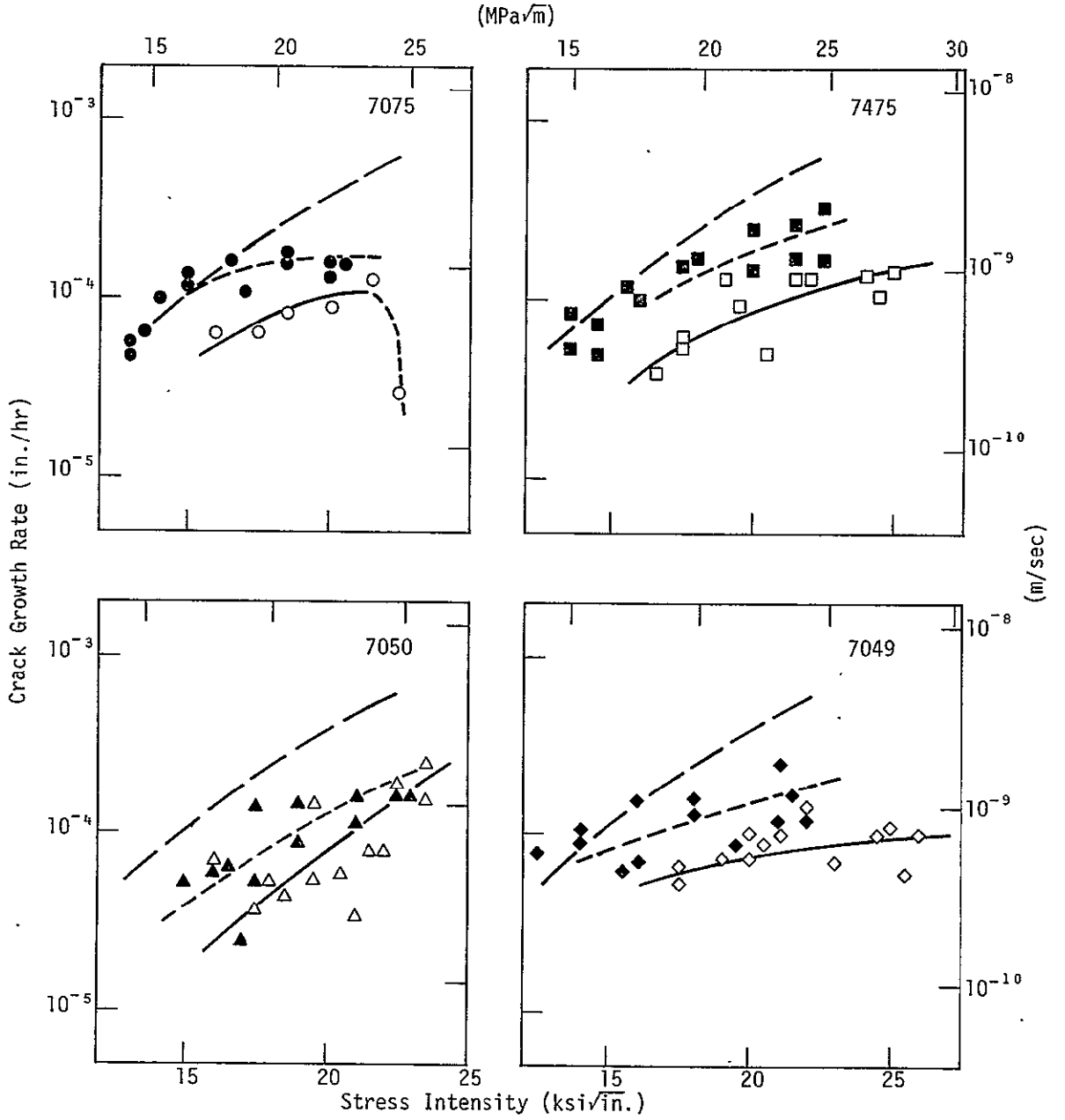

Figure 47. V-K plots for 1.25-in. thick -T73 temper plates in salt-chromate solution: SL orientation, pop-in precracks

Solid symbols: minimum temper condition
Open symbols: typical temper condition

Upper dashed curve represents 7075-T7651 in all cases. The 1.25-in. -T73 temper appeared much more susceptible in the salt-chromate solution than in the other environments. V-K plots were also flatter, trending towards a plateau.

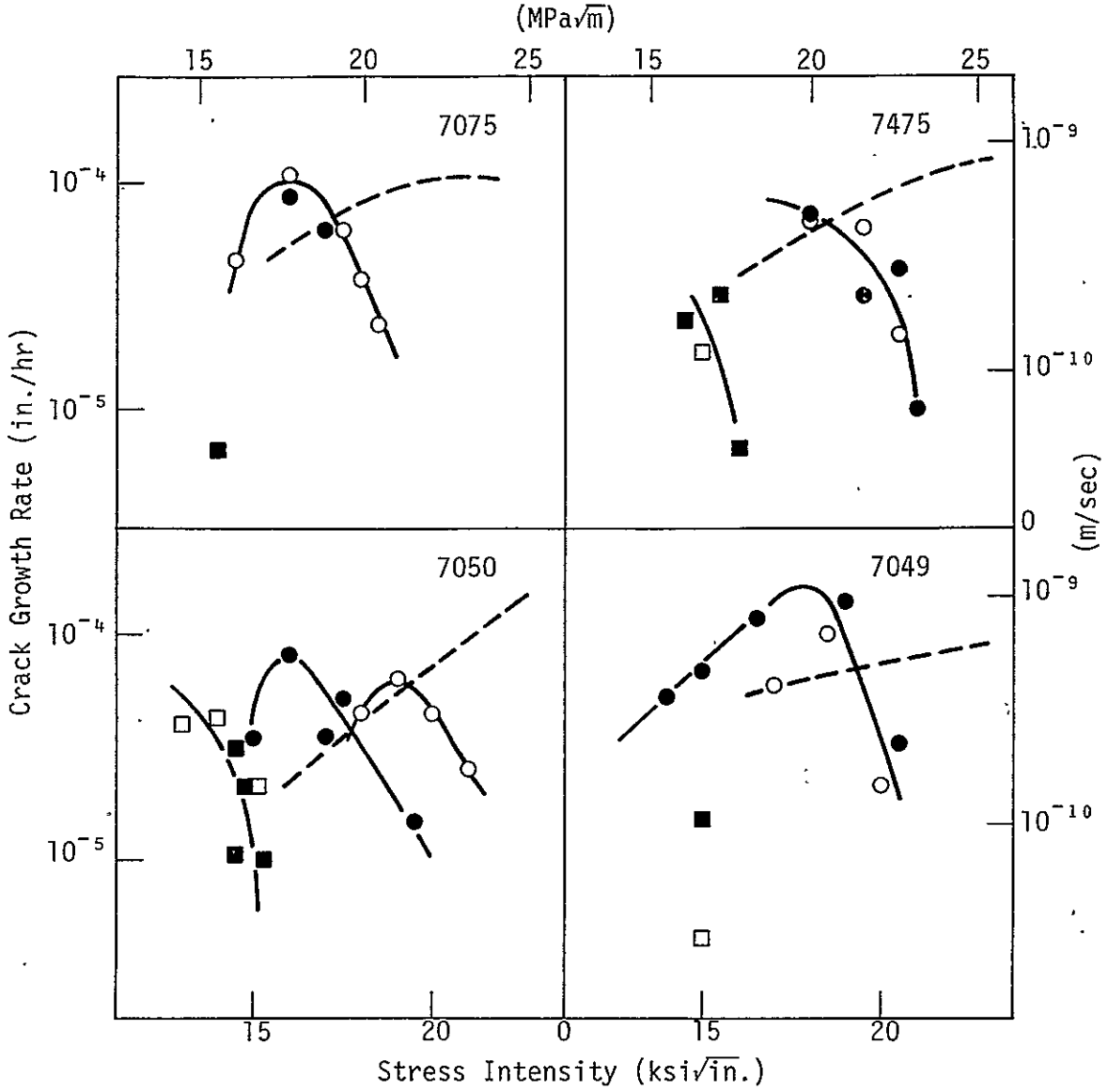

Figure 48. V-K plots for 1.25-in. thick -T73(T) temper plates in salt-chromate solution: SL orientation, fatigue precracks

Different symbols represent data from different specimens. Dashed line is for corresponding test using pop-in precracks. Pronounced inverse behavior due to incubation periods were evident.

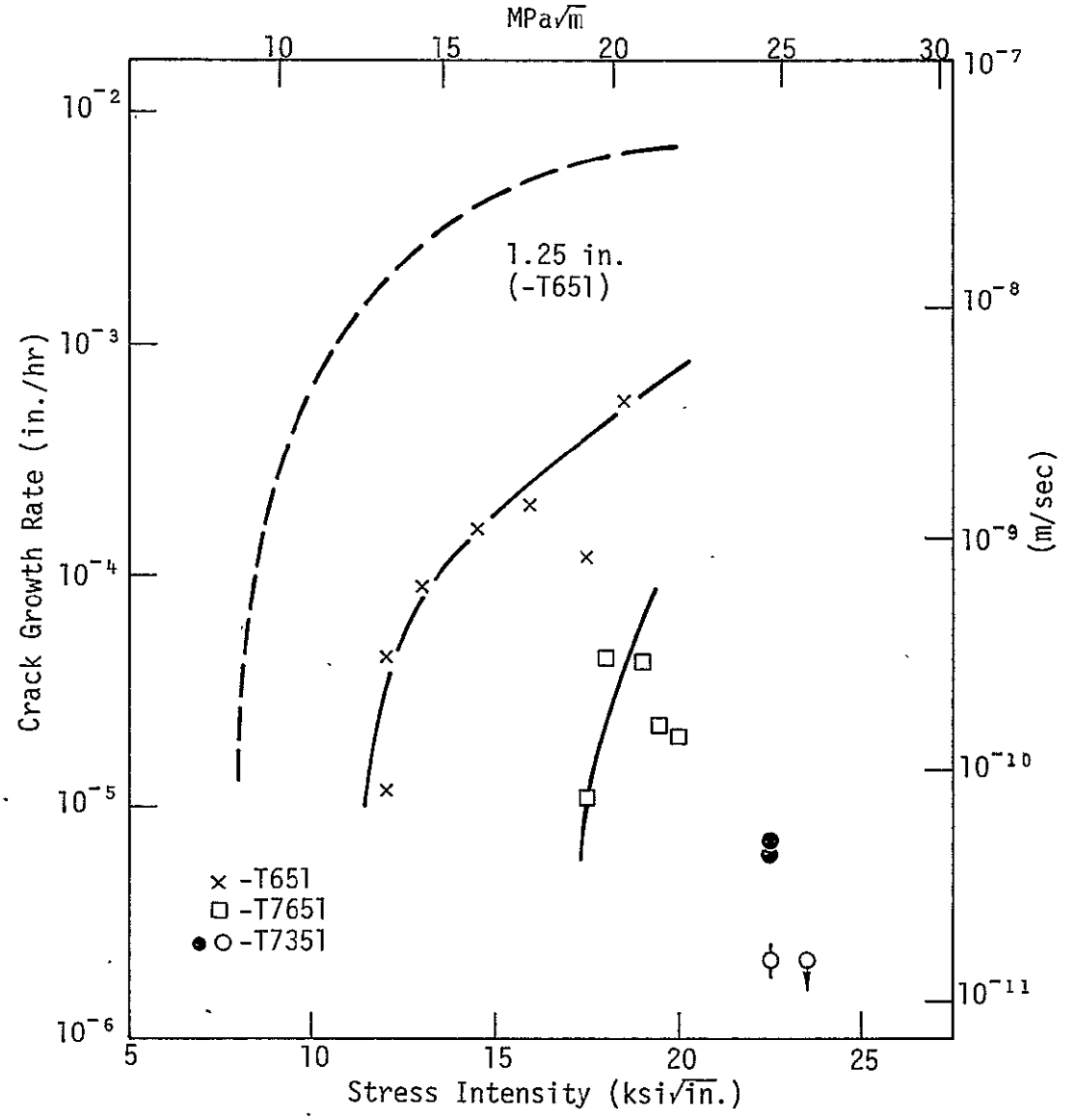

Figure 49. V-K data for 3.0-in. thick 7075 plates in salt-chromate solution: SL orientation, pop-in precracks.

Solid circles: Minimum -T73 temper
Open circles: Typical -T73 temper

All data points are for 25-mm high DCB specimens except that identified by ϕ which is for 75-mm high specimen. Crack growth rates were much slower than in corresponding 1.25-in. plates.

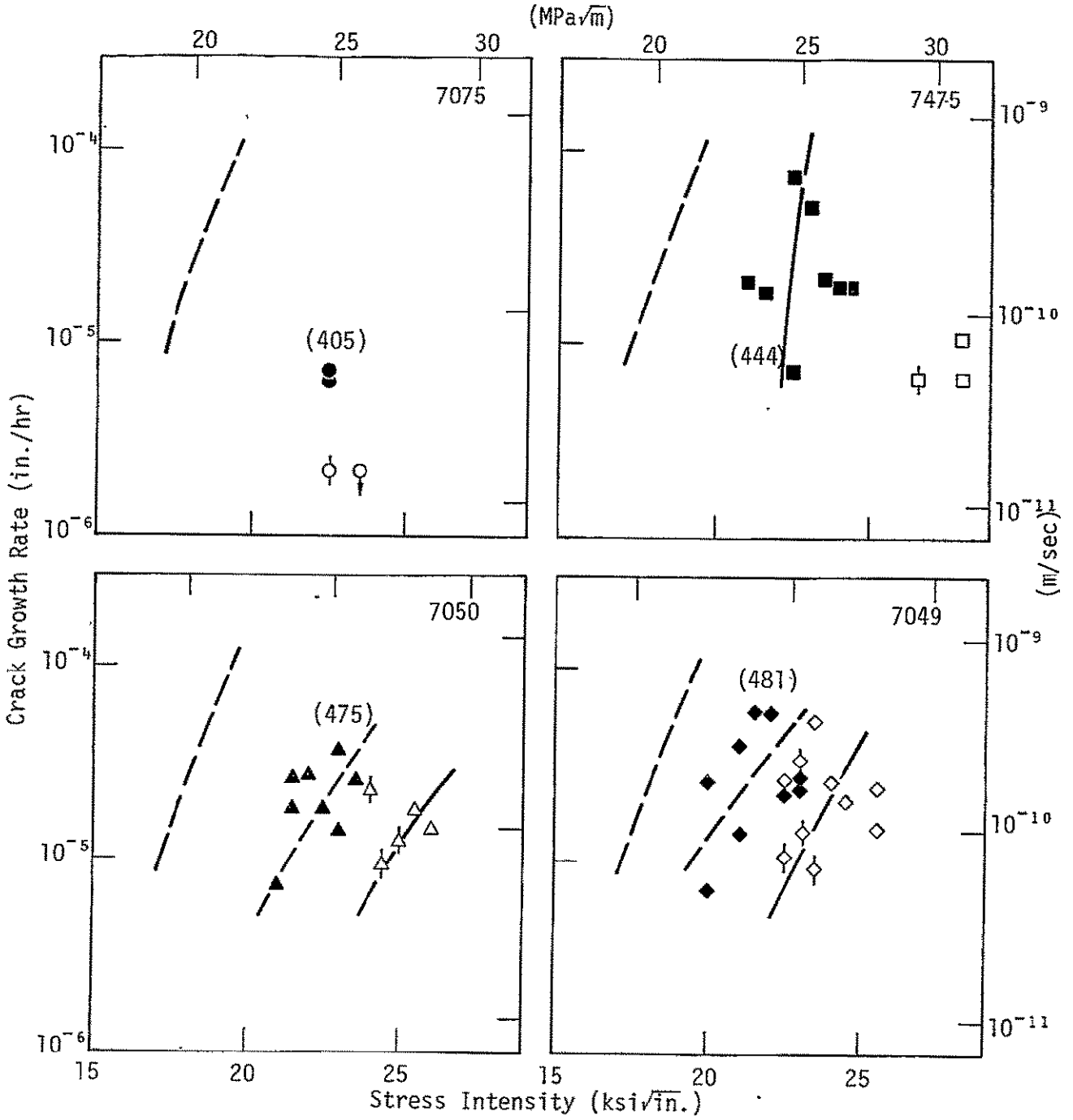

Figure 50. V-K data for 3.0-in. thick -T73 temper plates in salt-chromate solution: SL orientation, pop-in precracks.

Solid symbols: Minimum temper condition
Open symbols: Typical temper condition

Upper dashed curve represents 7075-T7651 in all cases (460 MPa yield strength). Numbers in brackets are LT yield strengths of minimum -T73 temper conditions. Slashed symbols: 75-mm specimens.

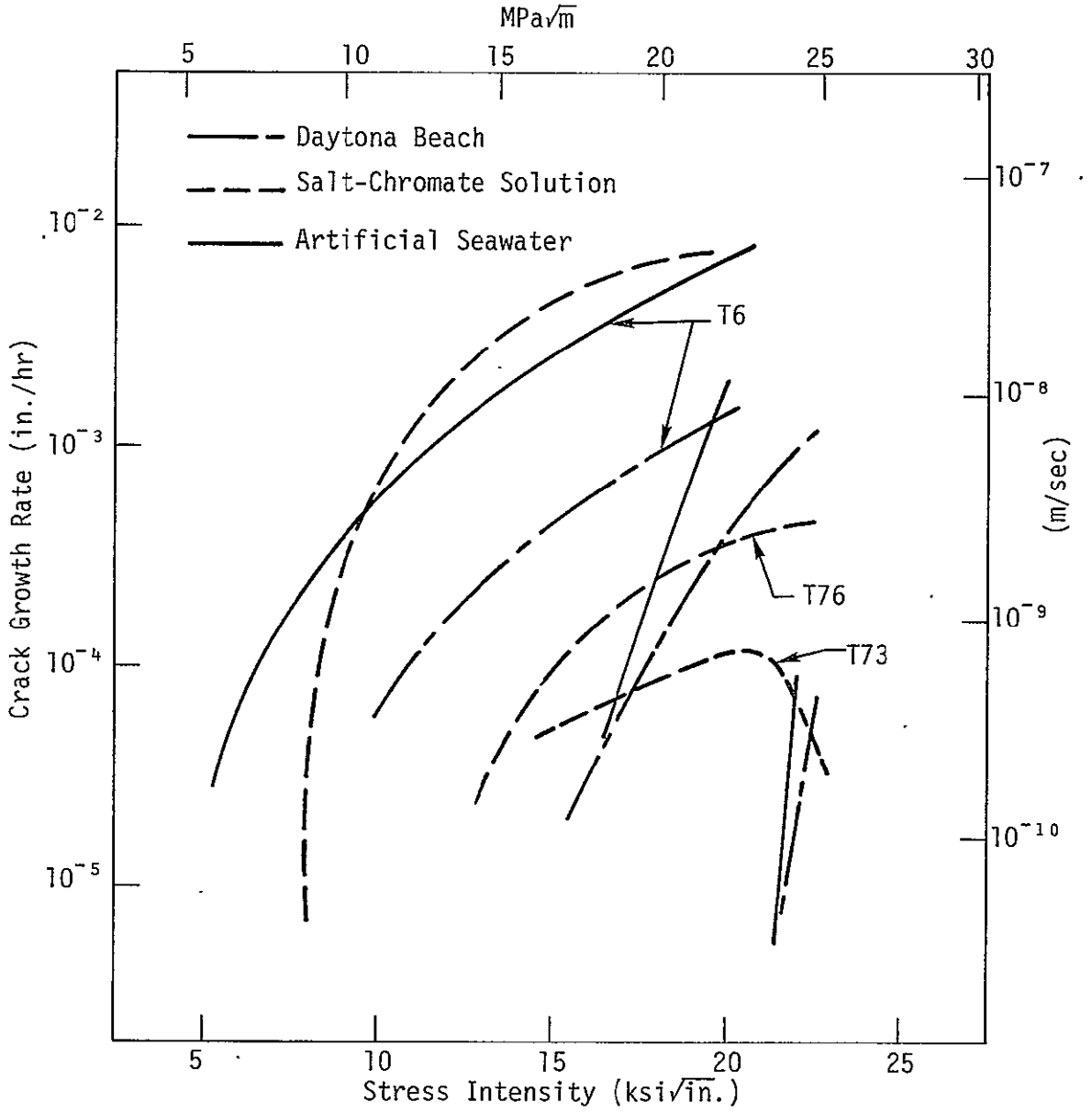

Figure 51. Effect of environment on crack growth behavior in 1.25-in. thick 7075 plate

In the -T6 temper, crack growth at Daytona Beach was slower than in the laboratory environments. Differences for the -T76 temper depended greatly on the stress intensity level, and in the -T73 temper, the salt-chromate solution was much more aggressive than the other environments.

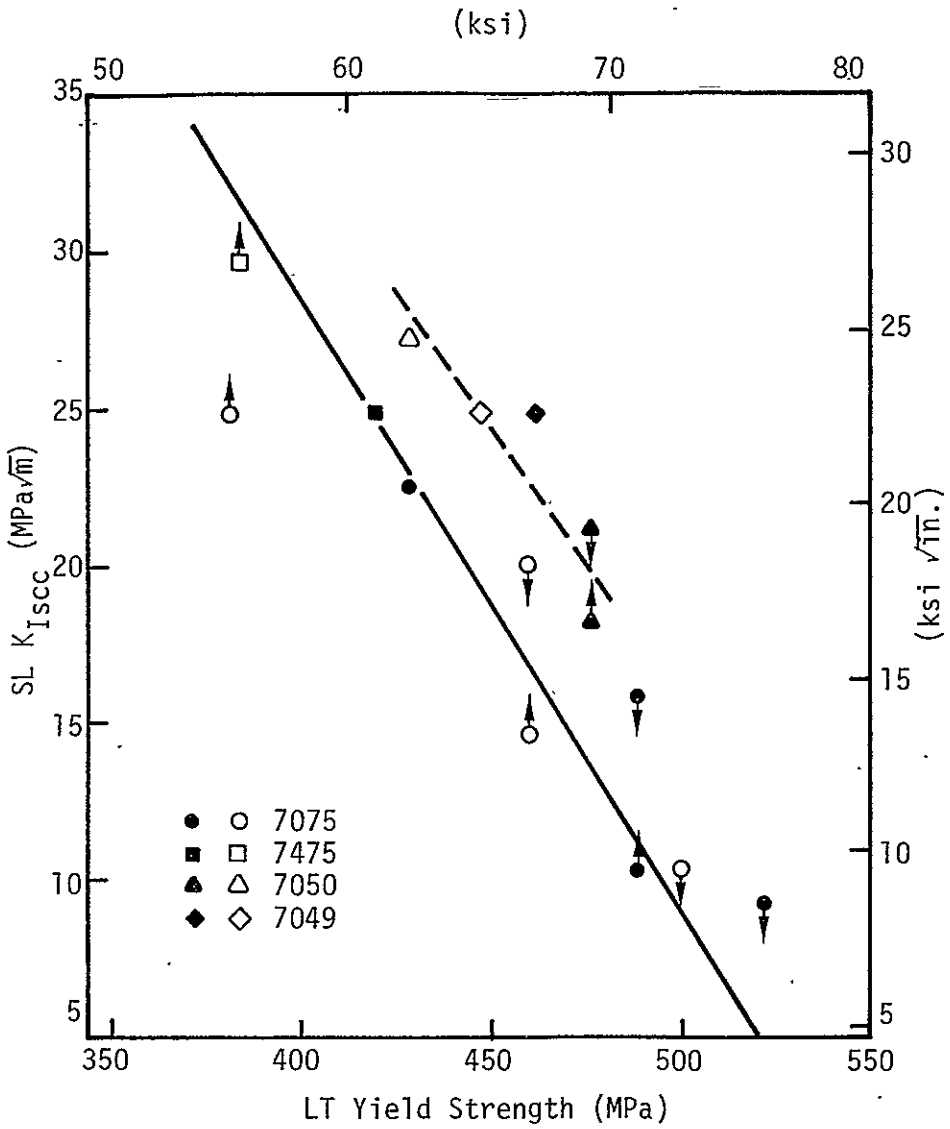

Figure 52. Dependence of SL threshold stress intensity (Daytona Beach) on strength

Solid symbols -- 1.25-in. plate
Open symbols -- 3.0-in. plate

For a given strength level, K_{Iscc} of 7050 and 7049 is about 4 MPa$\sqrt{m}$ greater than that of 7X75.

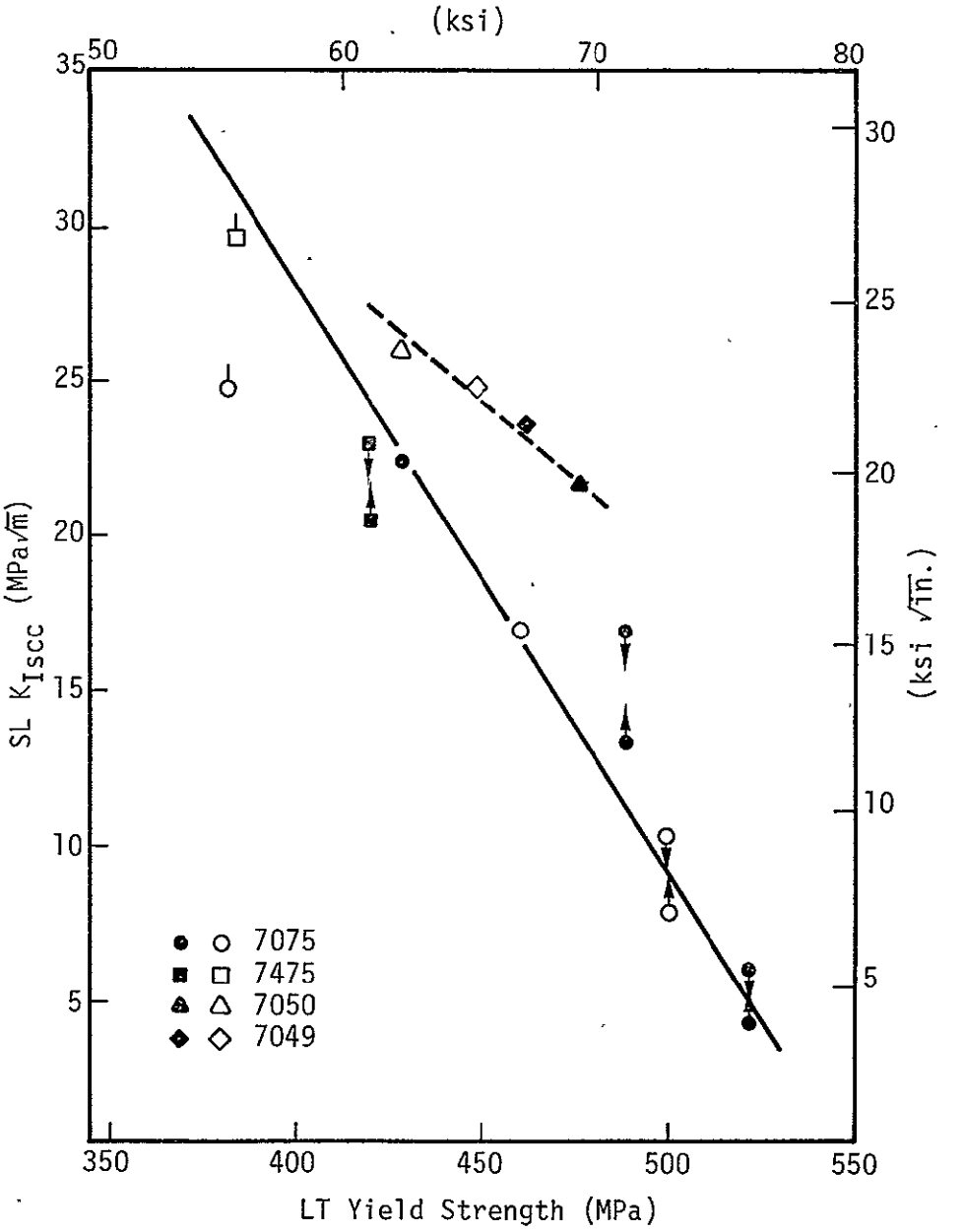

Figure 53. Dependence of SL threshold stress intensity (synthetic seawater) on strength

Solid symbols: 1.25-in. plate
Open symbols: 3.0-in. plate

K_{Iscc} of 7050 and 7049 is 3-5 MPa$\sqrt{m}$ greater than that of 7X75 for a given strength level.

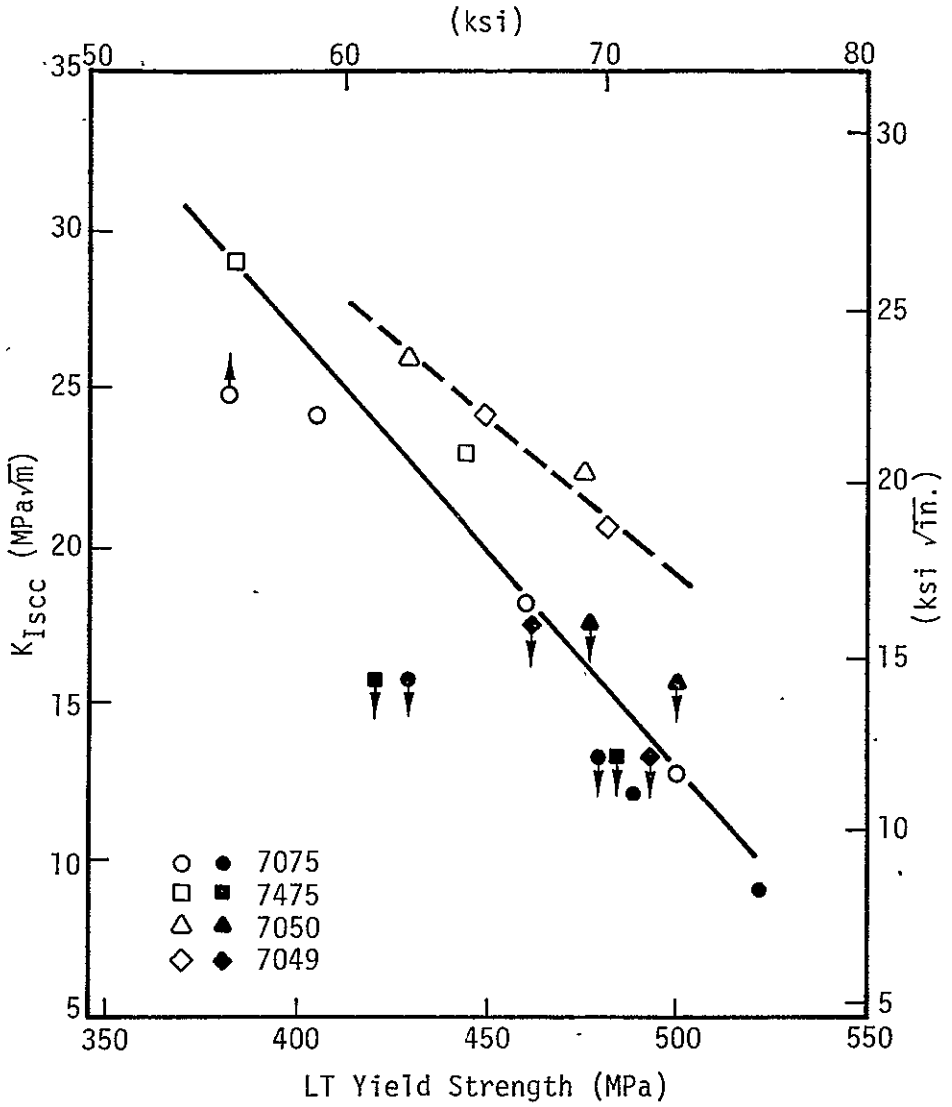

Figure 54. Dependence of SL threshold stress intensity (salt-chromate solution) on strength

Solid symbols: 1.25-in. plate
Open symbols: 3.0-in. plate

For 3.0-in materials, K_{Iscc} of 7050 and 7049 was higher than that of 7X75. K_{Iscc} values for 1.25-in. -T73 temper plates were not attained in this environment.

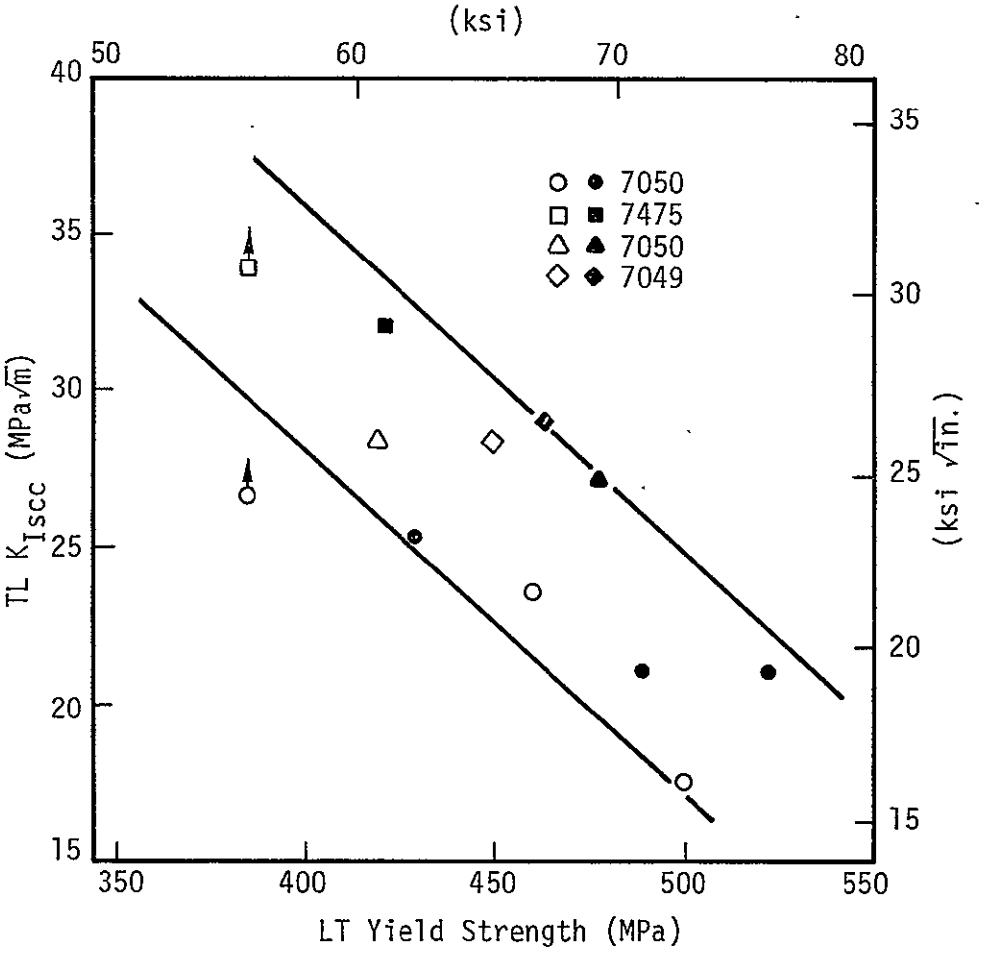

Figure 55. Dependence of TL threshold stress intensity (synthetic seawater) on strength

Solid symbols: 1.25-in. plate
Open symbols: 3.0-in. plate

All materials fell into the same general data band.

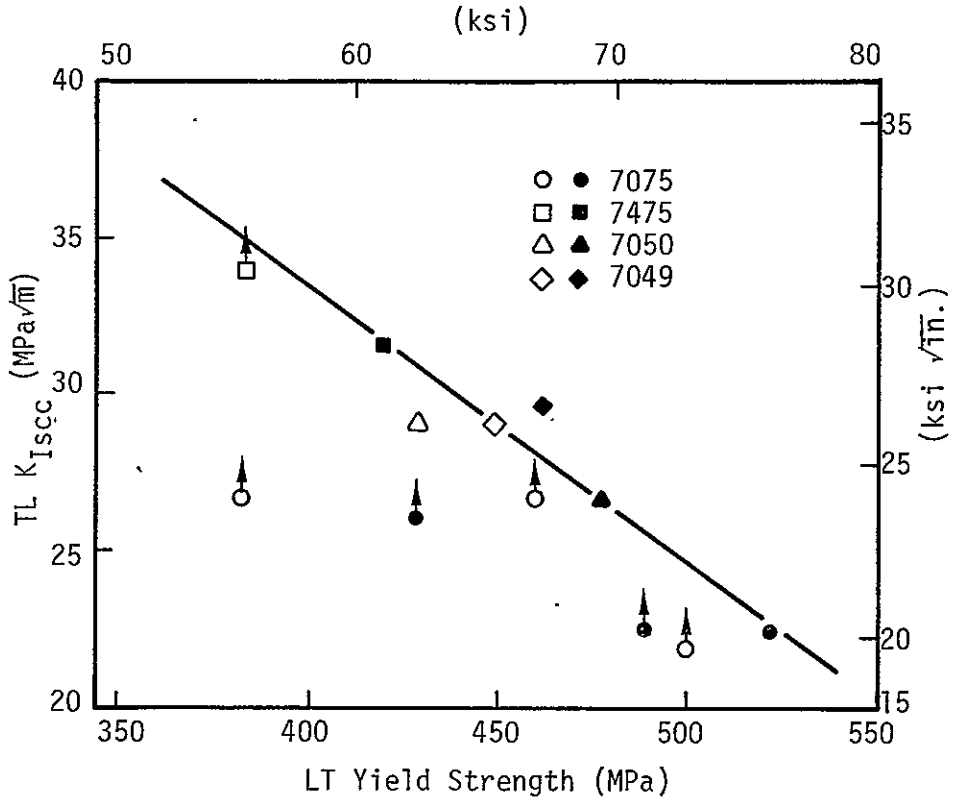

Figure 56. Dependence of TL threshold stress intensity (Daytona Beach) on strength

Solid symbols: 1.25-in. plate
Open symbols: 3.0-in. plate

There were no obvious alloy effects in the TL orientation.

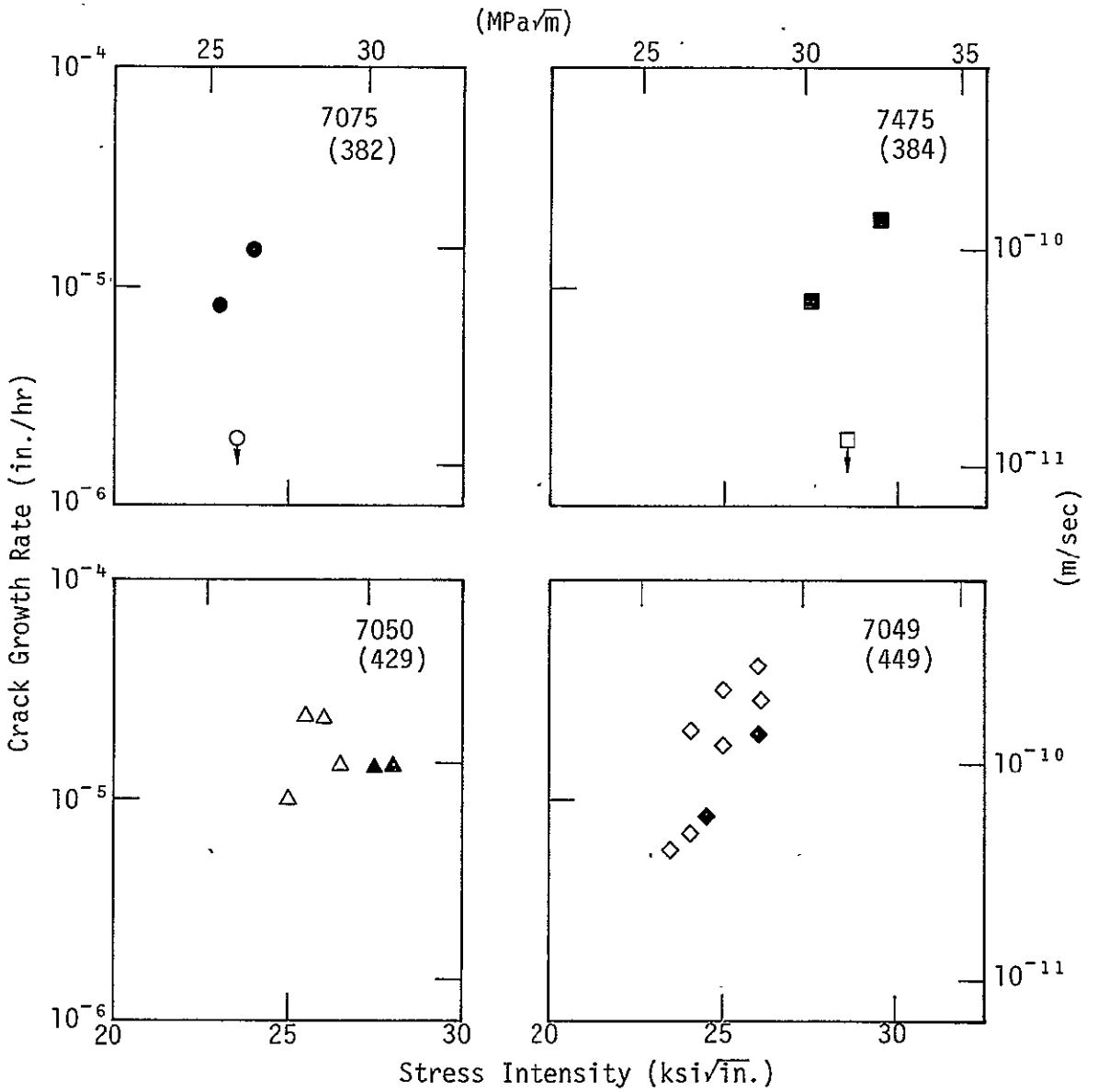

Figure 57. Comparison of V-K data in synthetic seawater for 3.0-in. -T73 temper plates: constant deflection (pop-in precrack) vs constant load (fatigue precrack)

Solid symbols: Constant load
Open symbols: Constant deflection

Numbers in brackets are LT yield strengths (MPa).

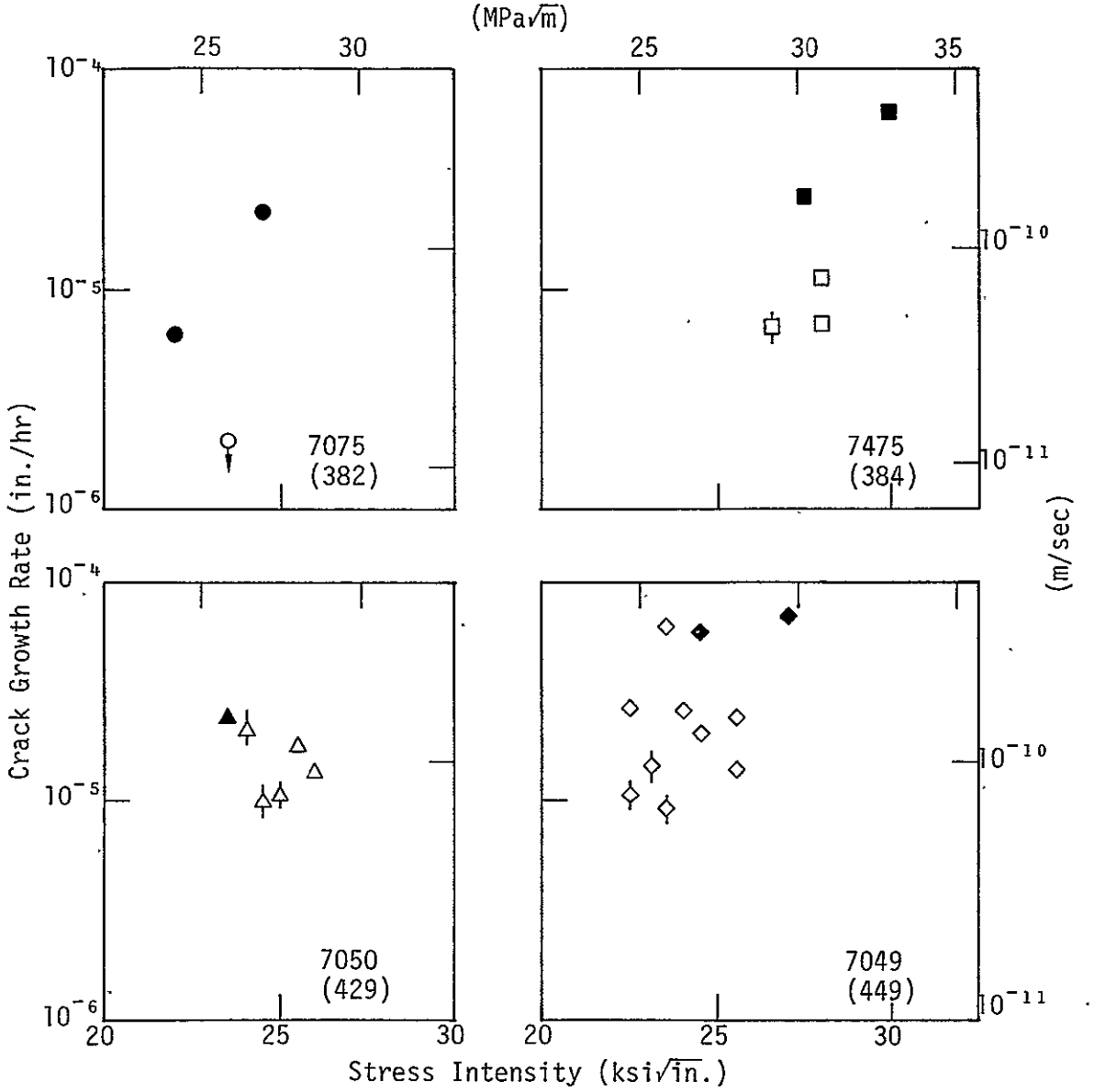

Figure 58. Comparison of V-K data in salt-chromate solution for 3.0-in. -T73 temper plates: constant deflection (pop-in precrack) vs constant load (fatigue precrack)

Solid symbols: Constant load
Open symbols: Constant deflection

All data points are for 25 mm-high specimens, except those identified by | which are for 75-mm specimens. Numbers in brackets are LT yield strengths (MPa).

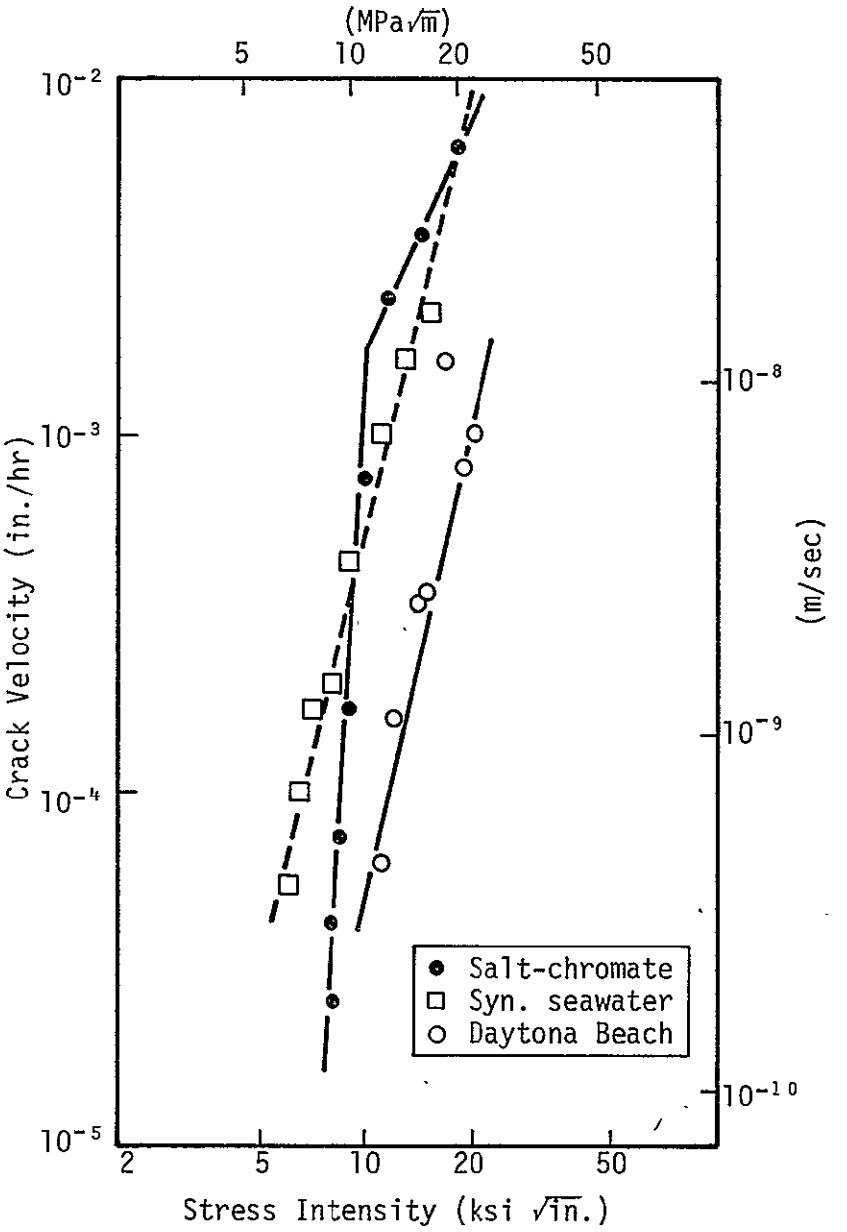

Figure 59. Crack velocity - stress intensity relationships for 1.25-in. 7075-T6 in various environments

Crack velocity in Region I was proportional to K^4 in synthetic seawater and at Daytona Beach. Exponent for salt-chromate test varied from 16 in Region I to 2 at beginning of Region II.

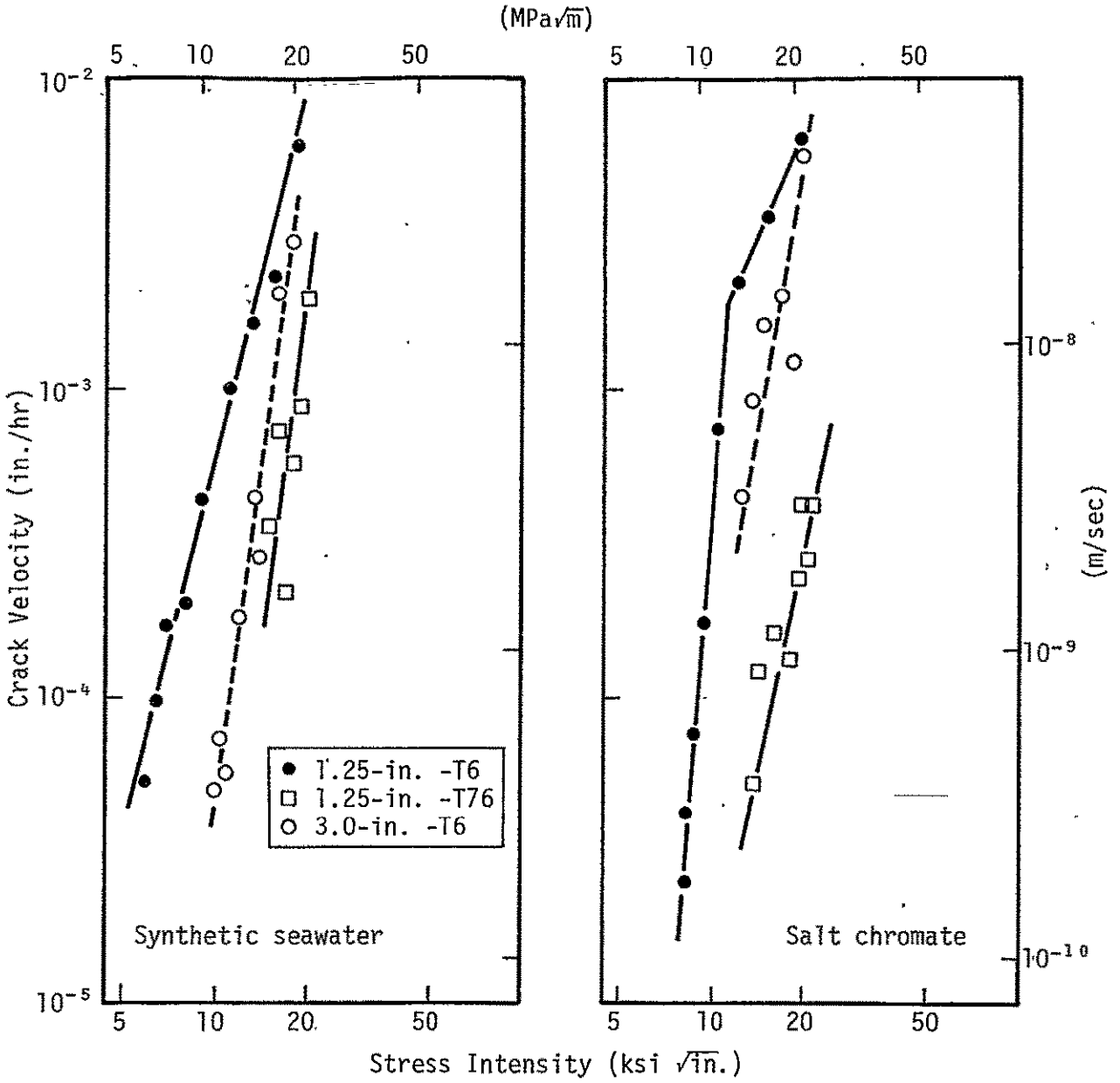

Figure 60. Comparison of crack velocity - stress intensity relationships for 7075-T6 and 7075-T76 in synthetic seawater and salt-chromate solution

Crack velocity in Region I was proportional to K^4-K^7 in synthetic seawater and K^5-K^{16} in salt-chromate solution.

APPENDIX A

FRACTURE MECHANICS CONCEPTS AND THEIR RELATIONSHIP TO STRESS-CORROSION

1. Fracture Mechanics Principles

Fracture mechanics forms the basis for most of the currently accepted methods of failure analysis. It is primarily concerned with the problem of evaluating the strength of materials in the presence of an existing crack and the conditions under which the crack propagates to failure. While metals usually fail in a ductile (plastic) manner, failure can still be described in terms of the elastic stresses or so-called "stress fields" surrounding the crack tip. All the stress field equations which describe the distribution of elastic stress near the crack tip contain the same proportionality factor, K, which is formally called the crack tip stress field intensity factor, or simply stress intensity factor. This factor reflects the magnitude of the crack tip stress field and, therefore, gives a measure of the intensification of stress at the crack tip caused by the applied load. For example, the stress intensity factor for an infinite plate containing a transverse crack of length 2a and subject to a uniform tensile stress, σ, is described by (Ref 3):

$$K_I = \sigma\sqrt{\pi a}$$

This equation shows that the stress intensity will increase with an increase in either the applied stress or crack length. Note also that the stress intensity factor has the dimensions of stress multiplied by the square root of the crack length, eg., $MPa\sqrt{m}$ ($ksi\sqrt{in.}$).

The determination of K factors for an infinite plate specimen requires only two dimensions, stress and crack length. Real specimens, on the other hand, have finite dimensions. Therefore, in addition to the magnitude of the loading forces and the crack size, K_I for finite specimens must be corrected for specimen size and shape, i.e.,

$$K_I = \sigma\sqrt{\pi a}\ \Phi$$

$$\text{or} \qquad K_I = \frac{P\sqrt{a}}{BW}\ \Phi\ ,$$

where P is the applied load, B is the specimen thickness, and W is the specimen width. The correction factor, Φ, is dependent on the geometry of the specimen and the method of loading. It also varies in a complex way with the specimen width and crack length. Various mathematical and experimental stress analyses are used to determine correction factors, and numerical solutions of K_I have been derived for a number of practical test specimens (Refs 3,4).

If the growth of a crack is controlled solely by the value of K, then the higher the stress intensity required to produce crack propagation, the greater is the resistance of the material to fracture. At the onset of fracture

$$K = K_C,$$

which is called the critical stress intensity for fracture or simply "fracture toughness". Provided that, among other things, certain requirements of crack length and specimen dimensions are satisfied, the fracture test can be conducted under a prescribed state of stress. Usually, the specimen dimensions are large enough to promote a plane-strain state of stress, in

which case the critical stress intensity for fracture is specially labeled K_{Ic} or plane-strain fracture toughness. Unstable fracture is more easily promoted under plane-strain conditions and, therefore, K_{Ic} is regarded as the minimum value required for crack growth by mechanical fracture.

2. Application to Stress Corrosion

A natural extension of the fracture mechanics approach to normal fracture is to view stress-corrosion cracking (SCC) as simply a form of subcritical crack growth. Accordingly, we retain the concept that the crack tip stress intensity provides the driving force for crack extension. The characterization of SCC in terms of a crack tip stress intensity factor is quite direct, but not without limitations. Fracture mechanics deals principally with the events which lead up to the point of crack instability, i.e., before the crack actually begins to grow. In SCC, however, we are concerned with moving cracks and, in particular, how fast they move. One of the unanswered questions is whether K can be used as the local load parameter which controls the rate of crack growth. As yet, there is no proof that it would if crack growth occurred solely by anodic dissolution, as it may in aluminum alloys. Nevertheless, the stress intensity does characterize the "mechanical environment" which exists in the region of the crack tip. Establishing a functional relationship between K and crack growth behavior may, therefore, add considerably to our understanding of how stress and mechanical fracture processes contribute to SCC.

Crack velocity as a function of stress intensity is usually expressed as a "V-K" curve. This curve is often divided into three parts or regions (Figure A1). At low stress intensities (Region I), crack velocity is strongly dependent on K. In

aluminum alloys, the velocity of stress-corrosion cracks can vary by several orders of magnitude: from 10^{-5} in./hr or less to 1 in./hr or more. At intermediate levels of stress intensity (Region II), the crack velocity may reach a limiting and constant value, independent of the level of stress intensity. Finally, at stress intensities approaching the critical stress intensity (K_{Ic}) for mechanical fracture, the velocity of crack growth may again become strongly dependent upon stress intensity. This is called Region III crack growth.

Regions I and II are of greatest practical interest, since most of the time spent in the growth of stress-corrosion cracks in aluminum occurs at stress intensities well below that for mechanical fracture. Region I holds special interest since it may be possible to develop K_{Iscc} data based on a minimum acceptable rate of crack growth. For example, some workers define K_{Iscc} as that level of stress intensity which produces a crack velocity of 10^{-5} in./hr (7×10^{-11}m/sec) or less. It should be recognized, however, that long periods of exposure are required to obtain crack growth data when the velocity approaches 10^{-5}in./hr.

There are several reasons for being interested in the kinetics of stress-corrosion cracking. Knowledge of crack growth rates should prove useful in alloy development and studies of the fundamentals of stress-corrosion cracking. In addition, the maximum rates at which cracks can grow should be of particular interest to design engineers since they may provide a means for estimating the (minimum) lifetime of real structures. And finally, we may be able to design a rapid test to measure stress corrosion performance in terms of how fast (or how far) cracks grow.

Fracture toughness and stress-corrosion susceptibility of wrought aluminum alloys depend on the orientation of the test specimen with respect to the direction grain flow produced by

the fabrication operation. Figure A2 shows the various specimen orientations possible; the short-transverse directions (SL and ST) generally have the lowest toughness and highest susceptibility to stress corrosion.

3. Previous Work

Although a considerable amount of V-K data has been determined for aluminum alloys that are susceptible to SCC (7079-T6, 7075-T6, 2024-T3, etc.), relatively little information exists for resistant materials such as 7075-T73. The results reported for previous investigations on a number of alloys are reproduced in Figure A3. As expected, materials such as 7075-T73, 6061-T6, 7049-T73, and 2024-T8 exhibit much lower crack velocities for a given stress intensity than the susceptible alloy/temper combinations.

These data also indicate that in general, alloys 7050 and 7049 in -T7X temper conditions are much superior to 7075-T6, but do not have quite the resistance of 7075-T73. It has also been claimed that although 7049 and 7050 are comparable in laboratory tests (3-1/2% NaCl environment), 7050 has a clear advantage in an industrial atmosphere. In fact, the data in Figures A3 f and g suggest that the crack growth rate of 7049-T73 in the industrial atmosphere is almost as fast as in 3-1/2% NaCl, alterate immersion. Care must be exercised in the interpretation of such data, however, because a valid comparison requires that certain conditions be met:

(1) samples should be from the same product form and section size

(2) specimens should be tested at the same time in the same environment, and

(3) strength levels should be comparable.

It is not clear to what extent the above criteria were satisfied in these evaluations.

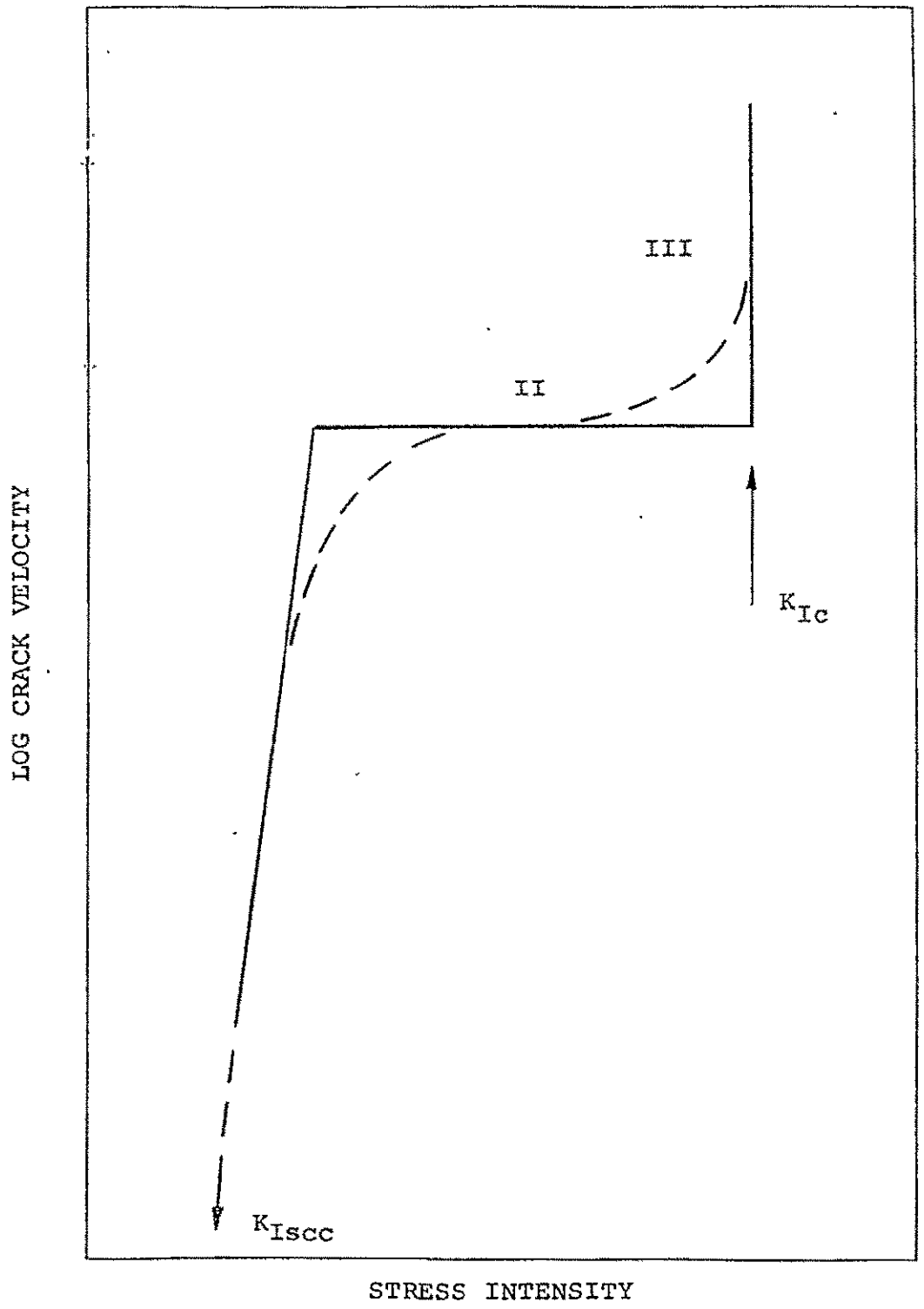

Figure A1. The general dependency of stress corrosion crack velocity on stress intensity

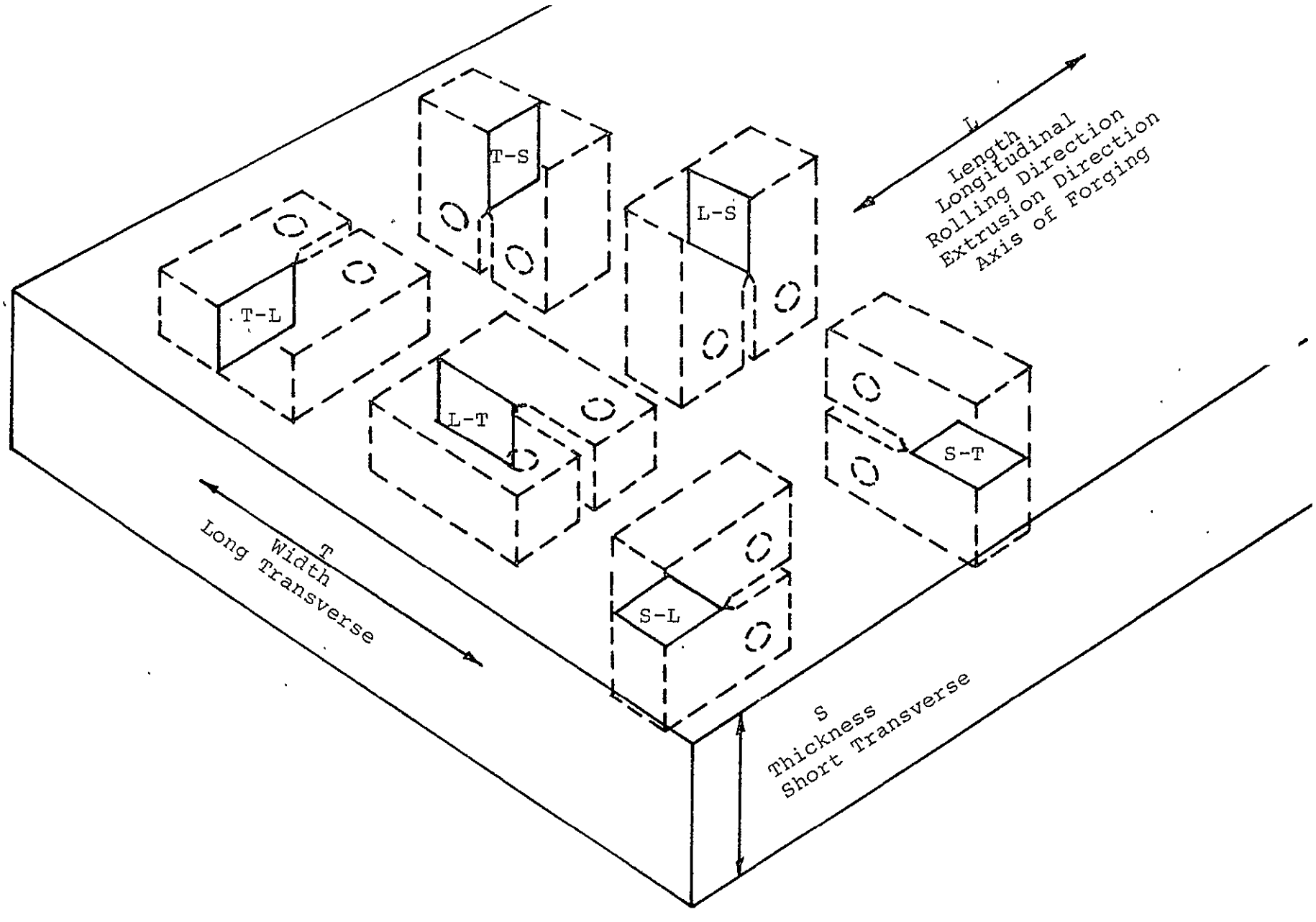

Figure A2. Fracture specimen orientations

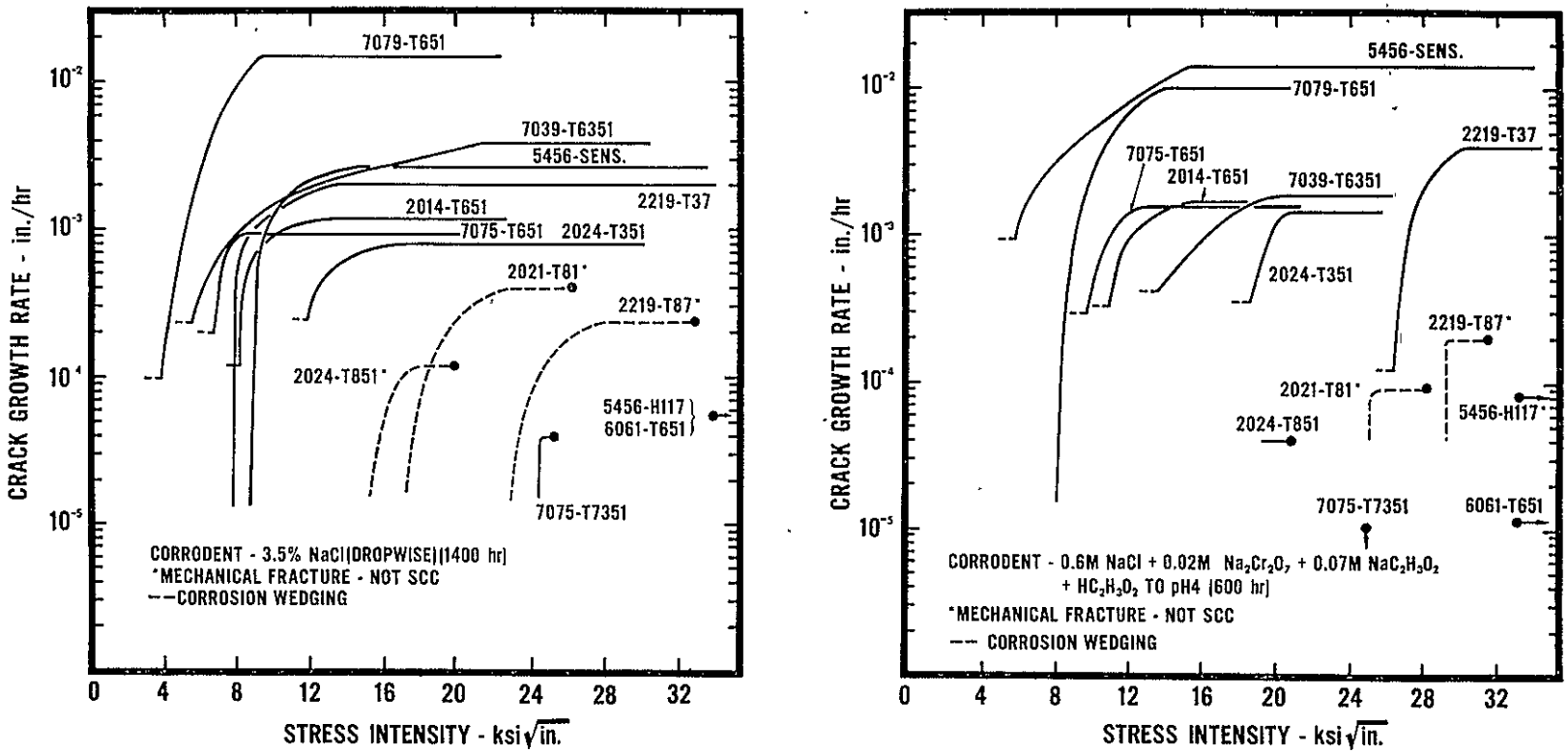

a. Pop-in Precracks-Ref 7

b. Pop-in Precracks-Ref 7

Figure A3. Summary of previously reported V-K plots for aluminum alloys: SL orientation

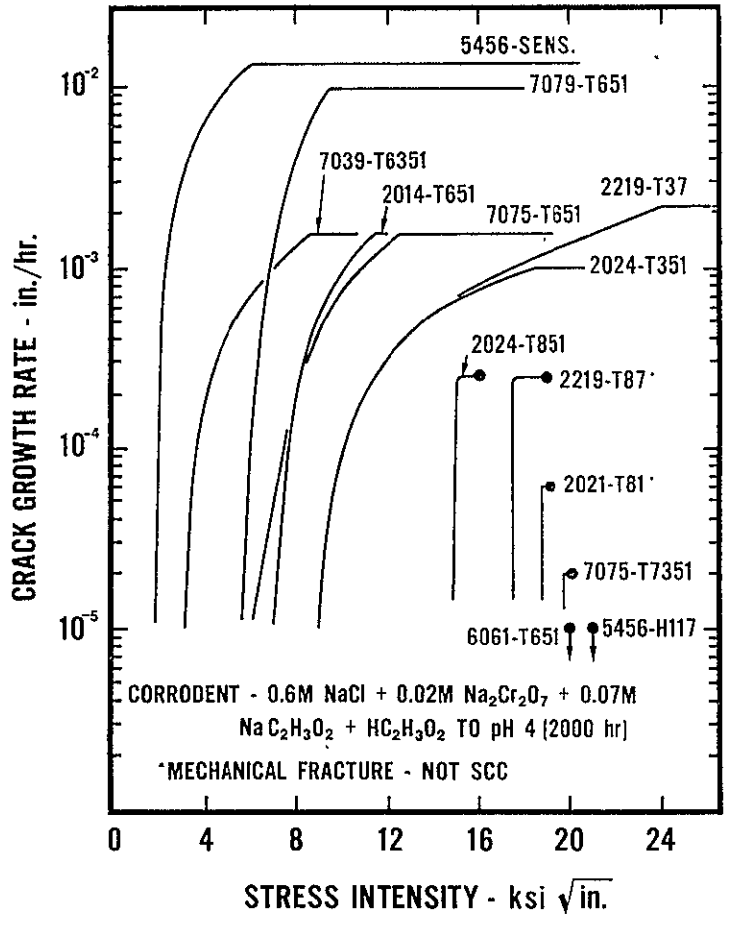

c. Fatigue Precracks-Ref 7

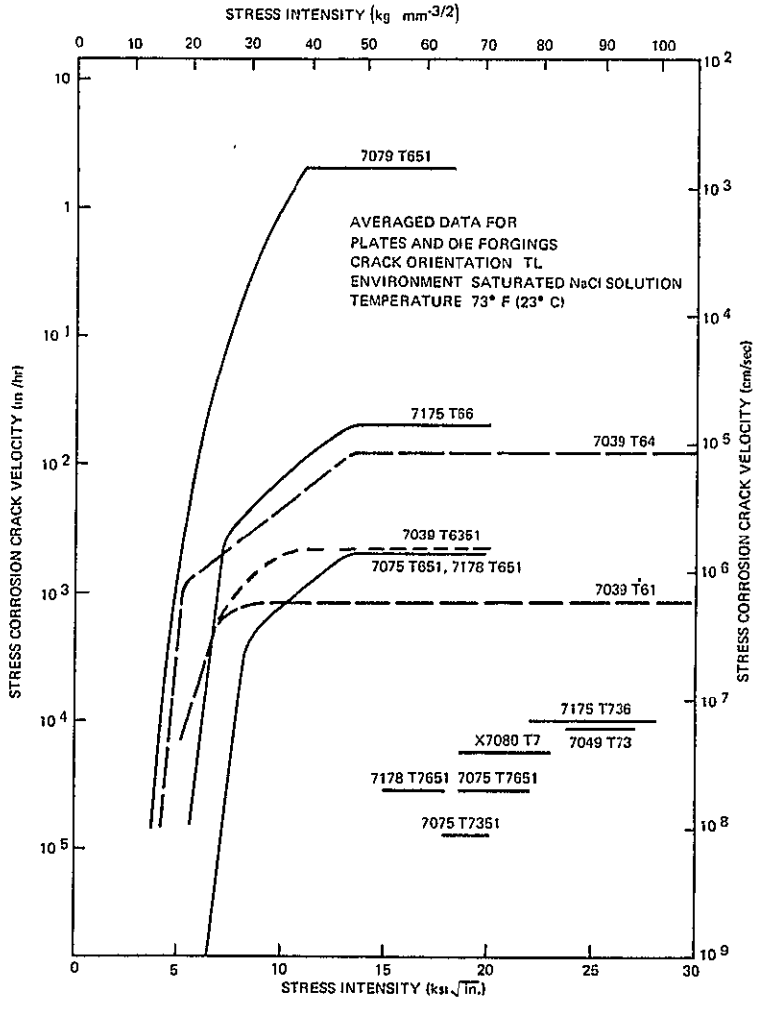

d. Pop-in Precracks-Ref 8

Figure A3. (Cont'd)

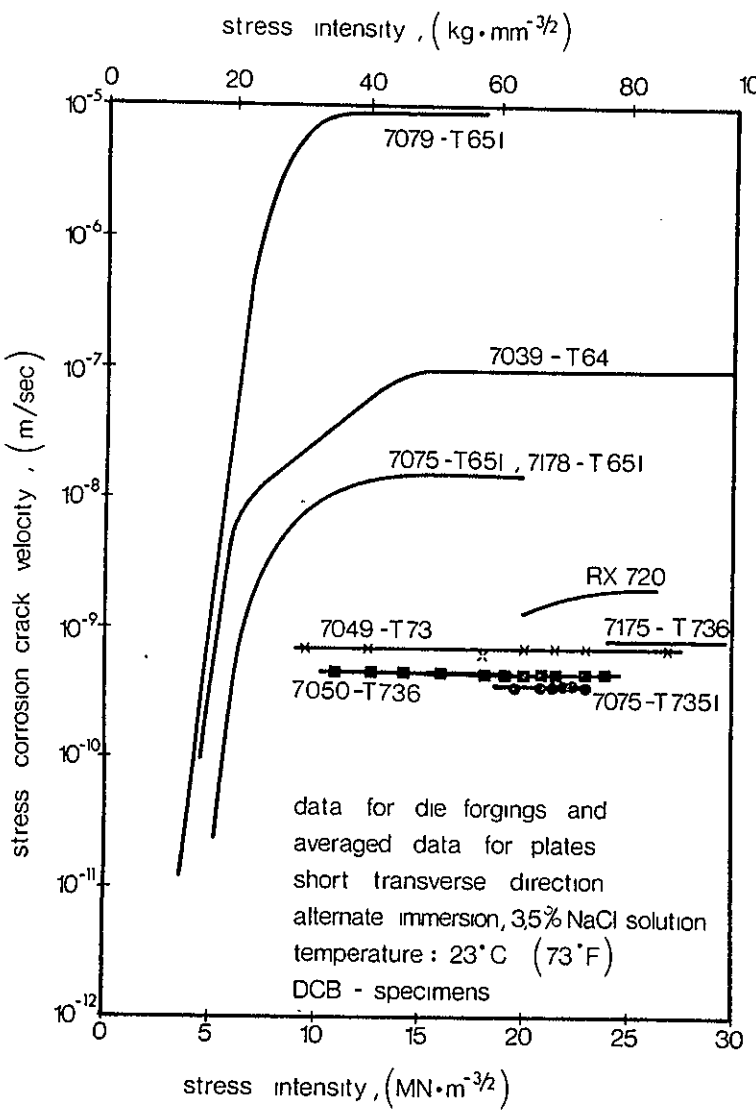

e. Pop-in Precracks-Ref 9

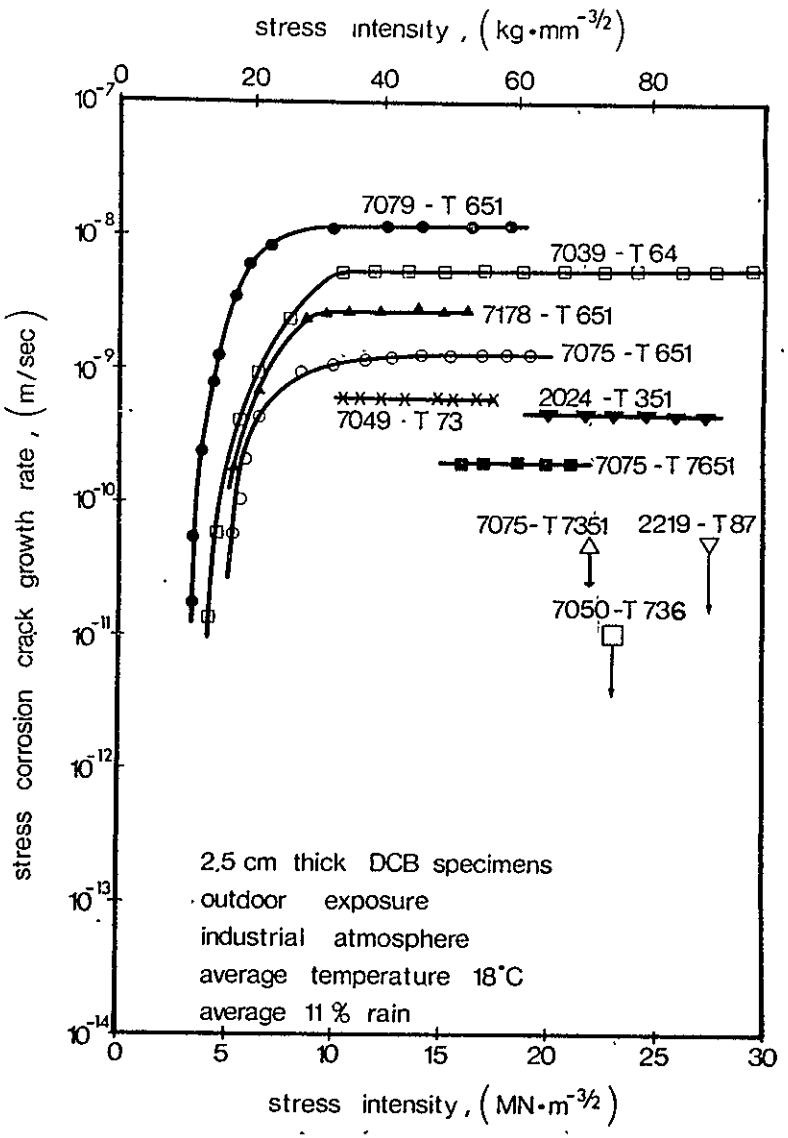

f. Pop-in. Precracks-Ref 9

Figure A3. (Cont'd)

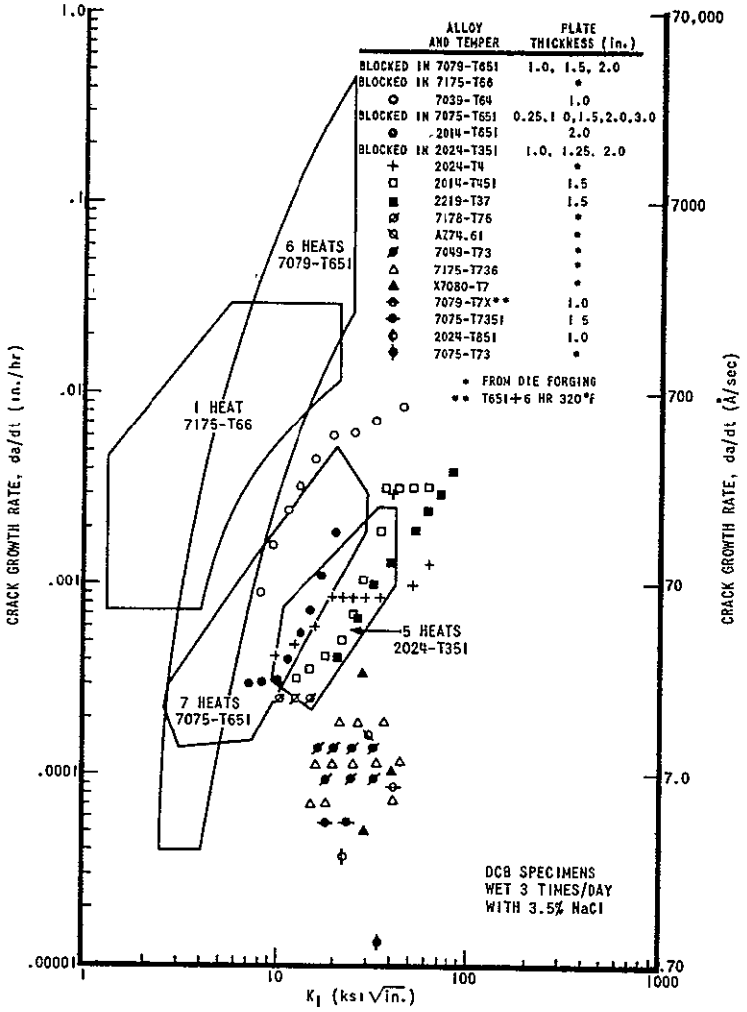

g. Pop-in Precracks-Ref 6

Figure A3. (Cont'd)

APPENDIX B

SYNTHETIC SEA WATER ALTERNATE IMMERSION STRESS CORROSION TEST METHOD

1. Solution make-up. 3.6% by weight commercial synthetic sea salt (Lake Products, Inc.) conforming to ASTM D1141. Fresh solution is prepared weekly. It shall have a pH of 8.2 when prepared, and be maintained to a range of 7.8 to 8.6 by the addition of NaOH or HCl.

2. Immersion cycle. The immersion cycle shall be such that the specimens are covered by the salt solution for 10 minutes of each hour and uncovered for 50 minutes.

3. Methods of cycling. Alternate immersion of the specimens is accomplished by moving the solution with a polyethylene pump from a tank to cover specimens which are stationary in a tray:

   a. To prevent galvanic corrosion, specimens do not touch one another nor any other bare metal during the alternate-immersion test period.

   b. Specimens of alloy containing deliberate additions of copper are not exposed to the same solution used for copper-free aluminum alloys.

4. Replacement of water lost by evaporation. The necessary amount of distilled water is added to maintain the proper salt concentration.

5. Temperature and relative humidity. Air temperature and relative humidity of the laboratory are controlled at 80° ± 2°F and 45 ± 6 percent, respectively. The solution temperature is thermostatically controlled at 75° ± 2°F.

6. Test duration. The test runs continuously for the time indicated or until failure occurs, with interrruptions only for changing solutions or examining specimens.

APPENDIX C

STRESS INTENSITY FACTORS FOR THE DCB SPECIMEN

The DCB specimen (Figure C1) can be loaded with pins and clevises in a conventional tensile testing machine or it can be self-stressed with bolts. In either case, use of the specimen depends upon knowledge of the relationship between the crack-tip stress intensity and crack length.

Two methods are used to obtain expressions for the stress intensity factor; one method is based on stress analysis and the other on specimen compliance (ratio of specimen deflection to load).

Experimental measurements of compliance show that in addition to the deflections due to bending and shear, some deflection also occurs because of rotations at the assumed "built-in" end of the beam (Ref 18). This contribution can be treated as an increase in crack length, and has been found to be approximately equal to 0.6h. This leads to the relations (Ref 18):

$$K_I = \frac{2P}{b}\left[\frac{3(a + 0.6h)^2 + h^2}{h^3}\right]^{1/2}$$

or

$$K_I = \frac{\delta E h^{3/2}[3(a + 0.6h)^2 + h^2]^{1/2}}{4[(a + 0.6h)^3 + h^2 a]}$$

where E is Young's Modulus, δ is the specimen deflection at the load point, and all other symbols are as shown in Figure C1. For a side-grooved specimen, K_I is multiplied by $(b/b_n)^{1/2}$; the use of 10% side-grooves increases K_I by about 5% (Ref 19).

The relationship between stress intensity, crack length, load and displacement is illustrated in Figure C2 for a DCB specimen with 2h = 25mm, b = 25 mm, b_n = 22.5 mm and E = 7.2 x 10^4 MPa. It is apparent that the stress intensity increases with crack length under constant load, but decreases with crack length at constant displacement, i.e., bolt loading. It is also apparent from Figure C2 that unique values of load and displacement are associated with a given crack length. In other words, crack length can be computed from measurements of load and displacement (compliance) or, at constant load, from measurements of displacement alone.

Figure C3 shows how stress intensity depends on crack length for bolt-loaded specimens having heights of 25 and 75 mm. For material having a given susceptibility to stress corrosion, the larger specimen would grow a longer crack in a given exposure time because K changes less rapidly with crack extension. Initial precrack length is also a factor; as Figure C4 shows, the shorter the precrack, the more dependent stress intensity becomes on crack length.

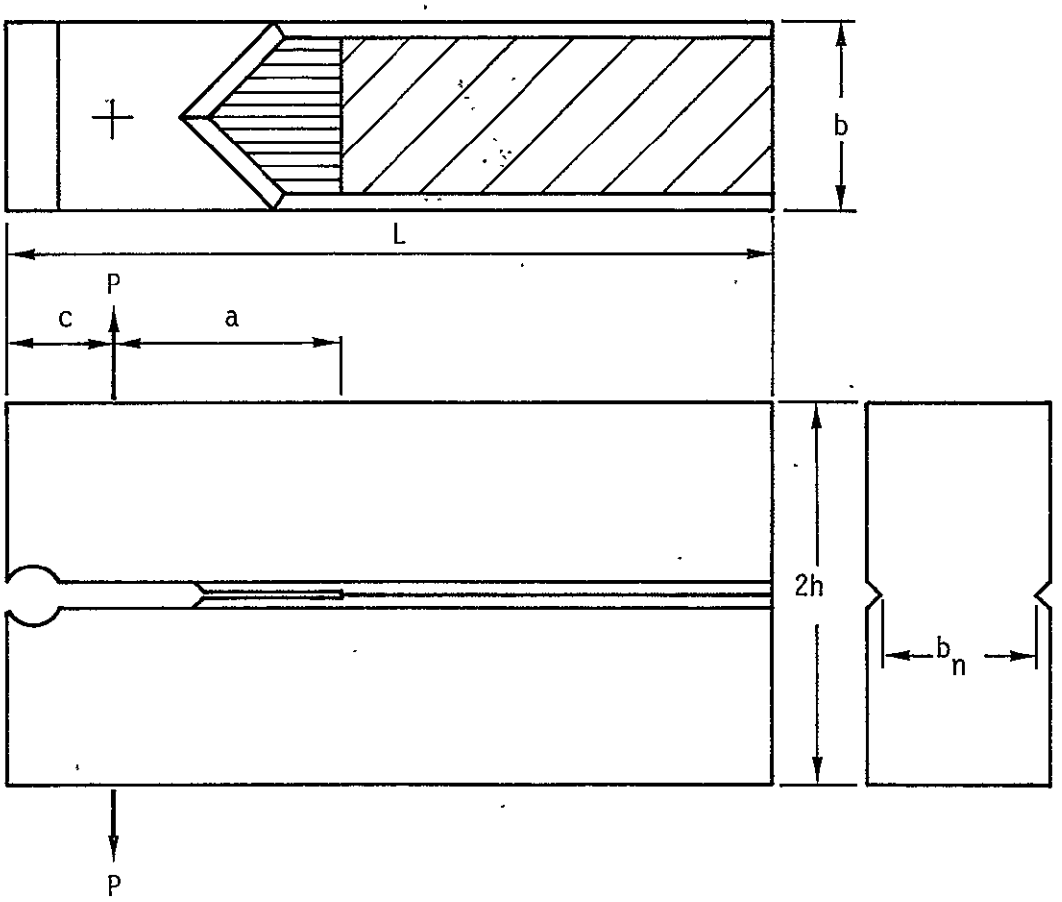

Figure C1. Double cantilever beam (DCB) specimen

P = Load
a = Crack length (measured from load point)
h = Specimen half height
b = Specimen thickness
b_n = Net thickness at crackline
L = Specimen length
c = Distance from load point to location of displacement measurement

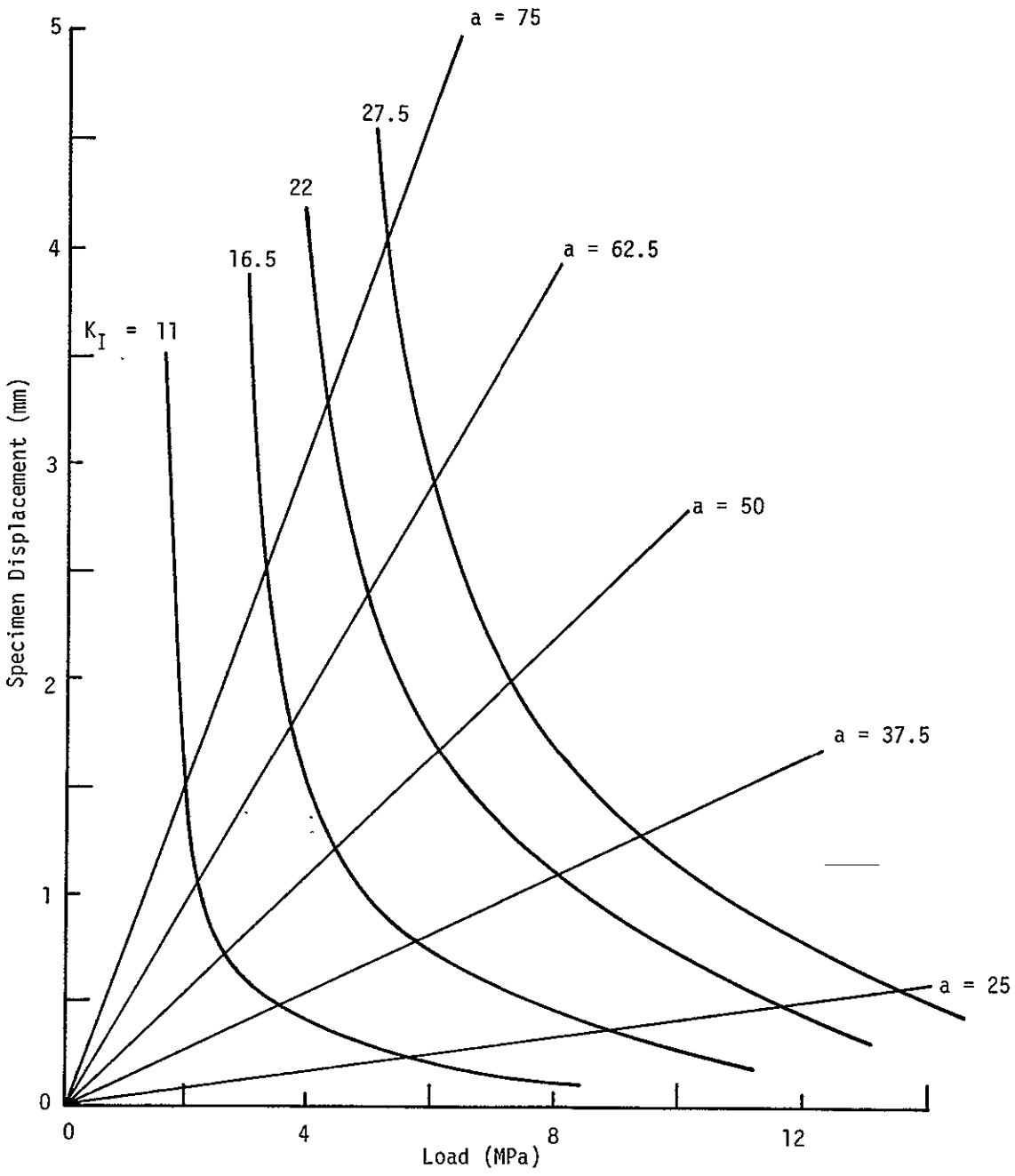

Figure C2. Compliance relationship for uniform DCB specimen

Relationships shown are for a specimen of height, 2h = 25 mm; thickness, b = 25 mm and b_n = 22.5 mm; and E = 7.2 x 10^4 MPa. Crack length, a in mm; and stress intensity, K_I in MPa$\sqrt{m}$.

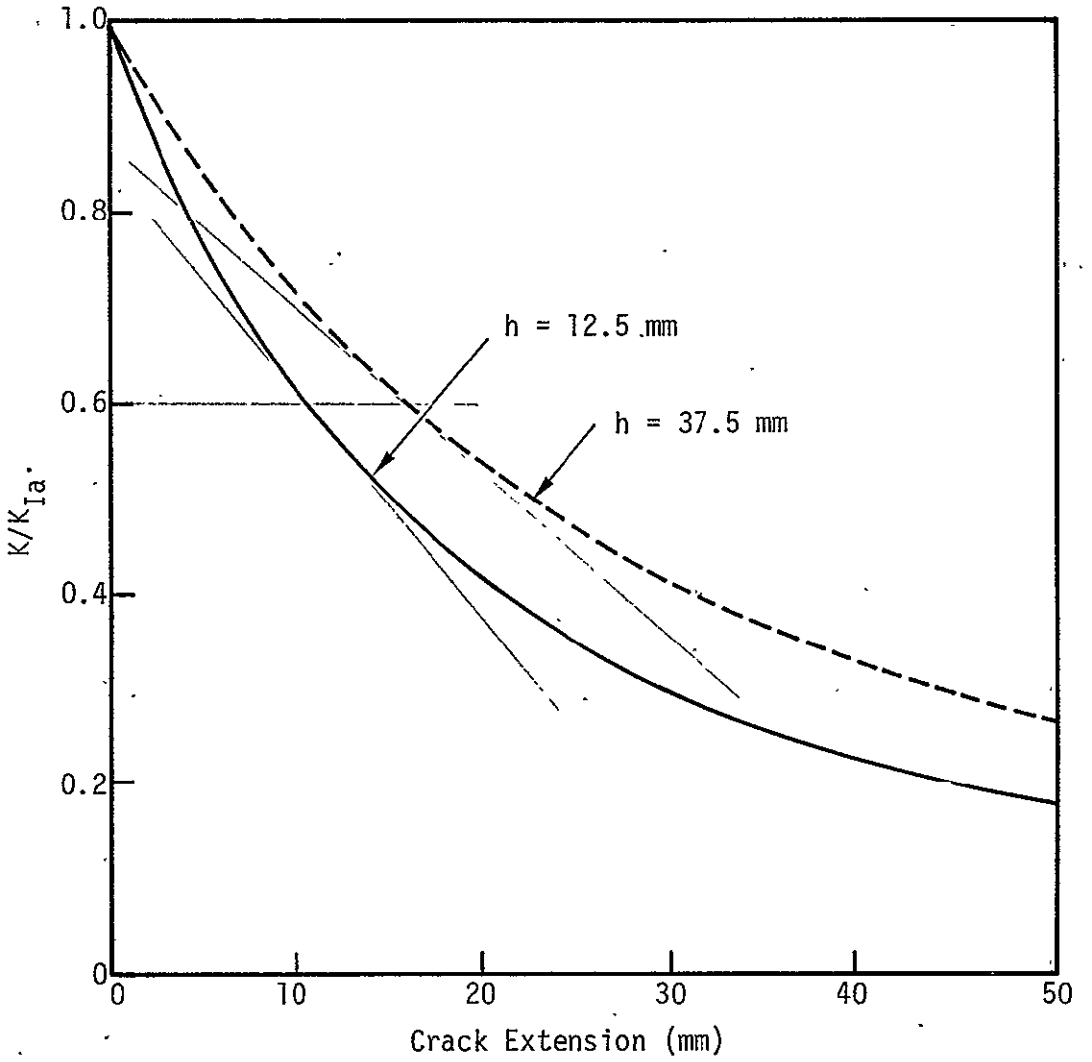

Figure C3. Stress intensity dependence on crack growth for different specimen heights

Precrack is assumed to be 25 mm from load point.

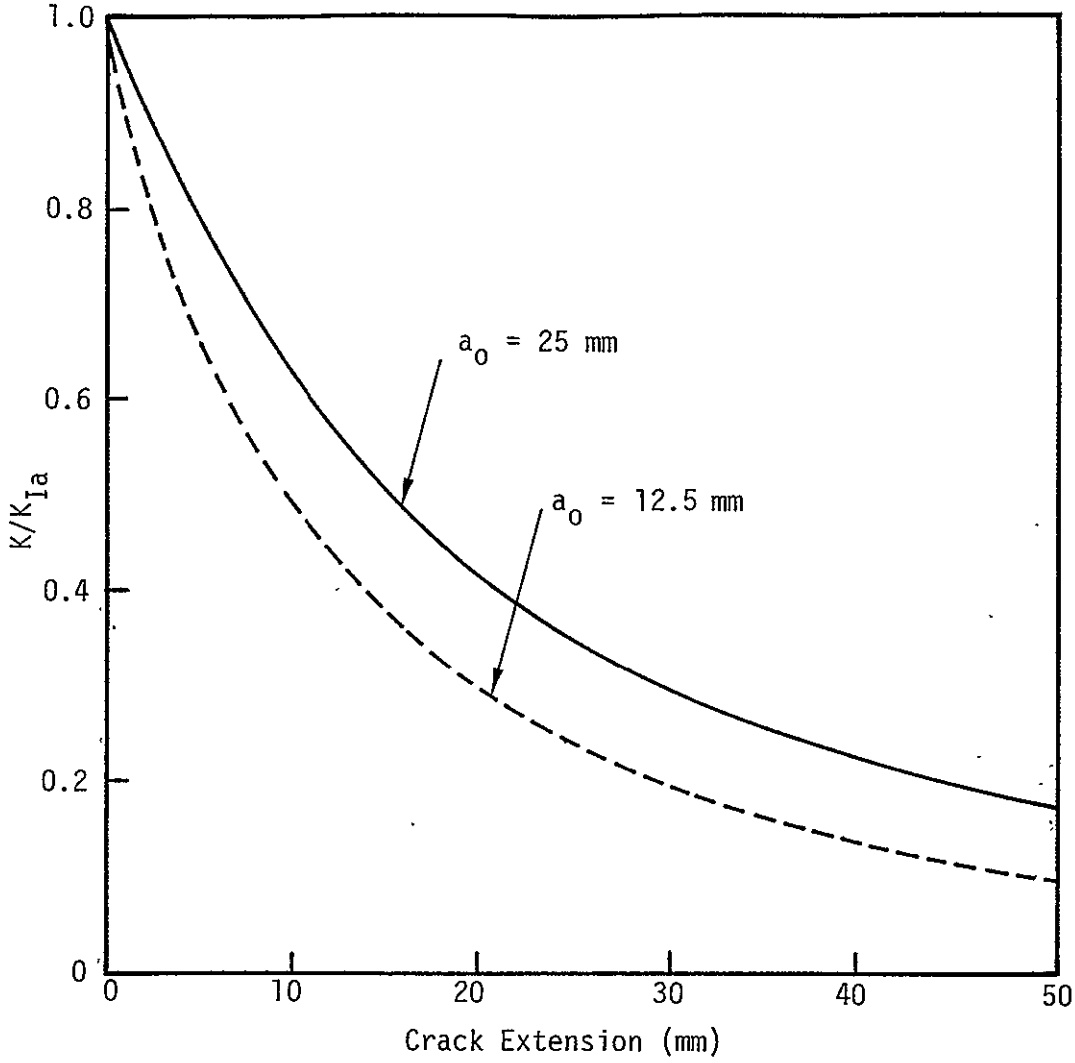

Figure C4. Stress intensity dependence on crack extension for different precrack lengths (a_o)

Specimen height is 25 mm.

APPENDIX D

STRESS INTENSITIES FOR CRACK ARREST (K_{Ia}) IN PRECRACKED DCB SPECIMENS

Stress intensity for crack arrest values as determined on the 25-mm high bolt-loaded DCB specimens are listed in Table D1 together with the fracture toughness (K_{Ic}) results. The data are also compared in a correlation plot in Figure D1 (data for the 3.0-in. plate, TL orientation, are not included because measurements were not conducted at the same location by each procedure).

As Figure D1 shows, both measurements gave quite comparable numbers, K_{Ia} on the average being slightly less than K_{Ic}. The agreement is much better than that reported by Sprowls et al (Ref 21) for 7075-TX51 plate materials, in which K_{Ia} was found to be up to 50% higher than K_{Ic} for specimens having similar dimensions. However, specimens in that study were not side grooved; high K values would therefore be expected (Ref 18) because deformation is not restricted to the plane of the crack, i.e., a shear-lip effect.

Although K_{Ia} might be expected to be lower than K_{Ic}*, there are a number of reasons why K_{Ia} as measured in this study could be relatively high. First, crack lengths were estimated from measurements at the specimen edges. An over-estimation of stress intensity would be expected since the crack fronts are often curved, leading slightly at the center of the specimen. Figure D2, for example, shows the fracture surface of a DCB specimen that was marked with dye during the precracking operation. For this particular specimen crackfront curvature caused the crack length

*For 7075-T6 Hoagland (Ref 22) showed K_{Ia} to be about 1.5 MPa$\sqrt{m}$ lower than K_{Ic}, both values determined on pop-in cracks.

to be underestimated by 1.5 mm; this would result in an 8% error in K_{Ia} for a 25-mm high specimen having a 25 mm crack length.

Another reason for high K_{Ia} values relative to K_{Ic} involves the different nature of the mechanical crack in each case. K_{Ic} measurements are made on a crack induced by fatigue at low stress intensity. K_{Ia}, on the other hand, is a measure of the stress intensity at which a crack induced by mechanical pop-in will arrest. This is a high stress intensity situation, and the plastic deformation involved could give a relatively high K_{Ia} value. In addition, a mechanical pop-in crack is probably blunter and more irregular than a fatigue precrack; this would also tend to increase K_{Ia}.

High apparent stress intensities in a DCB specimen can also be caused by an invalidation of the compliance relationship (from which the stress intensity formula was derived) due to plastic deformation of the specimen arms. Although simple stress analysis indicated that no such gross plastic yielding occurred at the strength and toughness levels involved in this study, we do not rule out the possibility that larger plastic zone sizes (relative to the beam height) than those encountered in establishing the compliance relation may have been achieved. A comparison of K_{Ia} values obtained on 25 and 75-mm high DCB specimens (Table D2), for example, shows slightly lower values for the larger specimen size. However, this difference could also be due to a smaller effect of underestimating crack length in the larger specimen (K changes less rapidly with crack length as the beam height increases).

The amount of scatter was somewhat greater with the DCB specimens than with the compact specimens (standard deviation of 1.1 $MPa\sqrt{m}$ vs. 0.8 $MPa\sqrt{m}$). This is quite likely due to lack

of precision in crack length determination; as discussed above this uncertainty could easily be eliminated by actual measurements on marked fracture surfaces. Marking the fracture surface would also allow measurements of both crack arrest and crack initiation toughness.

In spite of these limitations, a good correlation appears to exist between the K_{Ia} values and fracture toughness as measured by conventional methods. As expected, there were also the usual inverse relationships between K_{Ia} and yield strength as are commonly observed for K_{Ic} (Figure D3). We note, however, that good agreement between K_{Ia} (pop-in precrack, DCB specimen) and K_{Ic} (fatigue precrack, compact specimen) is specific to the family of alloys evaluated. Such a correlation for steels, for example, would be less likely, because they typically exhibit large differences between K_{Ia} and K_{Ic}. They are also more crack rate sensitive than aluminum alloys, and K_{Ia} appears quite dependent on the whole crack propagation history prior to arrest. Although this may also be true to some extent for aluminum alloys, a "K_{Ia}" test conducted under reproducible conditions should nevertheless correlate with true K_{Ic} values.

These results indicate that a simple bolt-loaded DCB specimen has promise as a practical alternative to those now used for routine fracture toughness testing of high-strength aluminum alloys* (Ref 23). However, additional work should be conducted on materials having higher toughness levels, and on other alloys such as 2124, 5086 and 6061. If the procedure proves out, it could greatly facilitate quality control testing at producing plants. Although machining costs may be no less than at present,

*This specimen was proposed for such purposes about 10 years ago (Refs 18 & 22).

the specimens do not have to be precracked; a tensile machine is not even necessary. All that is required is a clip-in strain gauge with electronic display (sufficiently accurate visual and/or mechanical methods of measuring deflection are also probably feasible), and a visual measurement of crack length, preferably on a dye-marked fracture surface.

Table D1. Comparison of K_{Ic} (Compact Specimen) and K_{Ia} (DCB Specimen) Values

Material[a]	Thickness in.	Stress Intensity (MPa$\sqrt{m}$) SL Orientation K_{Ic}[b]	SL Orientation K_{Ia}[c]	TL Orientation[d] K_{Ic}[b]	TL Orientation K_{Ia}[c]
7075-T651	1.25	24.2	21.3(3)	25.1	23.6(3)
7075-T7651	1.25	23.1	21.7(3)	25.2	23.8(3)
7075-T7351(M)	1.25	23.4	21.7(2)	-	-
7075-T7351(T)	1.25	24.3	23.8(15)	26.7	26.1(7)
7075-T651	3.0	19.6	19.8(3)	22.4	22.6(3)
7075-T7651	3.0	21.3	21.2(3)	22.0	23.8(3)
7075-T7351(M)	3.0	23.2	24.2(2)	-	-
7075-T7351(T)	3.0	23.5	24.8(7)	24.8	26.7(7)
7475-T7351(M)	1.25	25.7	24.0(2)	-	-
7475-T7351(T)	1.25	26.7	27.1(7)	31.7	32.8(7)
7475-T7351(M)	3.0	26.7	25.4(2)	-	-
7475-T7351(T)	3.0	29.7	30.0(7)	30.5	33.9(7)
7050-T73651(M)	1.25	25.7	24.2(2)	-	-
7050-T73651(T)	1.25	27.3	25.2(7)	31.2	28.3(7)
7050-T73651(M)	3.0	26.8	24.7(2)	-	-
7050-T73651(T)	3.0	27.9	28.3(6)	29.2	30.5(7)
7049-T7351(M)	1.25	25.9	23.0(2)	-	-
7049-T7351(T)	1.25	27.8	27.5(7)	31.2	30.9(7)
7049-T7351(M)	3.0	23.8	24.2(2)	-	-
7049-T7351(T)	3.0	27.6	26.3(7)	27.2	29.6(7)

[a] M indicates minimum-aged condition; T indicates typical condition.

[b] Triplicate specimens (best estimate of standard deviation, s = 0.8 MPa$\sqrt{m}$).

[c] DCB specimens were 25 mm high. Numbers in brackets give number of replicates (best estimate of standard deviation, s = 1.1 MPa$\sqrt{m}$)

[d] K_{Ic} and K_{Ia} values in 3-in. plate were not measured at the same location (1/4t for K_{Ic}; 1/2t for K_{Ia}).

Table D2. Comparison K_{Ic} (Compact Specimen) and K_{Ia} Values Determined on 25 mm and 75 mm High DCB Specimens: SL Orientation

Material[a]	Thickness, in.	Stress Intensity (MPa $\sqrt{m}$) K_{Ic}[b]	$K_{Ia(1")}$[c]	$K_{Ia(3")}$[d]
7075-T7351(T)	3.0	23.5	24.8	24.1
7475-T7351(T)	3.0	29.7	30.0	29.0
7050-T73651(T)	3.0	27.9	28.3	27.8
7049-T7351(T)	3.0	27.6	26.3	25.9

[a] T indicates typical condition.

[b] Compact Specimen: average of 3 replicates (s = 0.8 MPa$\sqrt{m}$).

[c] 25-mm high DCB specimen: average of 7 replicates (s = 1.1 MPa$\sqrt{m}$).

[d] 75-mm high DCB specimen: average of 6 replicates (s = 1.1 MPa$\sqrt{m}$)

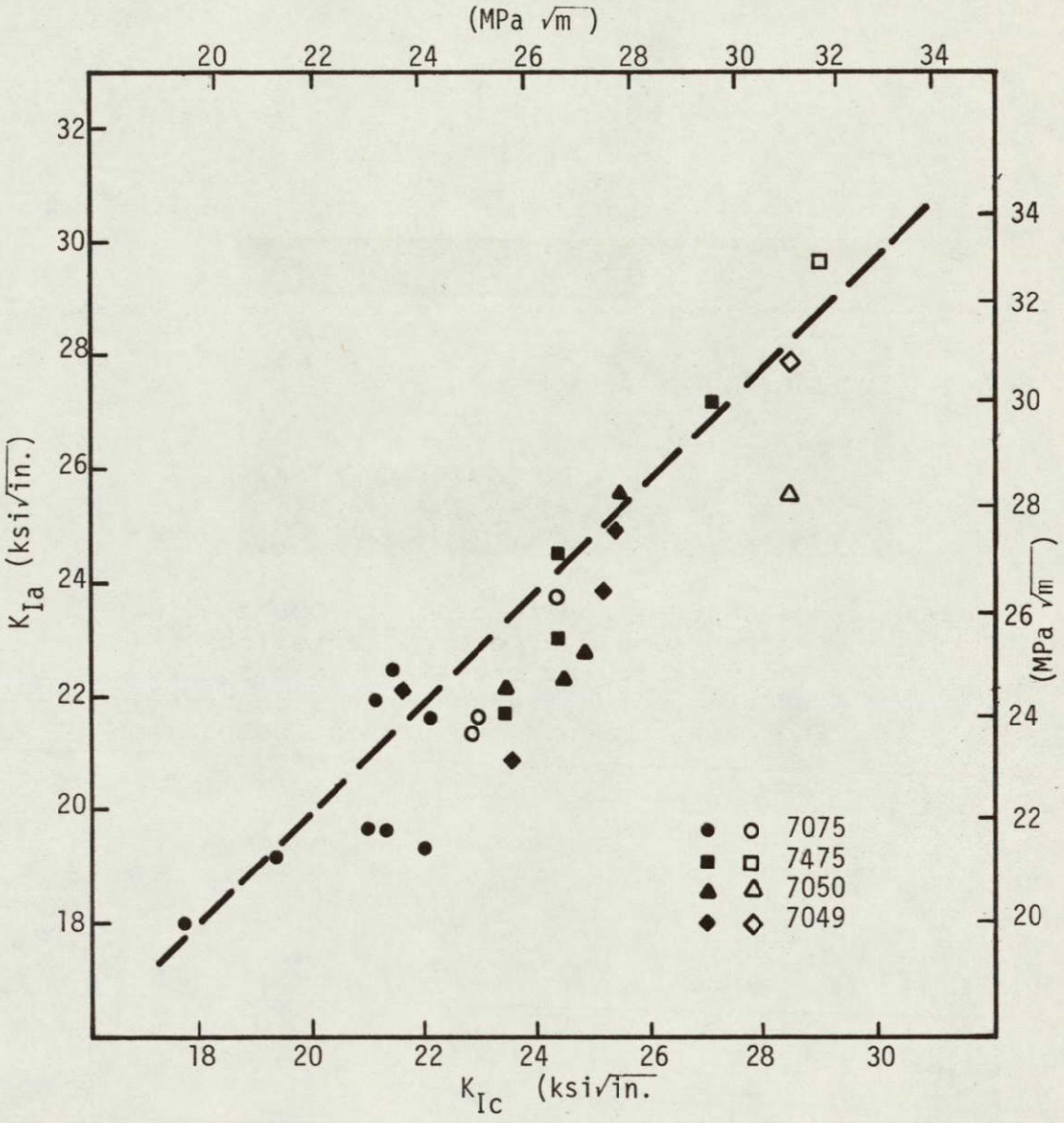

Figure D1. Correlation of SL and TL K_{Ic} (compact tension specimens) and K_{Ia} (25 mm DCB specimens) values for 1.25- and 3.0-in. thick plates; solid symbols: SL orientation, open symbols: TL orientation.

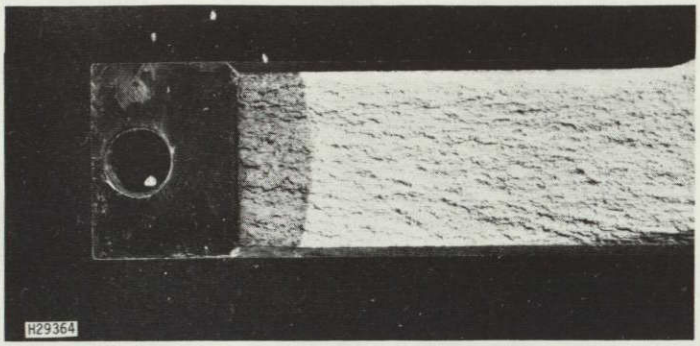

Figure D2. Mechanical pop-in crack in DCB specimen marked with dye before fracturing (1X). This particular specimen had a square starter notch, rather than a chevron notch as used in the present comparison study.

APPENDIX E

SURFACE AND CROSS SECTION EXAMINATIONS OF STRESS CORROSION CRACKS

Terminated DCB specimens tested in each environment were broken open for measurements of crack length and to examine crack morphology. The specimens were split lengthwise (normal to the fracture), and half of each specimen was broken open for examination of the fracture surface; the other half was polished for metallographic examination of the fracture cross section. Fracture surfaces of specimens tested in the salt-chromate solution are shown as tested (no cleaning was required). The right half of the fracture surface of specimens tested in marine atmosphere was cleaned in concentrated nitric acid to remove corrosion product. Study was centered on specimens tested in the marine atmosphere at Daytona Beach (Figure E1 series), since this represents a practical situation, and on specimens tested in the salt-chromate environment (Figure E2 series), since this test gave the clearest distinction between the precrack and subsequent stress corrosion.

As noted previously, general corrosion made it difficult to tell where the precrack ended and stress corrosion began in specimens tested in the marine atmosphere. (This transition was clearly defined in specimens tested in the salt-chromate environment.) In cross section, the cracks were non-planar with many unfailed ligaments remaining. Because of mixed mechanical/stress corrosion fracture at the start of the stress corrosion crack, it was not easy to tell exactly where the precrack ended in any given cross sectional view. General corrosion in the marine atmosphere specimens further obliterated this transition zone. The stress-corrosion cracks generated from

the fatigue precracks were much straighter than those associated with the pop-in precracks.

Stress corrosion cracks in the TL orientation were blunted by general corrosion. It appears that these cracks usually propagate transgranularly by following subgrain paths. In addition to the short TL cracks in these specimens, there were longer secondary cracks propagating normal to the plane of the precrack, i.e., SL oriented. These cracks are shown in greater detail in Figure E1 (f). These secondary cracks may have been generated by a combination of residual tensile stress in the plate interior (they were generally longer at the center of the specimen than at the edges), and the transverse tensile stress acting in the direction of the leading edge of the crack (σ_z). It is noteworthy that the length of these secondary cracks was approximately equal to the size of the plastic zone associated with the precrack tip ($r_p \simeq K_I^2/3\pi\sigma_y^2 \simeq 0.6$ mm). We also note that the cracks assumed a shape similar to that calculated for the plastic zone (Ref 32)--see Figure E3. It is apparent that these secondary cracks are self-limiting in length; the -T6 temper material, for example, grew cracks only slightly longer than those found in the resistant -T73 temper samples.

SL cracks in the 3.0-in. thick plates were also quite blunt, and in many locations were running out of plane, with a greater tendency towards branching than in the thinner plate.

Aside from the cleaner appearance of the fracture surfaces and better definition of stress corrosion at crack tips, the most noteworthy feature of specimens tested in the salt-chromate solution was the thin crack line shown in the 5X cross sections. Thicker cracks in specimens tested in marine atmosphere may have been caused by general corrosion on the fracture surfaces. This

may also indicate some wedging from corrosion product buildup occurred. (Specimens tested in 3.6% artificial seawater were similar to those tested in marine atmosphere in this respect.)

In view of the crack features noted (blunting, branching, jogs, unfailed ligaments, etc.), it becomes apparent that stress intensities measured in a precracked specimen probably bear little relationship to those actually present at the crack tip. In most cases, apparent (measured) stress intensities are higher than the actual average values. Differences between the actual and apparent values are probably smaller in fatigue-precracked specimens than in those containing a pop-in precrack. This difference would also tend to be smaller in the thinner materials; similarly, stress intensities would be overestimated to a greater extent in the TL orientation than in the SL orientation.

Figure E1. Fracture surfaces and cross sections of DCB specimens exposed for 6.5 months at Daytona Beach, Fla.

(a) 1.25 in. plate, pop-in precrack (SL)

(b) 1.25 in. plate, fatigue precrack (SL)

(c) 1.25 in. plate, pop-in precrack (TL)

(d) 3.0 in. plate, pop-in precrack (SL)

(e) 3.0 in. plate, pop-in precrack (TL)

(f) 1.25 in. 7049-T7351(T) specimen (TL)

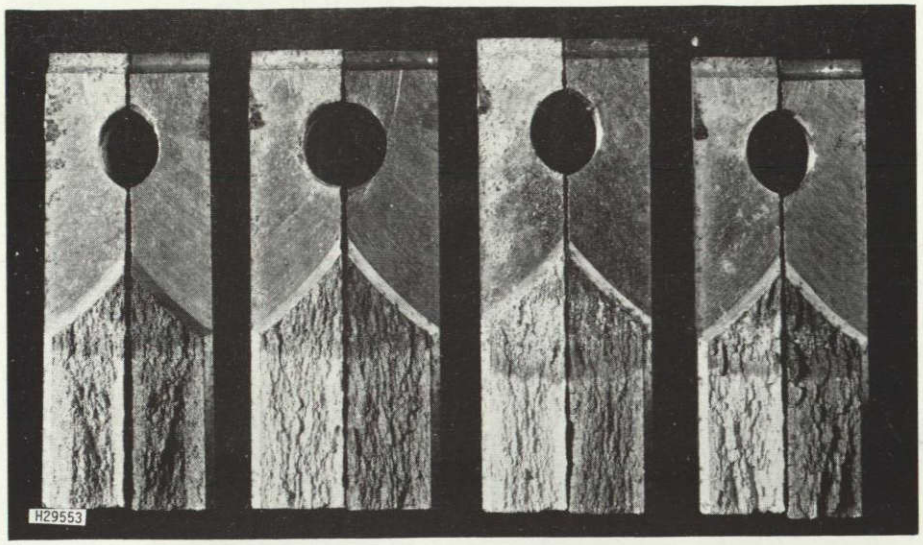

Fracture Surfaces 1X

2.0 2.8 5.8 3.6

Crack Extension mm

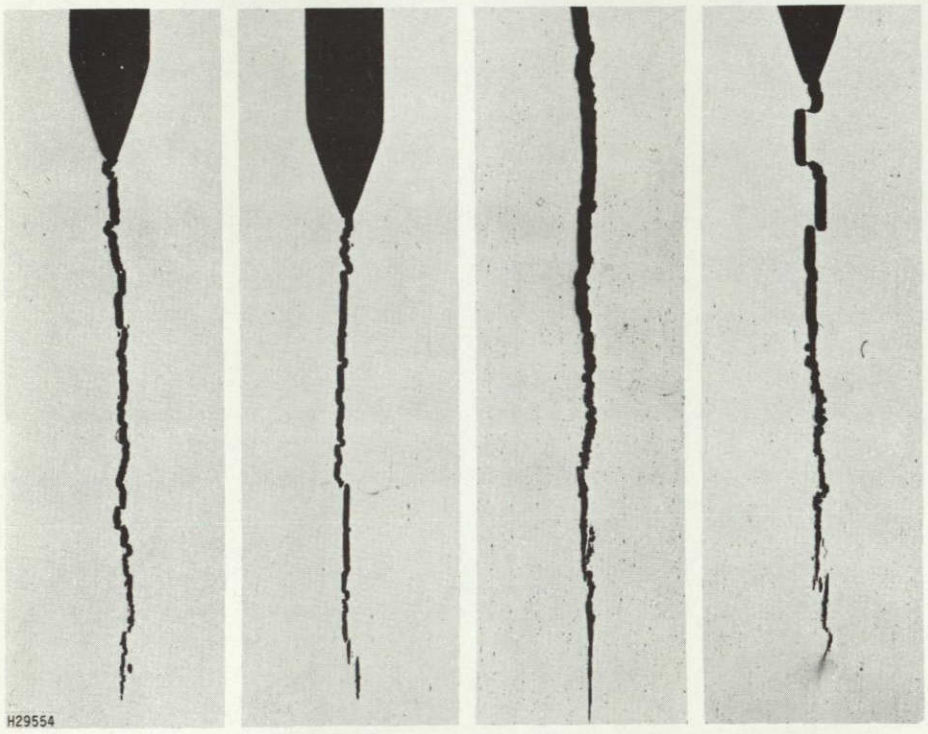

Cross Sections 5X

7075-T7351 7475-T7351 7050-T73651 7049-T7351

Material: 1.25 in. plate Typical temper condition

Test: 6.5 months marine atmosphere, Daytona Beach, Fla.

DCB Specimen: SL orientation 25 mm high, bolt loaded, pop-in precrack

Figure E1. (a)

Crack Tips - 200X

Etch: 10% H_3PO_4 at 120°F (3 min)

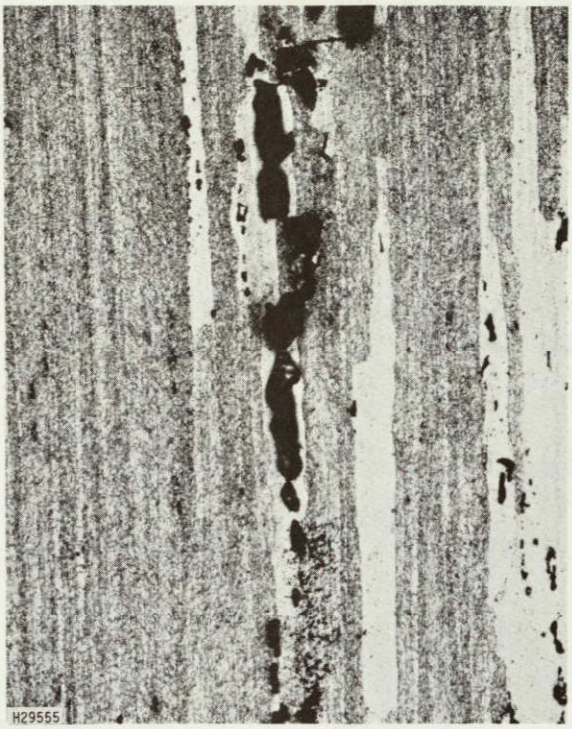

7075-T7351

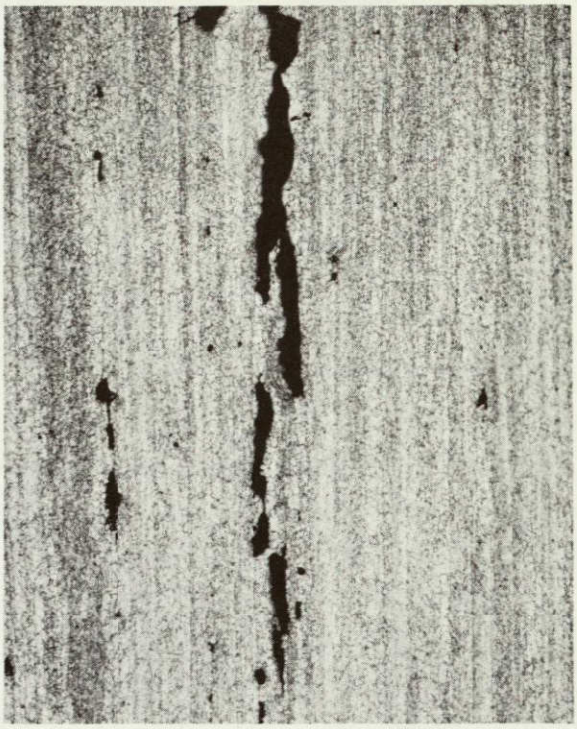

7475-T7351

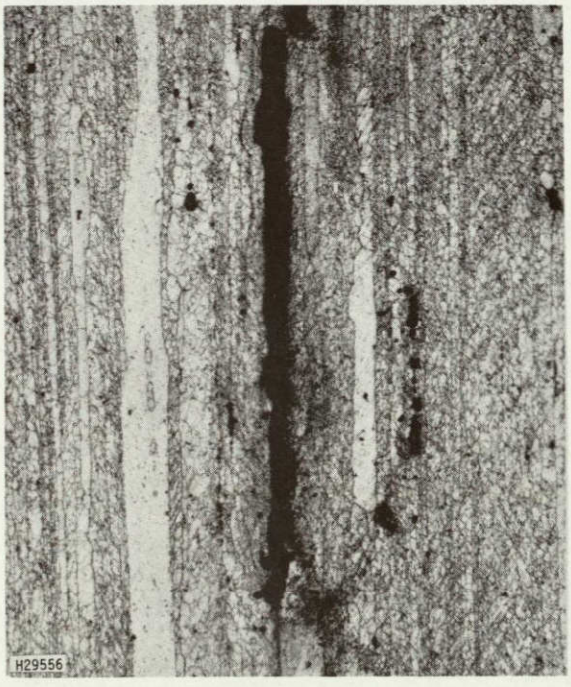

7050-T73651

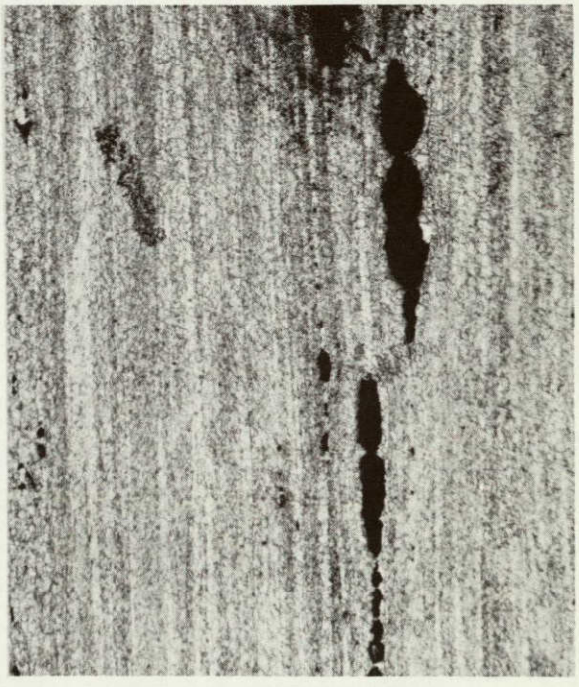

7049-T7351

Stress corrosion cracks in pop-in precrack DCB's were ragged with many jogs and unfailed ligaments remaining.

Figure E1. (a) Cont'd.

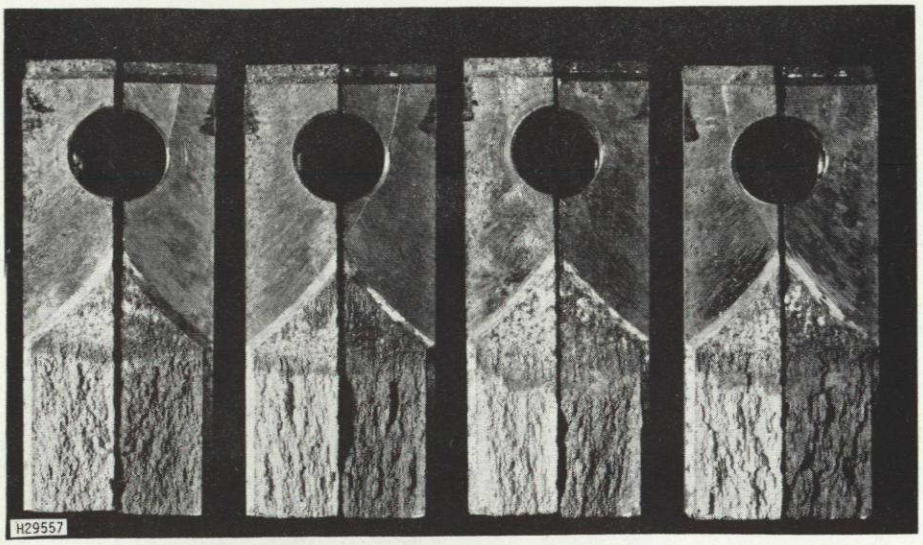

Fracture Surfaces 1X

1.3 2.3 5.1 3.6

Crack Extension mm

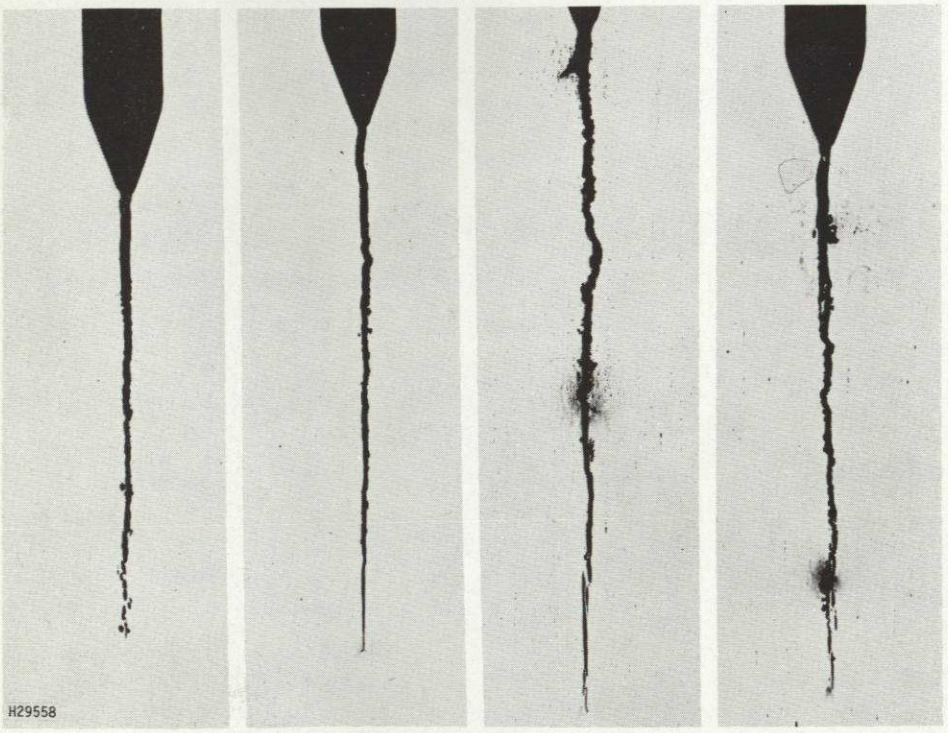

Cross Sections 5X

7075-T7351 7475-T7351 7050-T73651 7049-T7351

Material: 1.25-in. plate Typical temper condition

Test: 6.5 months marine atmosphere, Daytona Beach, Fla.

DCB Specimen: SL orientation 25 mm high, bolt loaded, fatigue precrack

Figure E1. (b)

Crack Tips - 200X

Etch: 10% H_3PO_4 at 120°F (3 min)

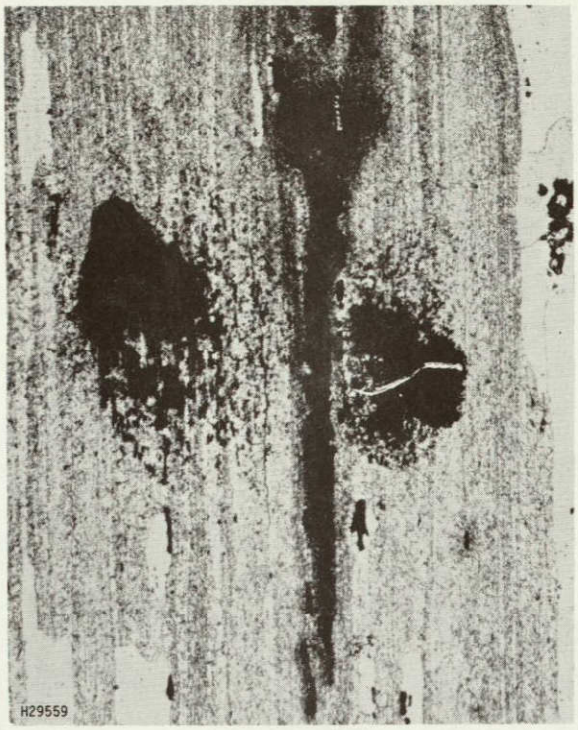

7075-T7351

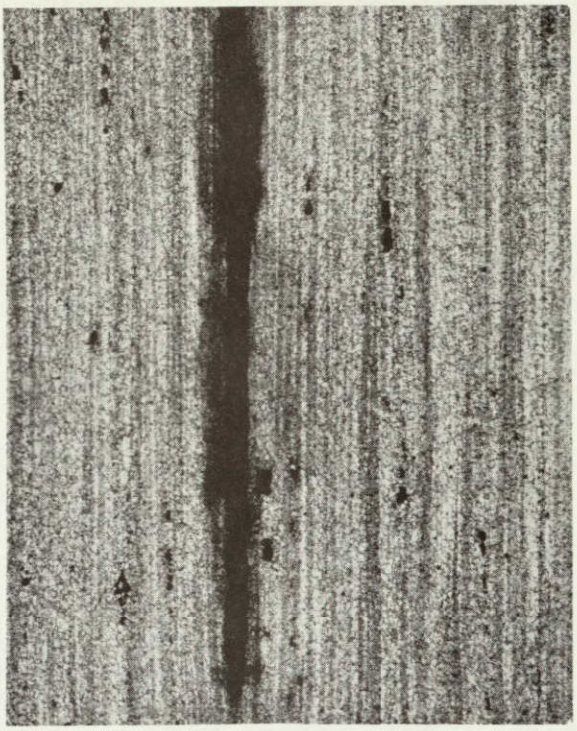

7475-T7351

7050-T73651

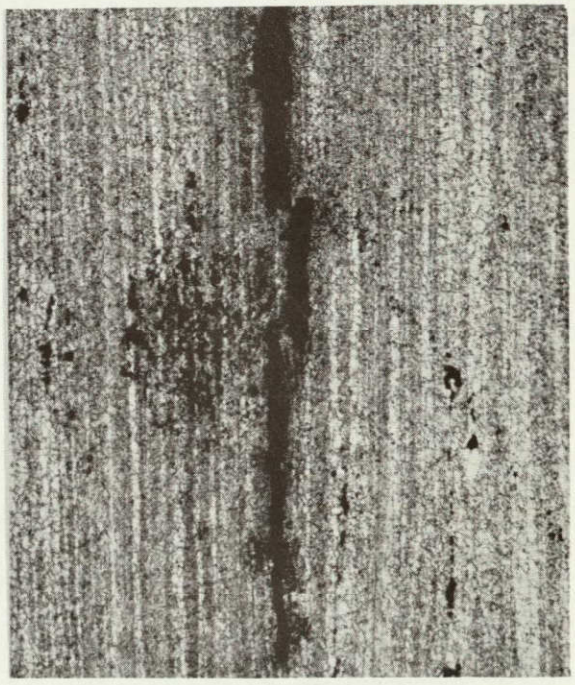

7049-T7351

Stress corrosion cracks in fatigue precracked DCB's were more planar than those generated from pop-in precracks.

Figure E1. (b) Cont'd.

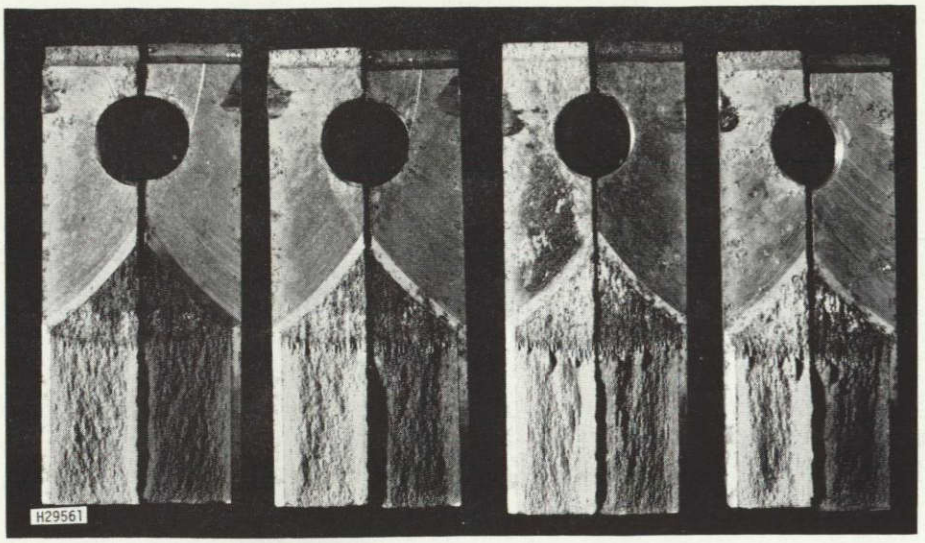

Fracture Surfaces 1X

0.8 1.3 1.8 0.8

Crack Extension mm

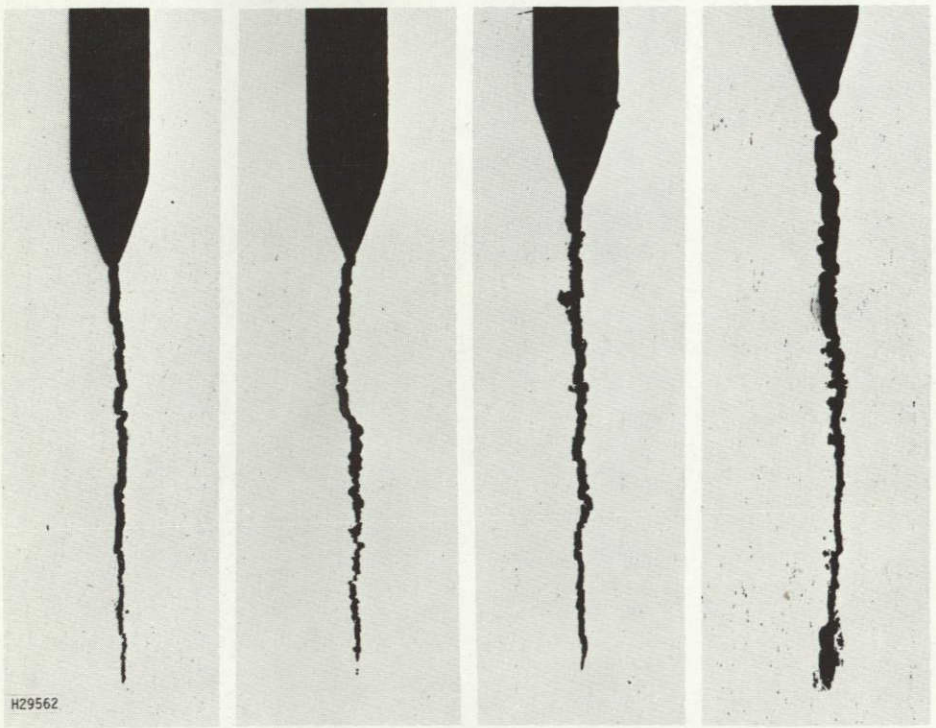

Cross Sections 5X

7075-T7351 7475-T7351 7050-T73651 7049-T7351

Material: 1.25-in. plate Typical temper condition

DCB Specimen: TL orientation 25 mm high, bolt loaded, pop-in precrack

Test: 6.5 months marine atmosphere, Daytona Beach, Fla.

Figure E1. (c)

Crack Tips - 200X

Etch: 10% H_3PO_4 at 120°F (3 min)

7075-T7351

7475-T7351

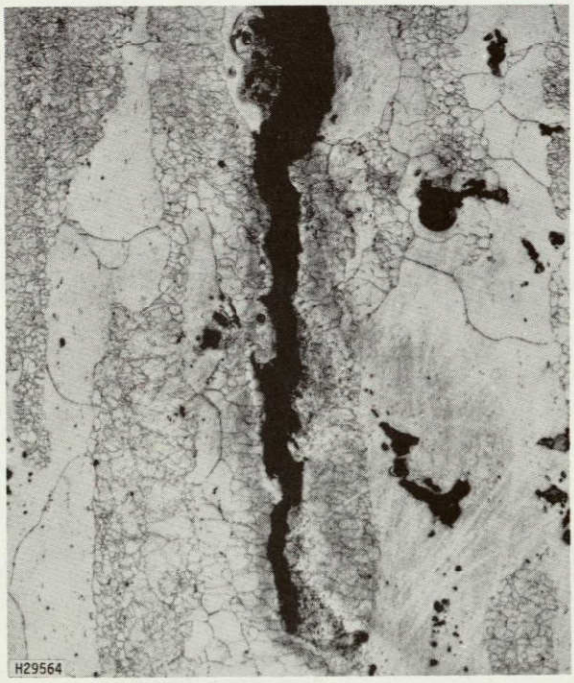

7050-T73651

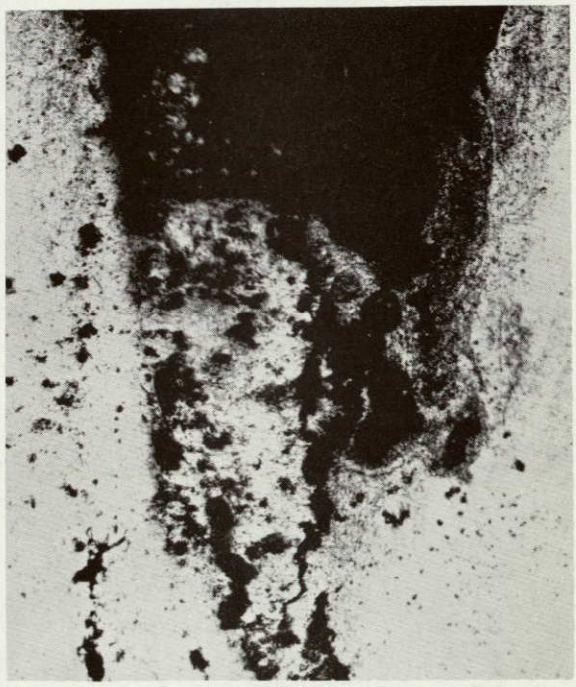

7049-T7351

Note cracks normal to and leading major crack plane in photo of fracture surfaces (opposite page). TL cracks were blunt and appeared to be progressing through subgrains.

Figure El. (c) Cont'd.

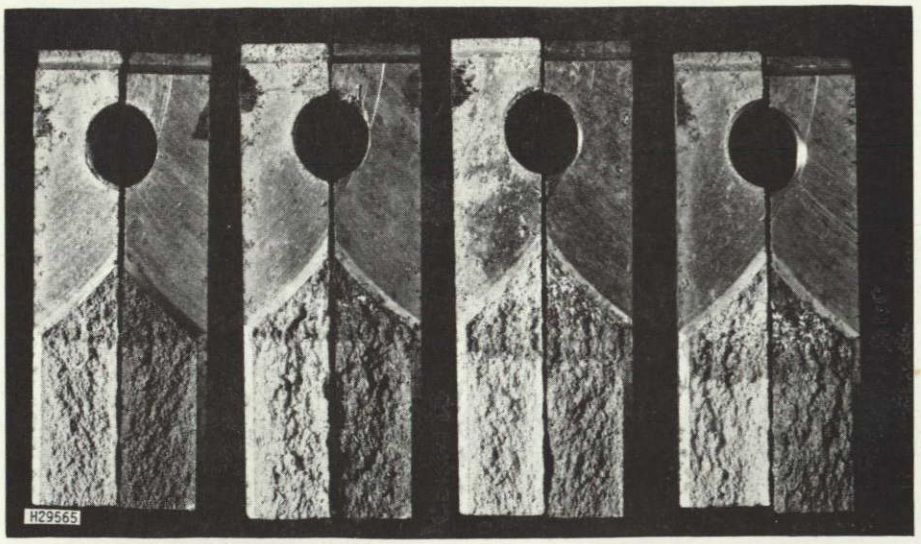

Fracture Surfaces 1X

0.5* 1.0 2.8 4.1

Crack Extension mm

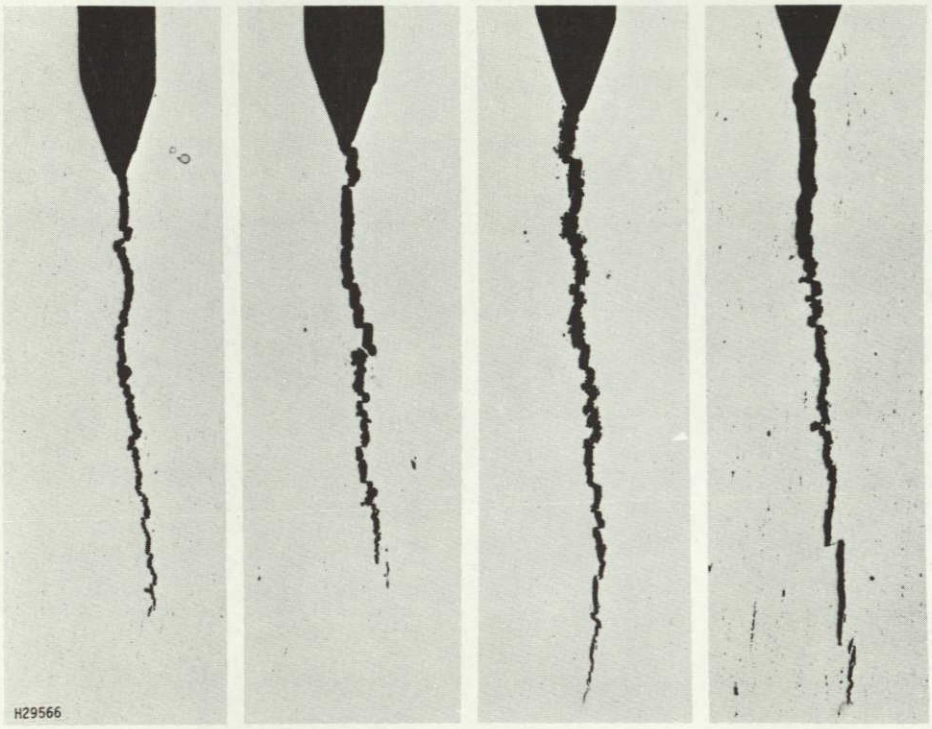

Cross Sections 5X

7075-T7351 7475-T7351 7050-T73651 7049-T7351

Material: 3.0-in. plate
Typical temper condition

Test: 6.5 months marine atmosphere, Daytona Beach, Fla.

DCB Specimen: SL orientation, 25 mm high, bolt-loaded, pop-in precrack

*No detectable stress corrrosion on fracture surface of 7075-T7351

Figure El. (d)

Crack Tips - 200X
Etch: 10% H_3PO_4 at 120°F (3 min)

7075-T7351

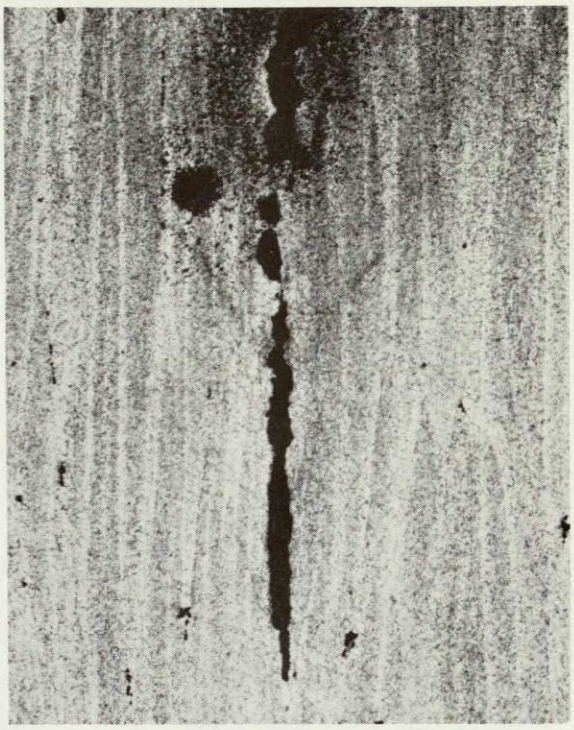

7475-T7351

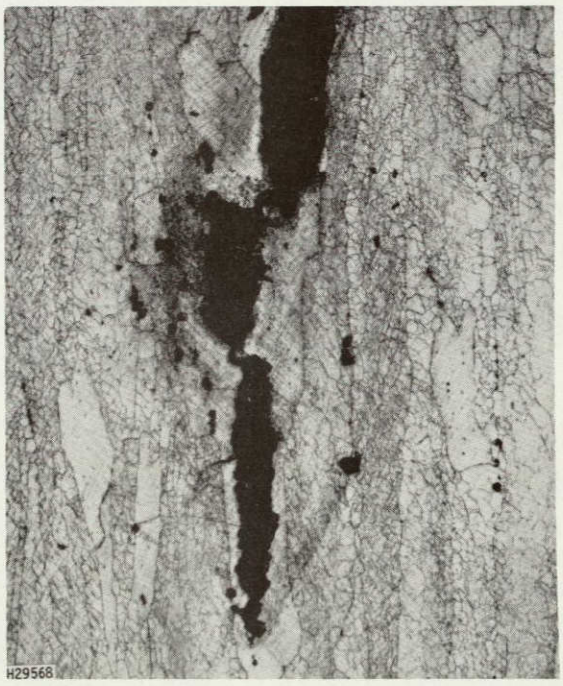

7050-T73651

7049-T7351

Cracks were quite blunt with a tendency towards branching. Note transgranular nature of crack in 7050 material.

Figure E1. (d) Cont'd

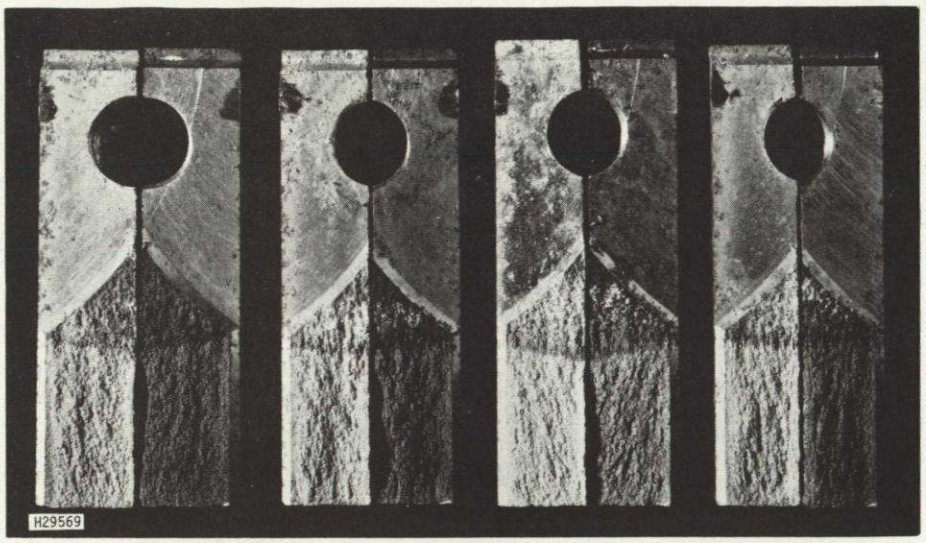

Fracture Surfaces 1X

0.8*	0.8*	-	0

Crack Extension mm

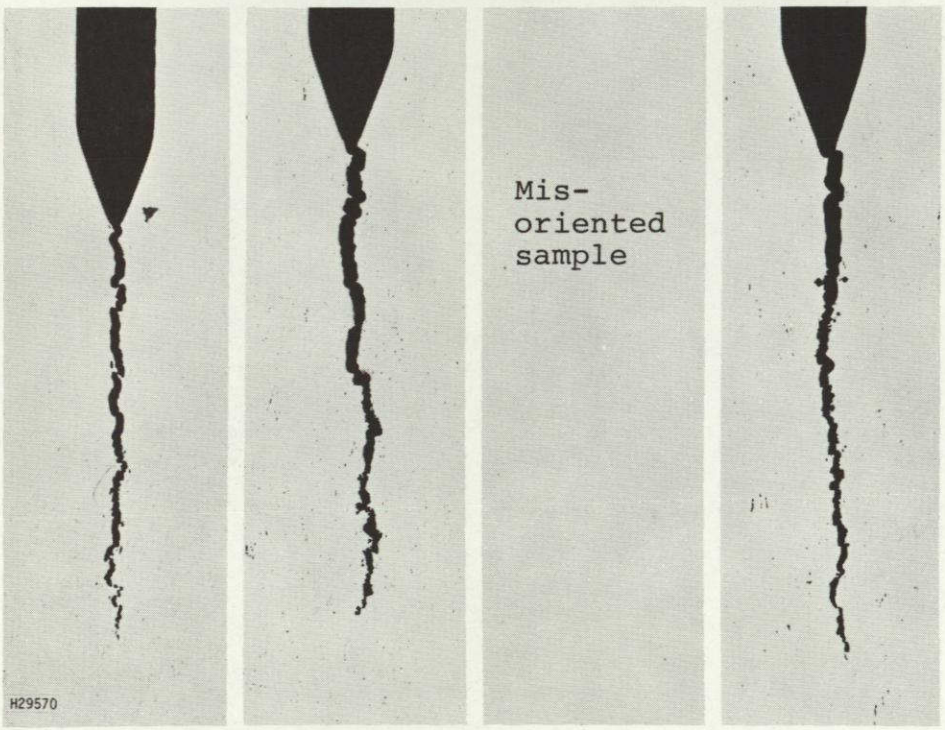

Cross Sections 5X

7075-T7351	7475-T7351	7050-T73651	7049-T7351

Material: 3.0-in. plate
Typical temper condition

DCB Specimen: TL orientation, 25 mm high, bolt loaded, pop-in precrack

Test: 6.5 months marine atmosphere, Daytona Beach, Fla.

*No detectable stress corrosion on fracture surface.

Figure E1. (e)

Crack Tips - 200X

Etch: 10% H_3PO_4 at 120°F (3 min)

7075-T7351

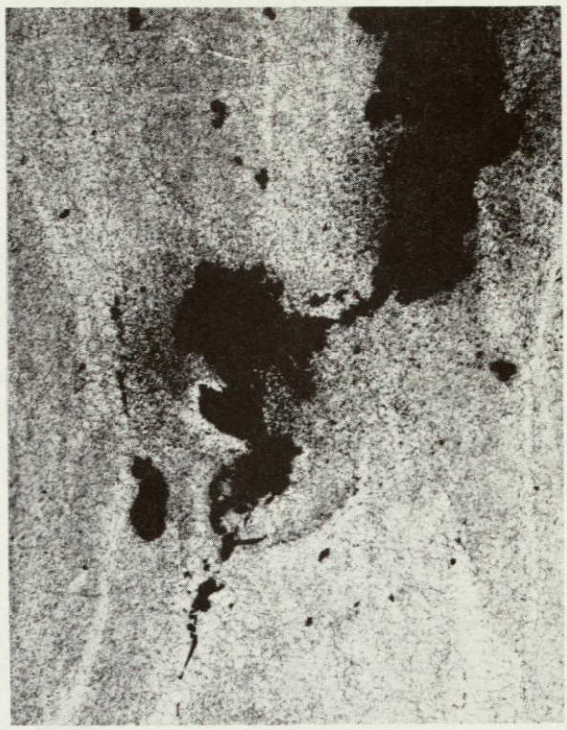

7475-T7351

Mis-oriented sample

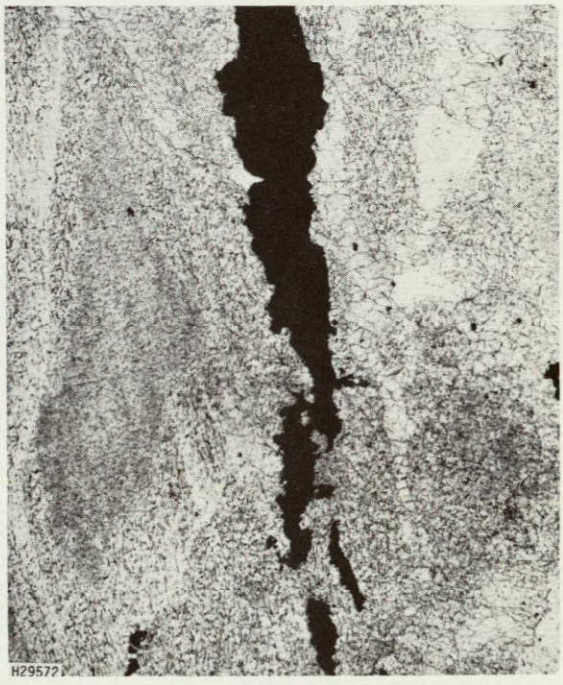

7050-T73651

7049-T7351

Although fracture surfaces did not show typical stress corrosion, there were small cracks normal to the fracture surface. The photomicrographs show short segments of apparent subgrain boundary attack.

Figure E1.(e) Cont'd

Specimen Edge

Specimen Center

8X

Figure E1. (f) Fracture surface of TL DCB from 1.25-in. 7049-T7351(T) plate exposed 6.5 mo. at Daytona Beach

Note numerous short transverse cracks normal to the fracture plane and extending in both directions, out of the apparent stress corrosion fracture area.

Figure E2. Fracture surfaces and cross sections of DCB specimens exposed for 6 months to salt-chromate solution, constant immersion

(a) 7075-T651 and -T7651 plate, pop-in precrack (SL)

(b) 7075-T651 and -T7651 plate, pop-in precrack (TL)

(c) 1.25-in. -T7351(M) plate, pop-in precrack (SL)

(d) 1.25-in. -T7351(T) plate, pop-in precrack (SL)

(e) 1.25-in. -T7351(T) plate, fatigue precrack (SL)

(f) 1.25-in. -T7351(T) plate, pop-in precrack (TL)

(g) 3.0-in. -T7351(M) plate, pop-in precrack (SL)

(h) 3.0-in. -T7351(T) plate, pop-in precrack (SL)

(i) 3.0-in. -T7351(T) plate, pop-in precrack (TL)

(j) 3.0-in. -T7351(T) plate, pop-in precrack (SL), 75 mm high specimen

(k) pop-in and fatigue precracks in 1.25-in. 7075-T7351(T) plate

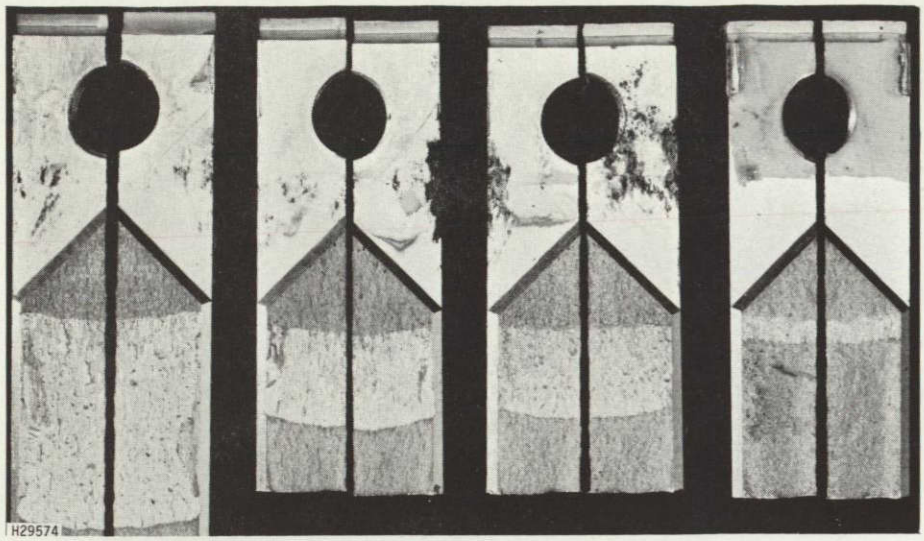

Fracture Surfaces 1X

27.4 13.0 11.7 3.0

Crack Extension mm

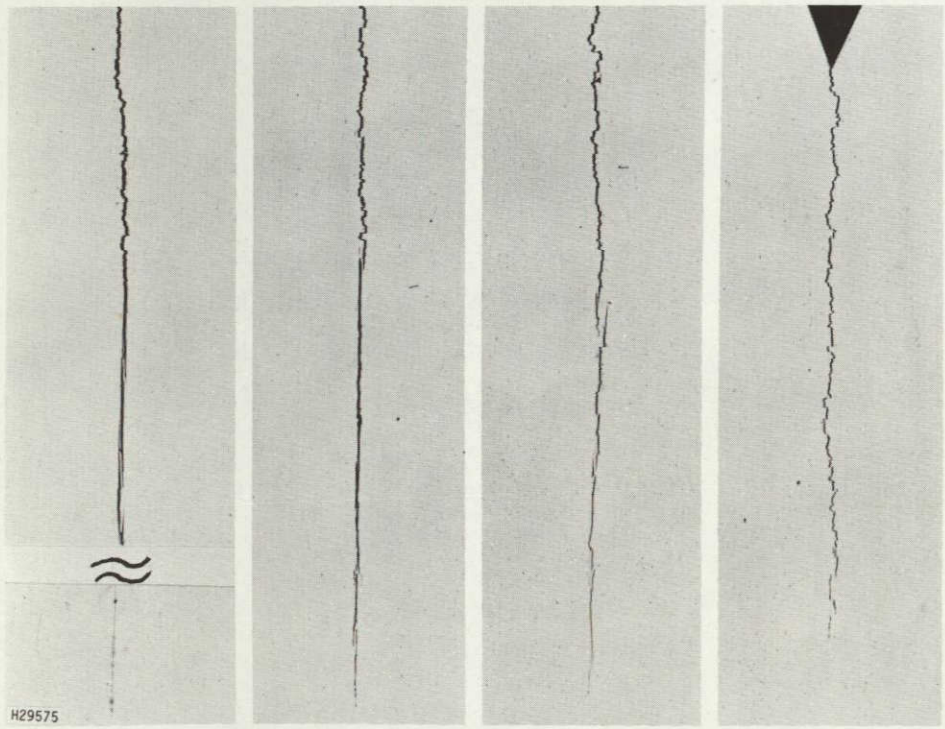

Cross Sections 5X

7075-T651 7075-T7651 7075-T651 7075-T7651

1.25-in. plate 3.0-in. plate

Test: 6 months salt-chromate constant immersion

DCB specimen: SL orientation, 25 mm high, bolt-loaded, pop-in precrack

Figure E2.(a)

Crack Tips - 200X
Etch: 10% H_3PO_4 at 120°F (3 min)

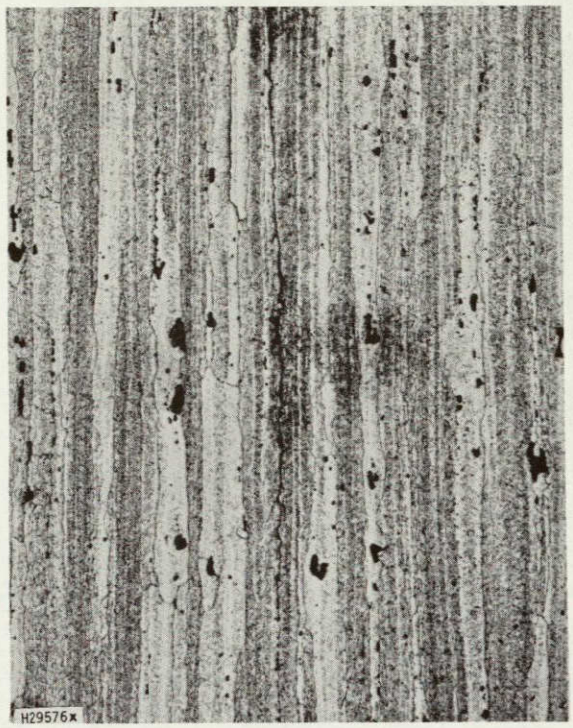

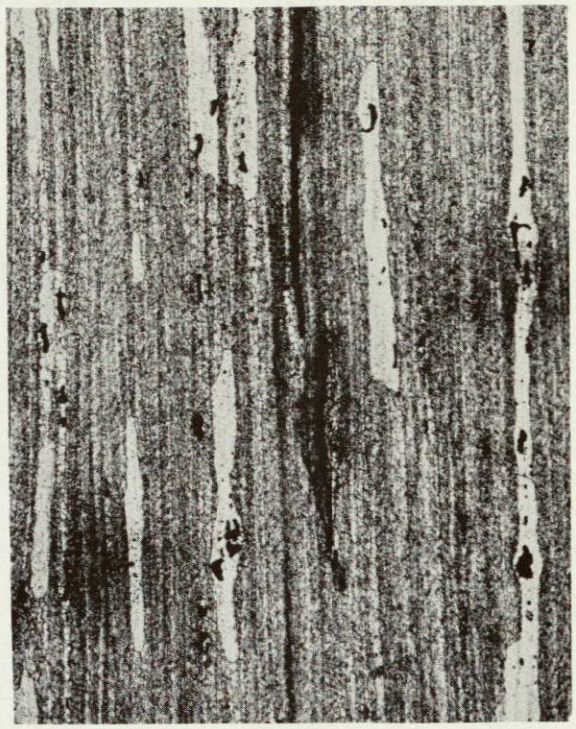

7075-T651 1.25-in. plate 7075-T7651

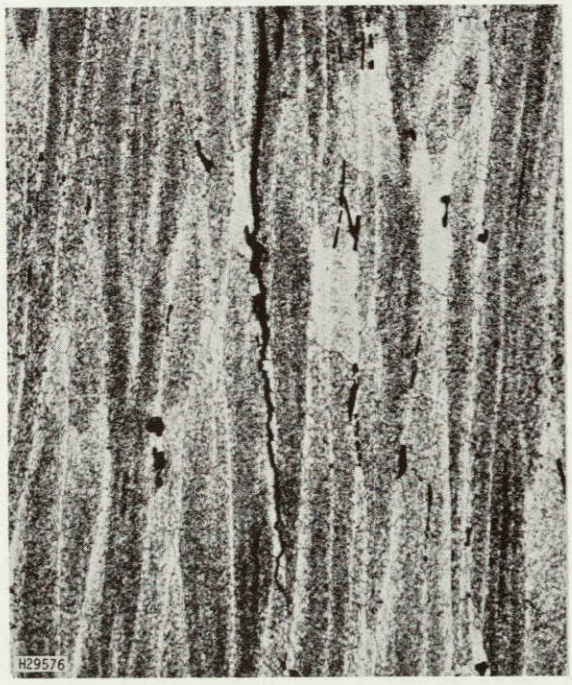

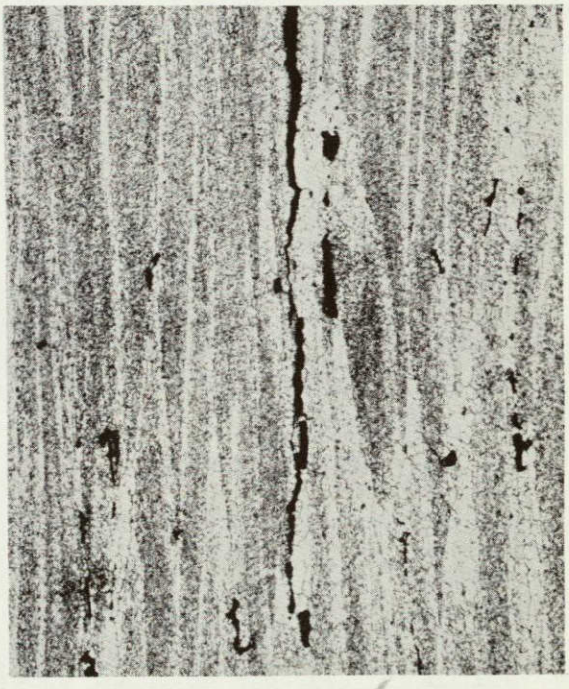

7075-T651 3.0-in. plate 7075-T7651

Figure E2.(a) Cont'd.

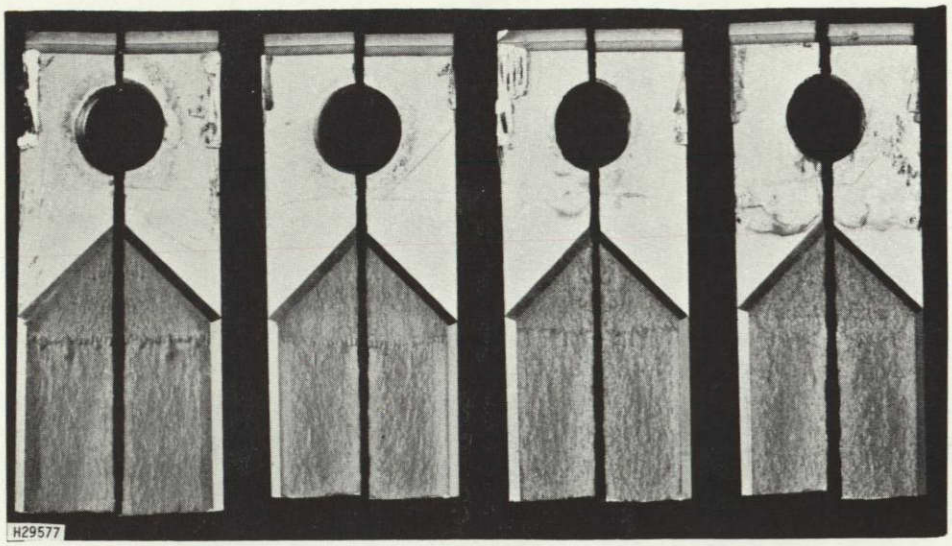

Fracture Surfaces 1X

1.8 0.8 0.5 0.0

Crack Extension mm

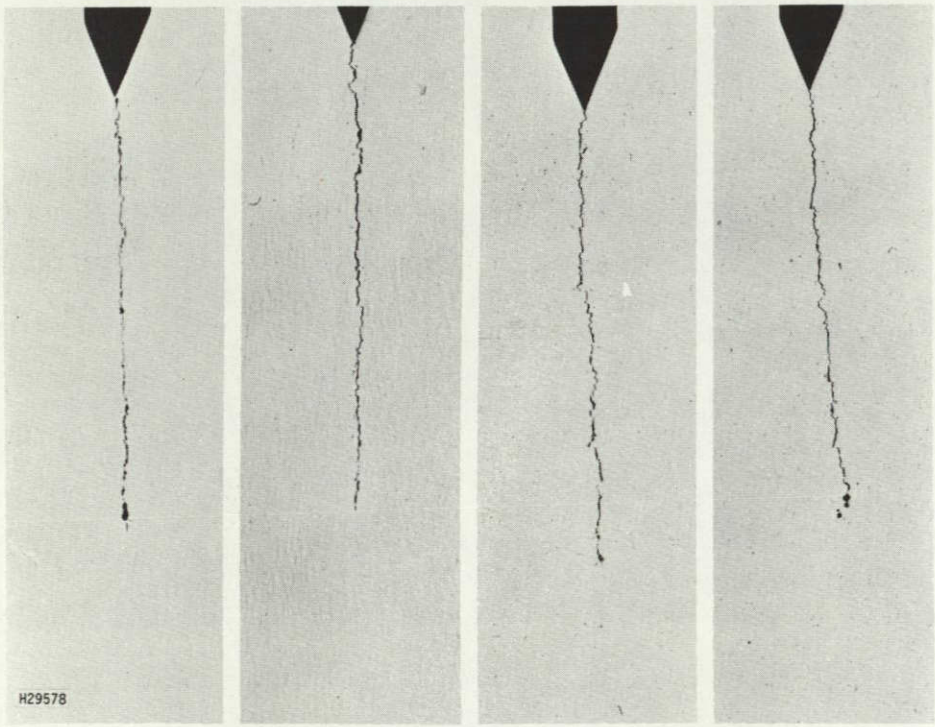

Cross Sections 5X

7075-T651 7075-T7651 7075-T651 7075-T7651

1.25-in. plate 3.0-in. plate

Test: 6 months salt-chromate constant immersion

DCB specimen: TL orientation, 25 mm high, bolt-loaded, pop-in precrack

Figure E2. (b)

Crack Tips - 200X

Etch: 10% H_3PO_4 at 120°F (3 min)

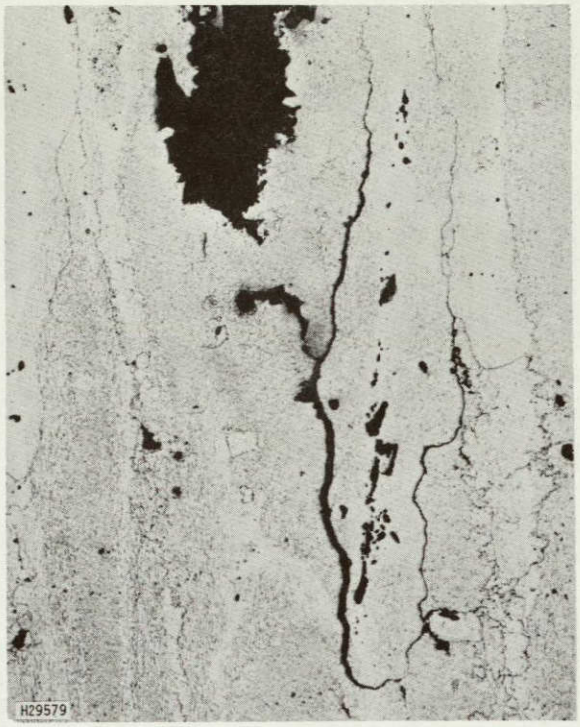

7075-T651 1.25-in. plate

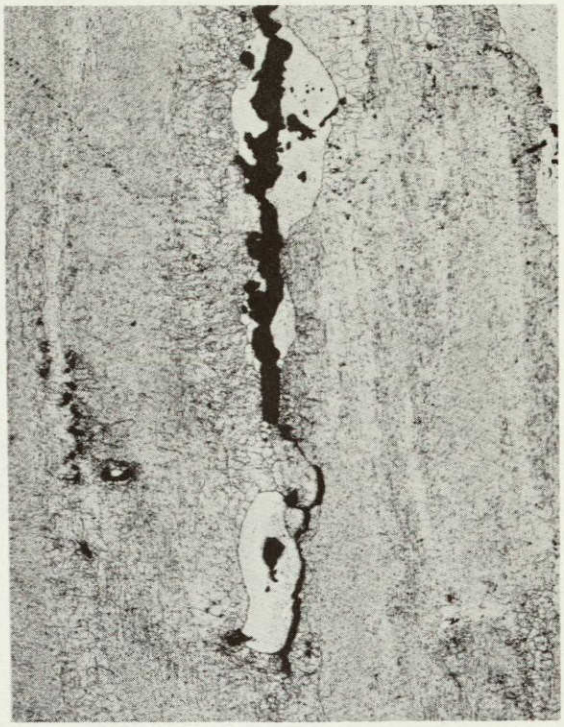

7075-T7651

7075-T651 3.0-in. plate

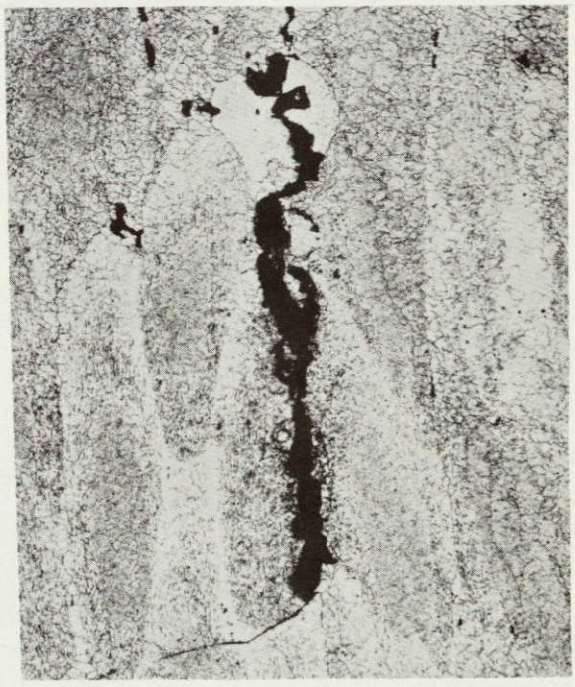

7075-T7651

Unlike the overaged materials, most -T651 and -T7651 TL specimens show definite stress corrosions cracks in the fracture plane as well as the small cracks normal to the fracture plane.

Figure E2. (b) Cont'd.

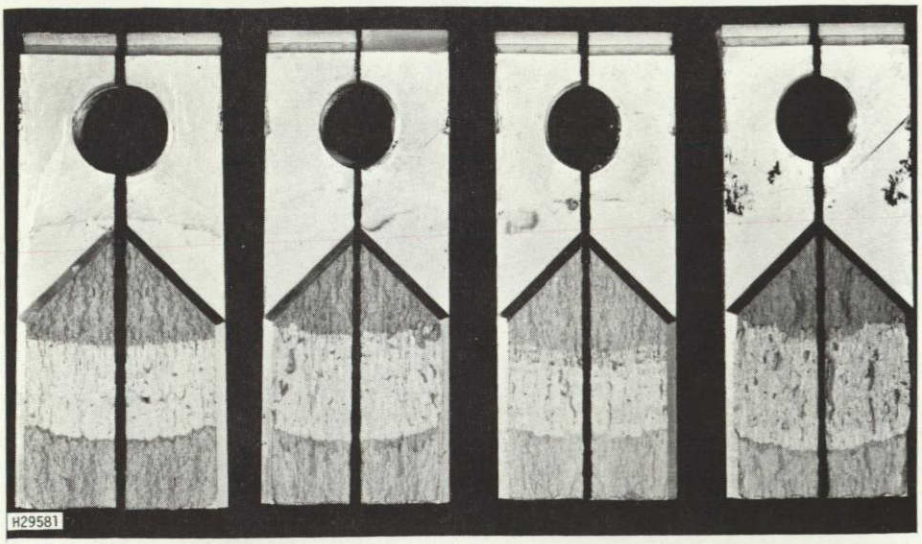

Fracture Surfaces 1X

12.2 13.0 12.4 14.5

Crack Extension mm

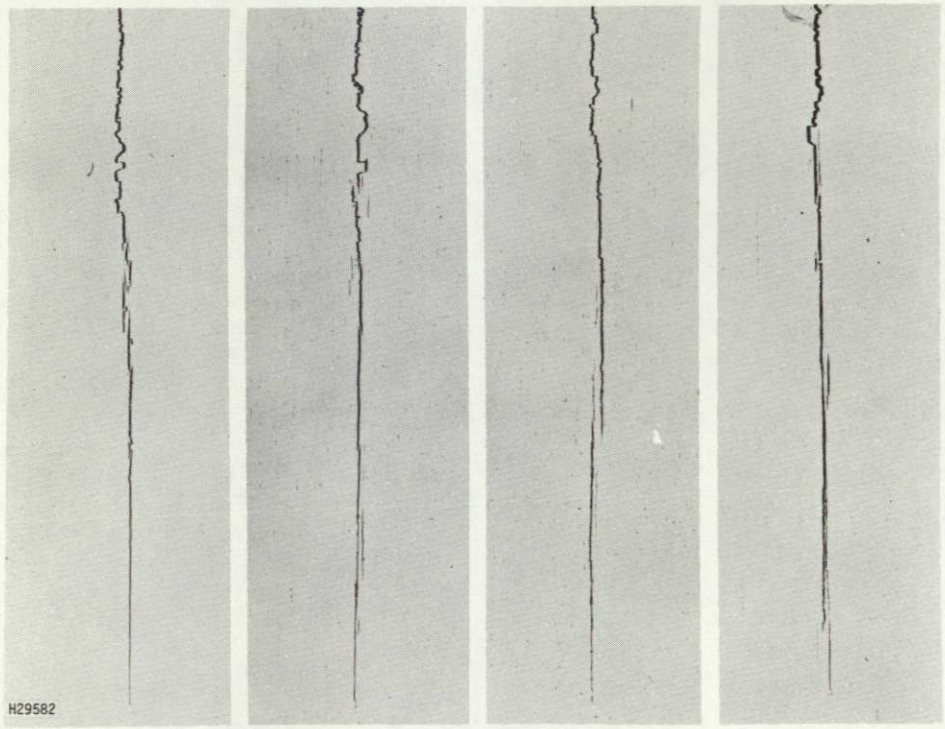

Cross Sections 5X

7075-T7351 7475-T7351 7050-T73651 7049-T7351

Material: 1.25 in. plate
Minimum temper condition

DCB Specimen: SL orientation, 25 mm high, bolt-loaded, pop-in precrack

Test: 6 months salt chromate constant immersion

Figure E2. (c)

Crack Tips - 200X

Etch: 10% H_3PO_4 at 120°F (3 min)

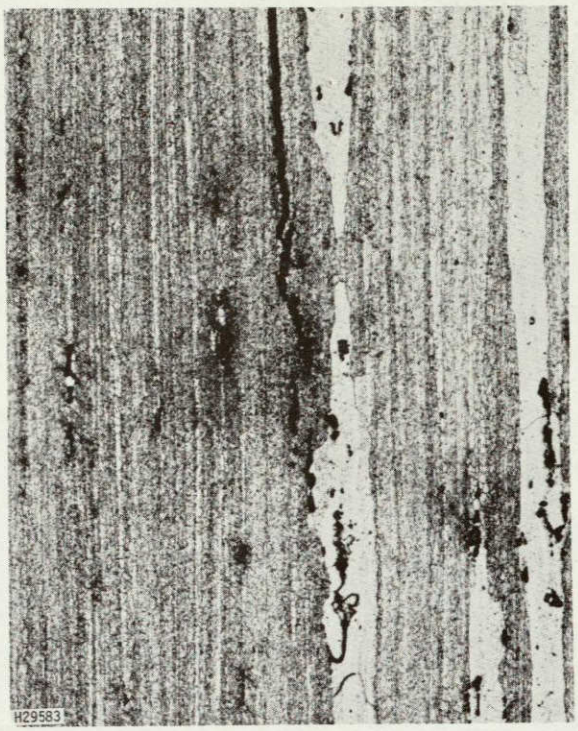

7075-T7351

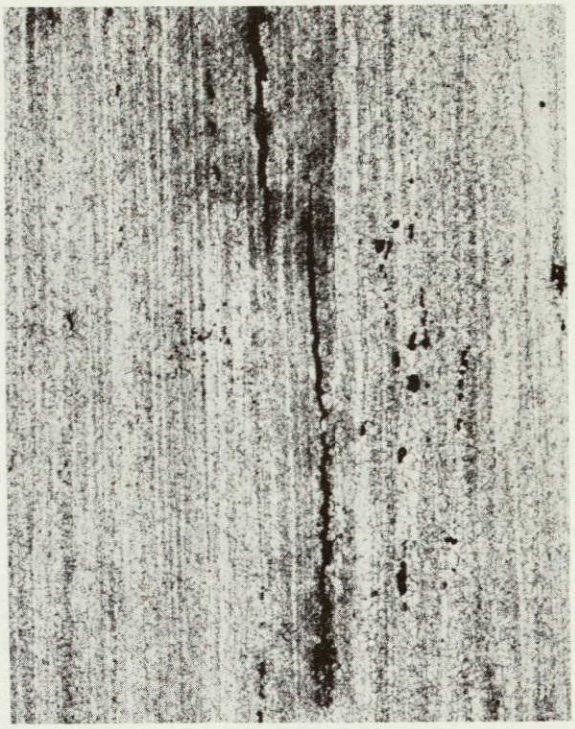

7475-T7351

7050-T73651

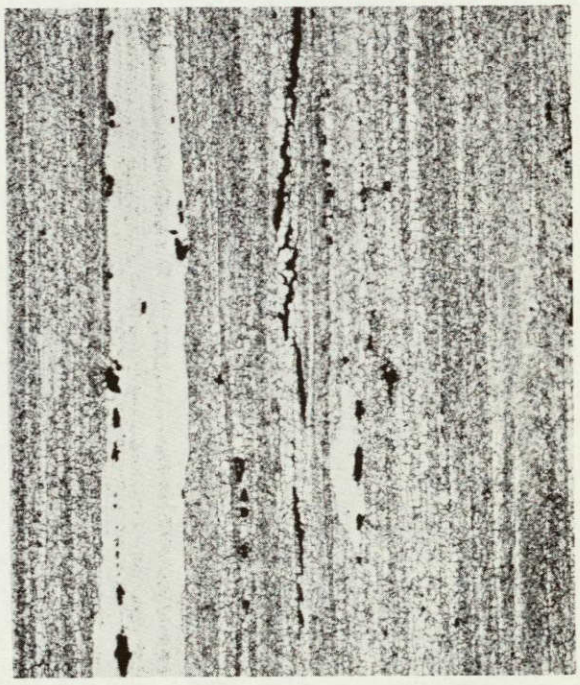

7049-T7351

Figure E2. (c) Cont'd.

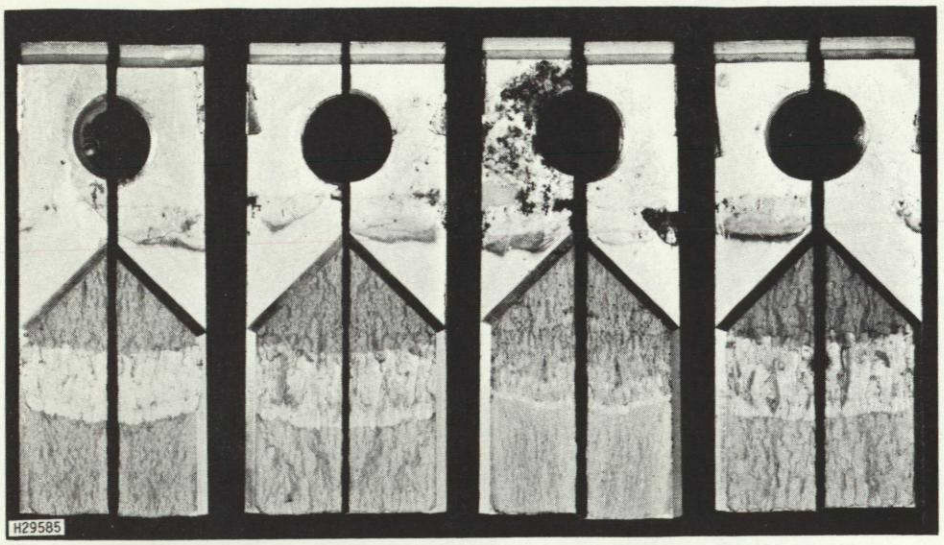

Fracture Surfaces 1X

8.9 9.9 7.9 10.1

Crack Extension mm

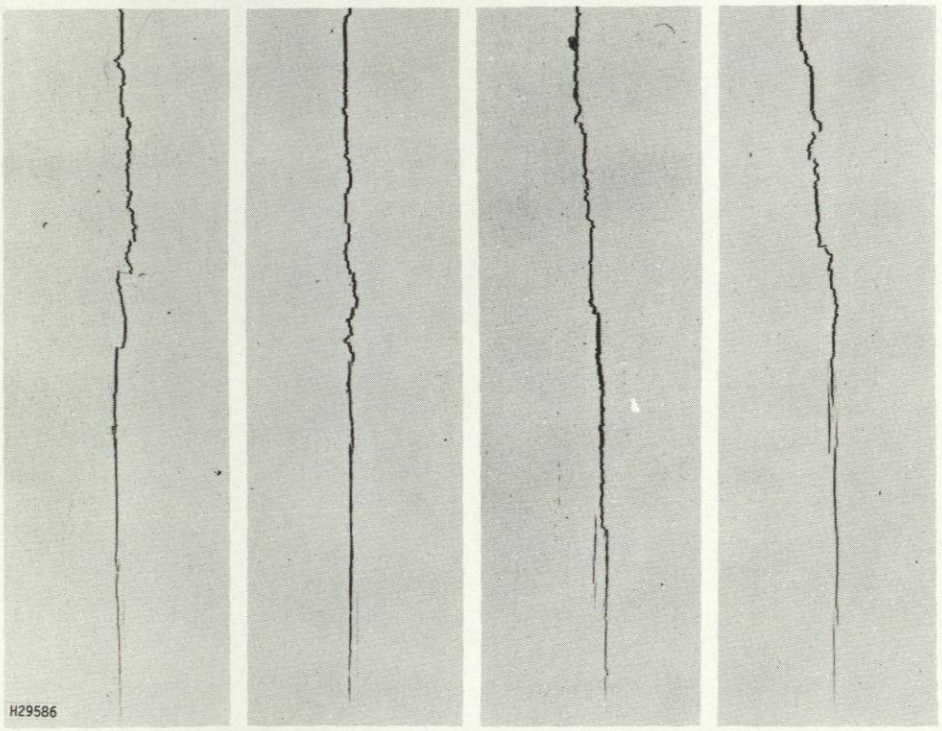

Cross Sections 5X

7075-T7351 7475-T7351 7050-T73651 7049-T7351

Material: 1.25-in. plate
Typical temper condition

DCB Specimen: SL orientation, 25 mm high, bolt-loaded, pop-in precrack

Test: 6 months salt chromate constant immersion

Figure E2. (d)

Crack Tips - 200X

Etch: 10% H_3PO_4 at 120°F (3 min)

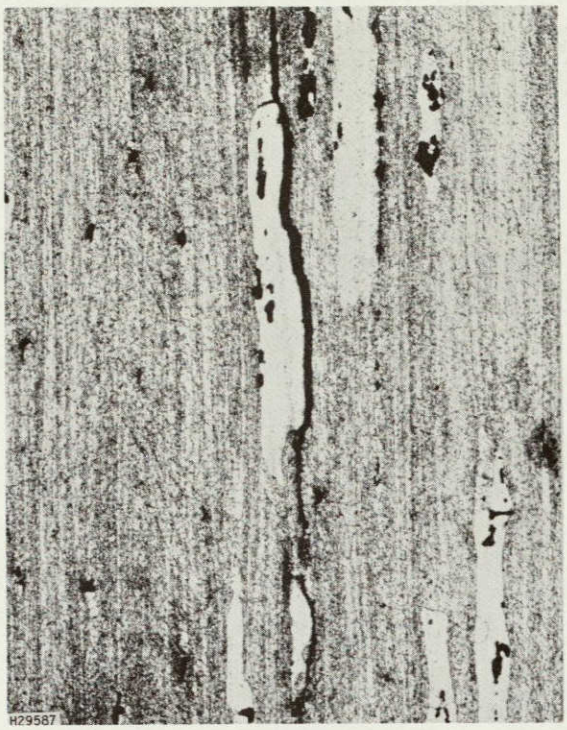

7075-T7351

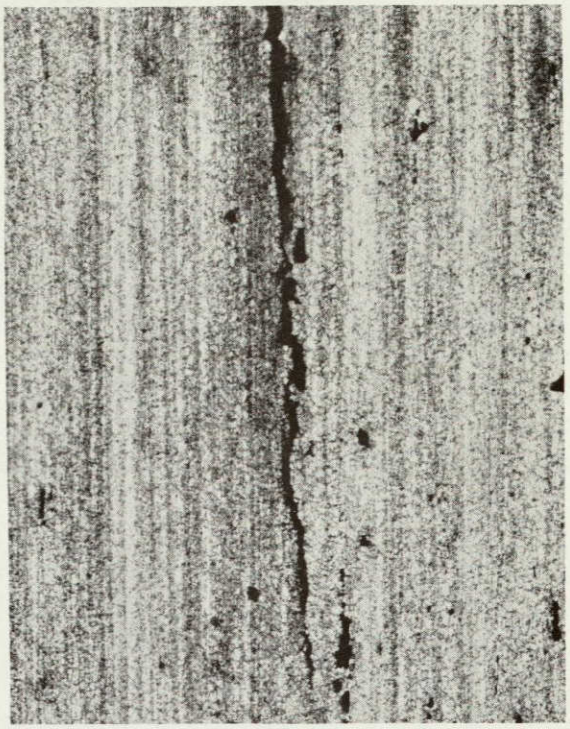

7475-T7351

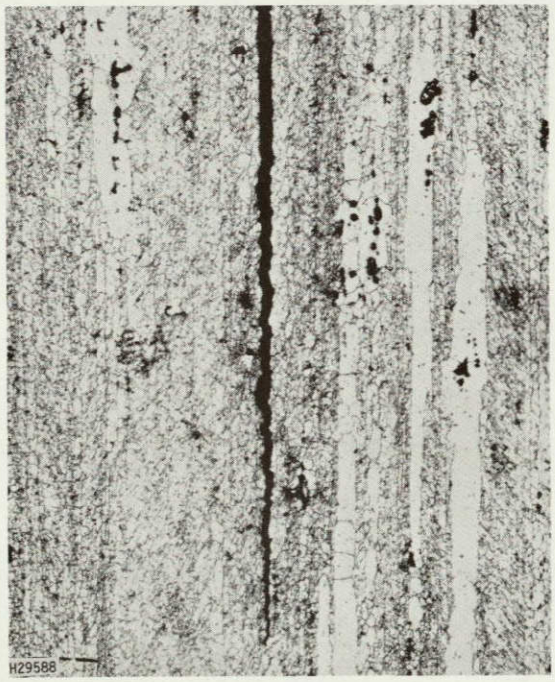

7050-T73651

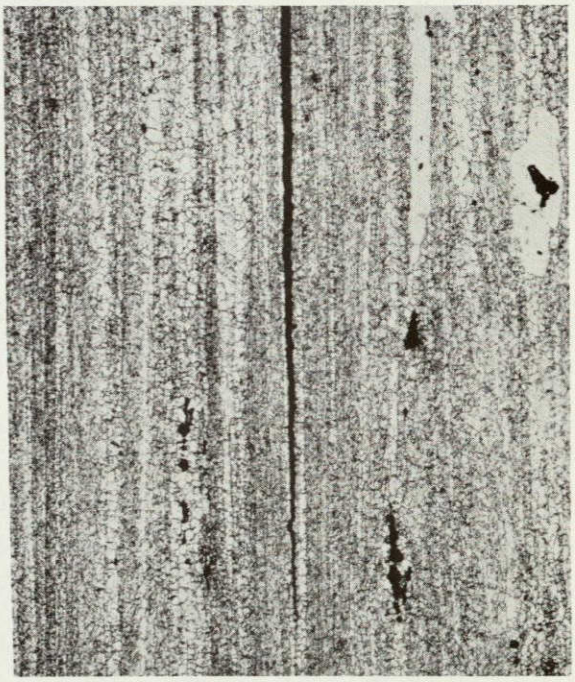

7049-T7351

The transition from precrack to stress corrosion crack is not well defined on the fracture surface of the 7050-T73651 specimen. This suggests a high percentage of mechanical fracture in the early stages of crack growth.

Figure E2. (d) Cont'd.

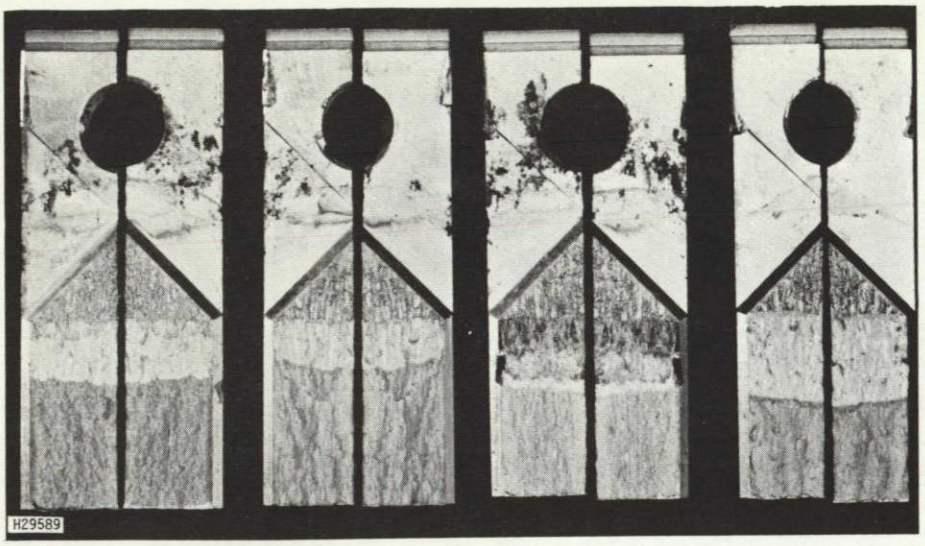

Fracture Surfaces 1X

6.6 4.8 8.6 10.4

Crack Extension mm

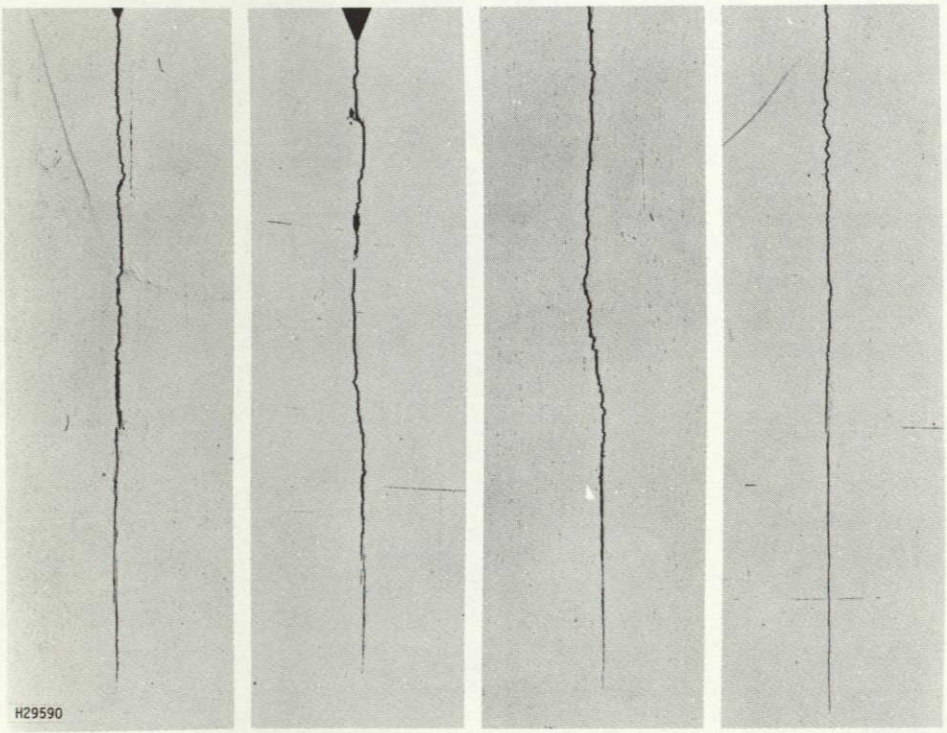

Cross Sections 5X

7075-T7351 7475-T7351 7050-T73651 7049-T7351

Material: 1.25-in. plate
Typical temper condition

DCB Specimen: SL orientation, 25 mm high, bolt-loaded, pop-in precrack

Test: 6 months salt chromate constant immersion

Figure E2. (e)

Crack Tips - 200X

Etch: 10% H_3PO_4 at 120°F (3 min)

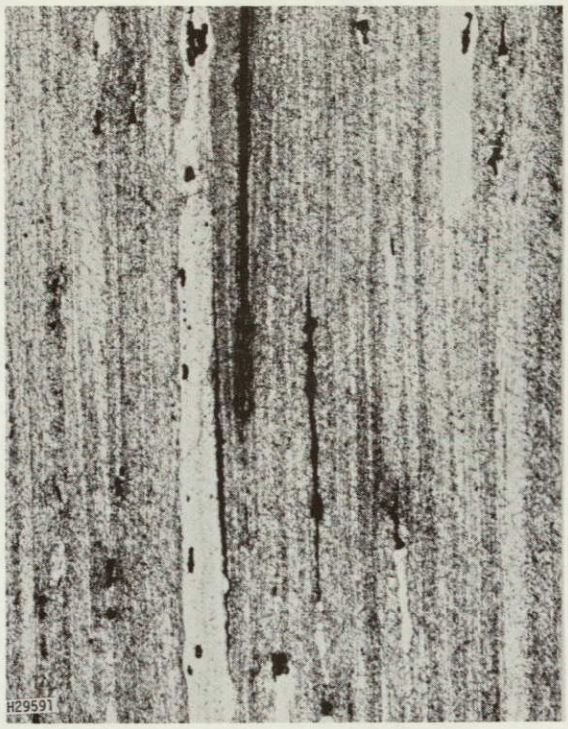

7075-T7351

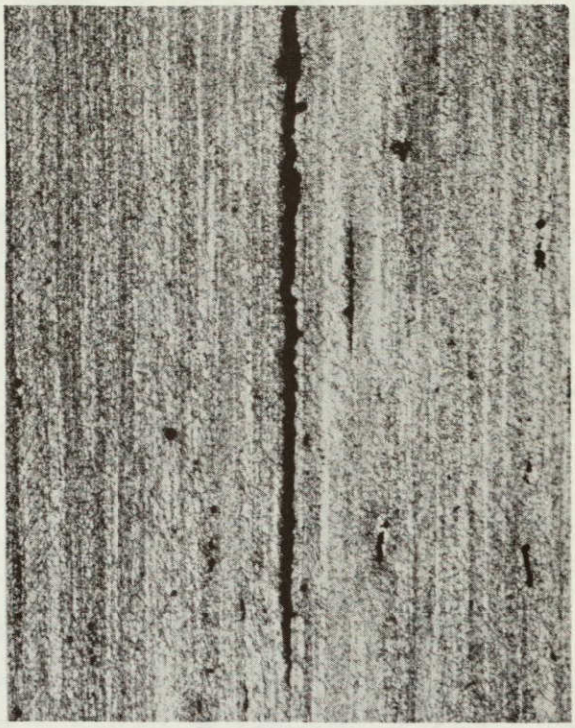

7475-T7351

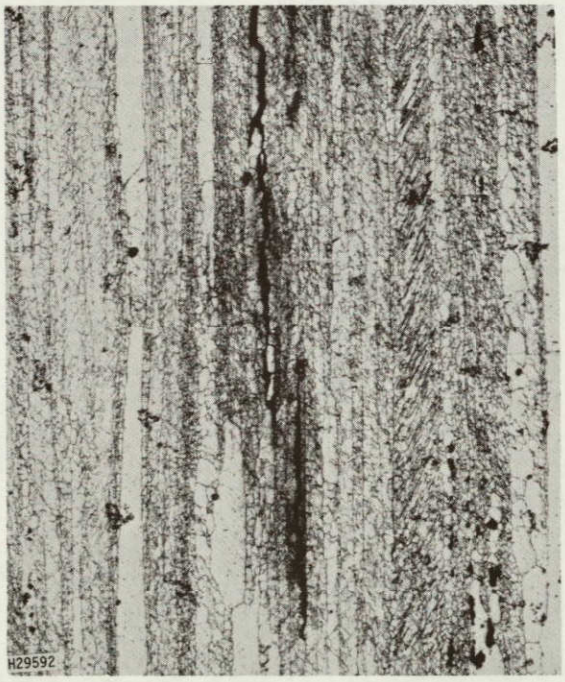

7050-T73651

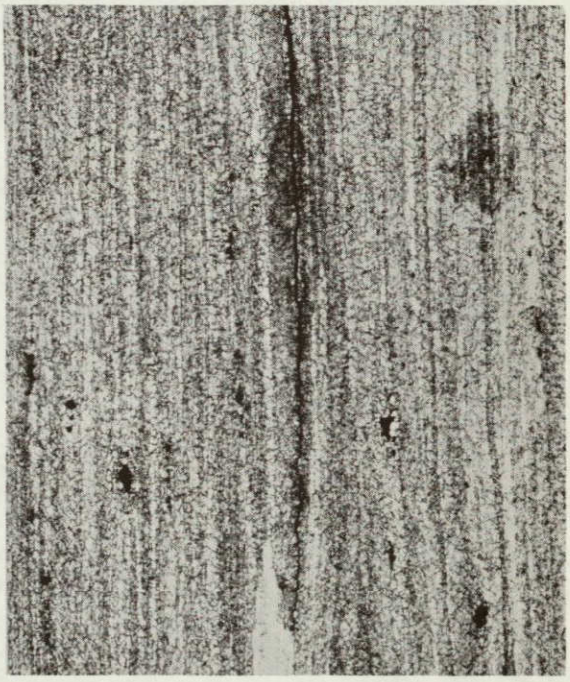

7049-T7351

Both precrack and stress corrosion cracks are straighter and have fewer delaminations than in specimens with pop-in precracks. The appearance of the 7050 fracture surface is notably different from the other three alloys.

Figure E2. (e) Cont'd.

C-3

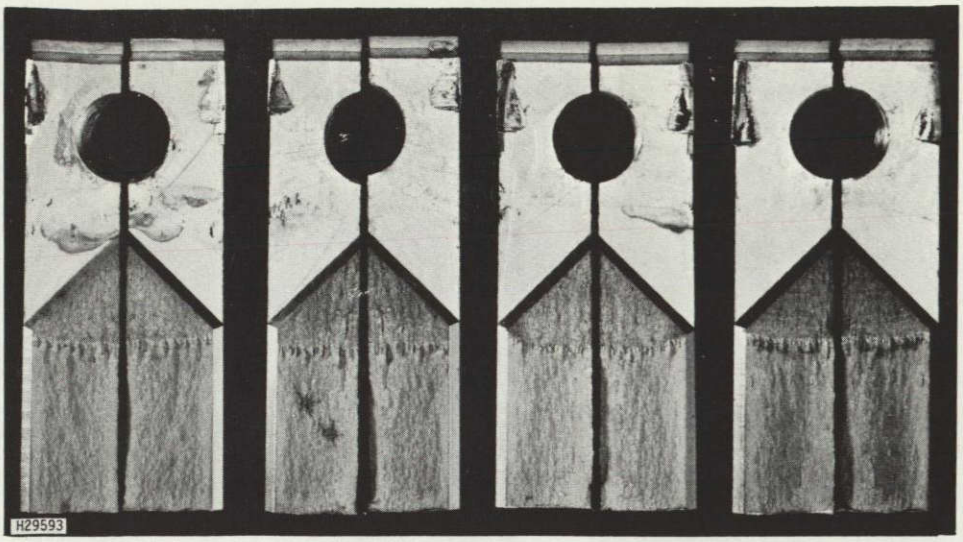

Fracture Surfaces 1X

1.3	0.5	0.5	1.8

Crack Extension mm

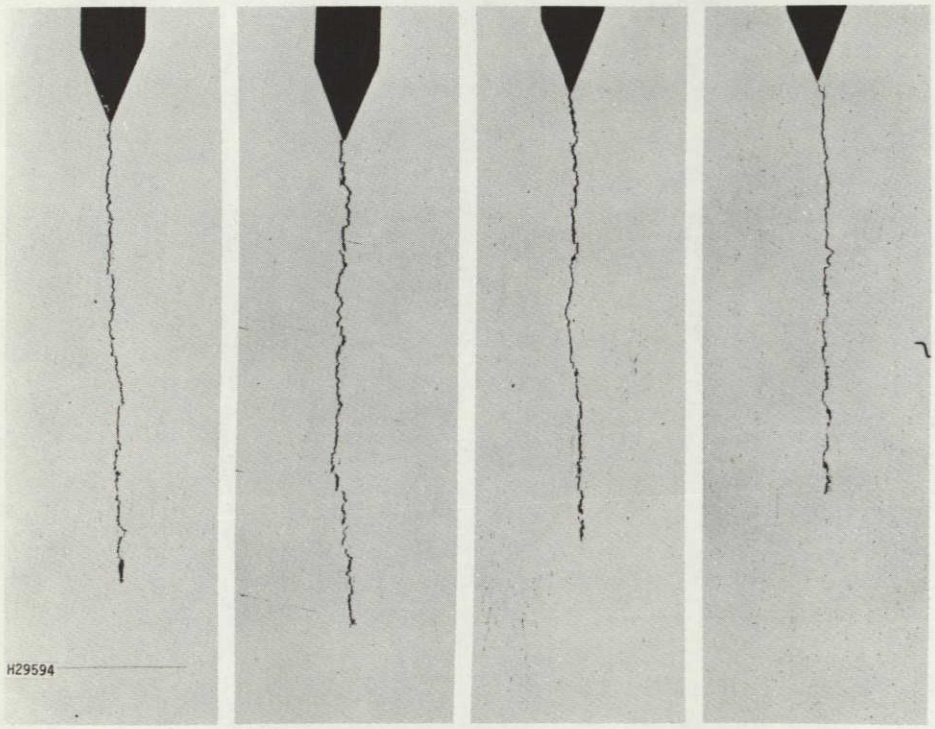

Cross Sections 5X

7075-T7351	7475-T7351	7050-T73651	7049-T7351

Material: 1.25-in. plate Typical temper condition

DCB Specimen: TL orientation, 25 mm high, bolt-loaded, pop-in precrack

Test: 6 months salt chromate constant immersion

Figure E2. (f)

Crack Tips - 200X

Etch: 10% H_3PO_4 at 120°F (3 min)

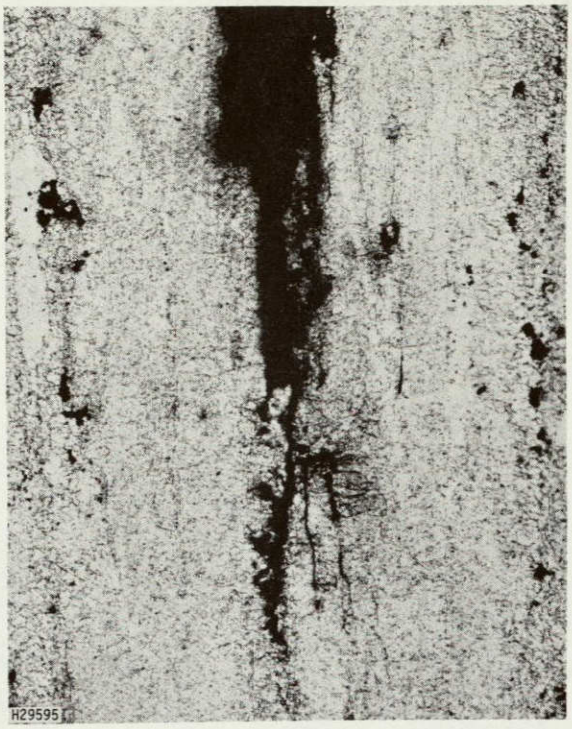

7075-T7351

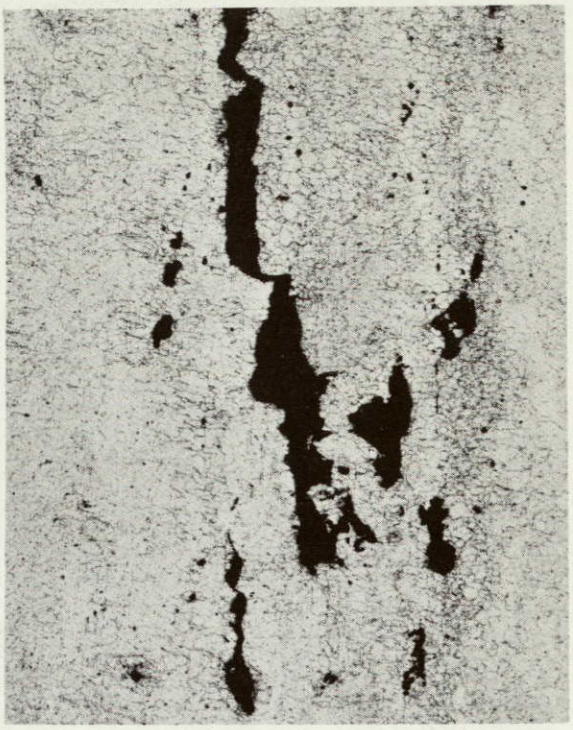

7475-T7351

7050-T73651

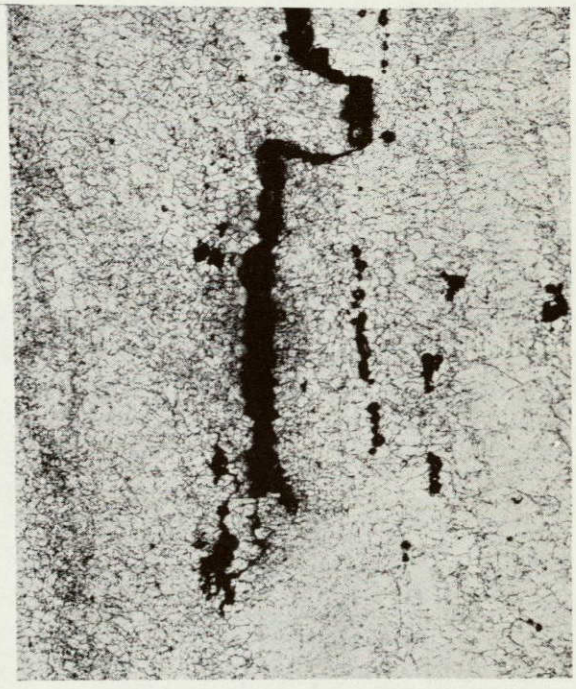

7049-T7351

Some stress corrosion cracking can be seen above, but cracks are typically blunt. Note cracks normal to fracture surface in photo at top of opposite page.

Figure E2. (f) Cont'd.

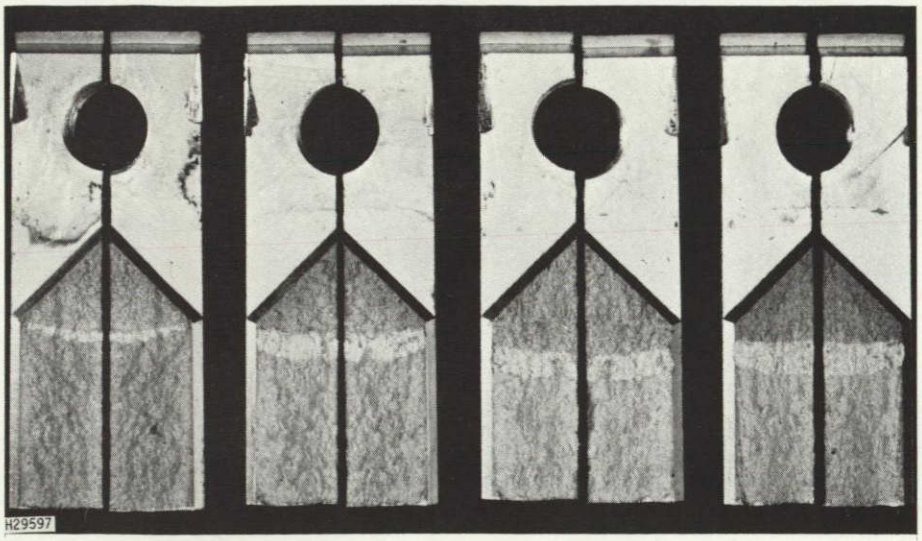

Fracture Surfaces 1X

0.8 3.6 4.1 4.8

Crack Extension mm

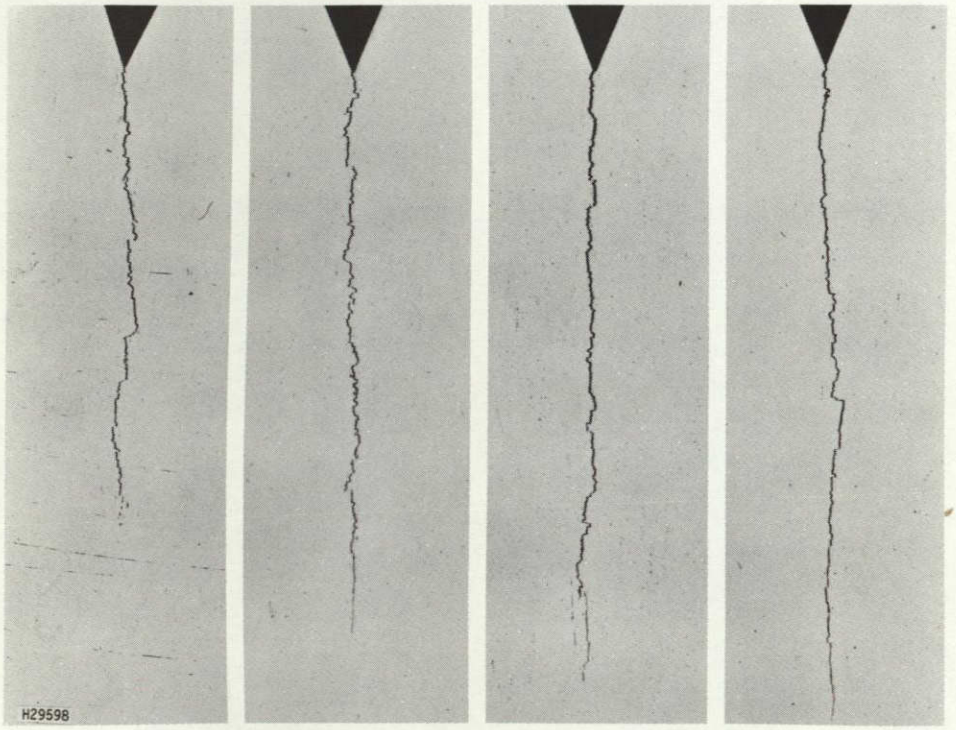

Cross Sections 5X

7075-T7351 7475-T7351 7050-T73651 7049-T7351

Material: 3.0-in. plate Minimum temper condition

Test: 6 months salt chromate constant immersion

DCB Specimen: SL orientation, 25 mm high, bolt-loaded, pop-in precrack

Figure E2. (g)

Crack Tips - 200X

Etch: 10% H_3PO_4 at 120°F (3 min)

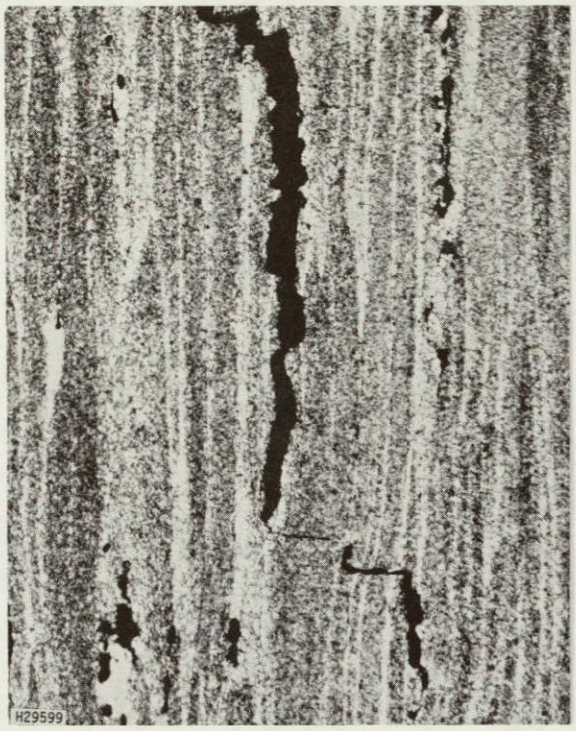

7075-T7351

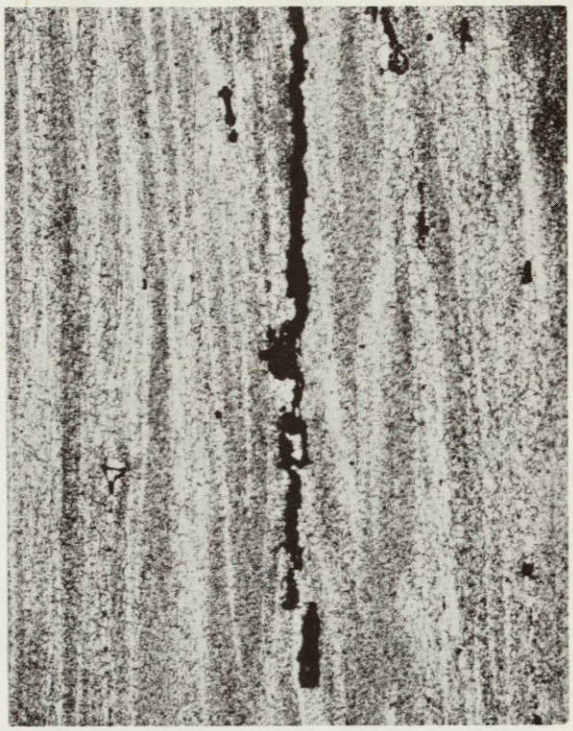

7475-T7351

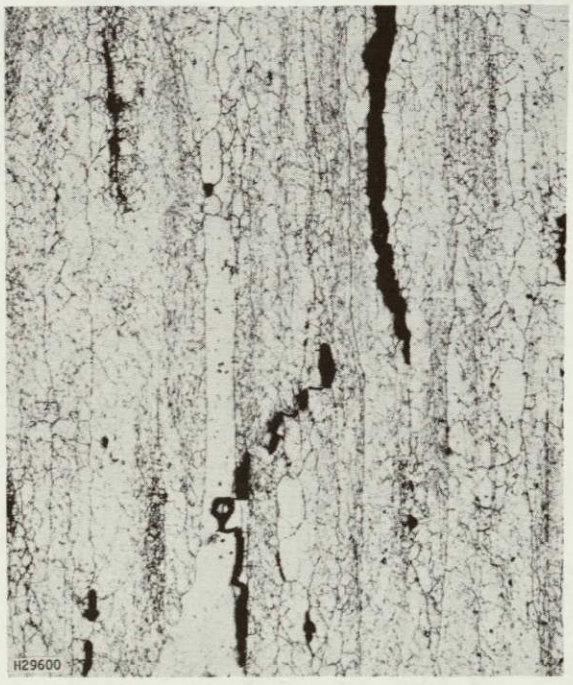

7050-T73651

7049-T7351

While significant stress corrosion crack growth can be observed on the fracture surfaces (opposite page), it's hard to identify as such in the cross sections of the crack tips. High stress intensities produce more mechanical fracture.

Figure E2. (g) Cont'd.

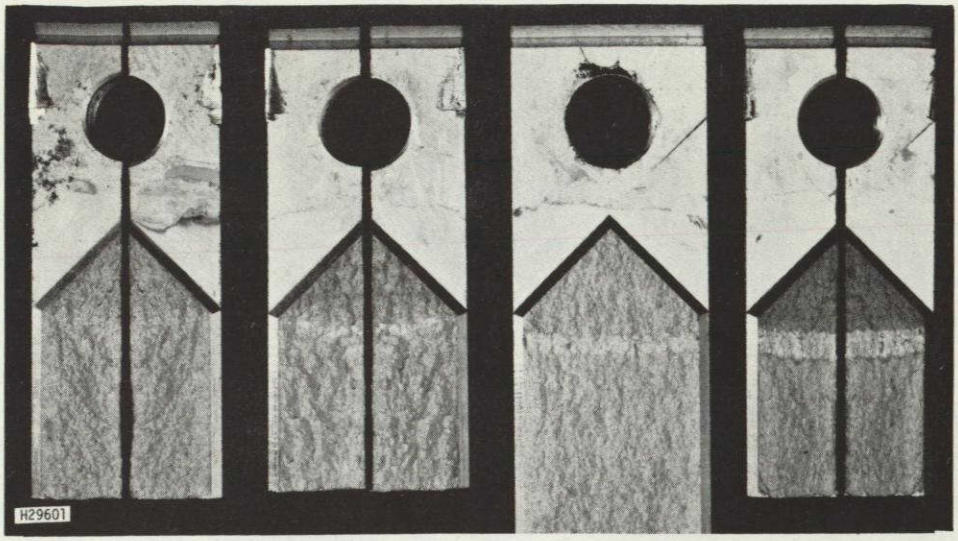

Fracture Surfaces 1X

0.5 0.8 2.5 3.3

Crack Extension mm

Cross Sections 5X

7075-T7351 7475-T7351 7050-T73651 7049-T7351

Material: 3.0-in. plate
Typical temper condition

Test: 6 months salt chromate constant immersion

DCB Specimen: SL orientation, 25 mm high, bolt-loaded, pop-in precrack

Figure E2. (h)

Crack Tips - 200X

Etch: 10% H_3PO_4 at 120°F (3 min)

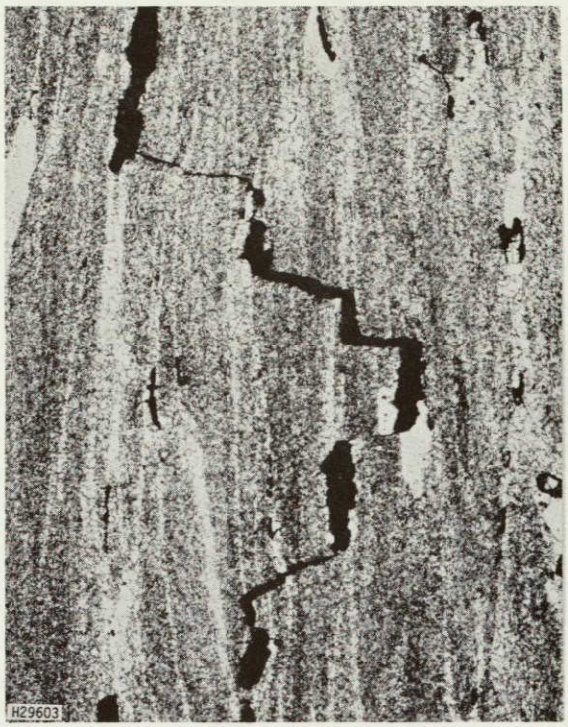

7075-T7351

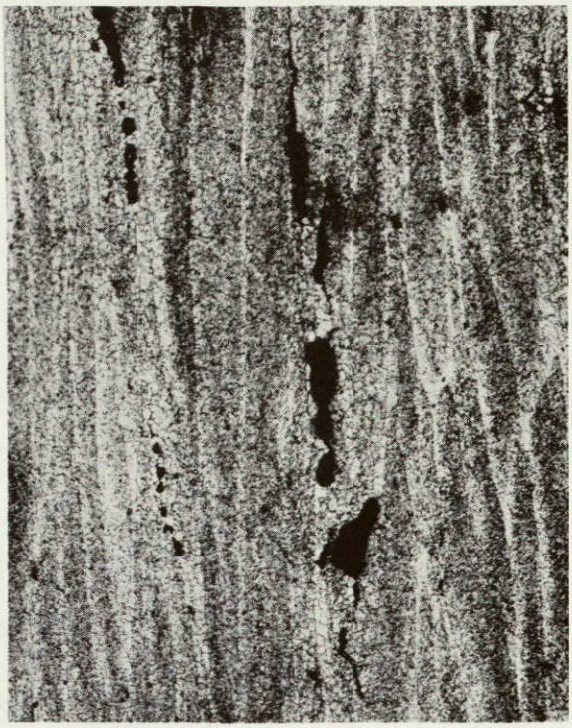

7475-T7351

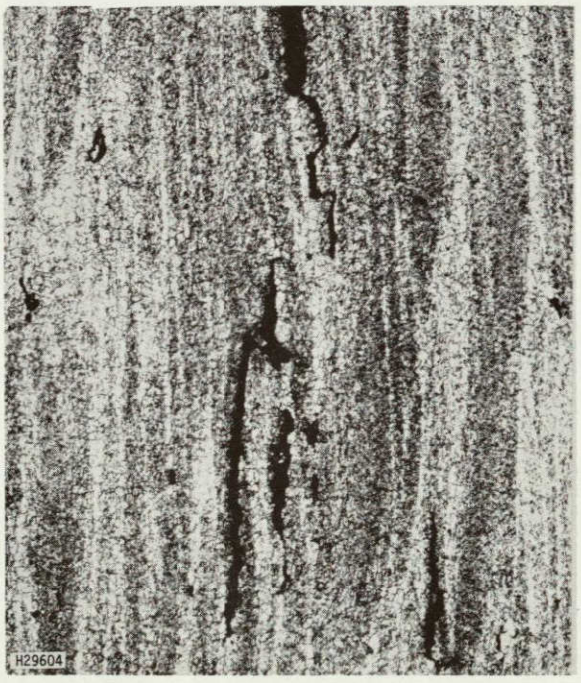

7050-T73651

Specimen
Mis-oriented

7049-T7351

The 7050 specimen chosen for cross sectioning was misoriented. The 7050 fracture surface shown is from the duplicate specimen.

Figure E2. (h) Cont'd.

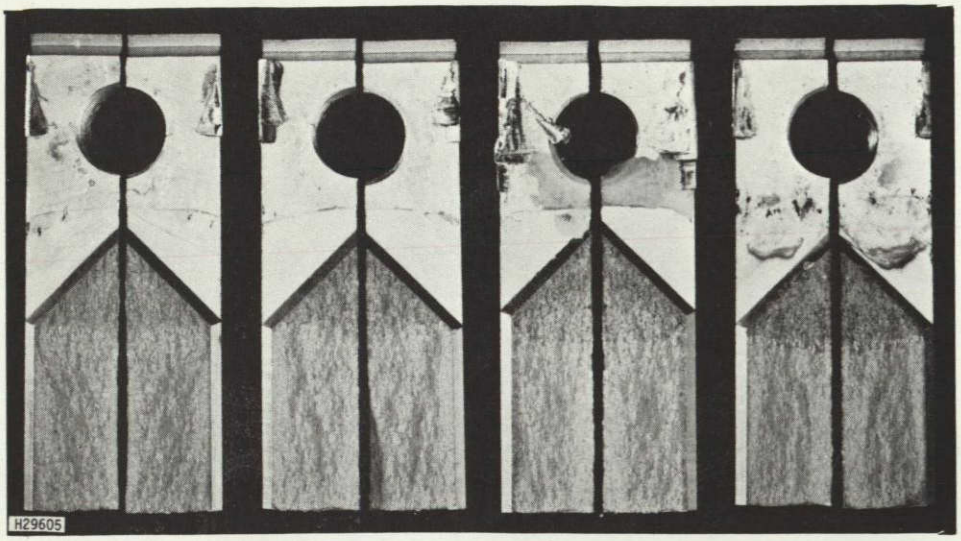

Fracture Surfaces 1X

1.0	0.0	0.3	0.0

Crack Extension mm

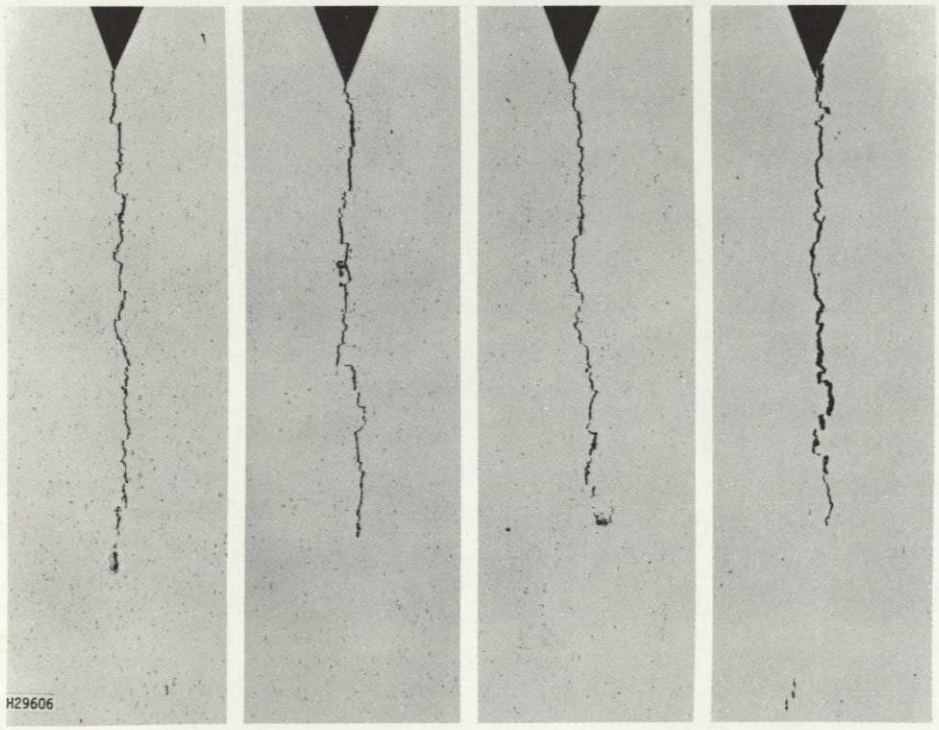

Cross Sections 5X

7075-T7351	7475-T7351	7050-T73651	7049-T7351

Material: 3.0-in. plate
Typical temper condition

DCB Specimen: TL orientation, 25 mm high, bolt-loaded, pop-in precrack

Test: 6 months salt chromate constant immersion

Figure E2. (i)

Crack Tips - 200X

Etch: 10% H_3PO_4 at 120°F (3 min)

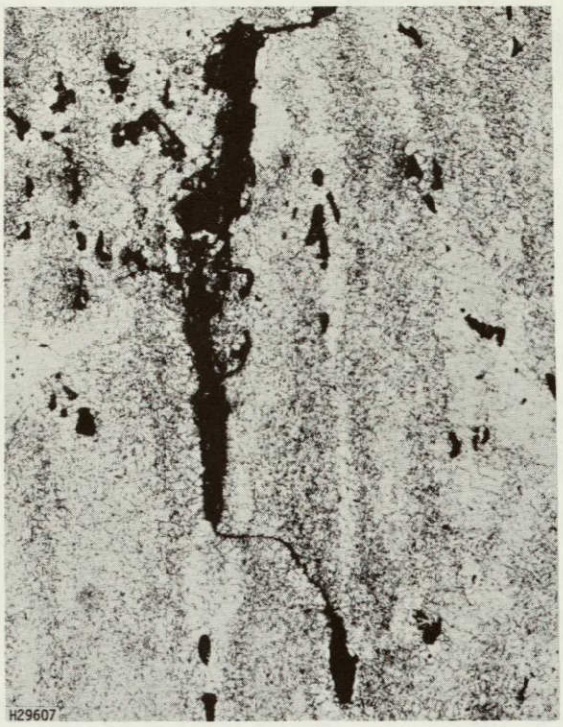

7075-T7351

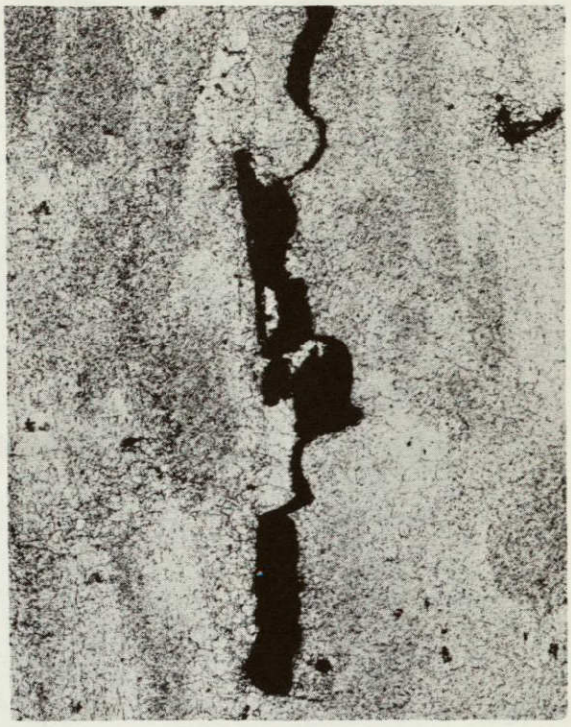

7475-T7351

7050-T73651

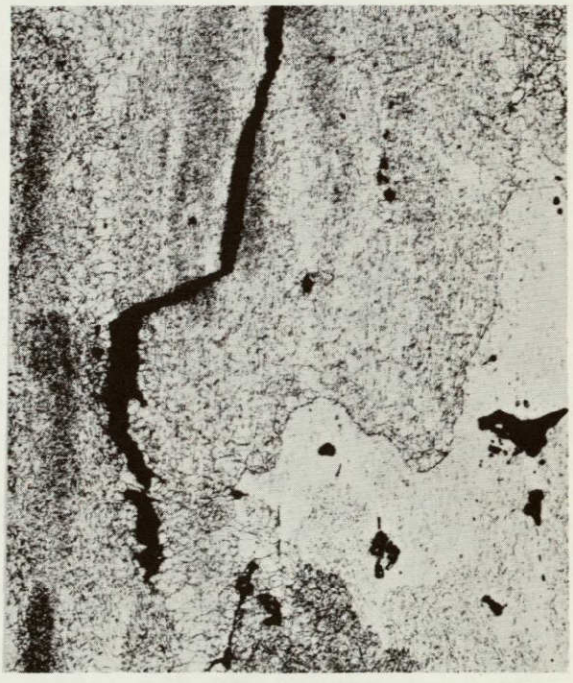

7049-T7351

Short cracks normal to the fracture plane are smaller than in 1.25-in. plate.

Figure E2. (i) Cont'd.

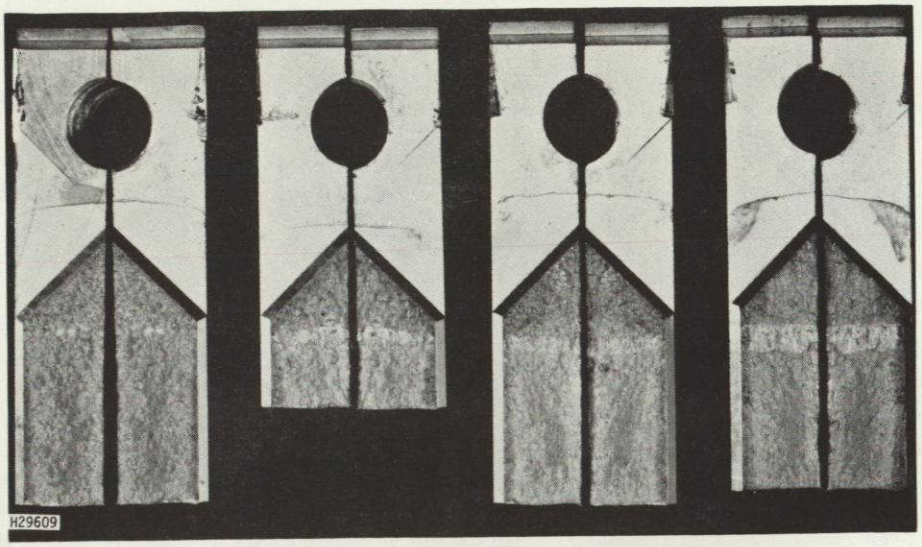

Fracture Surfaces 1X

0.3 1.3 2.3 2.3

Crack Extension mm

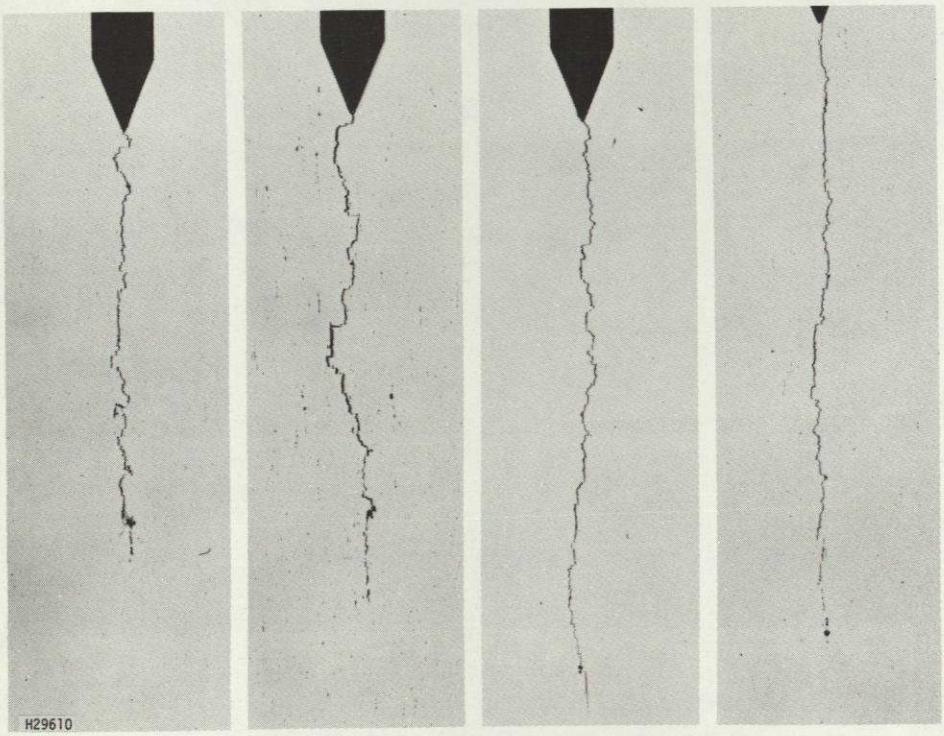

Cross Sections 5X

7075-T7351 7475-T7351 7050-T73651 7049-T7351

Material: 3.0-in. plate
Typical temper condition

DCB Specimen: SL orientation, 75 mm high, bolt-loaded, pop-in precrack

Test: 6 months salt chromate constant immersion

Figure E2. (j)

Crack Tips - 200X
Etch: 10% H_3PO_4 at 120°F (3 min)

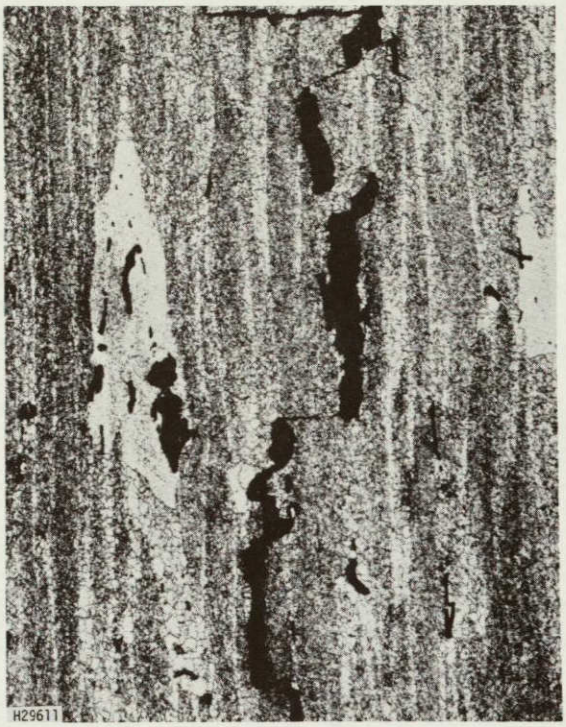

7075-T7351

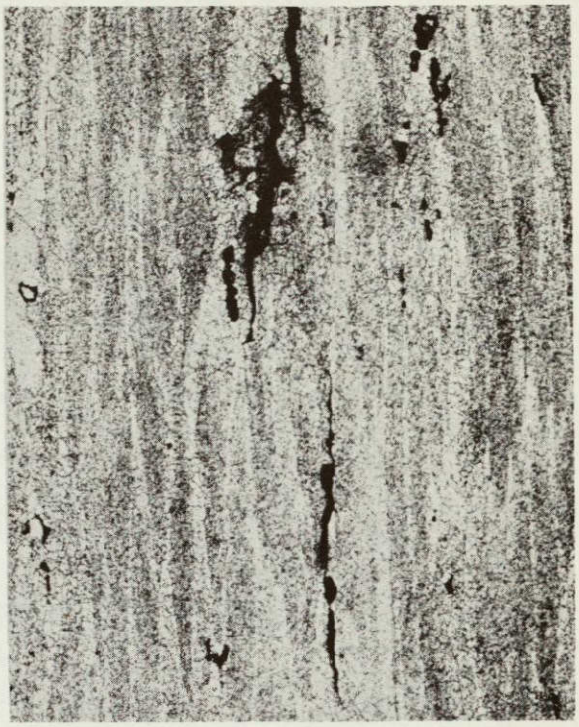

7475-T7351

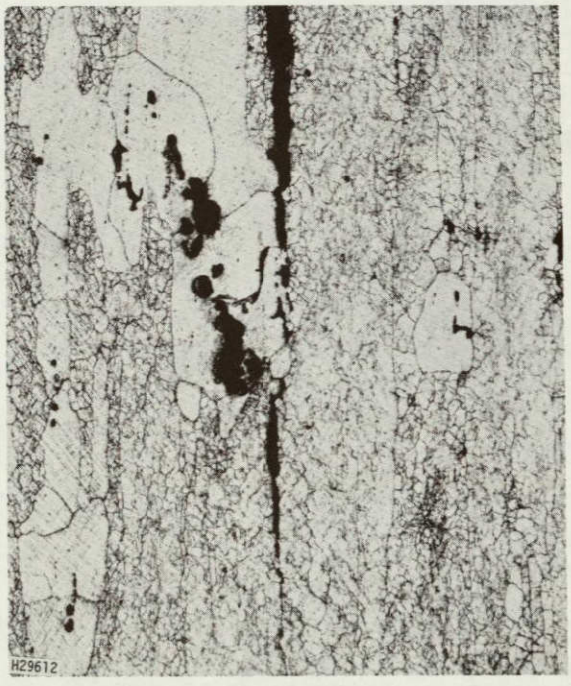

7050-T73651

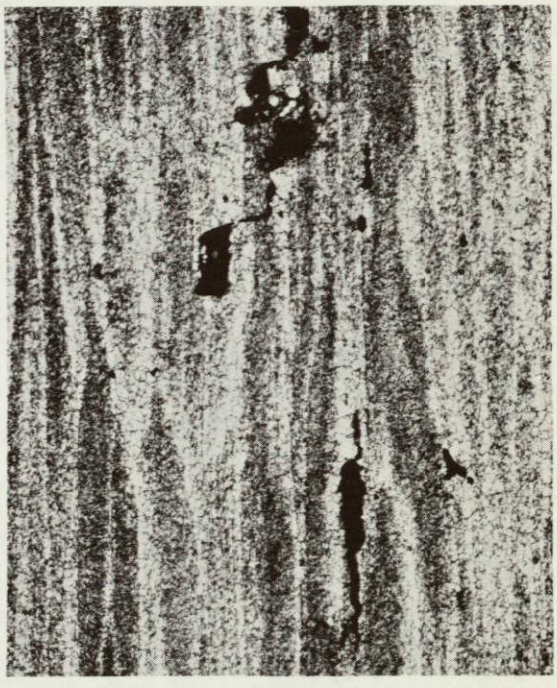

7049-T7351

Performance of 75-mm high specimen was similar to 25-mm high specimens except that stress corrosion was more apparent on fracture surface of 75-mm high 7075 specimen.

Figure E2. (j) Cont'd.

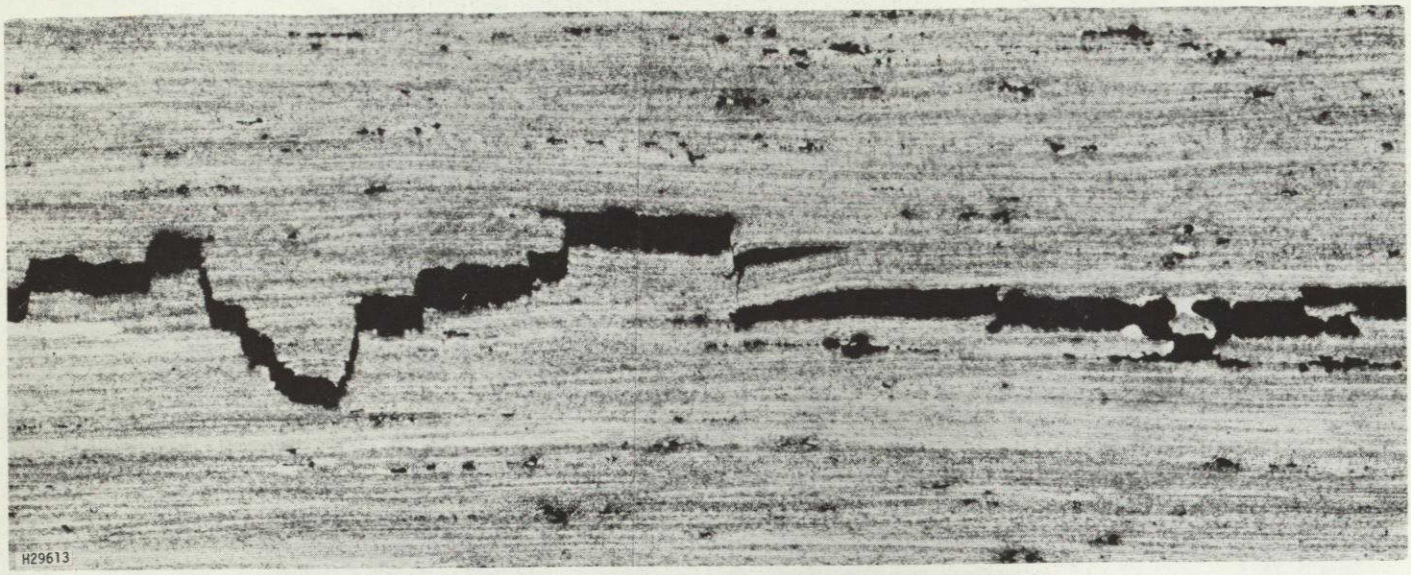

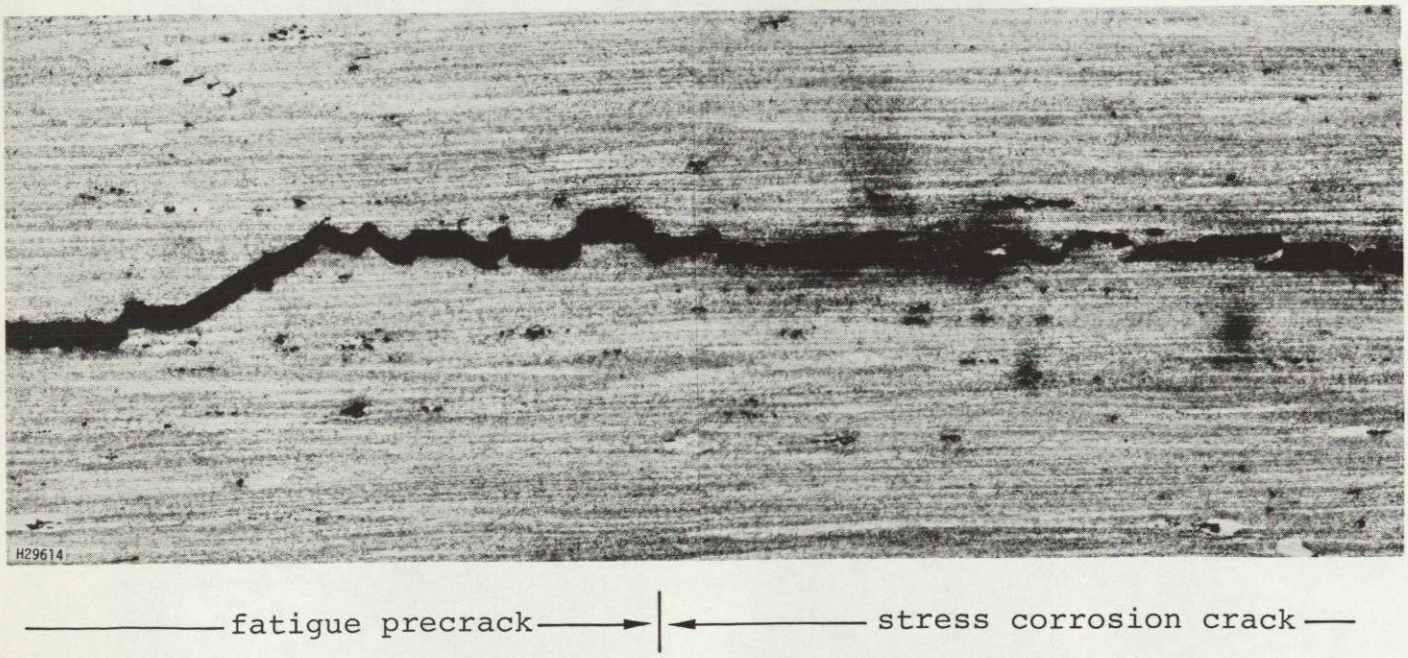

Figure E2. (k) Pop-in and fatigue precracks in DCB's from 1.25-in. 7075-T7351(T) plate - 100X

Note that transition from fatigue to stress corrosion is smooth, but delamination occurs at the transition from a pop-in precrack.

10X

20X

Figure E3. Cracks growing normal to precrack plane in TL specimen

Cracks have shape shown, which is similar to that of plastic zone.

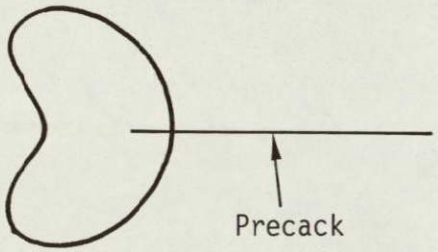

APPENDIX F

SCANNING ELECTRON MICROSCOPE VIEWS OF STRESS CORROSION CRACKS

The absence of significant general corrosion on the specimens tested in the salt-chromate environment allowed a clear examination of the precrack and stress-corrosion crack surfaces. Of particular interest was the interface region between the precrack and the stress corrosion crack.

Figure F1 shows the interface region in 7075-T7351(T) for a pop-in precrack. The interface was extremely uneven, with a great deal of mechanical rupture both ahead of and behind what was probably the original precrack front. There was also a considerable amount of overlapping, probably due to the non-planar nature of the pop-in precrack. This was then manifested as a fairly rough, uneven stress-corrosion surface.

In contrast, the transition to stress corrosion from a fatigue precrack was more uniform, with less mechanical rupturing (Fig. F2). Since the initial stress intensity was lower, mechanical fracture would be less likely. The stress-corrosion crack generated from the fatigue precrack appeared to be smoother with fewer delaminations than that associated with a pop-in precrack. Higher magnification of the transition zone between the transgranular fatigue precrack and the intergranular stress corrosion crack (Fig. F3) showed characteristics of both ductile tearing and stress corrosion in a plane normal to the precrack. It is probable that this could be a time-consuming process, and would quite likely lead to a pronounced incubation period as observed.

Examination of the stress corrosion surface ahead of the interface region continued to reveal a considerable amount of

mechanical rupturing (Fig. F4). It is quite clear therefore that any theories of stress corrosion cracking and V-K relationships must account for this feature of the process (Ref 30).

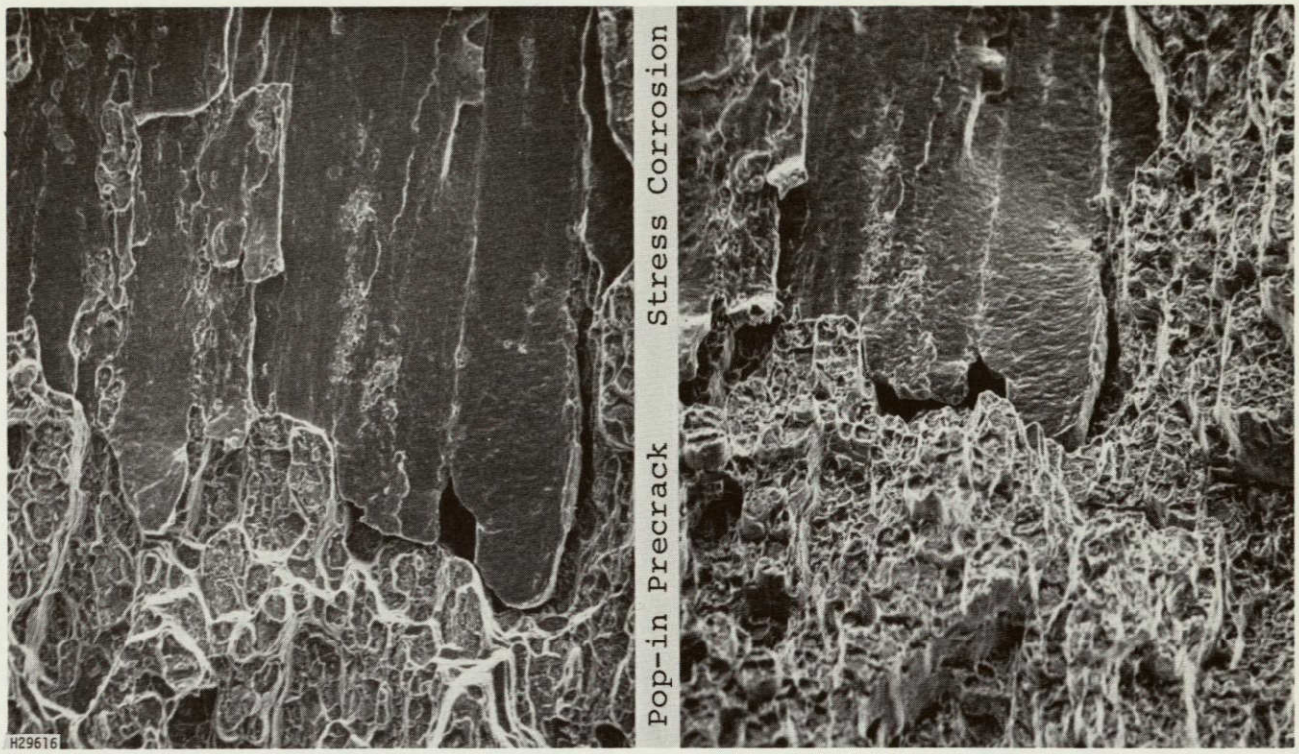

Figure F1. Pop-in precrack/stress corrosion interface on SL DCB from 1.25-in. 7075-T7351 plate: salt-chromate environment (100X)

The precrack and stress corrosion crack overlap on different planes. The original precrack front was probably straighter but fingers of stress corrosion grew back behind the precrack after stress corrosion was initiated. This may relate to the relatively slow initial crack growth rates observed at the specimen edge (incubation effect).

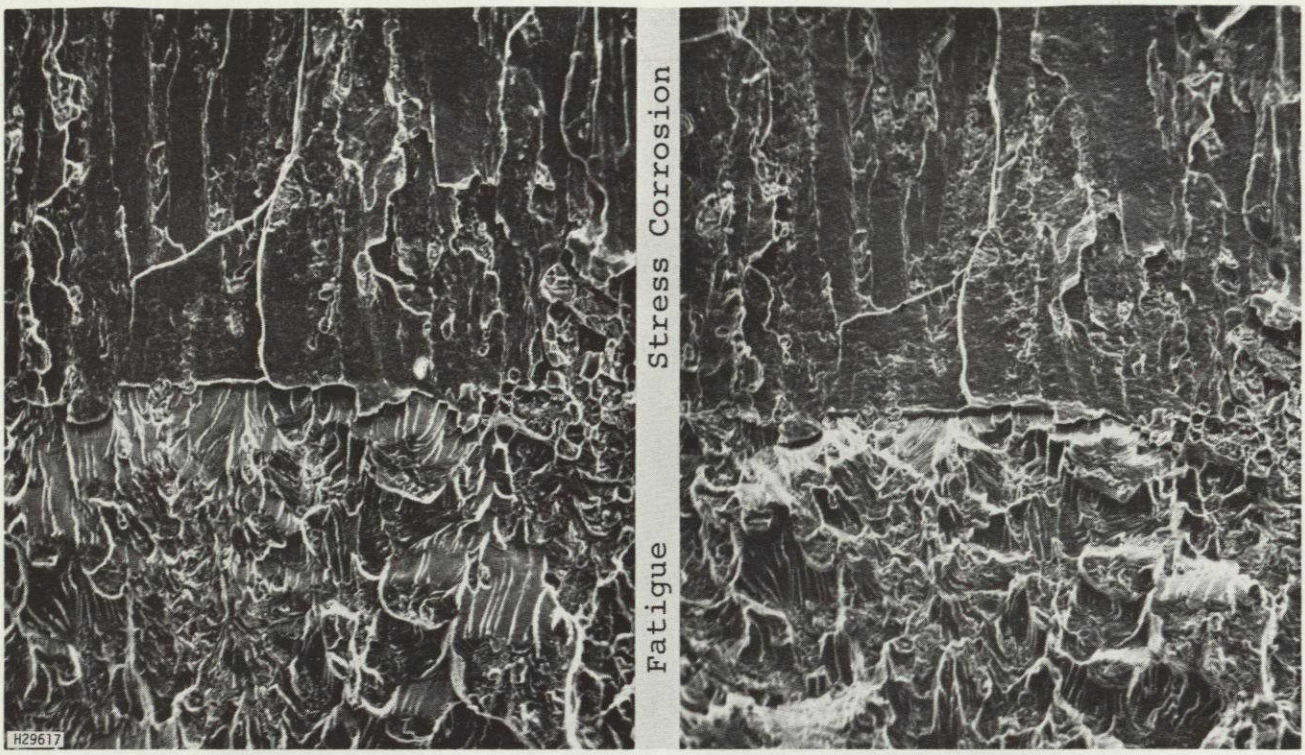

Figure F2. Fatigue precrack/stress corrosion interface on SL DCB from 1.25-in. 7075-T7351 plate: salt-chromate environment (100X)

Transition from precrack to stress corrosion was more uniform than with pop-in precrack. There was also less mechanical rupturing (as would be expected since the stress intensity was lower). Stress corrosion crack appeared to be flatter than that generated by pop-in precrack.

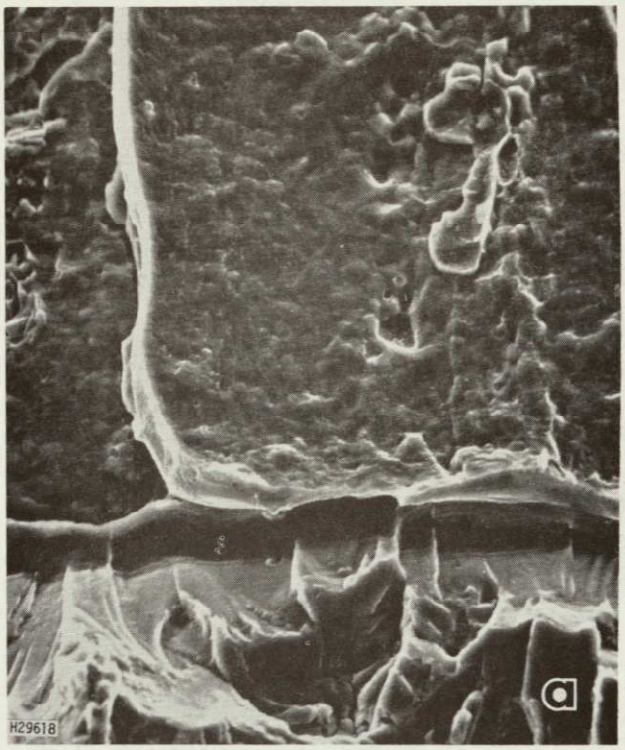

500X

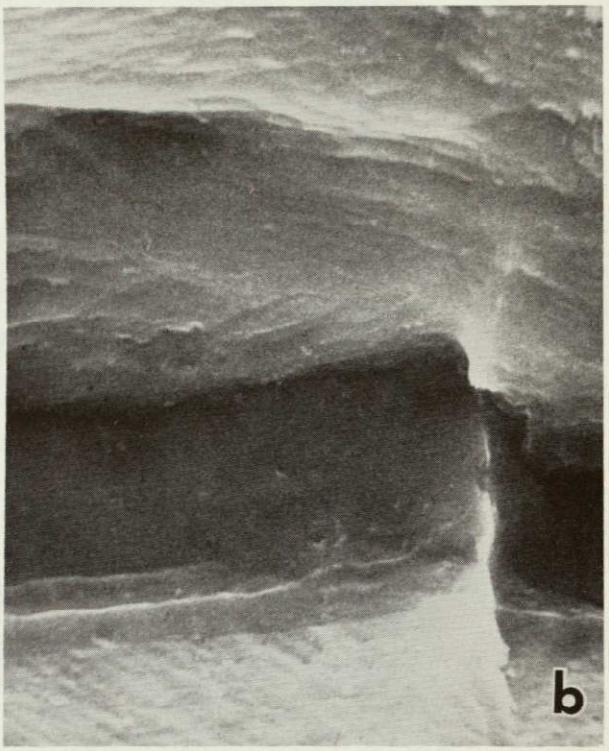

5000X

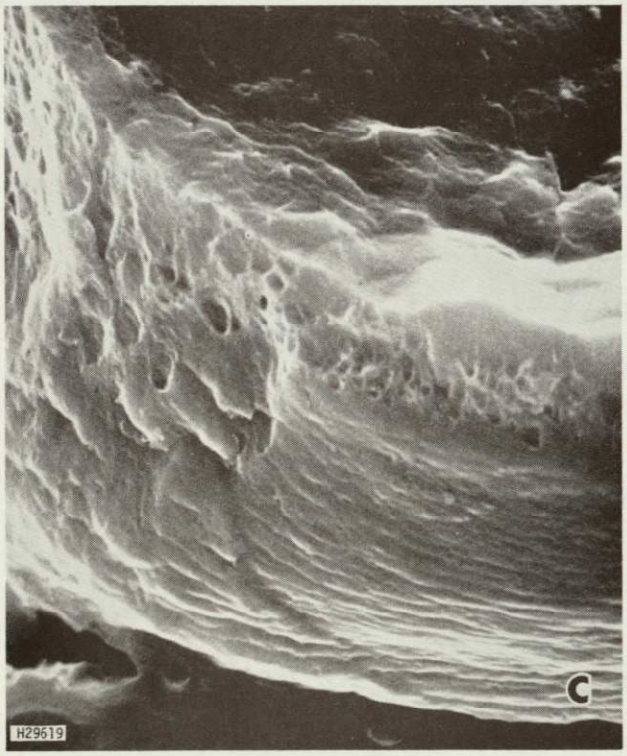

5000X

Figure F3. Fatigue precrack/stress corrosion interface of sample shown in Fig. F2. (45°)

In the transition region, areas of what could be both ductile tearing (b) and stress corrosion (c) were present.

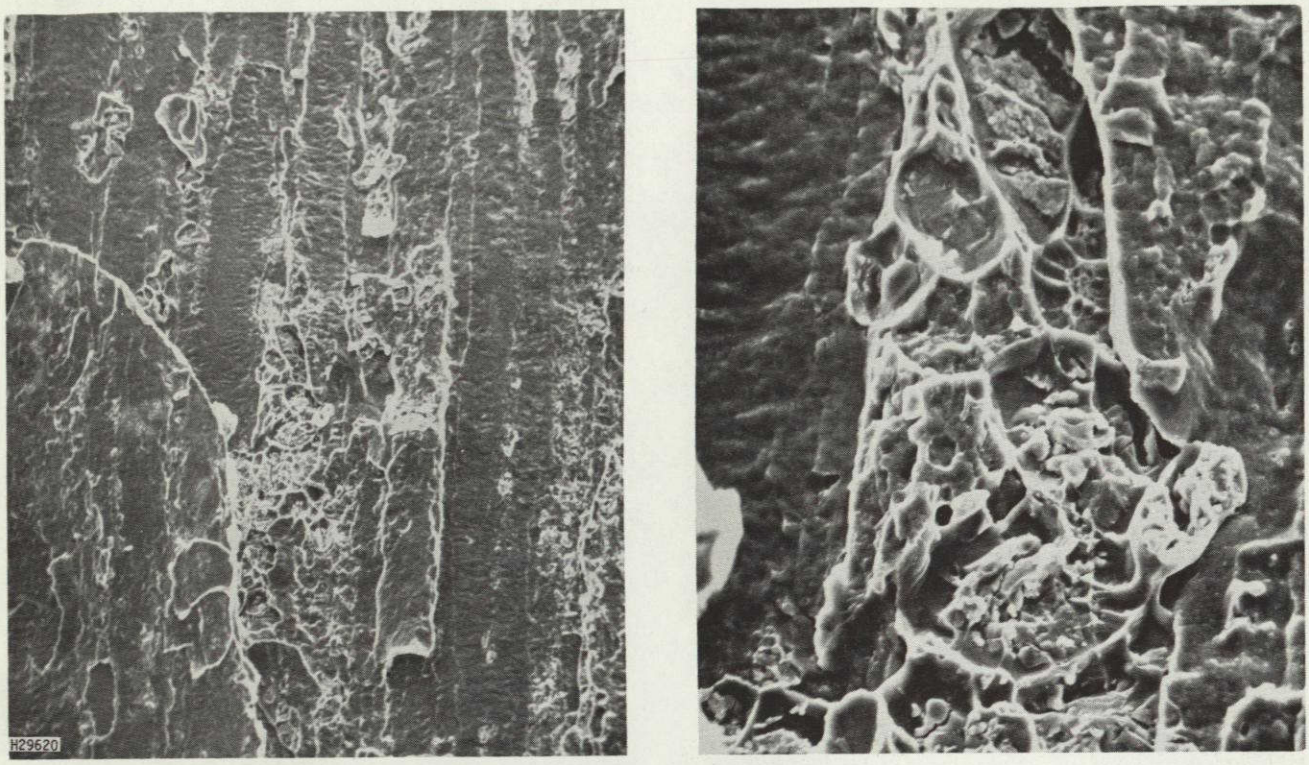

100X 500X

Figure F4. Stress corrosion fracture surface on SL-DCB specimen from 1.25-in. 7075-T7351 plate: salt-chromate environment (45°)

Areas of ductile rupture were commonly found in the stress corrosion crack.

5000X

10,000X

20,000X

Figure F5. Stress corrosion fracture surface on SL-DCB specimen from 1.25-in. 7075-T7351 plate: salt-chromate environment (45°)

Secondary texture of fracture surface is apparent at higher magnifications.

11. Air Force Materials Laboratory
Attn: A.W. Gunderson
Wright Patterson Air Force Base
Ohio, 45433

12. Alcan Aluminium Ltd.
Research Laboratories
Attn: M.A. Reynolds
Banbury, United Kingdom

13. Alcoa Technical Center
Chemical Metallurgy Division
Attn: D.O. Sprowls
Alcoa Center, PA 15069

14. Alcoa Technical Center
Engineering Properties & Testing Division
Attn: J.G. Kaufman
Alcoa Center, PA 15069

15. The American University
Chemistry Department
Attn: B.F. Brown
Washington, D.C.

16. Battelle Memorial Institute
Attn: D.N. Williams
505 King Avenue
Columbus, Ohio 43201

17. Bell Aerospace Company
Attn: J. V. Jackworth
P.O. Box 1
Buffalo, N.Y. 14240

18. Bell Helicopter Company
Attn: W.B. Bond
P.O. Box 482
Forth Worth, Texas 76101

19. Boeing Commercial Airplane Company
Attn: M.V. Hyatt
Mail Stop 73-43
P.O. Box 3707
Renton, WA 98124

20. Boeing Commercial Airplane Company
Attn: C.K. Clarke
Mail Stop K80-50
3801 S. Oliver Street
Wichita, KS 67210

21. Brown Boveri & Company Ltd.
Research Center
Attn: M.O. Speidel
Baden, Switzerland

22. Fairchild Hiller
Republic Aviation Division
Attn: J. Stock
Farmingdale, L.I., N.Y. 11735

23. General Dynamics/Convair Division
Attn: C. J. Kropp
Mail Zone 572-10
P.O. Box 1128
San Diego, CA 92112

24. General Dynamics/Fort Worth Division
Attn: T. E. Coyle
P.O. Box 748
Fort Worth, Texas 76101

25. Grumman Aircraft Engineering Corp.
Research Department
Attn: P. N. Adler
Bethpage, N.Y. 11714

26. Hughes Helicopter Corporation
Materials, Processes & Standards Dept.
Attn: J. C. French
Culver City, CA 90230

27. University of Illinois
Metallurgical Engineering Department
Attn: E. N. Pugh
Urbana, IL 61801

28. Istituto Sperimentale dei Metalli Leggeri
Attn: E. DiRusso
Via del Lavoro 2, CP 129
Novara, Italy

29. ITT Research Institute
Attn: H. Schwartzbart
10 West 35th St.
Chicago, IL 60616

30. University of Leeds
Department of Metallurgy
Attn: J. C. Scully
Leeds LS2.9JT, UK

31. Lehigh University
Dept. of Metallurgy & Materials Science
Attn: R. W. Hertzberg
Bethlehem, PA 18015

32. Lockheed-California Company
Materials Laboratory
Attn: J. M. Van Orden
P.O. Box 551
Burbank, CA 91503

33. Lockheed-Georgia Company
Attn: J. Carter
Dept. 72-34 Zone 26
Marietta, GA 30061

34. Lockheed Missiles & Space Co.
Metallurgy & Composites Laboratory
Attn: D. E. Piper
3251 Hanover St.
Palo Alto, CA 94304

35. Martin Marietta Aluminum, Inc.
Attn: W. Rotsell
19200 Southwestern Ave.
Torrance, CA 90503

36. Martin Marietta Corp.
Research Institute for Advanced Studies
Attn: A.R.C. Westwood
Baltimore, MD 21227

37. Materials Research Laboratories, Inc.
Attn: E.J. Ripling
22333 Governors Highway
Richton Park, IL 60471

38. McDonnell-Douglas Corp.
Materials & Process Division
Attn: R. H. Gassner
3855 Lakewood Blvd.
Long Beach, CA 90801

39. McDonnell-Douglas Corp.
Materials and Process Division
Attn: H. C. Turner
P.O. Box 516
St. Louis, MO 63166

40. McMaster University
Dept. of Metallurgy & Materials Science
Attn: J.D. Embury
Hamilton, Ontario, Canada

41. Midwest Research Institute
Attn: S.L. Levy
425 Volker Blvd.
Kansas City, MO 64110

42. University of Miami
School of Marine & Atmospheric Sciences
Attn: H.L. Craig, Jr.
Miami, FL 33149

43. National Aerospace Laboratory
Structures and Materials Division
Attn: H.P. Van Leeuwen
Amsterdam, Netherlands

44. National Bureau of Standards
Institute for Materials Research
Attn: G. M. Ugiansky
Washington, DC 20234

45. Naval Air Systems Command
Dept. of the Navy
Attn: R. Schmidt
AIR 520311
Washington, DC 20360

46. Naval Research Laboratory
Engineering Materials Division
Attn: R.W. Judy, Jr.
Washington, DC 20390

47. University of Newcastle
Department of Metallurgy
Attn: R.N. Parkins
Newcastle upon Tyne 1
United Kingdom

48. Northrup Corporation
Norair Division
Attn: D. Roda
3901 West Broadway
Hawthorne, CA 90250

49. Ohio State University
Dept. of Metallurgical Engineering
Attn: R. W. Staehle
Columbus, Ohio 43210

50. Reynolds Metals Company
Metallurgical Research Division
Attn: D. S. Thompson
4th and Canal Streets
Richmond, VA 23218

51. Rockwell International
Los Angeles Division
Attn: R. Brockett
International Airport
Los Angeles, CA 90009

52. Rockwell International
Rocketdyne Division
Attn: A. J. Jacobs
6633 Canoga Avenue
Canoga Park, CA 91304

53. Rockwell International
Science Center
Attn: W. L. Morris
Box 1085
Thousand Oaks, CA 91360

54. Rohr Aircraft Co.
Materials and Process Engineering
Attn: Supervisor
Chula Vista, CA 92012

55. Royal Aircraft Establishment
Materials Department
Attn: P. J. E. Forsyth
Farnborough, Hampshire
United Kingdom

56. Southwest Research Institute
Dept. of Materials Engineering
Attn: D. L. Davidson
8500 Culebra Road
San Antonio, Texas 78284

57. Sumitomo Light Metal Industries Ltd.
Research Laboratory
Attn: Y. Baba
Nagoya, Japan

58. United Aircraft Corp.
Sikorsky Aircraft Division
Attn: M. J. Salkind
Stratford, Conn. 06497

59. U. S. Steel Corporation
Applied Research Labs
Attn: S. R. Novak
Monroeville, PA 15146

60. Wyman-Gordon Company
Metallurgy Department
Attn: J. Long
North Grafton, MA 01601